Université Pierre et Marie Curie

Ecole Doctorale Cerveau Cognition Comportement

Neurospin / Unicog, ICM / Picnic

SIGNATURES ELECTRO-MAGNÉTIQUES

DE LA CONSCIENCE

DANS LE CERVEAU NORMAL ET PATHOLOGIQUE

---

par Jean-Rémi KING

Thèse de doctorat de neurosciences cognitives

dirigée par Stanislas DEHAENE

et co-dirigée par Lionel NACCACHE

Soutenue publiquement le 31 Janvier 2014

Devant un jury composé de :

Marcello MASSIMINI	Università di Milano	Rapporteur
Fabien PERRIN	Université de Lyon	Rapporteur
Habib BENALI	Université Pierre & Marie Curie	Examinateur
Victor LAMME	University of Amsterdam	Examinateur
Lionel NACCACHE	Université Pierre & Marie Curie	Examinateur
Stanislas DEHAENE	Collège de France	Examinateur

Université Pierre et Marie Curie

Ecole Doctorale Cerveau Cognition Comportement

Neurospin / Unicog, ICM / Picnic

CHARACTERIZING THE ELECTRO-MAGNETIC SIGNATURES OF CONSCIOUS PROCESSING IN HEALTHY AND IMPAIRED HUMAN BRAINS

Jean-Rémi KING

Dissertation submitted for the degree of

Doctor of Philosophy

Supervised by Prof. Stanislas DEHAENE

And co-supervised by Prof. Lionel NACCACHE

Publicly defended on the 31th of January 2014

Jury:

Marcello MASSIMINI	Università di Milano	Rapporteur
Fabien PERRIN	Université de Lyon	Rapporteur
Habib BENALI	Université Pierre & Marie Curie	Examiner
Victor LAMME	University of Amsterdam	Examiner
Lionel NACCACHE	Université Pierre & Marie Curie	Examiner
Stanislas DEHAENE	Collège de France	Examiner

ABSTRACT

We are not aware of everything our brain does. This dissociation between subjective experience and objective neural activity challenges both theoretical neuroscience and clinical practice. Indeed, not only are the neuronal mechanisms of conscious perception poorly understood, but it remains extremely difficult to determine whether vegetative state patients – who are thus awake but non-communicating – perceive their environment consciously. These theoretical and clinical questions constitute the two main axes of this thesis. In a first part, I develop, from the recent empirical and theoretical advances, a series of methods to characterize the neural and computational mechanisms of conscious perception. In particular, I show in a first study how multivariate pattern classifiers can decode magneto- and electroencephalographic recordings at the single trial level. In three successive studies, I then propose new signal processing methods to *i)* characterize the dynamical structure of stimulus-evoked processes *ii)* quantify the amount of information exchanged across cortical regions and *iii)* estimate the complexity of cerebral responses. At last, I show how a mathematical model based on Bayesian inference principles, can account for a large number of empirical findings observed in studies of conscious and unconscious perception. In a second part, I apply these methods on EEG recordings acquired from a large cohort of vegetative, minimally conscious and conscious patients. The results show that vegetative state patients present *i)* impaired late and sustained sound-evoked brain responses, *ii)* a reduction of the exchange of information across cortical regions *iii)* abnormal slow and medium EEG rhythms (<13Hz) and *iv)* a decrease of the EEG complexity. Ultimately, these various neural signatures of consciousness could be used in synergy to decode conscious contents and help to diagnose, predict and monitor the state of consciousness of non-communicating patients.

Nous n'avons pas conscience de l'ensemble des processus réalisés par notre cerveau à chaque instant. Cette dissociation entre l'expérience subjective et l'activité neuronale présente un défi majeur à la fois pour les neurosciences fondamentales, mais également pour la pratique clinique. En effet, non seulement les mécanismes neuronaux de la prise de conscience sont mal compris, mais il reste extrêmement difficile de déterminer si des patients en état végétatif – éveillés mais non-communicants – perçoivent leur environnement consciemment. Ces questions théorique et clinique constituent les deux axes principaux de cette thèse. Dans un premier temps, je développe, à partir des récentes avancées aussi bien empiriques que théoriques, une série d'outils permettant de caractériser les mécanismes neuronaux et computationnels de la perception consciente. En particulier, je montre dans une première étude comment les analyses de classification multivariée permettent de décoder les signaux magnéto- et électro-encéphalographiques à l'échelle de l'essai unique. De plus, dans trois études successives, je propose de nouvelles méthodes de traitement du signal permettant de *i)* caractériser la structure dynamique des processus évoqués par une stimulation sensorielle *ii)* de quantifier la quantité d'information échangées entre différentes régions corticales et *iii)* d'estimer la complexité des réponses cérébrales. Enfin, je montre comment un modèle mathématique utilisant les principes d'inférence bayésienne permet de rendre compte d'un grand nombre de résultats observés dans les études de la perception consciente et inconsciente. Dans un second temps, j'applique ces méthodes aux EEG d'une large cohorte de patients végétatifs, minimalement conscients et conscients. Les résultats montrent que les patients végétatifs présentent *i)* une altération des réponses corticales tardives évoquées par une stimulation auditive, *ii)* une diminution de l'échange d'information entre régions cérébrales, *iii)* des rythmes EEG moyens et lents (< 13Hz) anormaux et *iv)* une réduction de la complexité de l'activité EEG. A l'avenir, ces différentes signatures neurales de la conscience pourraient être utilisées en synergie pour décoder le contenu conscient et aider au diagnostic, au pronostic et au monitoring des patients non-communicants.

ACKNOWLEDGEMENTS

Ces trois années auraient été bien mornes sans mes collègues et amis quotidiens (voire, parfois, hebdomadaires). J'ai été très heureux de travailler avec des gens formidables tant sur le plan intellectuel qu'humain. Je suis particulièrement redevable envers Imen (et son tutututututu), Simon (et son appartement), Sébastien (et sa voiture), Pierre (et ses flops), Felipe (et son snowboard), mais aussi Anne (et sa musique), Catherine (et son enthousiasme loco-globalien), Clio (sans qui mon assiduité neurospinienne

A mon père,

TABLE OF CONTENTS

TABLE OF FIGURES

PUBLICATIONS OF THE AUTHOR

ARTICLES INCLUDED IN THE THESIS

Several chapters included in this thesis have been accepted in or submitted to international peer reviewed journals and were slightly adapted to increase consistency and facilitate readability.

CHAPTER 3. **KING, J-R.**, FAUGERAS, F., GRAMFORT, A., SCHURGER, A., EL KAROUI, I., SITT, J.D., ROHAUT, B., WACONGNE, C., LABYT, E., BEKINSCHTEIN, T., COHEN, L., NACCACHE, L., DEHAENE, S., (2013) Single-Trial Decoding of Auditory Novelty Responses Facilitates the Detection of Residual Consciousness, *Neuroimage*, 83: 726-738.

CHAPTER 4. **KING, J-R.**, GRAMFORT, A., SCHURGER, A., NACCACHE, L., DEHAENE, S. (in press) Two Distinct Dynamic Modes Subtend the Detection of Unexpected Sounds, *PLoS One*.

CHAPTER 5. **KING, J-R.**, DEHAENE, S., (in press) Characterizing the Dynamics of Mental Representations: the Temporal Generalization Method, *Trends In Cognitive Sciences*.

CHAPTER 6. **KING, J-R.***, SITT, J.D.*, FAUGERAS, F., ROHAUT, B., EL KAROUI, I., COHEN, L., NACCACHE, L., DEHAENE, S., (2013) Information Sharing in the Brain Indexes Consciousness in Noncommunicative Patients, *Current Biology*. 23(19): 1914-1919.

CHAPTER 7. SITT, J.D.*, **KING, J-R.***, EL KAROUI, I., ROHAUT, B., FAUGERAS, F., GRAMFORT A., COHEN, L., SIGMAN, M., DEHAENE, S., NACCACHE, L., (submitted) Large Scale Screening of the Neural Signatures of Consciousness in Vegetative and Minimally Conscious State Patients

CHAPTER 8. **KING, J-R.**, DEHAENE, S., (in press) A model of subjective report and objective discrimination as categorical decisions in a vast representational space, *Philosophical Transactions of the Royal Society: B*.

* The authors equally contributed to the work.

COMMENTS INCLUDED IN THE THESIS

COMMENT 1. **KING, J-R.**, BEKINSCHTEIN, T., DEHAENE, S. (2011) Technical Comment on "Preserved Feedforward But Impaired Top-Down Processes in the Vegetative State", *Science*, 334(6060)

COMMENT 2. SITT, J.D., **KING, J-R.**, NACCACHE, L., DEHAENE, S., (2013) Ripples of Consciousness, *Trends in Cognitive Sciences*, 17(11): 552-554.

OTHER PUBLICATIONS

CHARLES, L., **KING, J-R.**, DEHAENE, S. (in press) Decoding the dynamics of action, intention, and error-detection for conscious and subliminal stimuli, *The Journal of Neuroscience.*

EL KAROUI, I., **KING, J-R.**, SITT, J.D., MEYNIEL, F., VAN GAAL, S., HASBOUN, D., ADAM, A., NAVARRO, V., BAULAC, M., DEHAENE, S., COHEN, L., NACCACHE, L. (under review) Oscillatory and functional-connectivity facets of the MMN and P300: an intracranial study in humans.

ROHAUT, B., FAUGERAS, F., CHAUSSON, N., **KING, J-R.**, COHEN, L., NACCACHE, L. (submitted) Probing auditory semantic verbal processing in non-communicating patients: a high-density ERP study.

SHEYNIKHOVICH, D., GRÈZES, F., **KING, J-R.**, ARLEO, A. (2012) Exploratory Behaviour Depends on Multisensory Integration during Spatial Learning, *Artificial Neural Networks and Machine Learning,* 7552: 296-303.

DEHAENE, S., CHARLES, L., **KING, J-R.**, MARTI, S., (2014) Towards a computational theory of conscious processing, *Current Opinion in Neurobiology.*

INTRODUCTION

A BRIEF HISTORY OF THE INTUITIVE APPROACHES TO CONSCIOUSNESS

A soft jazz melody. The shimmering colour of a glass of red wine. The delectable smell of coffee in the early morning of summer. When it comes to writing an article, a chapter, or a book about consciousness, rare are the scientists who resist the urge to drop a few lyrical lines about their suddenly inspired inner life.

It is with slight embarrassment that we then admit that the vast majority of our research *really is* about blurry grey patches flashed on a computer screen. The conscious experience elicited by such stimuli is inevitably less exciting, but it raises fundamental questions: why do we experience anything at all? What is perception really made of?

FIGURE 0.1 THE "GABOR PATCH"

This gray stimulus one of the most common visual stimuli used in experimental psychology.

Before detailing how such stimuli helped us understanding the mechanisms of conscious perception, it is worth briefly summarizing some of the main philosophical proposals put forward across the last three millennia and that have served as theoretical foundations for the scientific study of consciousness. These proposals were not cautiously founded on scientific grounds to say the least. Indeed, when tackling the topic of consciousness, the most clear-sighted scientists and philosophers, also responsible for the theoretical and methodological foundations of contemporary science, have generally come round to one of two equally unsatisfactory routes: *dualism* and *panpsychism*.

The former is probably best incarnated by Descartes' infamous pineal gland proposition. Descartes was an immense scientist, whose interests spanned from philosophy and mathematics to cosmology and human anatomy. In this last topic he developed an expertise in the nervous system, which he described in great detail to mechanistically understand the way sensory information is transmitted to the brain. But the author of the *Discourse on the Method* struggled when it came to the question of conscious perception. It was seemingly too much for Descartes to believe that this 1.5 Kg of pinkish, wet and

squishy matter could in any way *host* and *produce* subjective experience. Rather, Descartes proposed that vision, smell and touch as well as all sensory information were transmitted to an immaterialist soul through the pineal gland. This little spherical body, roughly located at the centre of the brain would be the gate linking mind and matter, perception and reality.

This dualist view has persisted in parallel to panpsychist proposals. Panpsychism stems from the idea that mind and matter are not fundamentally distinct in nature but rather reflect two properties of the same thing. At the extreme, this view led many to argue that everything is more or less conscious. For instance, according to Diogenes, Thales believed that "*the universe is alive and full of spirits*" (HARE ET AL., 1982). Paradoxically, mixes of dualism and panpsychism have also been expressed: more than two millennia ago, Leucippus and Democritus developed a radically materialist theory, which continues to inspire contemporary physics. But sensations, Democritus argues, are composed of a fundamentally different type of atom than inert matter.

> "*[...] Soul and mind are, [Democritus] says, one and the same thing, and this thing must be one of the primary and indivisible bodies, and its power of originating movement must be due to its fineness of grain and the shape of its atoms; he says that of all the shapes the spherical is the most mobile, and that this is the shape of the particles of fire and mind.*",
> Aristotle, <u>De Anima</u>, referring to Democritus' theory of atoms and its relation to soul, mind and sensations.

Wild speculations are not the monopoly of ancient philosophers. The influential neurophysiologist Eccles and philosopher Popper (the very same Popper who forcefully defended the principle of refutability as a necessary condition for scientific theories) defended a radically dualist position in the 20th century (POPPER AND ECCLES, 1984). Still today, Chalmers continues to argue in favour of a dualist view of mind and matter (CHALMERS, 1996). Equally as controversial, Penrose and Hameroff argue, without any clear explanations, that consciousness results from the quantum mechanics properties of microtubules (PENROSE AND HAMEROFF, 2011).

However intuitive, convincing, or appealing these propositions might appear, they do not provide a satisfactory explanation to our original query: whether conceived of an immaterialist soul, or incarnated by a spherical atom of fire, or a Bose-Einstein condensate, conscious perception remains equally cryptic. More importantly, the way to empirically assess these proposals is equally mysterious. Fortunately, this situation changed radically with the rise of psychology and neuroscience. It may be difficult to span across all of the influential ideas developed by the founders of experimental psychology, but Helmholtz' proposal is worth mentioning here. Capitalizing on the physiological study of the human eye, he suggested that the quality of visual information was too poor to account for subjective experience. Rather, he argued, perception had to be an active process by which the brain makes *inferences* on sensory information. For the first time, perception was viewed as a constructive process rather than a self-sufficient substance or inaccessible essence. The study of visual illusions and brain-damaged patients comforted this view by demonstrating that perceptual inferences can go wrong. The mechanisms and the building blocks of perception could start to be dismantled, apprehended and comprehended.

At the time, however, experimental psychology was not the only approach to studying the mind. Other, less rigorous – if not completely esoteric – methods were also popular amongst the multiple scientific communities. It is probably for this reason that experimental psychology adopted the so-called behaviourist doctrine, which essentially consisted in focusing on behavioural predictions, rather than long literate phenomenological descriptions and mentalistic speculations. The notion of conscious perception did not appear to fit with this radical view, and was thus momentarily neglected, at least overtly. The scientific study of conscious perception finally reappeared when behaviourism gave way to what is now referred to

as cognitive science, a field in which the mind is explained in terms of mental processes involving computation, manipulation and the sharing of representational contents (BODEN, 2006).

FIGURE 0.2 THE RABBIT-DUCK ILLUSION (1892)

This visual illusion, popularized by Wittgenstein (1953), highlights the idea that perception is active interpretation and not a mere re-presentation of reality.

Progressively, theoretical and empirical approaches to consciousness have adopted what Dennett refers to as a "heterophenomenological" principle (DENNETT, 1992). Behind this complicated word lies the idea that psychology and neuroscience should explain the mechanisms by which subjects come to *report* seeing and hearing conscious experiences – as opposed to explaining consciousness in abstraction. Many scientists and philosophers now argue that explaining subjective reports will naturally provide an explanation to self reports and introspection, that can be viewed as the only mean by which one can be convinced of consciously experiencing an inner life. And indeed, as will be detailed in this thesis, a series of conceptual, computational and neural models of perception have now started to be sketched and empirically tested. In particular, the extraordinary technological progress that has marked the last fifty years have now allowed us to directly and objectively study the neural mechanisms that produce our stream of thoughts.

While the "quest for consciousness" (KOCH, 2004) used to be solely driven by a curiosity of the unknown, recent clinical applications have shifted the motivation. Indeed, as will be detailed in the literature review, there exist patients who, despite their awake state, lie still in their bed and fail to communicate with their environment. This so-called vegetative state provides an exceptional condition in which arousal and consciousness appear to be dissociated, providing a concrete way to the address the theoretical (What mechanisms allow one to be conscious?) and epistemological (How can we know whether someone is conscious?) questions initially raised by philosophers.

OUTLINE OF THE THESIS

After introducing the disorders of consciousness encountered in the clinics, I briefly summarize in CHAPTER 1. the scientific theories of consciousness, review their empirical supports, and show how they can be used to dissociate conscious and unconscious processing in non-communicative patients.

The scientific contribution detailed in CHAPTER 2. interconnects two main issues. The first, tackled in CHAPTER 3. , CHAPTER 6. and CHAPTER 7. , consists in characterizing the patterns of brain activity associated with different states of consciousness, using electrophysiological recordings (EEG) of patients suffering or recovering from disorders of consciousness. This clinical investigation aims at both improving patients' diagnosis, as well as confronting the contemporary theories of consciousness to a novel condition: i.e. when arousal and consciousness are seemingly dissociated. In brief, I show that vegetative state patients, present patterns of brain activity associated with unconscious processing: unlike conscious patients and healthy subjects, their electrophysiological responses to auditory stimuli is characterized by an impaired late evoked related potentials, a lowered amount of information sharing across distant brain regions, an increase of low frequency rhythms, and a decrement of complexity. These markers are similar to the ones observed in physiological, pharmacological, and clinical losses of consciousness, as well as in studies directly manipulating the visibility of stimuli presented to conscious subjects.

A second series of studies aims at providing original methods, empirical evidence, and theoretical concepts to refine the current models of consciousness, and is based on the behaviour and the brain activity of healthy subjects. CHAPTER 4. and CHAPTER 5. introduce novel decoding methods to detect and characterize the dynamics of different types of brain activity evoked by specific stimuli. In brief, I show that decoding tools applied to magnetoencephalographic recordings can extract information at the single trial level, and dissociates the type of brain dynamics associated with conscious and unconscious processes. Finally, I show in CHAPTER 8. how a simple Bayesian model can account for a large number of classic findings observed in the consciousness literature. This simple framework shows how conscious perception can be tackled in a perceptual decision perspective, and thus opens novel avenues to study its neural mechanisms.

CHAPTER I. LITERATURE REVIEW

1.1. THE VEGETATIVE STATE: CLINICAL AND THEORETICAL ISSUES

1.1.1. A DISSOCIATION BETWEEN AROUSAL AND CONSCIOUSNESS?

Every year, thousands of patients recover from coma. While many of them regain communication abilities, others evolve to particularly ambiguous states. This is the case of vegetative state (VS) patients, a condition in which patients present clear signs of wakefulness but are believed to remain utterly unaware of the self or the environment (JENNETT AND PLUM, 1972). More than a century ago, Rosenblath encountered the case of a 16-year-old tightrope-walker who fell into a coma after a terrible fall from his wire (ROSENBLATH, 1899). Two weeks after the event, the young patient recovered "to become strangely awake". He subsequently died from his injuries, after eight month of tube-feeding ((ROSENBLATH, 1899) reported by (STRICH, 1956) and (JENNETT, 2002)). Since, similar cases have been repeatedly reported (KRETSCHMER, 1940; FRENCH, 1952; STRICH, 1956; HASSLER ET AL., 1969), and referred to as "apallic syndrome"(KRETSCHMER, 1940), "severe traumatic dementia" (STRICH, 1956) and "encephalopathy" (JENNETT, 2002). But it was the English term "vegetative state", introduced by Jennett and Plum (JENNETT AND PLUM, 1972), that caught on in the medical and scientific communities. This term, argued Jennett and Plum appropriately characterizes these patients, because it implies "[leaving] a merely physical life devoid of intellectual activity [...] social intercourse [...] sensation and thought".
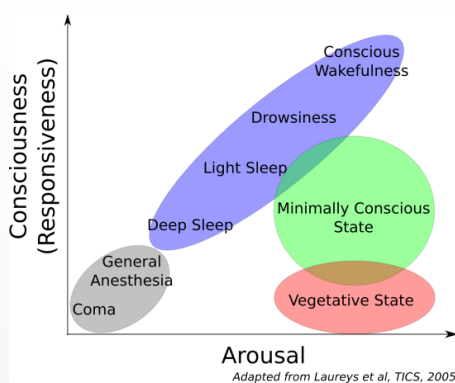
FIGURE 1.1 DISORDERS OF CONSCIOUSNESS: A DISSOCIATION BETWEEN AROUSAL AND CONSCIOUSNESS?

(Left) The vegetative state (VS) is characterized by a dissociation between patients' arousal (propensity to be awake and vigilant) and subjective reports. Unlike comatose patients, or deeply anesthetized subjects, these patients present relatively preserved wake-sleep cycles but remained completely unable to communicate with their environment. Minimally conscious state patients refers to similar patients who nevertheless presents fluctuating signs of consciousness.

(Right) Example of a patient who, after having been diagnosed in a vegetative state, communicated with a brain computer interface (OWEN ET AL., 2006) and hence demonstrated that he was in fact conscious of his environment.

The "vegetative" definition may appear straightforward at first: wakefulness and unawareness. Arousal is clearly defined as a set of behaviours – opening eyes, high and rapid muscle tone, *etc.* – and can thus be assessed unequivocally. Furthermore, its neural bases, the so-called ascending reticular activating system (ARAS), and its links to sleep-wake cycles are relatively well described and understood. However, determining whether the precise clinical definition of awareness should be of the self or the environment is challenging. How can we objectively assess such a subjective construct? Does the absence of overt behaviour imply an inner "life devoid of sensation and thought"? How can we know whether patients experience their surrounding environment when they are utterly unresponsive?

The concreteness of this simple question provides an unprecedented perspective to the fundamental question of consciousness. The vegetative state sweeps away the metaphysical considerations and the bizarre philosophical thought experiments and challenges both scientists and clinicians.

This clinical definition of consciousness is probably at the heart of ongoing debates that repeatedly engender novel, arguably more precise terminologies[1] and definitions (JENNETT, 2005; FINS ET AL., 2008; LAUREYS ET AL., 2010; LAUREYS AND SCHIFF, 2011; VON WILD ET AL., 2012) nonetheless condemned to an intrinsic limitation: an absence of behaviour does not necessarily imply a lack of consciousness. In practice, assessing supposedly conscious behaviour in severely impaired patients is extremely difficult, and often comes to differentiating between intentional[2] and command-following actions from random movements and reflexes. Besides, patients' arousal is fluctuating, and their behaviour does not necessarily replicate within and across clinical examinations. Current estimates indicate that between 15 and 43% of the patients diagnosed in a vegetative state present signs of residual consciousness when carefully examined by trained clinicians (CHILDS ET AL., 1993; ANDREWS ET AL., 1996; GILL-THWAITES, 2006; SCHNAKERS ET AL., 2009B).

In the present thesis, the meaning of "vegetative state" will thus be restricted to the clinical definition provided by the Coma Recovery Scale – Revised (CRS-R) (GIACINO ET AL., 2004). The CRS-R categorizes patients as in a vegetative state when they are consistently unable:

- to follow simple command
- to communicate, with gestural or verbal yes/no responses
- to verbalize intelligibly
- to demonstrate non-reflexive movements and/or emotional behaviour in contingent relation to relevant environmental stimuli (this includes sustained visual fixation, localization of nociceptive stimulations, emotional reaction to known faces, *etc.*)

Each of these abilities is assessed by trained clinicians with a precise set of tests resulting in a 23-point scale.

The reproducible demonstration of *at least one* of these abilities within the same clinical examination would result in a "minimally conscious state" (MCS) diagnosis. This term has only been recently introduced by Giacino and collaborators (GIACINO ET AL., 2002)[3], and together with the CRS-R has improved the diagnoses and scientific investigation of vegetative and minimally conscious state patients (GIACINO ET

---

[1] For instance, Laureys and collaborators have recently proposed to replace the term "vegetative state" by the less connoted and more descriptive "unresponsive wakefulness syndrome" (LAUREYS ET AL., 2010). This term has however not consensually be taken by the community (see a disagreement between Laureys and Schiff in their recent paper for example (LAUREYS AND SCHIFF, 2011)).

[2] Note that "intentional" implies a subjective perspective too, which does not simplify the clinical assessment.

[3] In 1995, the American Congress of Rehabilitation had already proposed the term "minimally responsive state" (MRS) to distinguish purely vegetative state patients from those who present inconsistent but clear signs of conscious behavior (GIACINO ET AL., 2002).

AL., 2009). Finally, it should also be noted that Bruno and collaborators have recently proposed to divide the minimally conscious category in two sub-entities (BRUNO ET AL., 2011B). MCS+ would refer to patients who respond to command, communicate, or present intelligible verbalization, whereas MCS- would refer to patients who only show minimal behavioural interaction, such as the orientation to noxious stimuli, the fixation of moving or salient stimuli or a behavioural response in relationship with their environment (*e.g.* appropriate smiling in response to a face).

The CRS-R is not the only scale that has been proposed to diagnose vegetative and minimally conscious state patients. A number of other scales have been proposed, including the Glasgow Coma Scale (GCS (GRAHAM ET AL., 2005)), the Western Head Injury Matrix (WHIM, (SHIEL ET AL., 2000)), the Western Neurosensory Stimulation Profile (WNNSP, (ANSELL AND KEENAN, 1989)), the Sensory Modality and Rehabilitation Technique (SMART, (GILL-THWAITES AND MUNDAY, 2004)) and the Full Outline of Un-responsiveness (FOUR, (WIJDICKS ET AL., 2005)). Although most of these scales have adequate reliability and validity, and measure various behaviours in response to auditory, visual and somato-sensory inputs, they often suffer from several important limitations (SCHNAKERS ET AL., 2008B). For example, the Glasgow Coma Scale is widely used across the world, but was originally developed to diagnose patients in acute coma stages. This scale is thus fairly limited when it comes to monitoring the progress of chronic vegetative and minimally conscious patients (GIACINO ET AL., 2004; SCHNAKERS ET AL., 2008B). In contrast, the CRS-R directly and formally defines states ranging from coma to minimally consciousness. Comparing these scales to one another on the same cohort of patients demonstrated that the CRS-R was better able to distinguish minimally conscious state patients from vegetative state patients (GIACINO ET AL., 2004; SCHNAKERS ET AL., 2008B). For these reasons, patients' state of consciousness is formally assessed with the CRS-R in the present studies.

1.1.2.   NEUROIMAGING: TOWARD NON-BEHAVIOURAL DIAGNOSES?

Vegetative and minimally conscious states are defined clinically and thus solely on patients' behaviour. However, unresponsiveness does not imply unconsciousness, limiting the accuracy of these behavioural diagnostic techniques. For example, complete paralysis is one condition that would lead, superficially, to the very same symptoms as a vegetative state patient. This possibility is not hypothetical. Locked-in syndrome (LIS) patients are completely aware of their environment but suffer from an *almost* complete inability to move. Fortunately, these patients are able to make some movements – they generally make eyes movements – and hence demonstrate to their clinicians and families that they are conscious (KOTCHOUBEY AND LOTZE, 2013). The possibility of misdiagnosing locked-in syndrome patients as vegetative state is therefore important to consider. Most of our senses and behaviours ultimately depend on the peripheral nervous system. Its integrity thus seems to necessarily determine the assessment of consciousness.

In a recent study, Owen and collaborators overcame the possibility of peripheral deficiencies and opted for a more direct communication channel: brain activity itself (OWEN ET AL., 2006). Healthy volunteers were asked to perform two different imagery tasks in the functional Magnetic Resonance Imaging (fMRI) scanner. The first task consisted in imagining playing tennis. This imaginary task interestingly recruits the supplementary motor area, and thus increases its BOLD response. The second task consisted in imagining visiting the rooms of their house, and activated the para-hippocampal gyrus, the posterior parietal cortex and lateral premotor cortex. The authors subsequently applied this experimental method to a series of patients and found that one patient diagnosed in a vegetative state demonstrated similar brain activations to healthy subjects. Although no sign of awareness could be observed behaviourally, this patient could demonstrate comprehension of complex instructions, and respond to them through her brain activity. A subsequent study revealed that, out of 23 vegetative state patients, four were able to wilfully modulate their brain activity (BYRNE ET AL., 2010). One vegetative state patient was even able to respond to

yes-or-no questions with this method. Recently, this approach has been adapted to a bedside setup using electroencephalography (EEG) (GOLDFINE ET AL., 2011; CRUSE ET AL., 2012). However, the validity of the statistical method in one of this study has been disputed (CRUSE ET AL., 2012, 2013A; GOLDFINE ET AL., 2012, 2013).

Command Following:

Tennis Imagery   Spatial Navigation Imagery

Tennis Imagery to Answer Yes
Spatial Navigation Imagery to Answer No

Do you have any sister?   Do you have any brothers?
"Yes"   "No"

Control

Patient

Adapted from Owen *et al.* (2006)   Adapted from Monti *et al.* (2010)
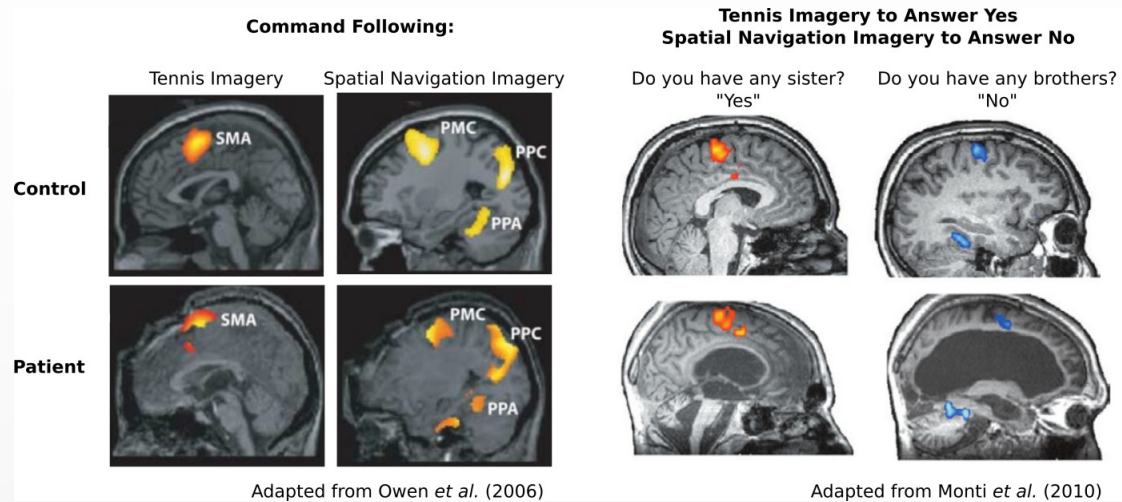
FIGURE 1.2 IMAGINING PLAYING TENNIS TO COMMUNICATE SIMPLE RESPONSES.

(Left) Patients diagnosed in a vegetative state may be unable to communicate because of deficits unrelated to the state of consciousness (e.g. paralysis). Owen and collaborators developed a simple neuroimaging protocol which required subjects to perform two different tasks: imagining playing tennis, or imagining moving around a house. Each of these tasks recruits different neural circuits as identified with fMRI (top). When testing a series of vegetative state patient, the authors found a patient who recruited similar networks to the control subjects, hence demonstrated covert command-following abilities (OWEN ET AL., 2006).

(Right) This protocol was adapted to answer simple yes/no questions (MONTI ET AL., 2010A). For example, subjects and patients were asked to imagine playing tennis to answer "yes", and imaging moving around a house to answer "no". The authors showed that one vegetative state patient was able to use this protocol to communicate with his environment.

Can such brain responses solve, once and for all, the difficult issue of consciousness diagnosis? This is not at all clear. Out of 31 minimally conscious state patients who were investigated in Monti *et al.*'s study (BYRNE ET AL., 2010), only one showed a significant brain response to the imaginary task. This approach failed to detect a modulation of brain activity in most of these patients, who could, nonetheless, demonstrate intentional behaviour in the clinic. Similar questionable results were obtained by Bardin and collaborators (BARDIN ET AL., 2011). The failure to accurately diagnose patients with neuroimaging techniques may be due to a number of factors, ranging from experimental difficulties to cognitive deficits. While the former may be improved with the advances of neuroimaging techniques, the latter could impose an important limitation to this method. Some patients may indeed be conscious of their environment and yet fail to respond to command because of a profound lack of motivation or an inability to understand instructions. Furthermore, in the same way that we can have conscious experiences while we are asleep, some patients may not be aware of their environment and yet experience conscious contents. In such cases, this neuroimaging approach would be doomed to fail.

In other words, whether these diagnostic methods are based on muscle or brain responses, they rely on subjects' ability to intentionally interact with their environment. Is it possible to take a simpler approach, and to test whether patients' brains respond to the environment, irrespective of their intention?

Putting this simple logic into practice faces a difficult issue: not all brain processes necessarily lead to conscious perception.

The so-called "blindsight" neuropsychological condition has marked, and in fact largely legitimated, the field of consciousness research. Popularized by Weiskrantz (WEISKRANTZ, 1986) (see (BRINDLEY ET AL., 1969; PÖPPEL ET AL., 1973; STOERIG ET AL., 1985) for earlier reports), blindsight designates the paradoxical ability to discriminate a visual stimulus above chance level, even when it is presented in a region of the visual field in which patients report not seeing anything, because of lesions in the primary visual cortex. Weiskrantz presented a dim light at the top or at the bottom of patients' blind field, and asked them to perform a two-alternative "forced-choice"[4] task which consisted in indicating the location of the stimulus. Although patients argued that they did not see any light, their guesses were systematically correct. Pathological blindsight has now been observed in many patients (see review in (STOERIG AND COWEY, 2009; COWEY, 2010)), and has been induced in monkeys (COWEY AND STOERIG, 1995). The existence of blindsight seemingly demonstrates that cognition and consciousness are dissociated: one can discriminate a stimulus without experiencing it. The corollary of this phenomenon is that brain activity elicited by a stimulus need not necessarily indicate its conscious perception. To determine whether an unresponsive subject is conscious of his/her environment, a top-down theoretical approach is thus needed in order to determine whether the mechanisms that subtend conscious perception are operational.

KEY POINTS

- "Vegetative state" (VS) is historically defined as wakeful unawareness of self and environment.
- VS is defined here with the Coma Recovery Scale – Revised (CRS-R) that assesses communication and goal driven behaviours.
- Minimally conscious state (MCS) refers to patients who demonstrate minimal communication and/or goal-driven behaviour.
- The clinical diagnosis of non-communicating patients is directly limited by the integrity of the peripheral nervous system (e.g. paralysis).
- Neuroimaging has recently been used as a tool to communicate intentions: subjects and patients imagining playing tennis or moving in their house to respond to yes-or-no questions.
- Previous neuroimaging and clinical diagnosis approaches both require patients to understand and memorize complex instructions.
- Could the diagnosis of consciousness be directly assessed by characterizing patients' brain activity (irrespective of their conscious perception of this activity)?

1.2. THEORIES OF CONSCIOUS ACCESS: FROM ABSTRACT TO NEURAL MODELS

The state of consciousness of awake but non-communicative patients is particularly difficult to establish, as there is no strict equivalence between conscious perception, brain activity and subjects' behaviour. To detect consciousness in the absence of subjective report, one must thus adopt a top-down theoretical approach. This strategy consists in first identifying the neural bases of consciousness in the labora-

---

[4] The term "forced-choice" indicates that patients do not have the ability to say that they do not know. In this case, they had to choose between 'top' and 'bottom'.

tory, and then applying a reverse inference in the clinic, by assessing whether these neural mechanisms are preserved in non-communicating patients.

In the last decades, a great deal of theories of consciousness has been sketched. After briefly reviewing the initial "box-and-arrow" models that have served as a basis for the contemporary theories of consciousness, I will summarize the main features of the recent neuronal models of conscious and unconscious processing. Although the exact computational and biological mechanisms responsible for conscious perception remain heatedly debated, we will see that several several key principles are starting to be consensually adopted.

1.2.1. ABSTRACT MODELS OF PERCEPTION AND ATTENTION

A multitude of philosophical concepts and analogies related to consciousness have been proposed throughout history, but it was not until the 20th century that computational models of conscious perception were investigated scientifically. The first models did not explicitly refer to "consciousness" (KOUIDER AND DEHAENE, 2007; GARDELLE AND KOUIDER, 2009) but the proposed principles of "selective" or "executive" attention, "visual short term memory" and "working memory" undoubtedly served as a basis for the current theories of consciousness. In particular, Broadbent detailed a simple but influential model of selective attention which dissociates two steps of processing: *i)* a set of parallel sensory buffers, and *ii)* a unique limited capacity "perceptual system", which would explain why we cannot perceive multiple things at the same time – the famous cocktail party effect (BROADBENT, 1957). Two decades later, Baddeley and Hitch (BADDELEY AND HITCH, 1975) formalized the idea of maintaining loops between these various steps[5]: the so-called "central executive" would coordinate, select, and trigger the maintenance of peripheral "slave" systems. In an action-selection model, Norman and Shallice (NORMAN AND SHALLICE, 1986) further clarified the distinction between processes that depend on a "supervisory attentional system" and those that can be applied independently and in parallel. This model introduced a distinction between automatic and consciousness-dependent processes which now constitutes one of the axioms of the contemporary models of consciousness (similar concepts are also present in (POSNER AND SNYDER, 1975; FODOR, 1983)).
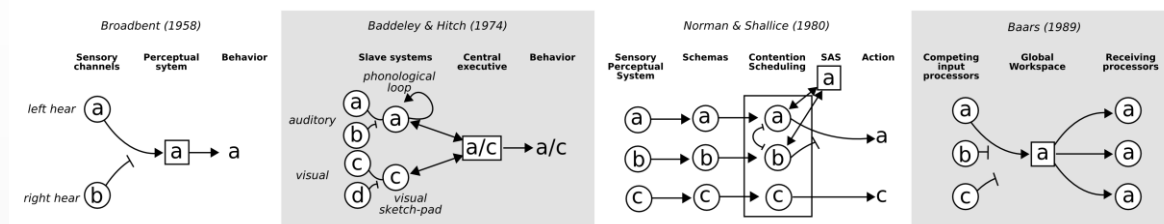
FIGURE 1.3 COGNITIVE MODELS OF CONSCIOUSNESS

Cognitive psychology has been marked by a series of influential models of perception. Broadbent proposed a very simple mechanistic model of attention in which sensory channels compete for a capacity limited perceptual stage. Baddeley and Hitch particularly formalize the notion of feedback loops to maintain information in the "slave systems" whose information is otherwise progressively lost. Norman and Shallice proposed an action selection model in which different streams of information processing ("schemas") are distinguished: some are automatic, and others depend on or are controlled by the supervisory attentional system (SAS), most notably when a competition between the schemas is detected. Baars suggested that the central component that organizes and controls behavior may be best viewed as a global workspace: peripheral modules compete for a central resource that allows them broadcasting their information to multiple receiving processors.

---

[5] Note that a maintaining loop was already proposed by Broadbent in his revision of the model (BROADBENT, 1957).

Each of these models has a central, yet obscure component ("perceptual system", "central executive", "supervisory attentional system"), often associated with conscious perception and deliberate behaviour and thus seemingly implies the existence of an internal observer and/or general coordinator. This premise is undoubtedly unsatisfactory. As forcefully argued by Dennett (DENNETT, 1992), the consciousness of an internal "homunculus" would still need to be explained. Current theories now favour highly distributed architectures which apparently escape the problem of the internal observer. One such model is Baars' "global workspace" theory (BAARS, 1989). Baars postulates that a myriad of parallel input processors compete for a capacity-limited central stage, which itself just serves as a broadcasting mechanism that transmits the information to many other processors. Baars employs the metaphor of a theatre (global workspace) in which actors (processors) compete to play on the stage, and thus be heard and seen by the rest of the audience[6]. According to the Global Workspace theory, each processor can thus compute information in two distinct modes: if its information is globally broadcasted it will be consciously accessible and therefore experienced. In contrast, if its communication is limited to set of modular processors, independently of the global workspace, then the activity would remain inaccessible and thus unconscious. In spite of their differences, these models converge on the idea that perception is subdivided into two steps: i) a set of peripheral processes which process information automatically and in parallel, and ii) a central bottleneck, which selects, in a goal-directed manner, the information that should receive dedicated computing resources to be maintained and memorized.

1.2.2. NEUROBIOLOGICAL MODELS OF CONSCIOUS ACCESS

These four decades of box-and-arrow models gave way to a new neurobiological era. For the first time, scientists were able to directly watch the human brain in action. The scientific study of consciousness, previously limited to abstract models and dry psychophysical experiments – or worse, thought experiments – suddenly appeared very tangible. Concrete questions could now be asked. What are the neural mechanisms responsible for consciousness? Is there a specific brain region, specific neurons dedicated to conscious processing? Can we objectify subjective experience and identify the biological bases of our feelings?

The number of biological theories of consciousness is, once again, too large to be extensively reviewed in the present manuscript (for a more exhaustive review see (SETH, 2007)). While the majority of models support the idea that consciousness is a distributed neural process, some authors have been arguing that it can be localized in specific regions. For instance, Zeki has argued that each cortical module *is* a bit of consciousness (or "micro-consciousness") (ZEKI, 2003). The activity in the cortical region V5/MT, specialized in motion detection, would accordingly be equivalent to the conscious perception of motion. Contrarily, Goodale & Milner have proposed different cortical pathways for (conscious) perception and (unconscious) action processing (GOODALE AND MILNER, 1992, 2005). They argue that the dorsal stream – a cortical pathway starting from the visual cortex and going all the way up to the parietal lobe – processes visual information in an unconscious manner and ultimately supports visually guided actions. Conversely, the ventral stream would be dedicated to the conscious recognition of visual items. Another cortical locus of conscious perception often encountered across the theoretical proposals is the prefrontal cortex (NORMAN AND SHALLICE, 1986; POSNER AND ROTHBART, 1991, 1998; POSNER AND SCENCESS, 1994). To take a recent example, Lau argues that conscious perception depends on the dorso-lateral prefrontal cortex (LAU, 2008), which would specifically host "higher order" – synonymous of "conscious" in Lau's view – representations (LAU, 2008; LAU AND ROSENTHAL, 2011). Finally, thalamic proposals have also been proposed. For example, Ward recently argued that "*the cortex computes the contents of consciousness whereas the thalamus displays, and thus experiences, the results of those computations*" (WARD, 2011).

---

[6] Dennett in fact still criticizes this idea, which remains a "Cartesian Theatre". Dennett proposed a slightly different version, the so-called "pandemonium metaphor" which, according to him, is immune to such issue.
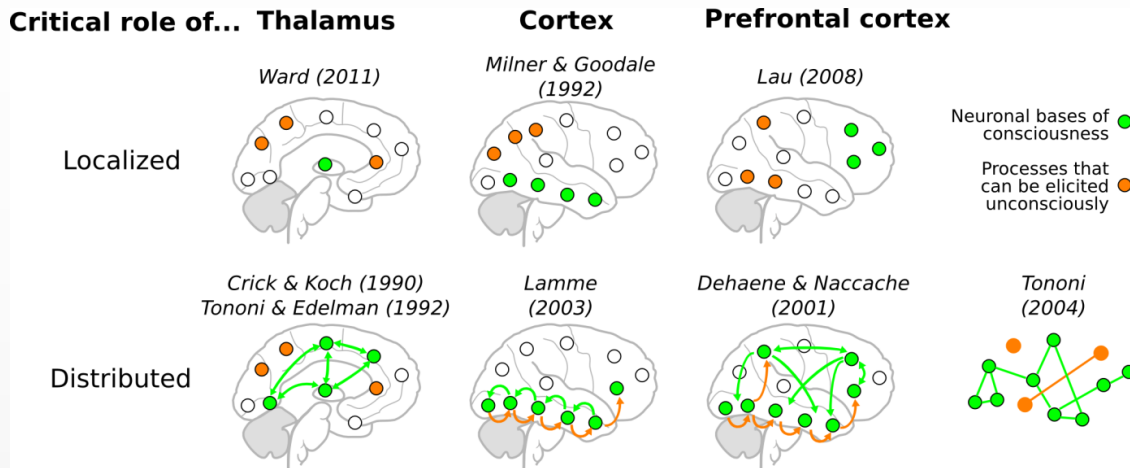
FIGURE 1.4 NEURONAL MODELS OF CONSCIOUS AND UNCONSCIOUS PERCEPTION.

Different neural mechanisms has been proposed to support conscious (in green) and unconscious (in orange) perceptual processing. While several models suppose that a unique (set of) brain region(s) host and/or support conscious perception (e.g. (WARD, 2011)), most models now argue in favour of distributed architecture (SETH, 2007). For example, Tononi and Edelman have proposed that thalamo-cortical loops could constitute a "dynamic core" corresponding to subjective experience (EDELMAN AND TONONI, 2000). Lamme has argued that feedforward activity (from sensory to associative cortices) was unrelated to conscious perception, whereas recurrent processing (horizontal and top down) would constitute the basis of conscious processing as it allows maintenance and information integration across cortical areas (LAMME, 2003, 2010). Dehaene et al. have proposed that the maintenance and integration mechanisms are supported by top-down feedback mechanisms mainly generated (DEHAENE ET AL., 2006; DEHAENE AND CHANGEUX, 2011).

In contrast to these localisationist models, others have argued that conscious processes are intrinsically distributed across the brain. In a pioneering paper, Crick and Koch proposed that conscious access is mediated through synchronous neuronal activity, "probably in the 40 - 70 Hz range" (CRICK AND KOCH, 1990A, 1990B). This proposal capitalizes on a series of empirical findings and computer simulations which suggest that synchronous (or "coherent") firing across distant areas may be a way to "bind" different features into a single unified percept (VON DER MALSBURG AND SCHNEIDER, 1986; GRAY AND SINGER, 1989; GRAY ET AL., 1989) (see (TALLON-BAUDRY AND BERTRAND, 1999) for a more exhaustive review). Indeed, since neurons can act as coincidence detectors when the mean inter-spike interval is longer than the integration interval, they would preferentially relay synchronized input and thus allow higher areas to selectively integrate different features (SINGER, 1993; SOFTKY AND KOCH, 1993; SINGER AND GRAY, 1995A; KÖNIG ET AL., 1996). Although Crick and Koch progressively abandoned this synchrony hypothesis[7], the theory was not forgotten. In particular, Llinás and colleagues have argued that synchronous activity around 40 Hz, engendered by thalamo-cortical loops would constitute the essential mechanism of conscious perception (LLINÁS AND PARÉ, 1991; LLINÁS ET AL., 1998). More recently, Singer's school, and Fries in particular (SINGER AND GRAY, 1995A; ENGEL ET AL., 2001; FRIES ET AL., 2001, 2008; WOMELSDORF ET AL., 2006; MELLONI ET AL., 2007), as well as others such as Tallon-Baudry (TALLON-BAUDRY AND BERTRAND, 1999; TALLON-BAUDRY, 2009) plead in favour of a functional role of neuronal synchrony in visual perception. Note that this view has been vigorously contested with the argument that the brain "*lacks the mechanisms needed to decode synchronous spikes*

---

[7] After this original synchrony theory, Crick and Koch argued that consciousness was linked to higher cortical areas (CRICK AND KOCH, 1998) that allow the formation of neuronal "coalitions" (KOCH AND CRICK, 2003). They provocatively suggested that the primary visual cortex (V1), one of the most studied brain region at the time, could not be a locus for visual consciousness partly because of its lack of direct connection to the prefrontal cortex (CRICK AND KOCH, 1998; KOCH AND CRICK, 2003). Koch now defends Tononi's theory of consciousness as integrated information (TONONI AND KOCH, 2008).

and to treat them as a special code" (SHADLEN AND MOVSHON, 1999). Perhaps a more consensual alternative is the idea that neuronal synchrony is a marker – as opposed to a mechanism – of information sharing.

A second important set of proposals relates to the concept of "re-entrant", "recurrent", or "feedback" processing. Although these concepts also suggest that conscious processing depends on the communication between different neuronal assemblies, they do not imply frequency-specific oscillations. Three models, differing in their specific physiological predictions, can be distinguished.

- First, Edelman and collaborators have proposed that *bi-directional re-entrant connections* allow the integration of different features across the cortex, and may thus serve as a basis for object segmentation, binding, and information maintenance (EDELMAN, 1989, 1993; SPORNS ET AL., 1989, 1991; SETH ET AL., 2004, 2006). The multiple re-entries across the thalamo-cortical system would be characterized by a specific functional cluster ("dynamic core") which would remain relatively stable for approximately 500 ms. Edelman and Tononi have argued that such dynamic cores would be characterized by two main properties; they would be highly differentiated (*i.e.* specific dynamic cores can be selected amongst a very large repertoire) as well as highly integrative (*i.e.* each core gathers a large amount of information across the thalamo-cortical system) (TONONI ET AL., 1998; EDELMAN AND TONONI, 2000; SPORNS ET AL., 2000; TONONI, 2004). Tononi subsequently proposed a mathematical formula to quantify the amount of integrated information in a given system (Tononi, 2004). However, this measure faces a number of practical issues. First, it depends on arbitrary parameters such as the spatial (neurons, cortical column) and temporal (milliseconds, seconds) scale considered for a given piece of information to have an impact. Second, in theory, it can only be tested by perturbing *each* part of the studied system. Third, this measure is currently too computationally expensive to be computable in complex systems (*e.g.* with 100 elements or more). Other similar measures have been proposed, some of which can be tested in the lab (TONONI ET AL., 1994; SETH ET AL., 2006, 2011; CASALI ET AL., 2013).

- Second, Lamme has argued for a strong equivalence between conscious perception and recurrent processing in the cortex (LAMME, 2003, 2010). He describes a two-step process in which a sensory stimulation first elicits a "fast feedforward sweep" of neuronal activity, and is subsequently followed by recurrent processing (LAMME AND ROELFSEMA, 2000). For instance, a visual stimulus would rapidly and successively recruit the striate and extra-striate cortices, the ventral and the dorsal pathways, potentially all the way up to the prefrontal cortex, depending on the strength of the stimulation and the available attentional resources. Each of these areas would first identify different features (colour, motion, shape, *etc.*) and would then share information via *horizontal* connections and *top-down* signals. Recurrent processing would *i)* maintain the various bits of information and *ii)* integrate them into a unified conscious percept. Lamme argues that the feedforward sweep can be elicited unconsciously, whereas recurrent processing is identical to conscious perception (LAMME, 2003, 2010).

- Finally, Dehaene, Naccache, and Changeux have proposed a "global neuronal workspace" model (DEHAENE ET AL., 1998A, 2006B; DEHAENE AND NACCACHE, 2001; DEHAENE AND CHANGEUX, 2005, 2011; SERGENT AND NACCACHE, 2012), based on Baars' theory (BAARS, 1989). They postulate that peripheral processors compete for a global workspace in a *winner-takes-all* fashion. The central resource then *i)* maintains the selected information via a top-down re-entrant signal and *ii)* diffuses this selected information to other peripheral processors. This central resource would be implemented through a *network of pyramidal neurons with long-range axons* particularly dense in the prefrontal, parietal, cingulate and temporal cortices. This model predicts that conscious perception should be marked by *i)* an "ignition" – sudden large activation of a broad set of regions including the prefrontal-parietal networks, and by *ii)* a maintenance of the activity in the selected sensory regions as well as in the global workspace region. The model also provides a functional descrip-

tion of the cortical layer, and of the main types of neurotransmitters associated with ignition (for recent review see (DEHAENE AND CHANGEUX, 2011)).

With the notable exception of Tononi's information integration theory (TONONI, 2004), most of these models progressively evolved from general concepts (connection to higher areas, synchrony, recurrence) to detailed bio-mimetic simulations (SPORNS ET AL., 1989, 1991; DEHAENE ET AL., 1998A, 2003; ENGEL AND SINGER, 2001; DEHAENE AND CHANGEUX, 2005; JEHEE ET AL., 2007; ZYLBERBERG ET AL., 2010). They thus offer a way to confront their predictions to empirical findings: what are the brain regions that can be activated unconsciously? What type of neural activity dissociates conscious and unconscious processing?

1.3. EXPERIMENTAL METHODS TO STUDY CONSCIOUS AND UNCONSCIOUS PROCESSES

I have briefly summarized above the neural theories of conscious processing. I will now outline the experimental method used in the laboratory and in the clinics to tests their respective predictions.

Blindsight is not the only case in which cognition and conscious perception are dissociated. Conscious and unconscious perceptual processes have also been studied via two families of experimental methods.

Conscious States				**Conscious Content**			
	Arousal				**Attention**		
		Low	*High*			*Low*	*High*
Subsequent Subjective Reports	*Low*	Deep Sleep General Anesthesia	Absence / Complex Partial Seizure	**Sensory Evidence**	*Low*		- Blindsight - Backward Masking - Crowding
	High	REM Sleep	Conscious Wakefulness		*High*	- Neglect - Change / Inattentional Blindness - Attentional Blink	- Multistable Perception

FIGURE 1.5 EMPIRICAL APPROACHES TO STUDY MINIMALLY DIFFERENCES BETWEEN CONSCIOUS AND UNCONSCIOUS PROCESSES.

1.3.1. CONSCIOUS OF: DISSOCIATING CONSCIOUS AND UNCONSCIOUS CONTENTS.

First, a series of studies has undertaken a minimalist contrastive approach (BAARS, 1989), which consists in minimizing the differences between the stimuli reported as "seen" and the stimuli reported as "unseen"[8]. A variety of experimental methods can limit, or even prevent, a stimulus from being consciously perceived (for review see (KIM AND BLAKE, 2005)). Most are based on three generic principles:

i)   degrading the quality of the sensory information
ii)   varying subjects' expectation about a stimulus and
iii)   altering subjects' attentional resources available to the stimulus processing.

The first technique can be simply implemented by adding noise to the stimulus, which obviously reduces the signal-to-noise ratio of sensory processes. Sensory information can also be deteriorated by

---

[8] Obviously this approach is not restricted to vision, but for simplicity, the vocabulary employed in this thesis will be restricted to the visual modality.

presenting a crowded stimulus in the periphery of the visual field (CAVANAGH, 2001; PARKES ET AL., 2001; WHITNEY AND LEVI, 2011) as well as by forward, backward and meta-contrast masking. Note that pattern masking is arguably a form of spatio-temporal crowding (WHITNEY AND LEVI, 2011; LEV ET AL., 2013), and may not be that different from spatial crowding. The invisibility induced by these experimental is hardly explained by attentional deficits: indeed subjects are asked and trained to focus their attention on the stimulus. By contrast, attentional blink (RAYMOND ET AL., 1997) and inattentional blindness[9] experiments (MACK AND ROCK, 1998; MACK, 2003) explicitly manipulate subjects' attention to reduce their ability to detect a critical stimulus, which is otherwise perfectly visible. For instance, the attentional blink experiment consists in asking subjects to report two quickly flash targets. When the delay between the two targets is low (<50 ms), the second target is often missed, as subjects' attention is still directed toward the processing of the first target (RAYMOND ET AL., 1997). Other methods such as change blindness (O'REGAN, 2006), some forms of inattentional blindness (MACK AND ROCK, 1998), and multistable perception such as the face/vase illusion and binocular rivalry (LOGOTHETIS ET AL., 1996; KIM AND BLAKE, 2005) can be modelled in terms of a combination of varying attention, masking and prior expectations. For example, change blindness is only efficient when *i)* subjects do not know which objects changes (low priors), and *ii)* there exists multiple salient objects on the screen (low attention), and *iii)* brief masks are flashed when the change occurs (masking).

These methods have different characteristics: they mask stimuli for different amounts of time, in different regions of the visual field, and differentially affect sensory processing (KIM AND BLAKE, 2005). Importantly however, while these forms of masking disrupt conscious perception, they still preserve some processes. Residual sensory processing can be identified by comparing forced-choice responses, reaction time, and neural activity under different conditions of visibility, and can thus help us identifying the neural bases of conscious and unconscious processes.

It may be useful at this point to clarify the vocabulary at play in each of these experimental methods:

- "Unseen" stimuli refer to items that subjects report not having seen when given the possibility to do so. Such a condition is thus referred to as a *subjective visibility report*.
- "Invisible" or "subliminal" stimuli refer to items that subjects are unable to detect, making stimulus discrimination or detection not significantly different from chance. This condition is thus often referred to as an *objective discrimination*.

Interestingly, the objective ability to detect a visual stimulus can differ from subjective visibility reports. This is for example the case of blindsight patients who report not seeing the stimulus presented in their blind field, but are yet able to discriminate it above chance in a forced-choice task. The case of blindsight thus contrasts with the subliminal perception experiments, in which subjects report not seeing the stimulus and are also unable to discriminate it. Whether the term "unconscious" should be restricted to invisible or unseen stimuli has been repeatedly debated over past decades (for a small set of opposing opinions, see (ERIKSEN, 1960; GREEN AND SWETS, 1966; MERIKLE, 1982; CHEESMAN AND MERIKLE, 1984; HOLENDER, 1986; SNODGRASS, 2002; DEHAENE ET AL., 2006B; SNODGRASS AND SHEVRIN, 2006; KOUIDER AND DEHAENE, 2007; LAU, 2008)).

---

[9] Depending on the exact paradigm, inattentional blindness experiments may also manipulate subjects' expectation about specific stimuli. In Simon & Chabris's famous experiment, naïve subjects are asked to count the number of passes made by one of the basket-ball teams recorded in a short video-clip (SIMONS AND CHABRIS, 1999). Performing this demanding task make them unaware that a person disguised as a gorilla had come right in the middle of their visual field in the middle of the video. Subjects' inability to consciously perceive the gorilla may however not only be solely due to attentional deficits, but is also affected by the fact that subjects had no reason to expect a gorilla in the video. Prior expectations may thus be crucial to "inattentional" blindness.

Indeed, each measure has its own advantages and disadvantages. Subjective reports can be analysed at the single trial level. They thus allow comparing objectively identical (DEHAENE ET AL., 2006B), or equally distinguishable stimuli (LAU AND PASSINGHAM, 2006; RAHNEV ET AL., 2011, 2012B), which are nevertheless associated with different visibility ratings. However, they are affected by responses biases. Response biases refer to the subjects' propensity to favour a particular answer. For example, a subject may adopt a "conservative" strategy, meaning that he/she rarely reports seeing the stimulus, even in cases he/she partially sees it. Such strategies are problematic because trials reported as "unseen" are contaminated by an important proportion of trials in which the subject did partially see the stimulus. Any measure (brain activity, reaction time, etc.) would thus not be representative of a purely unconscious condition.

Contrarily, objective measures of perception are robust to response biases. By estimating the difference of "seen" responses observed when the stimulus is present and when it is absent, one can estimate subjects' detection sensitivity independently of subjects' responses biases. However, such measure is necessarily computed across multiple objectively dissimilar trials. Consequently, objective measures dissociate conscious and unconscious processing from objectively different experimental conditions. For example, unconscious perception could be established by imposing a heavy masking on a faint stimulus, and making sure that subjects' detection sensitivity is not different from chance. Subjects' behaviour and brain activity could then contrasted to second condition, in which the stimulus is highly contrasted and poorly masked, so as to produce above chance detection sensitivity. The difference obtained between the two conditions may reflect differences related to stimulus properties rather than conscious perception *per se* (LAU, 2008).

While keeping these epistemic issues in mind, the term "unconscious" will hereafter be used to refer to either invisible or unseen stimuli, as long as it does not crucially interfere with the interpretation of the results. However, and as will be detailed and discussed in CHAPTER 8. , the general approach undertaken in the present thesis favours subjective reports over objective discrimination performance. This positioning stems from the premise that explaining how subjects come to make behavioural reports about their own thoughts and sensations is likely to help to understand how they come to report to themselves what they perceive.

1.3.2. CONSCIOUS OR NOT: DISSOCIATING THE STATES OF CONSCIOUSNESS.

The second family of studies consists in testing how the *state* of consciousness affects perceptual processing. Loss of consciousness can be induced physiologically (sleep), pharmacologically (anaesthesia) and pathologically (seizure).

First, information processing can be compared across different sleep stages (for brief reviews see (MCCARLEY AND SINTON, 2008; DIEKELMANN AND BORN, 2010)). Sleep induces a loss of responsiveness that can be easily reversed by a sensory stimulation, although the threshold of awakening varies depending on sleep stages (RECHTSCHAFFEN ET AL., 1966). Sleep stages are controlled by the ascending reticular activating system (ARAS), which modulates the thalamic and cortical activity. These sleep stages are empirically defined according to subjects' muscle activity and scalp EEG. Sleep stages 1 and 2 refer to the transition of wakefulness to sleep and are marked by the persistence of an important 10 Hz EEG oscillation. Sleep stages 3 and 4, also known as "deep" or "slow wave" sleep, are characterized by important low frequency oscillation (< 4 Hz, "delta waves"). Finally, rapid eye movement (REM) or "paradoxical" sleep present a similar EEG activity to wakefulness despite subjects' irresponsiveness. The exact state and content of consciousness in sleep remains difficult to assess, as dreams may formally constitute a conscious experience. Dreams generally occur in REM sleep, but have also been reported in non-REM sleep (MANNI, 2005). Furthermore, external sensory stimulations can be incorporated in dreams (BRADLEY AND MEDDIS, 1974; IBÁÑEZ ET AL., 2009).

A more profound loss of consciousness can be induced pharmacologically, with various anaesthetic substances such as propofol and sevofurane. General anaesthesia is closer to a reversible coma than to an artificial form of sleep, as subjects *i)* present a complete loss of responsiveness, *ii)* cannot be awakened by sensory stimulations and *iii)* form no memories of the situation. Despite being used in the clinics since the 19th century, the precise molecular and biological mechanisms of anaesthesia remain poorly understood. In particular, it remains debated whether anaesthetic substances primarily and directly affect the functioning of cortex by disturbing chemical communications across neurons, disrupting GABA receptors (NURY ET AL., 2011), for example, or whether anaesthesia primarily affects the ascending reticular activating system, which then deactivates the thalamo-cortical system (ALKIRE AND MILLER, 2006; ALKIRE ET AL., 2008; DEHAENE AND CHANGEUX, 2011). Although patients under dissociative anaesthesia, induced by substances such as ketamine, can preserve a form of conscious state, it is generally accepted that general anaesthesia unambiguously prevents a conscious experience of the environment.

Finally, loss of consciousness can also be caused by epileptic seizures. Epilepsy is a neurological disorder characterized by abnormal, generally excessive, hyper-synchronous neuronal activity. Two specific types of epilepsy – complex partial seizures and absences – may be particularly relevant to the study of conscious and unconscious processes. "Partial" seizures are initially spatially confined, most commonly in the temporal lobe, and can subsequently spread within the thalamo-cortical system (FISHER ET AL., 2005). When patients lose consciousness, the partial seizure is said to be "complex". After complex partial seizures (post-ictal period), patients may be disorientated, often report being exhausted, and generally reveal no memory of the events that occurred during the ictal period (ENGEL, 2013). "Absences" are symptomatic of "petit mal" epilepsy, a form of epilepsy most often observed in children and young adolescent. Absence mark a brief seizure-induced a loss of consciousness (*i.e.* lasts a few seconds), that starts and ends abruptly. Patients generally continue their activity as if nothing had happened. Unlike sleep and anaesthesia, absence and complex partial seizures do not dramatically affect subjects' arousal. While these patients are non-communicating, they remain awake, have their eyes opened and can even demonstrate stereotypical behaviour (ENGEL, 2013). Although the degree of consciousness varies between patients and seizures (BLUMENFELD, 2005; BAGSHAW AND CAVANNA, 2011), these pathologies offer clear evidence that wakefulness and conscious state can be dissociated (BARTOLOMEI AND NACCACHE, 2011; BAYNE, 2011).

In the various conditions, it is difficult to formally assess patients' and subjects' state of consciousness. The latter is generally based on *a posteriori* reports (*e.g.* do you remember having perceived something) or on online command following (*e.g.* press a button every time you hear a sound). Both of these measures are of course dramatically limited. *A posteriori* reports depend on the integrity of memory formation and retrieval, and command following may not always accurately reflect a conscious process (e.g. breaking at a red light). As a consequence, the study of consciousness states is necessarily based on a variety of convergent evidence rather than on a single key experiment.

1.3.3.   NEURAL CORRELATES, MARKERS, SIGNATURES AND BASES OF CONSCIOUSNESS

In summary, the two meanings of consciousness (*content* and *state*) have led to two main families of experimental methods – both of which can be used to identify the *neural signatures of consciousness*. Note that "signature" is used deliberately, and differs from the traditional term "neural correlate of consciousness" (NCC). Indeed, "correlate" does not imply the notion of specificity and could thus refer to any brain activity that has a relationship with consciousness. By contrast, and following the definition of the term in its classic meaning (*e.g.* signing a check), a signature has three properties (according to Wikipedia's definition). To be a neural signature of consciousness, the brain activity should be:

- **Specific**: it should not be observed in unconscious conditions (*e.g.* pupil size and heart rate correlate significantly with subjective reports. However, since they can vary independently of conscious perception, they are not specific enough).
- **A correlate**: the pattern of activity recorded is the product and not the mechanism, or "basis" by which subjects become conscious (*e.g.* arguing that gamma power is a neural signature of conscious access does not mean that anything oscillating at 40 Hz would represent consciousness).
- **Invariant**: the brain activity should be identical across the various ways conscious processing is investigated (i.e. a pattern of brain activity identified with a backward masking should be indicative of patients' level of anaesthesia).

As will be exposed in the following section, the unequivocal identification of a neural signature of consciousness is difficult. Studying anaesthesia, sleep and seizure-induced loss of consciousness indeed implies a number of methodological limitations. For example, significant differences between conscious and unconscious states may not be specifically related to consciousness *per se*, but rather reveal drug, seizure or arousal effects. Similarly, the difference of brain activity observed between masked and unmasked stimuli may reflect mask-specific effects rather than consciousness-specific properties. Furthermore, it remains possible that sleeping, anesthetized subjects and in patients having a seizure are conscious, but do not form any short or long term memory of their perception – in the same way that we dream every night and yet forget most of these experiences. Nevertheless, taken together, these various approaches will build a body of evidence that will undoubtedly help delineate the neural basis, and therefore signatures, of conscious processing.

The term "marker" will be used to refer to the patterns of brain activity that empirically correlate with consciousness in a specific manner. "Markers" will thus be preferred for experimental evidence (e.g. "A series of markers of consciousness was found in experiment X"), whereas "signature" will be reserved to the theoretical predictions (e.g. "Experiment X was designed to detect the signature of consciousness Y").

KEY POINTS

- Theories of consciousness predict that conscious perception should be associated with i) the maintenance and ii) the broadcasting/sharing/integration of iii) a limited amount of information.
- Different neural mechanisms have been proposed to implement such functions: information could be shared and bound by i) synchronizing the neuronal activity in the gamma band, ii) engaging a "global workspace" network and/or iii) triggering recurrent activity across distant regions via horizontal and top-down connections.
- Two main families of experimental methods can be used to test these predictions: i) those comparing the state of consciousness (e.g. wake *versus* sleep and anaesthesia) and ii) those comparing the content of consciousness (e.g. seen *versus* unseen stimuli generally presented at perceptual threshold).

1.4. EMPIRICAL FINDINGS

In spite of the wide range of methods cited above, neuroimaging studies have found converging evidence for a number of empirical phenomena related to conscious processing. After quickly reviewing

the neural activity that is unequivocally *not* specific to conscious processing, I will go over five families of putative neural signatures of conscious processing.

1.4.1.   THE SENSORY AND ASSOCIATIVE CORTICES CAN BE ACTIVATED UNCONSCIOUSLY

1.4.1.1.   Evidence from the manipulation of perceptual contents

Until the eighties, behavioural experiments, and priming studies in particular, had already demonstrated that automatic low level features (e.g. location, shape, etc.) could be rendered subliminal while still influencing behaviour. By contrast, it was often proposed that high-level processes such as semantic and executive functions necessitated conscious perception of the stimulus. Although several psychophysical experiments had already jeopardized this idea (for historical reviews see (MERIKLE, 1982; CHEESMAN AND MERIKLE, 1984; GAUCHET, 1992; DEHAENE AND NACCACHE, 2001; KOUIDER AND DEHAENE, 2007; NACCACHE, 2009) and meta-analysis (VAN DEN BUSSCHE ET AL., 2009)), the possibility of high level unconscious processing became unequivocal with the rise of neuroimaging studies, such as the one from Dehaene and collaborators (DEHAENE ET AL., 2001). The authors asked subjects to silently read briefly flashed words while their brain activity was recorded with fMRI. Half of these words were preceded and followed by visual masks that rendered the stimuli invisible. Yet, these invisible words elicited a significant brain response in the left extra-striate, fusiform and pre-central cortices – a network of brain areas associated with word reading in normal visibility conditions (FIEZ AND PETERSEN, 1998).
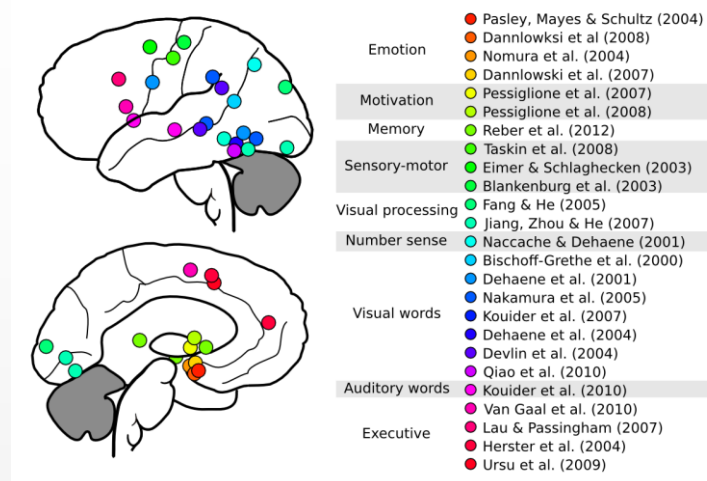
FIGURE 1.6 ACTIVATIONS ELICITED BY SUBLIMINAL STIMULI IDENTIFIED IN FMRI STUDIES.

Undetectable (e.g. invisible) or missed (e.g. unseen) stimuli can elicit activity in various cortical and subcortical regions. Note that this non-exhaustive review remains schematic as neither the exact location, nor the size, significance and the statistical corrections are mentioned. Note that the temporo-polar, prefrontal cortex and dorsal parietal cortex are generally not recruited by subliminal stimuli.

Numerous experiments have now confirmed that cortical modules could be unconsciously activated by orthographic or semantic features (BISCHOFF-GRETHE ET AL., 2000; DEHAENE ET AL., 2004; DEVLIN ET AL., 2004; NAKAMURA ET AL., 2005; QIAO ET AL., 2010). These results thus contribute to the redefinition of the depth of subliminal processing – a level now clearly deeper than basic visual feature recognition (FANG AND HE, 2005; EDDY ET AL., 2007; JIANG ET AL., 2007) and subcortical processing (WHALEN ET AL., 1998; MORRIS ET AL., 1999; NOMURA ET AL., 2004; PASLEY ET AL., 2004; DANNLOWSKI ET AL., 2007, 2008). Recent stud-

ies have also confirmed that subliminal processing is not restricted to the ventral stream[10]. Subliminal numbers can activate the parietal area responsible for quantity-estimation (NACCACHE AND DEHAENE, 2001A). Masked incentive items recruit basal forebrain nuclei such as the ventral striatum, associated with value and motivation (PESSIGLIONE ET AL., 2007, 2008). Faint auditory (DIEKHOF ET AL., 2009; SADAGHIANI ET AL., 2009; KOUIDER ET AL., 2010) and tactile stimuli (BLANKENBURG ET AL., 2003; TASKIN ET AL., 2008) can activate the primary auditory and sensory areas respectively even when subjects are unable to detect them. A recent study in fact suggests that invisible stimuli can trigger memory-related processes and activate the hippocampus – an area associated with *explicit* memory formation and retrieval (REBER ET AL., 2012). It may be noted, however, that these studies unequally control for residual conscious processing. In the last study by Reber et al. (REBER ET AL., 2012), for example, the target words were masked with white noise images, an unorthodox method that has been shown to only partially mask words (TURVEY, 1973; BREITMEYER AND OGMEN, 2000). Still, the accumulation of empirical evidence is undeniable. Multiple independent teams regularly demonstrate that a large number of cortical regions can be activated when subjects are unable to detect the target.

FIGURE 1.7 SENSORY ACTIVATION IN UNCONSCIOUS STATES.

Sensory stimulation can evoke activity in primary and secondary sensory cortices in anesthetized and sleeping subjects.
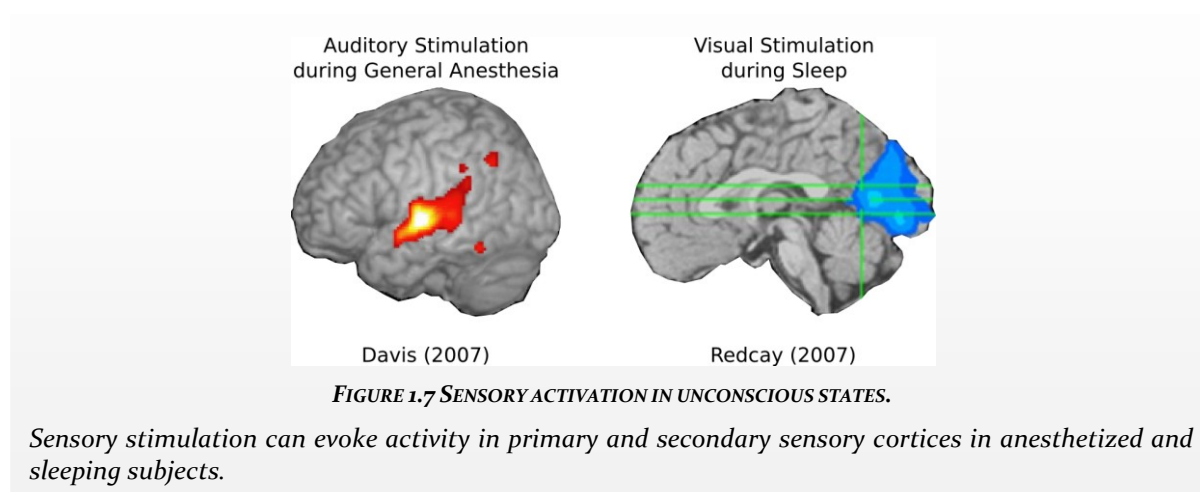
1.4.1.2. Evidence from the manipulation of consciousness states

Furthermore, similar findings have been obtained with normal (*i.e.* supra-threshold) stimuli presented to sleeping, anaesthetized and epileptic subjects. For example, various types of sounds have been shown to activate the auditory cortex, thalamus and caudate nucleus during non-REM sleep (PORTAS ET AL., 2000; CZISCH ET AL., 2002; TANAKA ET AL., 2003; REDCAY ET AL., 2007) including slow wave stages (ISSA AND WANG, 2011). Furthermore, the left amygdala and left prefrontal cortex (BA 46) differentially respond to pure tones and subjects' own name during various sleep stages, suggesting an extraction of the emotional content rather than a purely sensory activation (PORTAS ET AL., 2000). In fact, these neuroimaging studies confirm a well known phenomenon in the sleep literature; it has been repeatedly shown that meaningful stimuli more easily and more rapidly wake people up than neutral stimuli, suggesting that meaning must be partially processed during sleep (OSWALD ET AL., 1960; ZUNG AND WILSON, 1961; LANGFORD ET AL., 1974). Similar findings are observed in pharmacologically-induced loss of consciousness. Sounds activate several regions of the temporal cortex under deep anaesthesia (PLOURDE ET AL., 2006; DAVIS ET AL., 2007; LIU ET AL., 2012) and flashes activate the occipital lobe (REDCAY ET AL., 2007), although the depth of processing appears to be relatively superficial in this pharmacologically-induced loss of consciousness (PLOURDE ET AL., 2006; DAVIS ET AL., 2007). In the fMRI study by Redcay and colleagues, however, the patients were children and

---

[10] The ventral stream designates a series of regions that connect the occipital and the ventral temporal lobes. It is generally believed to host object recognition processes (GOODALE AND MILNER, 1992)

their sleep stages were not strictly monitored because of a lack of EEG (REDCAY ET AL., 2007). The results should thus be taken as indicative and interpreted cautiously.

1.4.2. LOCATING CONSCIOUS PROCESSES

A myriad of cognitive processes and their respective brain regions can be activated without subjects becoming aware of them. Nonetheless, this striking finding should not diminish the differences observed between conscious and unconscious brain responses.

1.4.2.1. Unmasked stimuli recruit the fronto-parietal networks

In Dehaene et al.'s study for example, subliminal stimuli elicited significant activity in brain areas related to reading, but this activity was dramatically reduced as compared to visible stimuli (DEHAENE ET AL., 2001). Furthermore, visible targets elicited activity in the prefrontal and parietal cortices, whereas these regions remained utterly unresponsive in the subliminal condition. The simultaneous increase of activity in specialized areas and the large activation of the multi-modal associative cortices typically distinguishes seen from unseen stimuli (REES ET AL., 2002; CARMEL ET AL., 2006; DEHAENE AND CHANGEUX, 2011). This pattern of results has been observed with various methods including binocular rivalry (LUMER, 1998), change blindness (BECK ET AL., 2001), stimuli presented at perceptual threshold (BOLY ET AL., 2007; DIEKHOF ET AL., 2009; SADAGHIANI ET AL., 2009), backward masking (GRILL-SPECTOR ET AL., 2000; DEHAENE ET AL., 2001) and attentional blink experiments (MAROIS ET AL., 2004). Furthermore, structural neuroimaging studies show that the gray matter density of the dorso-lateral cortex as well as the density of its white-matter tracks are specifically correlated with subjects' meta-cognitive abilities (FLEMING ET AL., 2010) – a process often associated with conscious processing (ROSENTHAL, 1997; LAU, 2008; LAU AND ROSENTHAL, 2011).
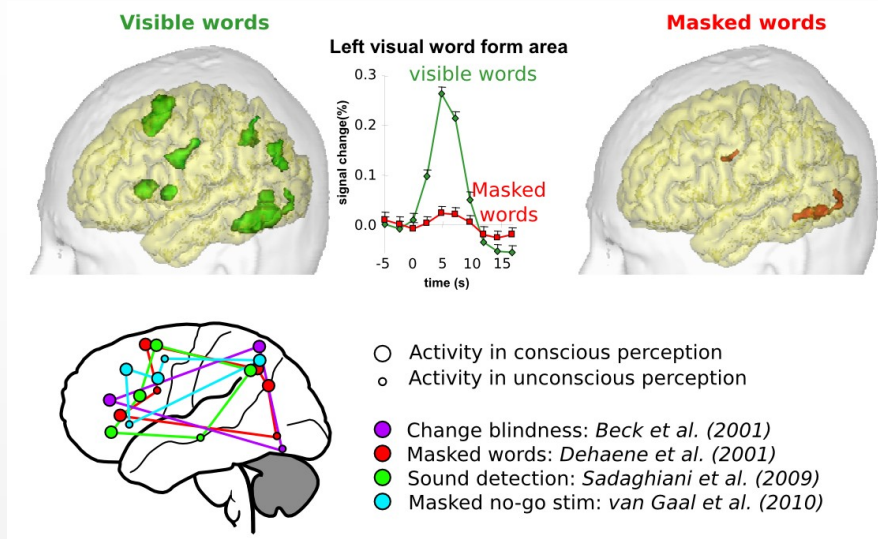
FIGURE 1.8 COMPARING SUBLIMINAL VERSUS SUPRALIMINAL STIMULI.

Although subliminal stimuli can elicit cortical activation, their amplitude is generally dramatically reduced as compared to supraliminal conditions. Furthermore, supraliminal conditions are typically marked by the recruitment of multiple brain areas, especially in the prefrontal and parietal cortices.

Intracranial recording studies demonstrate a strong correlation between subjective reports and the "level" of the cortical regions in the visual processing hierarchy. For example, binocular rivalry experiments showed that only 20% of the cells recorded in V1 and V2 fire when percept changes, whereas this proportion is doubled in V4 and V5 and reaches 90% in the infero-temporal cortex and superior temporal

sulcus (LOGOTHETIS ET AL., 1996; SHEINBERG AND LOGOTHETIS, 1997; WILKE ET AL., 2006). fMRI studies have shown that activity in early visual areas such as V1 (TONG ET AL., 1998, 2006; POLONSKY ET AL., 2000; HAYNES ET AL., 2005A), and even the lateral geniculate nucleus (HAYNES ET AL., 2005A), correlates with perceptual changes, but the BOLD response is likely to reflect top-down feedback. Indeed, Maier and collaborators have shown that while low-frequency local fields potentials correlated with the BOLD response in V1, efferent firing are apparently not affected by this change (MAIER ET AL., 2008).

1.4.2.2. Wakefulness is associated with fronto-parietal activations

A similar pattern of results is observed in sleeping and anaesthetized subjects: in these unconscious conditions, sensory stimulations fail to elicit frontal and parietal activations, and are generally associated with reduced sensory activity. This is particularly true in deep anaesthesia conditions (BONHOMME ET AL., 2001; KERSSENS ET AL., 2005; PLOURDE ET AL., 2006; DAVIS ET AL., 2007; RAMANI ET AL., 2007; LIU ET AL., 2012) as well as in REM and slow wave sleep (PORTAS ET AL., 2000; TANAKA ET AL., 2003; CZISCH ET AL., 2009; ISSA AND WANG, 2011). This reduced depth of cortical processing, and the specific lack of fronto-parietal responses fit with the fact that these regions are particularly (although not specifically) inactive during loss-of-consciousness. Indeed, positron emission tomography (PET) studies have shown that most anaesthetic substances lead to a general decrease of brain metabolism (ALKIRE ET AL., 1995, 1997) and particularly affect the dorso-lateral prefrontal cortex and the precuneus (KAISTI ET AL., 2002, 2003; LAITIO ET AL., 2007)[11]. Similarly, although the brain metabolism recorded in REM sleep is close to normal wakefulness (BRAUN ET AL., 1997; MAQUET, 1997, 2000; BUCHSBAUM ET AL., 2001), NON-REM sleep particularly reduces the metabolism in prefrontal and parietal cortices (MAQUET ET AL., 1996; BRAUN ET AL., 1997; MAQUET, 1997; MAQUET AND PHILLIPS, 1998). Conversely, fronto-polar activation typically mark lucid dreaming – a state in which subjects claim to be fully conscious but locked in their dream (DRESLER ET AL., 2011). Finally, abnormal prefrontal and parietal activity is also observed in partial complex epilepsy in which patients lose consciousness whereas simple partial seizures are characterized by isolated hyper-activation at the epileptic site that tends not to propagate to the associative cortices or to the rest of the cortex (SALEK-HADDADI ET AL., 2003; BLUMENFELD ET AL., 2004, 2009).

FIGURE 1.9 METABOLISM DEFICITS IN THE DIFFERENT TYPES OF LOSS-OF-CONSCIOUSNESS.

For each physiological (sleep), pharmacological (anaesthesia) and pathological (epilepsy) loss of consciousness, the level of metabolism is plotted as compared to normal (Minuses indicate hypometabolism, pluses indicate hypermetabolism).
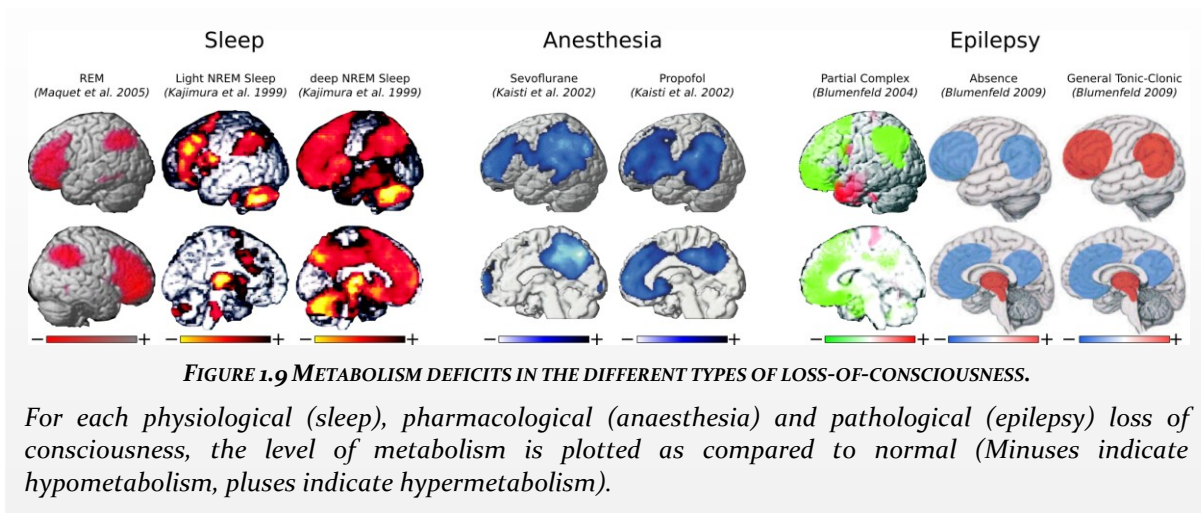
1.4.2.3. A causal role of the prefrontal cortex in conscious perception?

Beyond this correlational evidence, recent studies suggest that the prefrontal cortex is causally involved in conscious perception. Rounis and collaborators have shown that repetitive transcranial magnetic

---

[11] Note, however, that dissociative anaesthetic substances lead to an increased activity in the prefrontal cortex: *e.g.* (LEE ET AL., 2013).

stimulation (rTMS) over the dorso-lateral cortex reduces stimulus visibility without affecting discrimination performance (ROUNIS ET AL., 2010). However, the direct effect was relatively weak, and did not significantly differ from the sham TMS[12]. Furthermore, patients with left prefrontal lesions present an increased visibility threshold[13] to briefly flashed stimuli (DEL CUL ET AL., 2009). Although patients' objective discrimination performance was also affected, the change of visibility reports is significantly stronger than changes in discrimination performance.

Although most studies report a tight link between conscious perception and fronto-parietal activity, a few recent studies have shown that the prefrontal cortex could be activated by unconscious stimuli (HESTER ET AL., 2005; LAU AND PASSINGHAM, 2007; VAN GAAL ET AL., 2008, 2010; URSU ET AL., 2009; VAN GAAL ET AL., 2011). In particular, van Gaal and collaborators implemented a series of experiments demonstrating executive functions could be activated unconsciously (VAN GAAL ET AL., 2008; VAN GAAL ET AL., 2009, 2010; COHEN ET AL., 2009; VAN GAAL AND LAMME, 2011; VAN GAAL ET AL., 2011). Subjects performed a go/no go task in which they were asked to press a key as soon as a central annulus was presented on the screen (go trial). On some trials, a faint disk was briefly flashed just before the target, indicating that subjects should hold themselves from pressing the key (no-go trial). Crucially, the delay separating the disk from the annulus was varied such that long delays allowed subjects to consciously perceive the disk, whereas short delays rendered the disk invisible. Although subjects did press the key when the disk was subliminal, their reaction time significantly increased, suggesting that subliminal information can affect the executive system responsible for the go/no go task. Crucially, source reconstruction of subjects' EEG suggests this unconscious cognitive control was initiated by the prefrontal cortex. A follow-up fMRI experiment confirmed that activity in the pre-supplementary motor area (pre-SMA) was significantly increased by unconscious stimuli (VAN GAAL ET AL., 2010). Nevertheless, the unconscious prefrontal activation remained particularly small and spatially limited – two features which radically contrast with the visible condition: when the target was easily visible, a large activation could be observed over the right dorso-lateral prefrontal cortex, the superior and middle frontal gyri, the infero frontal cortex, the anterior cingulate and the parietal cortex. These experiments therefore suggest that, although some regions of the prefrontal cortex can be activated unconsciously, the large fronto-parietal recruitment remains characteristic of conscious perception.

1.4.2.4.   Involvement of the thalamus in conscious perception

Finally, another important region that differentiates consciousness states is the thalamus. This subcortical structure is known to gate sensory information to the cortex and to participate in regulating arousal (COENEN AND VENDRIK, 1972; STERIADE ET AL., 1993; MCCORMICK, 1997). The thalamus responds to auditory stimuli in non-REM sleep (PORTAS ET AL., 2000), and generally presents a hypometabolism in slow wave sleep (BRAUN ET AL., 1997; MAQUET, 1997, 2000; KAJIMURA ET AL., 1999) and general anaesthesia (FISET ET AL., 1999; KAISTI ET AL., 2002). Furthermore, thalamic activity increases in REM sleep when the dorso-lateral prefrontal cortex and the precuneus are seemingly deactivated (MAQUET ET AL., 1996), suggesting that it may participate in restoring a conscious state even during sleep. Finally, the thalamus is generally hyperactive in generalized and complex partial seizures (SALEK-HADDADI ET AL., 2003; BLUMENFELD ET AL., 2009), suggesting that its malfunctioning leads to an impaired conscious states. However, as fMRI and PET have a relatively low temporal resolution, it is unclear whether abnormal thalamic activity causes, results from,

---

[12] The fraction of visible trials is significantly reduced by the TMS, but this reduction is not significantly larger than the sham condition, thus leaving the possibility of a non-specific effect. The authors proposed using another measure than the fraction of visible trials: the difference between d' (the ability to discriminate the stimulus) and meta-d' (the ability to know that the stimulus was correctly discriminate), and demonstrate that this approach leads to a significant interaction.

[13] An increased visibility threshold indicates that one needs stimuli with a greater contrast or longer presentation time to make the same subjective visibility report.

or only correlates with changes of cortical activity. This issue will be further discussed below in the light of time-resolved studies.

KEY POINTS

- Numerous subcortical and cortical regions can be activated by stimuli without subjects' being able to detect them.
- While sensory cortices can be activated relatively easily unconsciously, higher regions, such as the prefrontal cortex, are more rarely recruited by subliminal stimuli.
- Contrary to invisible stimuli, visible stimuli are marked by a large response in the sensory cortices and the recruitment of higher areas, and the fronto-parietal networks in particular.
- Loss-of-consciousness is associated with a general reduction of brain metabolism which particularly affects the frontal and parietal cortices.
- Lesions studies suggest that prefrontal impairments leads to reduced visibility reports.
- fMRI and PET studies suggest that thalamic activity indexes subjects' consciousness state.

1.4.3. TIMING CONSCIOUS PROCESSES

The differences between conscious and unconscious processes observed with fMRI and PET studies can be further characterized by time-resolved neuroimaging techniques. In particular, EEG, MEG and intracranial recordings tend to show that unconscious perception early-evoked responses are largely preserved but late and sustained brain activity are drastically diminished.

1.4.3.1. Impact of stimulus visibility on early and late brain responses

It is perhaps not surprising that the electrophysiological dynamics of conscious and unconscious processes were already under scrutiny in the 1960s, given that EEG had been invented ninety years earlier (CATON, 1875), and applied to human subjects for thirty years (BERGER, 1929; HAAS, 2003). In 1964/1965, three independent teams simultaneously[14] discovered a link between the late event-related potentials (ERPs) and subjects' ability to report the presence of a stimulus (DAVIS, 1964; HAIDER ET AL., 1964; DESMEDT ET AL., 1965B; SPONG ET AL., 1965). To only illustrate one of them, Desmedt, Debecker and Manil compared the evoked EEG response to a faint tactile stimulus that was either presented alone or was predicted by a preceding sound. When predicted, the stimulus was detected 88% of the time, and elicited both early (< 300 ms) and late ERPs (> 300 ms). By contrast, detection dropped to 50 % in the absence of the auditory cue. While early ERPs in response to the unpredicted stimuli remained identical, late ERPs were completely absent. Unfortunately, to avoid a motor-response artefact, the authors asked their subjects to count the number of detected targets, rather than provide a subjective report at each trial. This late ERP may thus index counting processes rather than conscious perception *per se*. A few years later, Hillyard and collaborators compared the P300 elicited by the same physical stimulus when it was consciously detected or missed (HILLYARD ET AL., 1971). The authors demonstrated that the P300 was only present when subjects were able to report having seen the stimulus. In contrast, early responses, such as the N1 component were present even in missed trials (provided that the stimulus intensity was sufficiently strong). Subsequent investigations suggested that "*N1* [relates to] *the quantity of signal information received and P3* [reflects] *the certainty of the decision based upon that information*" (SQUIRES ET AL., 1973A).

The P300 component was then dissociated into two components. Whereas the P3a is a transient frontal component, probably generated by the frontal cortex, and is elicited by unexpected events (SUTTON

---

[14] Two of these studies were even published in the same issue of Science (DAVIS, 1964; HAIDER ET AL., 1964)!

ET AL., 1965; POLICH, 2007), the P3b, is a sustained components, likely generated by a variety of areas including the frontal and parietal cortices, is characterized by a centro-posterior positivity (HALGREN ET AL., 1998; DEL CUL ET AL., 2007; POLICH, 2007), and is only elicited by visible and relevant stimuli (SQUIRES ET AL., 1973B, 1975A, 1975B, 1976; DEHAENE ET AL., 2006B; POLICH AND CRIADO, 2006; POLICH, 2007; DEHAENE AND CHANGEUX, 2011). A variety of experimental methods have shown that the P300b, or its magnetic equivalent (VAN AALDEREN-SMEETS ET AL., 2006; GUTSCHALK ET AL., 2008) best indexes conscious perception. This includes perceptual threshold (HILLYARD ET AL., 1971; SQUIRES ET AL., 1973A; SEKAR ET AL., 2013), masking (DEL CUL ET AL., 2007; GUTSCHALK ET AL., 2008; LAMY ET AL., 2009; SALTI ET AL., 2012), attentional blink (VOGEL ET AL., 1998; SERGENT ET AL., 2005), form completion (HEALTH ET AL., 1978; STUSS ET AL., 1992; VIGGIANO AND KUTAS, 2000) as well as change blindness experiments (NIEDEGGEN ET AL., 2001; FERNANDEZ-DUQUE ET AL., 2003; WOODMAN AND LUCK, 2003). Together, these experiments converge on the idea that the amplitude of early ERPs do not necessarily correlate with subjective report, whereas the P3b tends to.

This early – late dissociation is also supported by lesions studies. Faces presented to the neglected visual field of neglect patients still elicits an N170 despite being reported as unseen (VUILLEUMIER ET AL., 2001). Similarly, a cortically-blind two-year-old child presented robust visual evoked potentials between 80 and 180 ms (WYGNANSKI-JAFFE ET AL., 2009). Finally, lesions of the dorso-lateral prefrontal cortex diminish the ability to perceive a target. In these patients, the N1 component is relatively preserved, but later components, including the N2 and the P3b, are drastically reduced in amplitude (BARCELÓ ET AL., 2000).
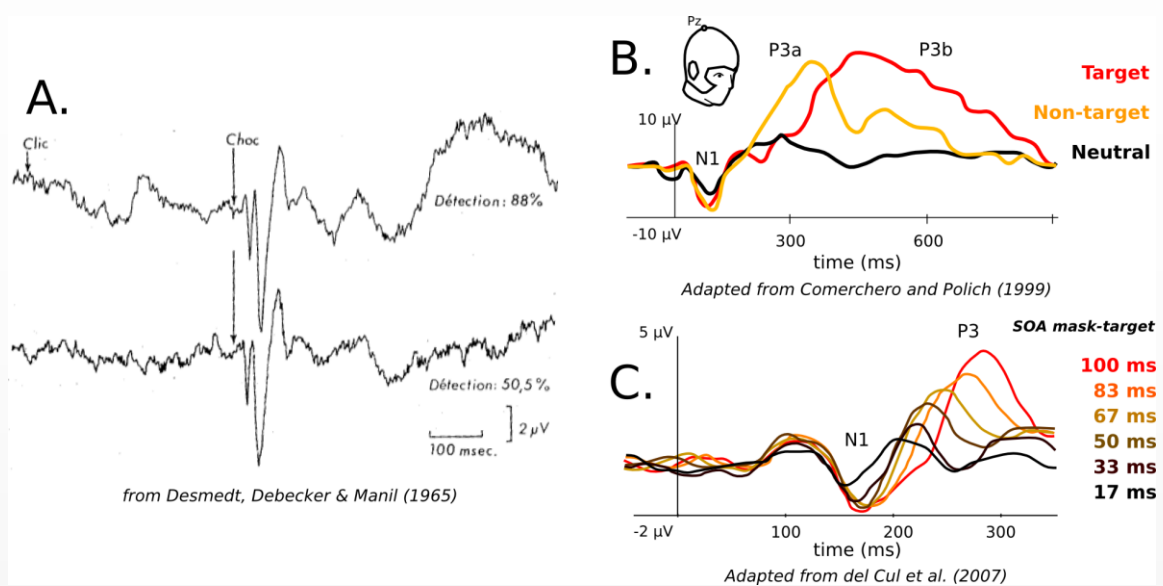
FIGURE 1.10 EARLY VERSUS LATE EVENT RELATED POTENTIAL UNDER DIFFERENT ATTENTION AND VISIBILITY CONDITIONS.

A. *Desmedt, Debecker & Manil asked subjects to detect a brief and faint tactile stimulation (DESMEDT, DEBECKER, & MANIL, 1965). (top). When the target was preceeded by an auditory cue, detection performance was high, and EEG activity revealed both early and late event related potentials (ERP). By contrast, when the same stimulus was presented without any cue, detection performance dropped, and late ERP disappeared.*

B. *(COMERCHERO & POLICH, 1999). The P3 component can be divided into two types of neural events. The P3a refers to a transiant, frontal positivity following the presentation of irrelevant stimuli. By contrast, the P3b component is characterized by a sustained posterior positivity*

C. *Subjects performed a discrimination task on differentially masked stimuli (DEL CUL, BAILLET, DEHAENE, & CUL, 2007). By varying the stimulus onset asynchrony (SOA), visibility of the stimulus could be parametrically varied. EEG results suggests that, unlike other components, the P300 indexes subjects' visibility reports.*

Finally, intracranial recordings also dissociate early and late neural activity (SUPÈR ET AL., 2001; ROELFSEMA ET AL., 2002; DECO ET AL., 2007; JONES, 2007; QUIROGA ET AL., 2008; GAILLARD ET AL., 2009). The strongest intracranial evidence comes from Roelfsema and Lamme. In a series of experiments, they showed that subjective reports systematically correlated with the later[15] part of the neural activity (ROELFSEMA ET AL., 1998, 2004; LAMME AND ROELFSEMA, 2000; LAMME ET AL., 2000). In particular, Supèr, Spekreijse & Lamme trained monkeys to saccade toward a figure presented in their peripheral visual field (SUPÈR ET AL., 2001). Electrical activity showed that figures independently activated the primary visual cortex between ~40 and 100 ms after stimulus onset. However, the subsequent activity was significantly increased when monkeys made a saccade toward the figure as opposed to when they kept fixation. Similarly, Gaillard and collaborators investigated the neural activity of implanted patients in a backward masking task (GAILLARD ET AL., 2009). The results demonstrated that masked and unmasked stimuli elicit similar early brain responses in the occipital, fusiform and frontal cortex. By contrast, later ERPs were markedly different between the two visibility conditions.
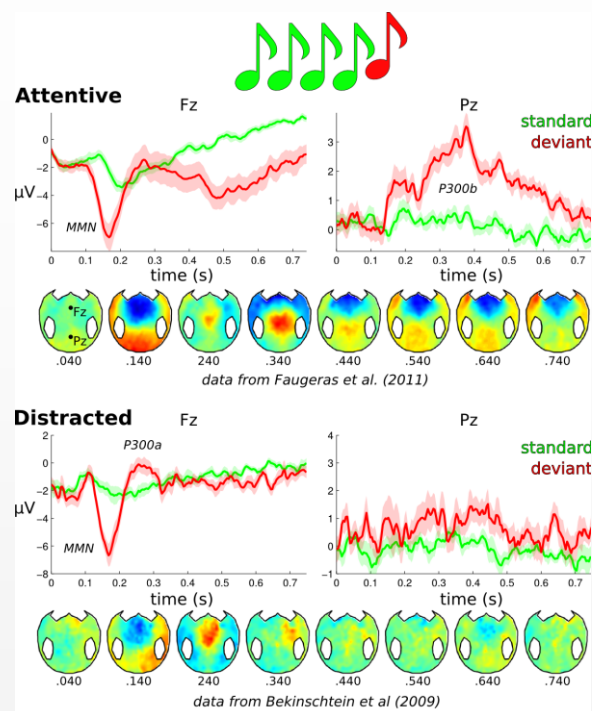
FIGURE 1.11 IMPACT OF ATTENTION ON THE AMPLITUDE OF THE MMN AND THE P300

The auditory oddball paradigm consists in presenting a series of identical sounds (green) intermixed with rare deviant sounds (red). The change of sounds elicits two components. The mismatch negativity (MMN), peaking around 170 ms, is followed by a P300 component. Unlike the P300, the MMN can be observed even when subjects are paying attention away from the auditory stimuli.

1.4.3.2.   Impact of consciousness states on early and late brain responses

The temporal dissociation between conscious and unconscious processing is also supported by loss of consciousness studies. Several experiment used an "oddball" protocol, in which a series of identical auditory stimuli are intermixed with rare deviant tones. These rare events, in normal awake subjects, lead to a negative deflation of the N1, referred to as the mismatch negativity (MMN) component (NÄÄTÄNEN

---

[15] This "later part" remains however relatively early: the activity elicited before 100 ms is identical in visible and invisible conditions, whereas its later part is correlated with subjective reports.

AND PICTON, 1987; NÄÄTÄNEN ET AL., 2007), and are often followed by a P300 component. Following the findings mentioned previously, the MMN is very robust, regardless of attention (ZHAO AND LI, 2006; BEKINSCHTEIN ET AL., 2009; HAROUSH ET AL., 2011), and is seemingly present at perceptual threshold (SAMS ET AL., 1985) although it is unclear whether it can be triggered by a completely subliminal stimulus[16].

Although the amplitude of ERPs tends to dramatically decrease with loss of consciousness (PAAVILAINEN ET AL., 1987; BASTUJI ET AL., 1995; ELTON ET AL., 1997; ATIENZA ET AL., 2001), a significant MMN can be observed under anaesthesia (SIMPSON ET AL., 2002; HEINKE ET AL., 2004; KOELSCH ET AL., 2006; CZISCH ET AL., 2009) as well as in REM sleep (NASHIDA ET AL., 2000; SCULTHORPE ET AL., 2009). Note, however, that these findings have not been systematically replicated (SALLINEN ET AL., 1996), and that the presence of the MMN in non-REM sleep remains still unclear (PAAVILAINEN ET AL., 1987; NIELSEN-BOHLMAN ET AL., 1991; WINTER ET AL., 1995; ATIENZA ET AL., 1997; ELTON ET AL., 1997; VAN HOOFF ET AL., 1997; COTE ET AL., 2000; SCULTHORPE ET AL., 2009) (for review of the MMN under various conscious stages see (ATIENZA ET AL., 2001; NÄÄTÄNEN ET AL., 2007)). In contrast, the vast majority of the above studies indicate that the P3 component largely vanishes with subjects' loss of consciousness.
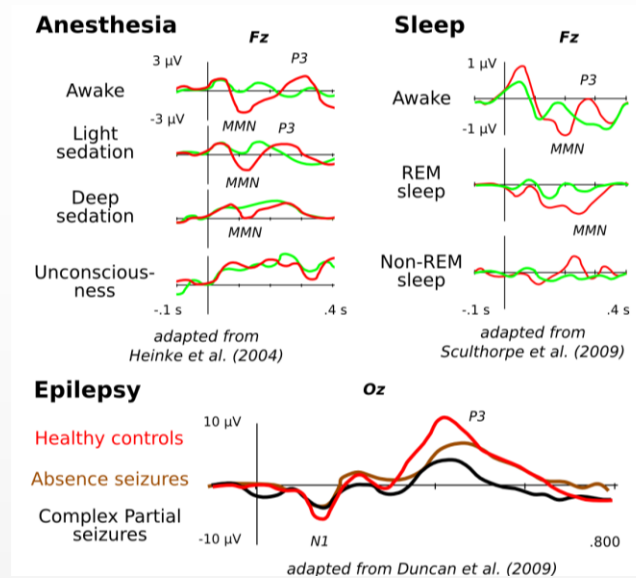
FIGURE 1.12 EFFECTS OF VARIOUS TYPES OF LOSS OF CONSCIOUSNESS ON THE MMN AND THE P3.

(Top) The oddball paradigm has been tested across various states of consciousness. In some studies, the MMN is found in light and deep sedation (HEINKE ET AL., 2004) as well as in REM sleep (SCULTHORPE, OUELLET, & CAMPBELL, 2009), whereas the P300 is only observed under wakefulness and light sedation.

(Bottom) During seizure induced loss-of-consciousness, auditory and visual stimulations elicit preserved early evoked related potentials (N1) but diminished P300 (DUNCAN, MIRSKY, LOVELACE, & THEODORE, 2009).

Finally, a small number of studies suggest a similar pattern of results in absence and complex partial epileptic seizures. Both animal (INOUE ET AL., 1992) and human studies (ORREN, 1978; DUNCAN ET AL., 2009; CHIPAUX ET AL., 2013) suggest that early evoked potentials are preserved, and/or that late components are largely impaired. In a recent study, Chipaux and collaborators presented visual flashes to epileptic children during absence epilepsy (CHIPAUX ET AL., 2013). Although patients were completely unresponsive and

---

[16] *Allen and colleagues* (ALLEN ET AL., 2000) *claimed to a subliminal change in the frequency of a tone could elicit a mismatch negativity, however the component they report does not clearly resemble the traditional MMN. For example the component peaks at 350 ms.*

presented no recollection of the ictal events, significant visual evoked potentials were observed over the occipital electrodes around 250 ms, thus suggesting the existence of residual visual processing in this pathological loss of consciousness. However, the study remains subject to potential caveats. The visual stimulation was indeed rhythmically presented at 2Hz. Yet, absence seizures are typically characterized by a 3-4Hz rhythm (BLUMENFELD, 2005). It is thus possible that evoked potential entrained the thalamic activity, which would consequently lead to a cortical activation in phase with the visual potential. Furthermore, the authors only report the EEG components recorded over the occipital lobe. It thus remains unclear whether the P3 component is affected in this specific case.

1.4.3.3. A complicated link between conscious perception and late event related potentials

Although the precise timing of conscious perception appears to vary as a function of the precise experimental set-up, studies commonly suggest that early neural activity can be triggered unconsciously whereas late neural responses are tightly linked to stimulus reportability. Nonetheless, several studies may complicate this overall picture.
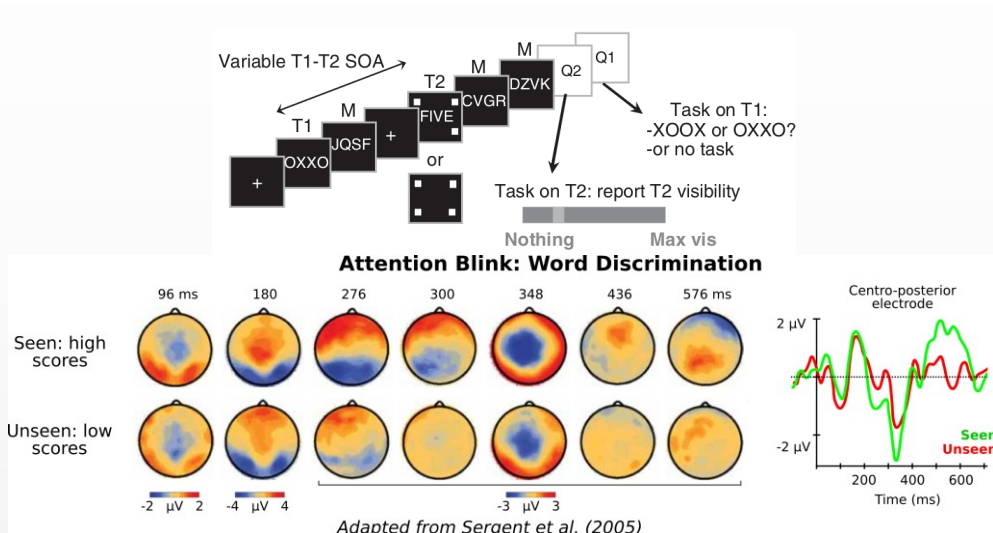
FIGURE 1.13 EVIDENCE OF A LATE ERP ELICITED BY AN UNCONSCIOUS STIMULUS.

Sergent et al. (SERGENT, BAILLET, & DEHAENE, 2005) showed in an attentional blink paradigm, which consists in detecting two successive stimuli, that a strong N400 component could be elicited by the stimuli reported as unseen . Conversely, the following positivity varied as a function of visibility reports.

First, the N400, a centro-posterior negative EEG component that is believed to index semantic processes (KUTAS AND FEDERMEIER, 2011), can be elicited by stimuli rendered invisible in an attentional blink experiment (VOGEL ET AL., 1998; SERGENT ET AL., 2005). Results show that the N400 peaks *after* the P3, and its large intensity appears independent from the visibility of the stimulus. Similar findings have also been established in backward masking experiments (KIEFER AND BRENDEL, 2006; EDDY ET AL., 2007). Furthermore, congruous and incongruous words elicit a significantly different N400 in REM and stage II sleep (BRUALLA ET AL., 1998; PERRIN ET AL., 2002; IBÁÑEZ ET AL., 2006; DALTROZZO ET AL., 2012) as well as in slow wave sleep (BRUALLA ET AL., 1998; LOPEZ ET AL., 2001; IBÁÑEZ ET AL., 2009). To my knowledge, no N400 has ever been observed under general anaesthesia. Overall, these results advocate against a direct link between timing and conscious access: late components may remain unconscious. Furthermore, these findings seem to invalidate the idea that early event related potentials could be consciously perceived but rap-

idly forgotten (*e.g.* (WOLFE, 1999)[17]). Rather, the possibility of a large late unconscious ERP suggests that some *types* of neural activity are consciously accessible and some others remain inaccessible.

Second, although "the most consistent finding in non-REM sleep is the lack of P3" (LAUREYS, 2005A), several studies did find unconscious P3 components. Although reduced, the P3 may be elicited in REM sleep (SALISBURY ET AL., 1992; PERRIN ET AL., 1999). Cote and Campbell even found a strong P3b component in REM sleep. However, it was elicited by a tone presented at 90 dB (the equivalent of a police whistle) (COTE AND CAMPBELL, 1999)! Several studies have found significant P3 elicited by invisible (BERNAT ET AL., 2001A, 2001B; VAN GAAL ET AL., 2011) and unseen stimuli (DEL CUL ET AL., 2007; HENSON ET AL., 2008; LAMY ET AL., 2009). For example, Bernat and colleagues showed that a briefly flashed (1 ms) stimulus elicited a small (2 µV) but significant P3 in spite of subjects' inability to detect the target (BERNAT ET AL., 2001B). Masked stimuli eliciting cognitive control (VAN GAAL ET AL., 2011) or familiarity processes (HENSON ET AL., 2008) induce small but significant late centro-posterior positivity. Furthermore, unseen stimuli that are correctly discriminated present a larger P3 than unseen but incorrectly identified stimuli (LAMY ET AL., 2009). Finally, Del Cul, Baillet and Dehaene showed that masked stimuli elicit a large increase of centro-posterior activity between 200 ms and 600 ms as compared to the conditions with the mask only. The increase of the P300 amplitude may therefore not systematically index conscious perception.
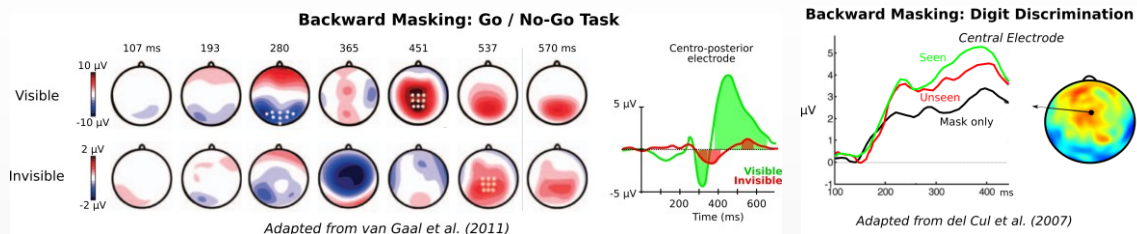
FIGURE 1.14 *EVIDENCE OF UNCONSCIOUS P300.*

(Left) In a backward masking paradigm, van Gaal et al. (VAN GAAL, LAMME, FAHRENFORT, & RIDDERINKHOF, 2011) *showed that a no-go stimulus could elicit a small centro-posterior positive component, traditionally associated with conscious perception. However the amplitude of this component is drastically reduced as compared to the visible condition.*

(Right) Del Cul et al. showed that the unseen masked stimuli elicit a significantly larger P300 than the mask only condition (DEL CUL, BAILLET, DEHAENE, & CUL, 2007)*. The amplitude of the P300 however correlates with subjective visibility reports.*

Finally, the P300 may not systematically be the first EEG component that dissociates subjective visibility reports. For example, Melloni and colleagues have recently shown that the P300 indexes conscious visibility *only when the stimulus is unexpected* (MELLONI ET AL., 2011). By contrast, when subjects know which stimulus is going to be presented, visibility reports best correlated with the P200 component. Likewise, Pitt, Martinez and Hillyard showed that the P300 only indexes visibility reports when it is task-relevant. In this study however, visibility was not probed at each trial but was roughly assessed at the end of the session (PITTS ET AL., 2012). Following the literature on attentional blindness (MACK AND ROCK, 1998), it may thus be the case that they were not as conscious of the stimuli than the experiment suggests. Further investigation would thus be necessary to clarify these issues in determine the condition under which the P300 sensitively and specifically indexes subjective reports of visibility.

---

[17] In a similar view, Crick & Koch noted that "[the stimuli used in subliminal perception studies] may affect ongoing mental processes, including higher order processes, without being registered in working or long-term memory." (CRICK AND KOCH, 1990A)
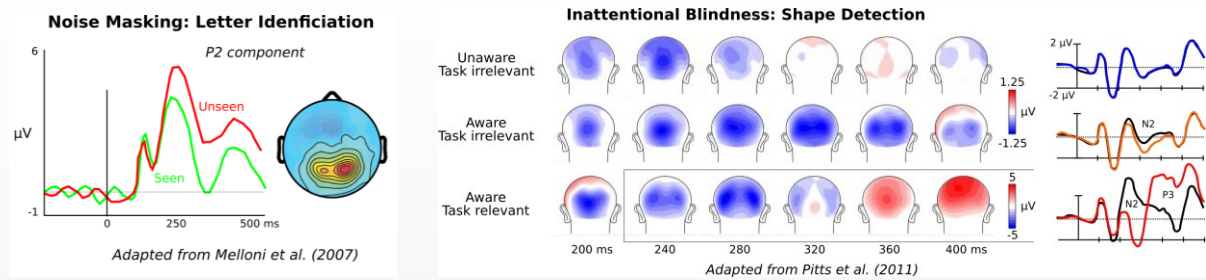
FIGURE 1.15 EXPERIMENTAL CONDITIONS MODULATE THE TIMING OF THE FIRST ERPS INDEXING VISIBILITY REPORTS.

(Left) Melloni et al. showed in a hysteresis paradigm that stimuli whose identity is correctly expected by the subjects, elicit different P200 component as a function of visibility reports (MELLONI, SCHWIEDRZIK, MÜLLER, RODRIGUEZ, & SINGER, 2011).

(Right) Pitts et al. showed that visible stimuli do not elicit the traditional large P300 components when they are task-irrelevant (PITTS, MARTÍNEZ, & HILLYARD, 2012).

Overall, it appears that brain events rising before 200 ms can be easily dissociated from subjects' ability to report their presence. The processes that occur after 200 ms still need to be clarified. While most studies demonstrate that task-relevant stimuli lead to strong and sustained centro-posterior positivity, likely elicited by a distributed network of brain regions, the precise neural bases of consciousness when stimuli are predictable or task irrelevant remain currently unclear (ARU ET AL., 2012B; SERGENT AND NACCACHE, 2012).

KEY POINTS

- Event-related potential (ERP) studies indicate that early brain activity can be elicited under unconscious states and by undetectable stimuli.
- Late ERPs tend to correlate with subjective reports and index a conscious and attentive state.
- The precise timing of the brain activity corresponding to subjective report may vary depending on the precise experimental protocols.

1.4.4. BRAIN RHYTHMS & INFORMATION COMPLEXITY

Event-related potentials (ERP) represent a small category of the human brain electric responses: those whose amplitude is phase-locked to the stimulus. Other forms of responses such as oscillations (BUZSAKI, 2009) and scale-free dynamics (MILLER ET AL., 2009) can be investigated after transforming the amplitude of single trial signals into time-frequency maps. Five broad frequency ranges are generally used to summarize the obtained results, and are denoted by historically- rather than alphabetically- ordered Greek letters (delta: 0-4 Hz, theta: 4-8 Hz, alpha: 8-13 Hz, beta: 13-30 Hz and gamma:>30 Hz).

A change of power of each of these frequencies is often referred to with the terms "synchrony" (for increasing power) and "desynchrony" (for decreasing power), because it is believed to reflect a local (de)synchronization of the neuronal activity. Indeed, a single neuron generates too little changes in the electric and magnetic fields to be recorded with scalp EEG or MEG. Rather, electrophysiological recordings reflect the summation of synchronous firing of millions of neurons that have a similar spatial orientation (HÄMÄLÄINEN ET AL., 1993). Consequently, an increase of power in a particular frequency suggests a local synchronization (and/or increase) of the neuronal activity. However, to avoid confusion, the term "synchrony" will be reserved to signal correlation across distant brain regions which, as detailed below, is assessed by fundamentally different methods. Each of these frequencies has been proposed to

index various brain functions. Although directly linking EEG frequencies and cognitive functions is probably a simplistic approach (BUZSAKI, 2009; TALLON-BAUDRY, 2009), several patterns of results deserve to be reviewed quickly.

1.4.4.1. Studies manipulating the content of conscious perception

• *Reviewing the gamma proposal*
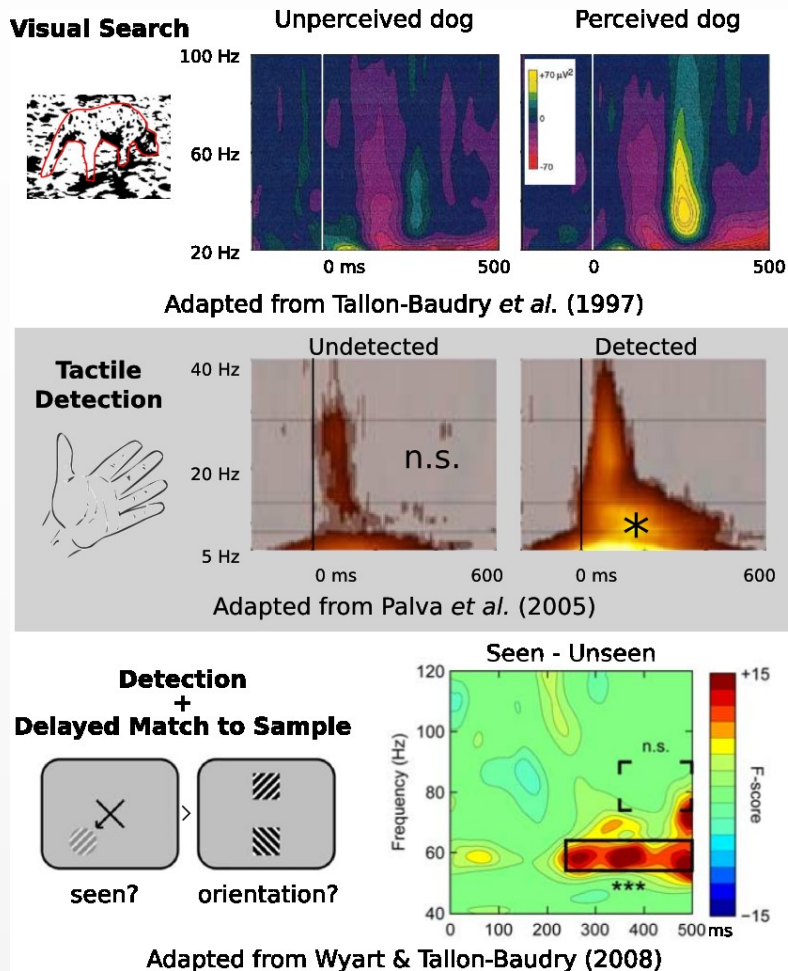
FIGURE 1.16 EEG AND MEG RHYTHM CORRELATING WITH CONSCIOUS PERCEPTION.

(Top) Tallon-Baudry et al. presented subjects to a Dalmatian hidden in a black and white background and compared conditions in which subjects were able to detect the dog, to conditions in which subjects were unaware of the presence of the dog (TALLON-BAUDRY, BERTRAND, DELPUECH, & PERNIER, 1997). EEG recordings revealed that the perceived conditions was associated with a strong increase in the gamma range, around 280 ms after the onset of the stimulus.

(Middle) A tactile stimulus presented at perceptual threshold elicits a stronger increase in alpha and beta power when it is detected than when it is not (PALVA, LINKENKAER-HANSEN, NÄÄTÄNEN, & PALVA, 2005).

(Bottom) Wyart and Tallon-Baudry asked subjects to determine the orientation of a poorly contrasted grating as well as whether they saw it or not (WYART & TALLON-BAUDRY, 2009). A preceding cue indicating most the targets' location was used to manipulate subjects' spatial attention. Contrasting seen versus unseen targets revealed a significant increase of power around 60 Hz, approximately 220 ms after the stimulus onset.

Conscious perception has repeatedly been associated with an increase of power in the gamma range (> 30 Hz). This change is generally observed at the time of the P3 following the recognition (TALLON-BAUDRY ET AL., 1997; RODRIGUEZ ET AL., 1999) and detection of a masked (SUMMERFIELD ET AL., 2002; ARU AND BACHMANN, 2009A; GAILLARD ET AL., 2009; LUO ET AL., 2009), attended (BATTERINK AND NEVILLE, 2013) or faint stimulus (WYART AND TALLON-BAUDRY, 2008) – although earlier changes of gamma power have also be observed at earlier time window (FISCH ET AL., 2009). Furthermore, the gamma power recorded from EEG in blindsight patients distinguished the activity elicited by a stimulus presented in the healthy visual field as compared to the impaired one (SCHURGER ET AL., 2006). Similarly, intracranial recordings demonstrated that gamma power (together with firing rate) recorded in area V4 – but not V1 and V2 – strongly correlated with rhesus macaques' visibility responses in a perceptual suppression experiment (WILKE ET AL., 2006).

However, several findings suggest that the gamma band may not be specific to conscious perception. First, Wyart and Tallon-Baudry recently showed that seen and unseen targets are marked by differences in the gamma band ~250 ms *before* the onset of the stimulus (WYART AND TALLON-BAUDRY, 2009). A similar, although much noisier, finding was simultaneously reported by an independent team (ARU AND BACHMANN, 2009B). Second, small but significant transient gamma responses can be elicited unconsciously (PALVA ET AL., 2005; FISCH ET AL., 2009; GAILLARD ET AL., 2009; LUO ET AL., 2009), including in anaesthetized subjects (GRAY ET AL., 1989; SUPP ET AL., 2011). For example, Supp *et al.* have recently demonstrated that tactile stimuli induced a transient gamma response over the sensori-motor cortex independently of the level of anaesthesia (SUPP ET AL., 2011). By contrast the stimulus-induced theta rhythm (4-8 Hz) disappeared as soon as subjects became unresponsive and seemingly unconscious.
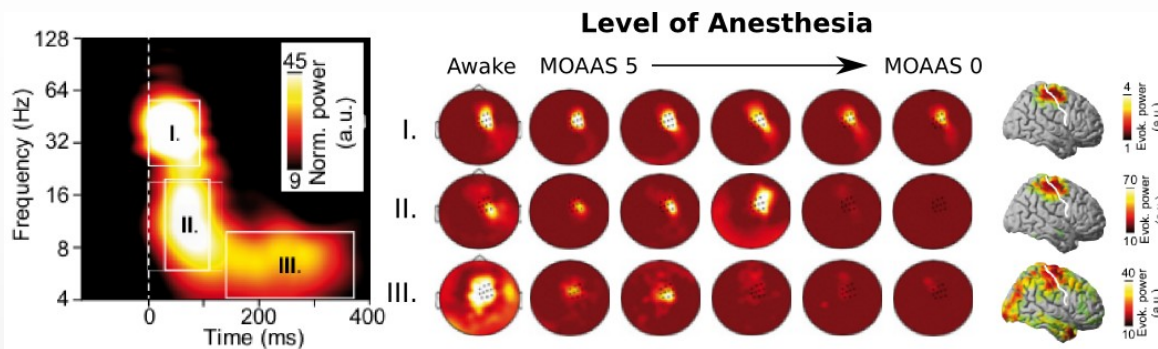
Adapted from Supp *et al.* (2011)

FIGURE 1.17 CHANGES OF TACTILE-INDUCED OSCILLATIONS AS A FUNCTION OF AESTHETIC CONCENTRATION.

Supp et al. *(2011) showed in a tactile stimulation paradigm, that high frequency power is relatively preserved across all levels of anaesthesia, whereas the power in lower frequency ranges, and in the theta band in particular, strongly correlates with subjects' state of consciousness (SUPP ET AL., 2011).*

As it is well known that attention increases gamma power (ENGEL ET AL., 2001; FRIES ET AL., 2008) (FRIES ET AL., 1997, 2001, 2008; SIEGEL ET AL., 2008; WYART AND TALLON-BAUDRY, 2008) – although in potentially distinct specific frequency range (WYART AND TALLON-BAUDRY, 2008) – it may be the case that the increase of gamma power reflects a facilitation of bottom-up processing, which itself may facilitate - but not necessary index - conscious perception. This possibility is particularly strengthened by two recent experiments. Aru *et al.* parametrically varied the visibility of a complex image by either changing the strength of the sensory input, or changing subjects' expectation about the stimulus – two psychophysical factors known to favor visibility (ARU ET AL., 2012A). The intracranial recording revealed that gamma power solely indexed stimulus strength but did not differ as a function of subjective visibility reports. Additionally, Batterink *et al.* investigated the effect of attentional blink on gamma power (BATTERINK ET AL., 2012).

The attentional blink experiment consists in asking subjects to detect two subsequent targets T1 and T2. When the lag between T1 and T2 is short, T2 is generally not consciously perceived, as subjects attention is driven away from it (RAYMOND ET AL., 1997). Batterink *et al.* showed that, at a short lag, T2 elicited higher gamma power when correctly than when incorrectly identified, whereas the P300 did not distinguish these two conditions (BATTERINK ET AL., 2012). By contrast, this pattern of results was completely reversed at long lag: correctly and incorrectly discriminated trials differed in the amplitude of the P3 but not in the power of gamma rhythms. Unfortunately, visibility was not assessed at each trial. It thus remains to be confirmed that subjective visibility reports are best indexed by the P300 than by gamma power.
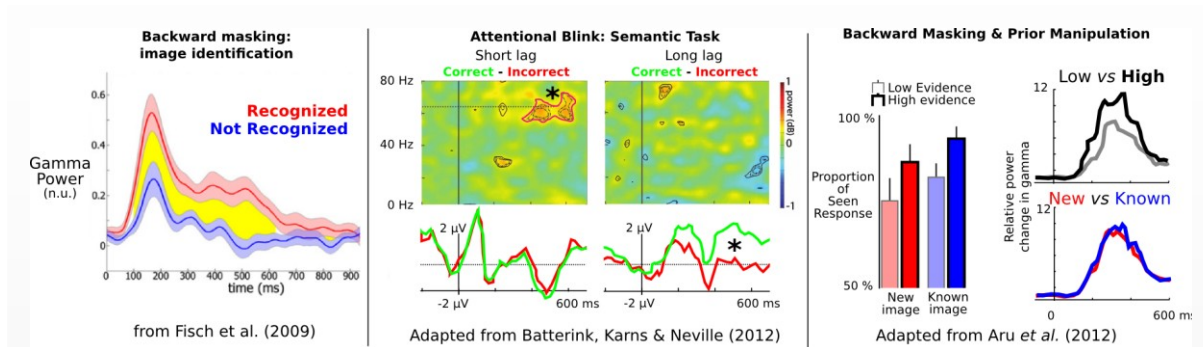
FIGURE 1.18 GAMMA POWER CAN BE ELICITED INDEPENDENTLY OF SUBJECTIVE REPORTS

(Left) Fisch et al. *showed with intracranial recordings that gamma power could be elicited by masked stimuli even when subjects failed to recognized them (FISCH ET AL., 2009).*

(Middle) Batterink et al. *showed in an attentional blink paradigm that gamma power dissociate correct from incorrect trials only at short lag (generally corresponding to an invisible condition), whereas the P300 well distinguished correct and incorrect trials at long lag (generally corresponding to a visible condition) (BATTERINK, KARNS, & NEVILLE, 2012).*

(Right) Aru et al. *showed in a noise masking experiment that changing subject's prior knowledge affect visibility threshold, but does not affect gamma power recorded with intracranial electrodes. By contrast, gamma power was only affected by the strength of the stimulus evidence (ARU ET AL., 2012).*

- • *The paradoxical effects of alpha*

The power changes in the gamma band are generally opposite to the ones observed in the alpha band. This 10 Hz oscillation has long-lastingly been observed to anti-correlate with subjects' visual attention towards a relevant stimulus. Particularly present when eyes are closed (ADRIAN AND MATTHEWS, 1934), the increase of alpha power typically marks a disengagement of attention from visual inputs (KLIMESCH ET AL., 2007). Conversely, attention towards a stimulus tend to induce a strong and lasting decrease of the alpha power over the occipito-parietal electrodes (YAMAGISHI ET AL., 2003; PALVA ET AL., 2005; WILKE ET AL., 2006; JOKISCH AND JENSEN, 2007; RIHS ET AL., 2009; WYART AND TALLON-BAUDRY, 2009). MEG source reconstruction (SIEGEL ET AL., 2008) and intracranial recordings (BOLLIMUNTA ET AL., 2008) suggest that the alpha rhythm is generated by a thalamo-cortical loop involving the layers 5-6 of the occipital cortex. Moreover, changes in alpha power succeeds rather than precedes spiking and gamma activity (WILKE ET AL., 2006). The alpha rhythm is thus often associated with a top-down mechanisms that allows regulating bottom-up information processing (KLIMESCH ET AL., 2007; SADAGHIANI ET AL., 2010; JENSEN ET AL., 2012). In this view, the alpha rhythm would disrupt irrelevant/unattended information in order to facilitate the detection of relevant/attended information. Accordingly, this mechanism would lead to the paradoxical idea that alpha waves are necessary to conscious perception (in order to specifically select relevant information) but are anti-correlated with it (the more alpha, the more visual information is discarded). This modulatory hy-

pothesis[18] fits with recent studies: not less than five independent teams almost simultaneously showed that the phase and the power of alpha waves predict whether or not subjects will detect a subsequent stimulus presented at perceptual threshold conditions (HANSLMAYR ET AL., 2007; VAN DIJK ET AL., 2008; BUSCH ET AL., 2009; MATHEWSON ET AL., 2009; WYART ET AL., 2012), as well as when generated by a TMS pulse (ROMEI ET AL., 2008A, 2008B).

1.4.4.2. Studies comparing brain activity under different states of consciousness

The above studies essentially focused on the way stimulus processing modulates EEG rhythms and *vice versa*. Nonetheless, the resting EEG rhythms are also indicative of subjects' state of consciousness. In particular, the various types of loss of consciousness are associated with power changes in all frequency bands, and predominantly in low frequency rhythms. Indeed, general anaesthesia (KISHIMOTO ET AL., 1995; MAKSIMOW ET AL., 2006; LEWIS ET AL., 2012), non-REM sleep (DANG-VU ET AL., 2005; MURPHY ET AL., 2009) as well as absence (HOLMES ET AL., 2004; CHIPAUX ET AL., 2013) and complex partial epileptic seizures (LEMIEUX AND BLUME, 1986; BLUME AND LEMIEUX, 1988; BLUMENFELD, 2005) are generally marked by a loss of the alpha oscillation and by large delta (<4Hz) waves, predominantly observed over anterior electrodes[19]. Interestingly, recent neuroimaging and computer simulations suggest that delta oscillations are mainly generated in the frontal lobe, and subsequently propagate to the rest of the cortex, causing cortical malfunctioning (AMZICA AND STERIADE, 1998; DANG-VU ET AL., 2005; MURPHY ET AL., 2009). In particular, the prefrontal hypometabolism is directly correlated with the delta waves amplitude (DANG-VU ET AL., 2005), which suggests a direct bridge between the PET, fMRI and time-resolved neuroimaging results.
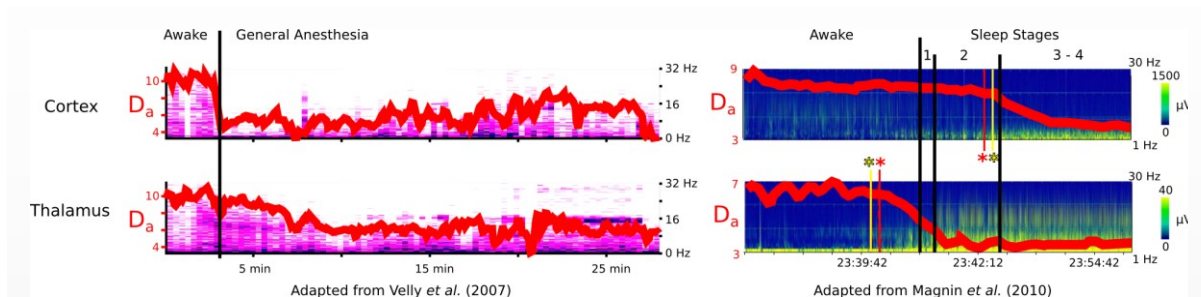
FIGURE 1.19 DISSOCIATION OF CORTICAL AND THALAMIC ACTIVITY IN THE TRANSITION TO A LOSS OF CONSCIOUSNESS.

(Left) Using spectral and complexity measures, Velly et al. showed that the dimension of activation (Da) of cortical activity successfully indexes subjects' rapid loss of consciousness (VELLY ET AL., 2007). By contrast, the Da of thalamic and/or para-thalamic activity progressively decreases to reach a plateau approximately 10 min after subjects' loss of consciousness.

(Right) Magnin et al. found a similar dissociation in sleep (MAGNIN ET AL., 2010): thalamic activity starts decreasing before sleep onset and progressively diminishes until sleep stage II. By contrast, cortical activity is characterized by a high Da during wake and until sleep stage II. Cortical Da drops during deep sleep.

Recently, the theories of information and dynamical systems have also been used to shed a different light on EEG activity (DIMITROV ET AL., 2011). These frameworks provided a series of novel methods such as permutation entropy (BANDT AND POMPE, 2002), dimension of activation (GUILLEMANT ET AL., 2004),

---

[18] The hypothesis is sometimes referred to as "phasic alertness" to dissociate it from arousal (wake versus sleep) and selective attention (STURM AND WILLMES, 2001; SADAGHIANI ET AL., 2010)

[19] As for the PET studies, some dissociative anaesthetic such as ketamine are not accompanied by an increase in delta power, however the state of consciousness in such cases is less clear as subjects tend to report dream-like experiences. See (BONHOMME ET AL., 2011) for a recent review.

algorithmic complexity, and spectral entropy. In theory, these measures characterize signal properties that are not necessarily unveiled by traditional spectral frequency decomposition (STAM, 2005). In practice, these measures show that the complexity of EEG signals is directly correlated with the state of consciousness. For instance, permutation entropy, which quantifies the regularity of the EEG signals, after decomposing them into a set of discrete temporal pattern, dramatically drops during general anaesthesia (JORDAN ET AL., 2008; LI ET AL., 2008). Similarly, dimension of activation, which consists in embedding the EEG signal into a high dimensional space in order to identify its attractors, drops when subjects fall asleep (REY ET AL., 2007; MAGNIN ET AL., 2010) or enter a general anesthetized state (VELLY ET AL., 2007).

Interestingly, these tools showed that the rhythms of the cortex and of the thalamus are dissociable. In REM sleep, the thalamus is characterized by important delta waves while the rest of the cortex shows a quasi normal spectrum (MAGNIN ET AL., 2004), suggesting that the cortex may then be functioning but disconnected from external inputs. In the wake-sleep transition, the thalamus shifts towards low frequency rhythms before the cortex does (MAGNIN ET AL., 2010). Finally, spectral edge, median power and dimension of activation in the scalp EEG are closely related to the state of consciousness of anaesthetized subjects, whereas thalamic / para-thalamic areas present little changes across consciousness states (VELLY ET AL., 2007). Taken together, these results suggest that the thalamus may not directly host or coordinate conscious information processing. Rather, and following neuromimetic modelling (DESTEXHE, 2000), its deactivation may result from a decrease of cortico-thalamic feedback (ALKIRE, 2009).

KEY POINTS

- Gamma power is likely to reflect increased processing, but may not necessarily index perceptual reports.
- Alpha power is likely to often reflect a filtering mechanism: its presence would thus index a functioning attentional mechanism.
- Increased low frequency power, and loss of the alpha oscillation traditionally mark loss of consciousness
- Novel information-theoretic tools can be used to characterize the dynamical patterns of electrophysiological signals, and show that conscious states are correlated with the complexity of cortical but not thalamic activity.

1.4.5.   FUNCTIONAL CONNECTIVITY

FIGURE 1.20 STIMULUS INDUCED FUNCTIONAL CONNECTIVITY INDEX VISIBLE AND TASK-RELEVANT STIMULI.

Maintaining (left), selecting (middle) and detecting (right) a visual stimulus is associated with a significant increase of the phase correlation in the beta range across various cortical sites.
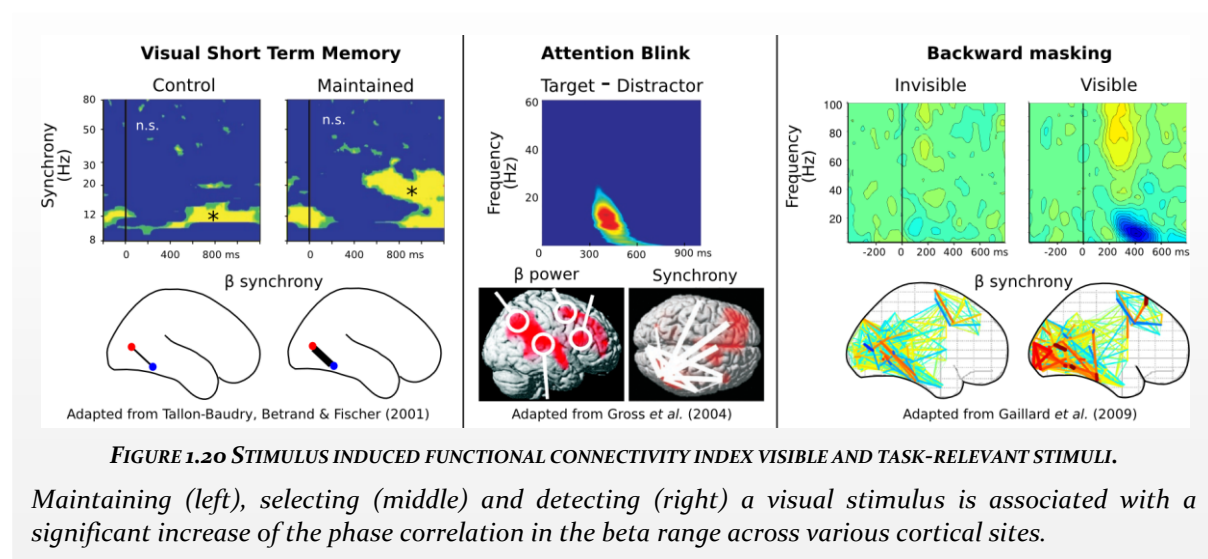
It is important to note that the dynamics of the electrophysiological signals recorded from scalp EEG and MEG present an indirect method to probe the functional architecture of the human brain. Indeed, none of the complex EEG patterns and oscillations would be observed at the scalp level if neurons were disconnected from one another, as the microscopic electric and magnetic fields generated by each neuron generates would not sum up to global coherent patterns. Rather, and as mentioned earlier, different rhythms are thought to reflect thalamo-cortical horizontal or top-down cortical connections. It should be stressed however that these rhythms do not just reflect the brain anatomical structures. As mentioned above, brain rhythms can be modulated within a few milliseconds, and thus suggest an underlying functional and dynamical architecture. A number of studies have thus directly attempted to quantify these functional connections, by systematically quantifying the amount of correlated signals observed across different brain regions.

1.4.5.1. Functional connectivity induced by conscious and unconscious stimuli

As fMRI studies have shown that conscious perception is associated with stronger and more widespread activity over the cortex, it is perhaps not surprising that visible stimuli elicit significantly higher functional connectivity than invisible targets (VUILLEUMIER ET AL., 2001; HAYNES ET AL., 2005B). Nonetheless, EEG, MEG and intracranial recordings have recently clarified this overall picture and demonstrated that long-distance functional connectivity was observed in specific frequency ranges. In particular, seen stimuli generally induce higher long distance functional connectivity in the beta band (TALLON-BAUDRY ET AL., 2001; GROSS ET AL., 2004; GAILLARD ET AL., 2009). Similarly, several backward masking studies have reported significantly higher long-distance gamma synchrony in seen than unseen conditions (MELLONI ET AL., 2007; GAILLARD ET AL., 2009). It may also be noted that synchrony in the gamma range is particularly affected by subjects' spatial attention (SIEGEL ET AL., 2008; GREGORIOU ET AL., 2009A, 2009B). By definition, these correlations do not distinguish bottom-up from top-down information flow. This specific issue can be investigated by "causality" analyses, such as Granger causality and transfer entropy. These methods consist in estimating whether a given temporal signal is useful to predict the future of a distinct signal. Despite its name, causality analyses remains purely observational, and therefore correlational. Granger analyses suggest that the increase in beta synchrony reflect an increase of both bottom-up and top-down information flow (GAILLARD ET AL., 2009; GREGORIOU ET AL., 2009A). Furthermore, TMS experiments, in which information processing is believed to be specifically and temporally disrupted, suggest that feedback information is crucial to conscious perception (PASCUAL-LEONE AND WALSH, 2001; RO ET AL., 2003; BOYER ET AL., 2005; SILVANTO ET AL., 2005; LAMME, 2006A). For example, Pascual-Leone & Walsh have shown that visual phosphenes[20] are elicited when supra-threshold stimulation over MT/V5 is followed 30 ms later by a sub-threshold stimulation over V1. By contrast, when V1 is stimulated before V5, subjects do not report seeing phosphene. This experiment has been proposed to reflect an asymmetrical effect of bottom-up and top-down processing on conscious perception: bottom-up information (V1 -> V5) would be less likely to be associated with conscious perception than top-down information (V5 -> V1).

The above studies specifically investigated the functional connectivity induced by sensory stimulation. However, the human brain presents interesting functional connectivity patterns in passive conditions too. In particular Raichle *et al.* (RAICHLE ET AL., 2001) showed that a number of brain areas, including the precuneus, medial prefrontal cortex, and bilateral temporo-parietal junctions, were paradoxically more active at rest than during demanding cognitive tasks. The discovery of this so-called default mode network (DMN), has opened a vast field of research on resting-state functional connectivity (see reviews in (BUCKNER ET AL., 2008; NORTHOFF, 2012)), which suggests that brain areas continue to share information even when subjects are passive. Furthermore, several networks identified in resting state conditions in-

---

[20] Phosphenes are brief and faint visual perceptions elicited by TMS pulses over the visual cortex.

clude a prefrontal components (DEHAENE AND CHANGEUX, 2011), suggesting that this area shares information with many different circuits. However, the precise link between such resting state networks and conscious processing remains debated. On the one hand, the coupling strength of these networks correlates with consciousness state (BOLY ET AL., 2009).On the other hand, these networks can be found in sleeping (HE ET AL., 2008) and anaesthetized subjects (VINCENT ET AL., 2007; GREICIUS ET AL., 2008). Furthermore, some of these networks, such as the DMN, can be *suppressed* during the presentation of a consciously perceptible target (FOX ET AL., 2006), and this suppression disappears during anaesthesia (HE AND RAICHLE, 2009). On the contrary, the DMN is particularly active during mind-wandering and auto-biographical tasks (BINDER ET AL., 1999; MASON ET AL., 2007) (although see (GILBERT ET AL., 2007)). For example, Christoff et al.(CHRISTOFF ET AL., 2009) asked subjects to perform a particularly easy task. On some trials, subjects were asked to report whether they were focusing on the task, or mind-wandering. The results show that the mind-wandering trials were associated with a stronger DMN activation prior to probe. Overall, while the preservation of the resting-state networks is indicative of subjects' state of consciousness, each of these neural circuits might be recruited by different types of conscious processing such as attention to external stimuli or internal processing (BOLY ET AL., 2007; BUCKNER ET AL., 2008; DEHAENE AND CHANGEUX, 2011).

1.4.5.2. Differences in functional connectivity across consciousness states

Although the above studies demonstrate a tight link between functional connectivity and conscious perception, the empirical evidence obtained in altered states of vigilance suggests a more complicated picture. On the one hand, and as mentioned above, loss of consciousness (partially) preserves the neural activity in primary cortical areas but strongly limits their ability to relay sensory information to higher order regions (*e.g.* (MOELLER ET AL., 2009; MARTUZZI ET AL., 2010; BONHOMME ET AL., 2011; LIU ET AL., 2012)). Furthermore, the spatio-temporal organization of the functional networks recorded at rest is dramatically disrupted when vigilance drops. In particular, the default-mode-network is particularly disturbed in non-REM sleep and anaesthesia (*e.g.* (SCHROUFF ET AL., 2011; SCHRÖTER ET AL., 2012), see (GULDENMUND ET AL., 2012) for recent review). On the other hand, the presence of large slow waves in deep sleep and general anaesthesia (CIMENSER ET AL., 2011; FRANKS AND ZECHARIA, 2011) as well as complex epileptic seizures ((GUYE ET AL., 2006; ARTHUIS ET AL., 2009), although see (AMOR ET AL., 2009) for a more precise description of the change in synchrony during epileptic seizures), seemingly suggest that the whole brain is in fact "hypersynchronous" and therefore highly connected (TONONI AND EDELMAN, 1998). A recent intracranial study may however jeopardize this classic idea. Lewis et al. indeed showed that slow oscillations induced by propofol anaesthesia occur asynchronously over the cortex (LEWIS ET AL., 2012). The authors provide evidence that neurons fire in phase with the trough of the local delta wave. Because delta waves are asynchronous over the cortex, neurons would generally be at a suppressed phase when they receive distant cortical inputs. It remains unclear, however, how such asynchronous delta waves recorded over the cortex, eventually lead to such a strong coherent delta activity at the scalp level.

In any case, an increase of functional connectivity does not necessarily indicate an increase of transmitted information across the cortex. As forcefully argued by Tononi and collaborators (EDELMAN AND TONONI, 2000; TONONI, 2004; LAUREYS AND TONONI, 2008; TONONI AND KOCH, 2008), although functional connectivity may increase in deep sleep and under anaesthesia, the overall amount of information the brain carries is most likely diminished. To take an exaggerated example, if each neuron is connected to all other neurons, the hypothetical brain could only store 1 bit of information: either all neurons are active, or none are. This high-connectivity/low-information hypothesis fits with the evidence reviewed above: information-theoretic analyses of the EEG signals show that unconscious states are typically characterized by lower entropy (ANDERSON AND JAKOBSSON, 2004; KUMAR ET AL., 2007; LI ET AL., 2008; SHALBAF ET AL., 2013) and a lower dimension of activation (GUILLEMANT ET AL., 2004; GIFANI ET AL., 2007; REY ET AL., 2007; LEE ET AL., 2009) which both suggests that the unconscious brain's capacity to store information is low.

The link between information sharing and consciousness states has been particularly strengthened by a series of combined EEG/TMS experiments conducted by Massimini and collaborators (MASSIMINI ET AL., 2005, 2010, 2012; FERRARELLI ET AL., 2010; ROSANOVA ET AL., 2012; CASALI ET AL., 2013). The authors show that TMS pulses elicit a less complex neuronal activity in non-REM sleep (MASSIMINI ET AL., 2005) and anaesthesia (FERRARELLI ET AL., 2010) than in normal wakefulness (CASALI ET AL., 2013). In particular, during wakefulness, TMS pulses elicit activity in a series of different brain regions which differ depending on the stimulation site. In contrast, stimulations during non-REM sleep and anaesthesia only activate areas in the vicinity of the TMS.

FIGURE 1.21 FUNCTIONAL CONNECTIVITY ELICITED BY TMS PULSES INDEX STATES OF CONSCIOUSNESS.

Massimini and colleagues (MASSIMINI ET AL., 2005, 2010, N.D.; FERRARELLI ET AL., 2010; ROSANOVA ET AL., 2012; CASALI ET AL., 2013) showed that the pattern of brain activity elicited by a TMS pulse has qualitatively different dynamics depending on subjects' state of consciousness. When subjects are unconscious, the TMS pulse elicits a simple activation of the area(s) underneath the TMS, and potentially spreads over across the cortex homogeneously (top left). By contrast, when subjects are conscious, the TMS pulse elicits a neural response whose main locus varies across time (bottom left). (Right) Analyzing the complexity of these patterns using a novel index (Pertubational Complexity Index) proved to sensitivity and specifically index the state of consciousness in a variety of physiological and clinical conditions (CASALI ET AL., 2013). This last study is further commented in COMMENT 2.

KEY POINTS

- Stimulus-induced increase of functional connectivity correlates with subjective reports.
- The integrity of intrinsic (resting state) functional networks is strongly correlated with states of consciousness.
- It remains unclear whether the states dominated by low frequency rhythm reflect a hypersynchronous or asynchronous functional connectivity pattern. In any case, the amount of shared information across cortical areas is likely to be correlated with the state of consciousness.

1.5. TOWARD FINDING THE SIGNATURES OF CONSCIOUSNESS IN NON-COMMUNICATING PATIENTS

1.5.1. INTERIM SUMMARY

In spite of the diversity of the above experimental methods, neuroimaging studies of consciousness converge on a number of empirical findings and thus allow for testing of the previously reviewed theoretical proposals. First, many different cortical regions, including the ventral temporal cortex (KOUIDER AND DEHAENE, 2007) and the frontal lobe (VAN GAAL AND LAMME, 2011), can be activated by invisible and unseen stimuli. This finding thus strongly challenges the view that recruiting any (ZEKI, 2003) or some cortical regions (GOODALE AND MILNER, 1992, 2005) suffices to perceive a stimulus consciously. Second, the fronto-parietal network is frequently observed as a key player of conscious perception: i) subjective visibility reports are often marked by a late and large increase of neural activity in these areas ("ignition", (DEHAENE AND CHANGEUX, 2011)) and ii) the malfunctioning of these brain regions generally marks a loss of consciousness (LAUREYS, 2005B). Third, the presence of local or distant 40 Hz synchrony in both subliminal and loss of consciousness conditions, makes it unlikely that this frequency range plays a major and specific role in conscious perception (CRICK AND KOCH, 1990A). Finally, the dissociation between consciousness state and thalamic activity weakens the idea that this subcortical structure is a receptacle or a crucial coordinator of conscious processing (CRICK AND KOCH, 1990A; TONONI ET AL., 1994).

By elimination, it may be thus tempting to conclude that conscious perception is directly supported by the prefrontal cortex (DEHAENE ET AL., 2006B; LAU, 2008) and/or the exchange of information across neural assemblies (LAMME, 2006B; DEHAENE AND CHANGEUX, 2011). However, the precise spatio-temporal features of conscious processing remain insufficiently clear to unequivocally support a single theory of consciousness. Depending on the experimental method, and particularly on the way conscious perception is experimentally defined and assessed, the first electrophysiological activity that correlates with subjective reports can be relatively early (~150 ms) (SUPÈR ET AL., 2001; PINS, 2003; KOIVISTO ET AL., 2006; LAMME, 2006A; BOEHLER ET AL., 2008; MELLONI ET AL., 2011) or late (~300 ms) (DESMEDT ET AL., 1965A; SERGENT ET AL., 2005; DEL CUL ET AL., 2007; GAILLARD ET AL., 2009; MELLONI ET AL., 2011; NEUROSCIENCE ET AL., 2012). Similarly, it is insufficiently clear whether conscious perception is specifically supported by local recurrent processing (LAMME AND ROELFSEMA, 2000; PASCUAL-LEONE AND WALSH, 2001; SILVANTO ET AL., 2005; SCHOLTE ET AL., 2006; FISCH ET AL., 2009), long distance information sharing (BECK ET AL., 2001; MELLONI ET AL., 2007; GAILLARD ET AL., 2009; SCHRÖTER ET AL., 2012), frontal cortices (DEHAENE ET AL., 2006B; LAU, 2008; DEHAENE AND CHANGEUX, 2011), or a combination of these neural substrates.

One of the critical tests for these neural theories of consciousness relates to their ability to provide accurate and useful predictions in the clinic. In particular, these theories should be able to discriminate conscious and unconscious patients independently of their behaviour. As mentioned earlier, the comparison between vegetative and minimally conscious state patients offers a particularly interesting contrast, as it separates the brain activity of minimally different types of patients who nevertheless present supposedly different state of consciousness. The logic is simple: if one of the putative neural signatures of consciousness discriminates vegetative from minimally conscious state patients, it may reflect a neural mechanism relevant to conscious perception.

1.5.2. BRAIN ACTIVITY IN THE VEGETATIVE STATE

The number of neuroimaging studies of vegetative and minimally conscious state patients is rapidly increasing (for extensive reviews see (LAUREYS ET AL., 2004; LAUREYS, 2005B; OWEN ET AL., 2009B;

LAUREYS AND SCHIFF, 2011)). I will now briefly review the main findings that have been observed over the past two decades.

1.5.2.1.   A lowered metabolism in the prefrontal cortex, the precuneus and the thalamus

The brain metabolism of vegetative state patients is extraordinarily reduced and can reach half of its normal level (LAUREYS ET AL., 2004). Although this reduction affects the entire thalamo-cortical system (LEVY ET AL., 1987; DEVOLDER ET AL., 1990; TOMMASINO ET AL., 1995; RUDOLF ET AL., 2000), the anterio-cingulate, the medial and lateral prefrontal cortex, as well as the precuneus (posterior cingulate) are particularly impaired (LAUREYS ET AL., 1999B; BEUTHIEN-BAUMANN ET AL., 2003; BRUNO ET AL., 2010). It is generally argued that this general hypometabolism is caused by an important neuronal degeneration (OWEN ET AL., 2009A)).
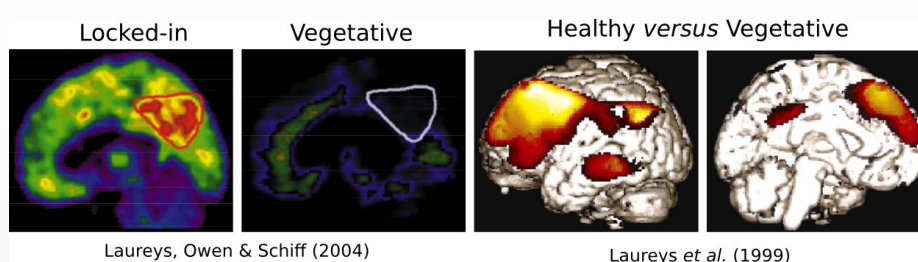
FIGURE 1.22 BRAIN METABOLISM IN CONSCIOUS AND VEGETATIVE SUBJECTS.

Studies quantifying brain metabolism with Positron Emission Tomography (PET) show that vegetative state (VS) patients present an overall decrease of activity both in cortical and in subcortical structures. However, following the patterns observed in physiological, pharmacological and clinical loss of consciousness (FIGURE 1.9), the dorsolateral prefrontal cortex, the medial prefrontal cortex as well as the precuneus appear particularly impaired in VS.

1.5.2.2.   Locating the brain activity elicited by sensory stimulations: fMRI and PET

In spite of these general impairments, several neuroimaging studies have demonstrated that vegetative state patients can process sensory information (GIACINO ET AL., 2006). For example, Menon and collaborators showed that complex natural images elicited higher activity in the extra-striate cortex than scrambled images (MENON ET AL., 1998)[21]. Similarly, simple and complex sounds elicit reliable activations in the auditory cortices (DE JONG ET AL., 1997; BOLY ET AL., 2004; OWEN ET AL., 2005; COLEMAN ET AL., 2007) and tactile stimuli activate the sensory cortex (LAUREYS ET AL., 2002; SILVA ET AL., 2010). Several responses have been observed in associative cortices (BOLY ET AL., 2004; SCHIFF ET AL., 2005; DAVIS ET AL., 2007) and even prefrontal activations have been reported (SCHIFF AND PLUM, 1999; GIACINO ET AL., 2006; DAVIS ET AL., 2007). However, these activations appear dramatically reduced and spatially limited as compared to healthy controls, conscious and even minimally conscious patients. Finally, the activity in the fronto-parietal networks is generally not correlated with primary sensory areas (LAUREYS ET AL., 2004; SCHNAKERS ET AL., 2006; LAUREYS AND SCHIFF, 2011).

---

[21] Although see (SCHIFF AND PLUM, 1999) for potential confounds in this study.
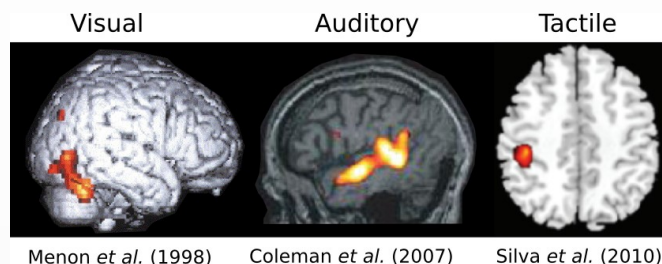
FIGURE 1.23 STIMULUS EVOKED CORTICAL ACTIVITY IN VEGETATIVE STATE PATIENTS.

(Left) Menon et al. (MENON ET AL., 1998) used PET to compare the brain activity elicited by faces versus random images. The results revealed significant activity in the fusiform gyrus, classically associated with face processing.

(Middle) Coleman et al. (COLEMAN ET AL., 2007) presented a variety of auditory stimuli (noise, unintelligible sounds, unambiguous speech, ambiguous speech) to vegetative and minimally conscious state patients and showed that some 3/7 VS patients presented significant speech processing abilities, as assessed by comparing ambiguous and non-ambiguous sentences. The present figure is an example of VS patients showing a significantly higher activity to sound versus silence.

(Right) Similar results can be observed with VS patients recorded with PET during a tactile stimulation (SILVA ET AL., 2010).

Overall, these results suggest that VS patients can present preserved cognitive processing. However, and following the patterns of activation elicited by unconscious stimuli (Figure 8-10), the corresponding brain activation are generally restricted to limited neural circuits, and do not tend to recruit the fronto-parietal networks.

1.5.2.3. Timing the brain activity elicited by sensory stimulations: EEG and MEG
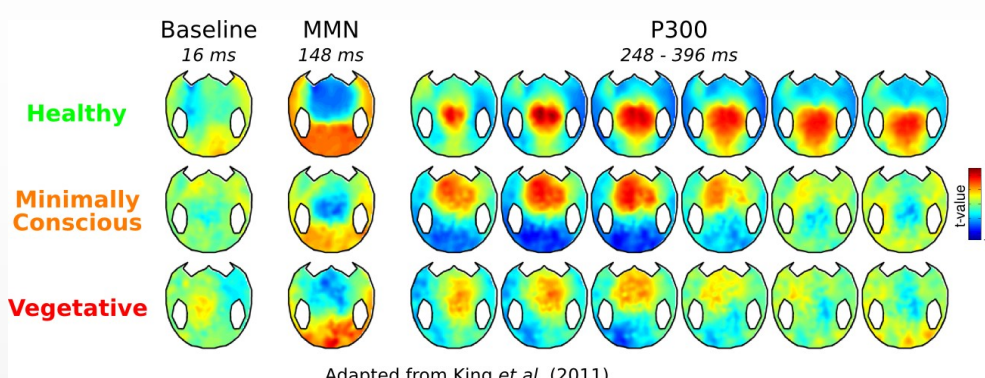
FIGURE 1.24 SPECIFIC IMPAIRMENT OF LATE ERPs.

When presented to a variation of the auditory oddball paradigm (BEKINSCHTEIN ET AL., 2009; FAUGERAS ET AL., 2011), vegetative and minimally conscious state patients can present a preserved mismatch negativity (MMN) in response to deviant tone. The following P300 is however dramatically lowered in amplitude and shortened in time. The above figure has been generated from data collected by Frédéric Faugeras and Lionel Naccache and generously provided for a technical comment available in Supplementary Material (COMMENT 1).

EEG and MEG studies demonstrate that vegetative state patients can present preserved event related potentials (ERP). In particular, auditory oddball experiments have been repeatedly implemented to

test the presence of the mismatch negativity (MMN) component. The results demonstrate that a large proportion of unambiguously vegetative state patients present significant MMN (FISCHER ET AL., 2004, 2010; DALTROZZO ET AL., 2007; BEKINSCHTEIN ET AL., 2009; FAUGERAS ET AL., 2011) and show that this component significantly predict subsequent recovery (FISCHER ET AL., 2004; DALTROZZO ET AL., 2007). Other supposedly automatic ERPs can also be observed in vegetative state patients. In particular, the N400 which seemingly indexes automatic semantic processes, has been observed in some vegetative state patients (SCHOENLE AND WITZKE, 2004; BALCONI ET AL., 2013; STEPPACHER ET AL., 2013). For example, Schoenle and Witzke analyzed a large cohort of 120 patients, and showed that 12% of the vegetative state patients presented a significant N400, whereas up to 77% minimally conscious patients[22] showed a significant N400 (SCHOENLE AND WITZKE, 2004). In contrast, the amplitude of the P300 is generally indicative of a patient's state of consciousness: the P300 elicited by meaningless auditory oddballs is indeed larger and more often observed in conscious and minimally conscious state than in vegetative state patients (PERRIN ET AL., 2006; BEKINSCHTEIN ET AL., 2009; FISCHER ET AL., 2010; FAUGERAS ET AL., 2012). Furthermore, several studies have shown that the P300 was a significant predictor of subsequent recovery (LUAUTÉ ET AL., 2005; DALTROZZO ET AL., 2007; CAVINATO ET AL., 2009; FAUGERAS ET AL., 2012) suggesting that this ERP component could index a clinically unobserved restoration of consciousness.

1.5.2.4. Rhythms

FIGURE 1.25 ELECTROPHYSIOLOGICAL SPECTRUM AND FUNCTIONAL CONNECTIVITY OF VEGETATIVE, MINIMALLY CONSCIOUS AND CONSCIOUS STATE PATIENTS.

(Left) EEG studies (LEHEMBRE ET AL., 2012; J LEON-CARRION, MARTIN-RODRIGUEZ, DAMAS-LOPEZ, BARROSO Y MARTIN, & DOMINGUEZ-MORALES, 2008; JOSE LEON-CARRION ET AL., 2012) suggest that minimally conscious, and a fortiori vegetative state patients present a predominance of low frequency rhythms (0-4 Hz). An abnormally low alpha oscillation has also been reported (e.g. (LEHEMBRE ET AL., 2012)). Furthermore, functional connectivity measures based on phase synchrony in specific frequency bands suggests that patients with disorders of consciousness present functional connectivity impairments in the alpha band (8 – 13 Hz).

(Right) fMRI analyses of patients' default mode network (DMN) suggests that the integrity of this circuits is correlated with patients' state of consciousness (VANHAUDENHUYSE ET AL., 2010).

Vegetative state patients generally present an abnormal EEG spectrum. As in the sleeping and anesthetized states, the EEG is typically dominated by large low frequency waves, especially over frontal regions (*e.g.* (BABILONI ET AL., 2009; LEHEMBRE ET AL., 2012; VAROTTO ET AL., 2013)). Furthermore, alpha oscil-

---

[22] *The authors refer no "near vegetative state patients" which is not a usual clinical category, but nevertheless grossly resembles the minimally conscious state.*

lations, generally peaking over centro-posterior electrodes, are often absent or slowed down to a theta rhythm (BABILONI ET AL., 2009; LEHEMBRE ET AL., 2012; VAROTTO ET AL., 2013). The alpha wave amplitude has been shown to be correlated with patients' recovery (BABILONI ET AL., 2009). Spectral summary and complexity measures revealed similar patterns of results. The bi-spectral index (BIS) is correlated with patients' states of consciousness, significantly lower in vegetative than in minimally conscious state patients (SCHNAKERS ET AL., 2008A). Similarly, EEG entropy is lower in vegetative state patients than in minimally conscious state patients, although this difference was found in acute, but not chronic, patients (GOSSERIES ET AL., 2011).

1.5.2.5.   Functional connectivity

Finally, numerous studies suggest that vegetative state patients are characterized by an impaired functional connectivity. PET and fMRI studies suggests that thalamo-cortical and cortico-cortical connectivity may be present, but largely impaired in the vegetative state (LAUREYS ET AL., 1999A, 2000A, 2000B; BOLY ET AL., 2004; ZHOU ET AL., 2011; KOTCHOUBEY ET AL., 2013). In particular, auditory stimuli induce more widespread activation, and recruit distant brain regions in healthy subjects (LAUREYS ET AL., 2000B, 2002) and in minimally conscious state patients (BOLY ET AL., 2004) than in vegetative state patients. Similar results were observed with tactile stimuli: contrary to healthy subjects, vegetative state patients' bilateral parietal cortices (Brodmann area 40) are less activated and not correlated to the activity in primary sensory motor cortex (SILVA ET AL., 2010). Furthermore, minimally conscious state patients show impaired functional connectivity between sensory cortices and the cortical midline in response to painful stimuli (BOLY ET AL., 2008). It has been recently argued that such functional connectivity impairments would solely reflect top-down deficits, and that bottom-up information processing would conversely be preserved in vegetative state patients (BOLY ET AL., 2011). However, and while this hypothesis remains plausible, we underlined severe methodological issues which invalidate the data presented in support of this claim (KING ET AL., 2011) (COMMENT 1).

Numerous studies indicate that resting-state functional connectivity is also impaired. Silva and collaborators found that the ascending reticular activating system (ARAS) activity normally correlated with the precuneus' in healthy subjects but not in vegetative state patients (SILVA ET AL., 2010). The integrity of the default mode network is also directly correlated with consciousness states (BOLY ET AL., 2009; CAUDA ET AL., 2009; VANHAUDENHUYSE ET AL., 2010) and recovery (LAUREYS ET AL., 2000B). For instance, Vanhaudenhuyse *et al.* showed that the default mode network is correlated with patients' CRS-R score (VANHAUDENHUYSE ET AL., 2010), although not necessarily each of the assessed abilities independently (BRUNO ET AL., 2010). Note, however, that the detection of resting state connectivity depends on the use of adequate series of preprocessing steps that are not always thoroughly applied (ANDRONACHE ET AL., 2013).

These studies generally demonstrate weak differences between vegetative and minimally conscious state patients. Furthermore, they are directly dependent on the way functional connectivity is modelled, and can thus be subject to a number of artefacts (ROGERS ET AL., 2007; KING ET AL., 2011; ANDRONACHE ET AL., 2013). A more direct method to assess cortico-cortical connectivity is to use combined EEG and TMS. As mentioned above, Massimini and colleagues have demonstrated that the electrophysiological activity elicited by TMS pulses is more complex in normal wakefulness than in sleep and anaesthesia (MASSIMINI ET AL., 2005, 2007; ROSANOVA ET AL., 2012) (COMMENT 2). More specifically, the location of the peak activation only changes over time if subjects are awake. Applying this method to vegetative, minimally conscious, and conscious state patients as well as locked-in syndrome patients demonstrated a very strong correlation between patients' clinical states of consciousness and the complexity of the TMS-induced EEG activity (ROSANOVA ET AL., 2012; CASALI ET AL., 2013). This result was recently replicated by an independent team (RAGAZZONI ET AL., 2013). Not only does this result strongly suggest that functional connectivity is im-

paired in vegetative state patients, but it provides a method that is independent of the integrity of patients' afferent and efferent pathways and of their ability to understand instructions.

The possibility of a causal relationship between patients' state of consciousness and the thalamo-cortical connections is particularly well supported by interventional studies. Giacino, Schiff and colleagues showed that stimulating the central thalamus bilaterally with deep brain stimulation (DBS) electrodes restored arousal regulation and improved responsiveness of a minimally conscious state patient, who had been unable to communicate reliably for six year prior to the operation (SCHIFF ET AL., 2007). Interestingly, after a five-month period, behavioural improvements could be observed even when the electrodes were not active. Although promising, this highly invasive study has not been applied to a vegetative state patient. It thus remains unclear whether central thalamic impairments are the unique cause of disorders of consciousness. Although several anatomical studies found centro-thalamic lesions in vegetative state patients (KINNEY ET AL., 1994; MAXWELL ET AL., 2006), these patients are generally characterized by multi-focal white and gray matter injuries (TSHIBANDA ET AL., 2009; NEWCOMBE ET AL., 2010).

Adapted from Rosanova *et al.* (2012)
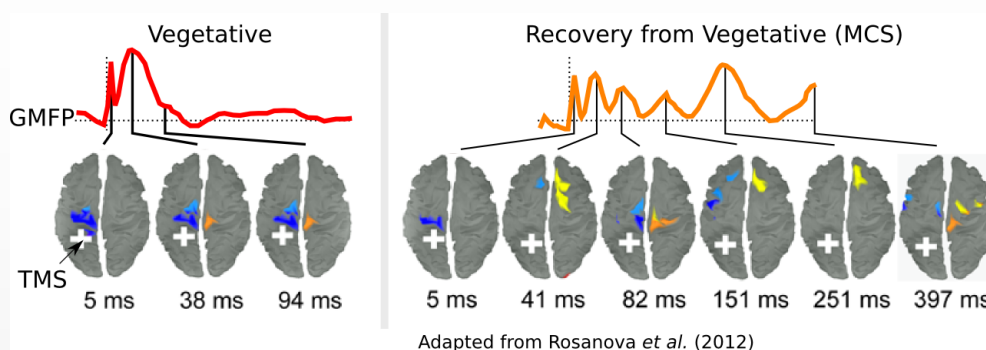
FIGURE 1.26 EFFECTIVE CONNECTIVITY ASSESSED WITH TMS & EEG IN VEGETATIVE AND MINIMALLY CONSCIOUS STATE PATIENTS.

Rosanova and colleagues quantified the effective connectivity of vegetative and minimally conscious state patients with following Massimini et al.'s original protocol (MASSIMINI ET AL., 2005). The results demonstrate that TMS pulses elicit, in vegetative state patients, a peak of activation which is stable across time. By contrast minimally conscious patients present a brain response similar to conscious subjects (see FIGURE 1.21 and COMMENT 2).

KEY POINTS

- Vegetative state (VS) patients' brain metabolism is dramatically reduced, especially in the fronto-parietal regions.
- VS patients can demonstrate residual sensory activation, but activations of the frontal and associative cortices are extremely rare.
- VS patients can present preserved early ERPs (P1, N2, MMN). Late ERPs (P3, N4) are generally correlated with consciousness states and recovery.
- VS patients' EEG spectrum at rest is dominated by low frequencies (<4Hz) and an absent, or slowed, alpha rhythm (10 Hz).
- VS patients' anatomical and functional thalamo-cortical and cortico-cortical connectivity is largely impaired.

Chapter 2. Introduction to the Experimental Contribution

2.1. Outstanding questions

The recent neuroimaging developments have radically changed the theoretical advances in consciousness research. Initiated with metaphors and abstract concepts, the current theoretical proposals now provide detailed neural mechanisms. Each of these putative processes predicts that conscious perception should be marked by specific patterns of neural activity observable independently of subjects' ability to behaviourally report their subjective contents. A critical test for these theories thus points towards their ability to discriminate two minimally different types of patients: vegetative state patients and minimally conscious state patients, who remain either completely or largely impaired in communicating despite their preserved arousal. More specifically, these empirical results lead to five specific questions that have motivated the present work:

- Which of the putative neural signatures of consciousness maximally differentiates vegetative state from minimally conscious state patients?

The putative neural signatures of conscious perception have been established through a number of different experimental methods. However, the extent to which each of these markers can be used to distinguish vegetative from minimally conscious state patients remains unknown. Two different approaches will be presented in the present experimental contribution. The first consists in testing the current models of consciousness in their respective ability to successfully apply to the vegetative and minimally conscious clinical cohort. The second approach consists in systematically testing a large battery of potential markers in order to test whether the present models of consciousness account for all of the differences observed between vegetative and minimally conscious state patients.

- Can the neural markers of conscious processing be used to make predictions at the single subject level? Can they be used to make predictions at the single trial level?

A key challenge to clinical research is to go beyond group statistics and provide tools that are directly applicable to each patient. While most of the studies reviewed above show statistical differences between groups of vegetative and minimally conscious state patients, the sensitivity (does the marker detect consciousness?) and the specificity (does it detect other things than consciousness?) of each putative neural signature of consciousness is generally not assessed. A key challenge is thus to *quantify* the ability of each of these putative markers to distinguish vegetative and minimally conscious state patients. Ultimately, the most discriminative marker could allow single trial detection and thus open the possibility of monitoring consciousness states in real time. Furthermore, such advance would also offer a new family of experimental paradigms in conscious access could be probed at each trial without asking for subjective report.

- Can the putative neural markers of conscious processing be compared and combined?

As most clinical and empirical studies investigate a single type of brain activity at a time, it is unclear whether the various putative signatures of consciousness occur in synergy. Systematically comparing and contrasting them could lead to two important consequences. First, it could help differentiate the processes that are necessary but not sufficient to consciousness, from those are specific to it. Second, each neural marker could contain substantially different information about the underlying conscious processing.

- What are the computational mechanisms responsible for conscious perception, and do their respective elementary generate different patterns of neural activity?

Identifying and isolating the computational components allowing one to consciously perceived his/her environment is a central question in the present thesis. While a great deal of research has focused on determining which brain region, and which types of brain activity index conscious perception, it often remains insufficiently clear why these specific neural responses produce conscious perception. For example, models emphasizing on the role of gamma synchrony in consciousness (CRICK AND KOCH, 1990A; TALLON-BAUDRY AND BERTRAND, 1999) generally rely on the premise that conscious perception is directly linked to information binding. Analogously, the global workspace theory (BAARS, 1989; DEHAENE ET AL., 2006B; DEHAENE AND CHANGEUX, 2011) equates consciousness to information access and, to a lesser extent, information maintenance. Yet, the evidence reviewed above questions such premises. For example, unconscious semantic priming suggests that complex and integrated semantic information may be processed unconsciously (NACCACHE AND DEHAENE, 2001B; KOUIDER AND DEHAENE, 2007). Similarly, blindsight demonstrate that one can use (and thus access) unconscious information for behavioural reports (WEISKRANTZ, 1986; STOERIG AND COWEY, 2009). Such evidence suggests that the present frameworks and their respective computational mechanisms should be clarified and formalized.

- Can novel methods provide new insights to the theories of conscious access?

Each theory of consciousness probably arose from methodological advances: time frequency analyses were followed by models of conscious access based on synchronous oscillations; event-related potentials studies engendered theoretical proposals distinguishing early and late activity; information theoretic equations have been tightly linked to the proposals equating complexity and consciousness. To extend the current models of conscious access, original methods should thus be proposed and tested in the context of conscious and unconscious processing.

2.2. OVERVIEW OF THE THESIS

The questions outlined above will be tackled along three general axes of research:

- First, the methods to detect the putative electrophysiological signatures of consciousness will be implemented, and supplemented with original analyses characterizing the patterns of brain activity associated with conscious and unconscious processes.
- Second, the ability of the resulting markers to discriminate between vegetative state and minimally conscious state patients will be tested.
- Third, each of these methods will be discussed in terms of their ability to improve the current theories of conscious access.

These general aims are tackled across six distinct studies.

In a first study, I show how multivariate pattern analyses (MVPA) can be used to decode, at the single subject level as well as at the single trial level, the early and late brain responses to two distinct auditory novelties encountered in an experimental setup introduced by Bekinschtein and collaborators (BEKINSCHTEIN ET AL., 2009). The so-called "Local Global" protocol is specifically designed to dissociate early and late event related potentials and thus offer an interesting possibility of isolating consciousness-dependent from consciousness-independent processes. Following the classic oddball task described in the literature review, "local" novelties indicate a change of sound within a given trial and elicit a mismatch negativity (MMN) around ~150 ms. By contrast, "global" novelties indicate a change of auditory sequence across trials and elicit a late P300b but not MMN. After testing the decoding methods with a scalp and intracranial EEG as well as MEG, and under different active, passive and distractive tasks, I demonstrate that only late ERPs vanish under distraction.

In a second set of papers, I show how the decoding analyses developed in the first study can be extended and used in an original way so as to characterize the dynamics of mental processes. In particular, I show that the resulting "temporal generalization" method differentiates serial processes and sustained neural responses. The dissociation between serial and sustained processing can be empirically observed in an MEG version of the Local Global protocol implemented in the first study. The results demonstrate that a change of sound within a given trial (local mismatch) gives rise to a sequence of different brain responses. By contrast a global change of the auditory pattern elicits a late and sustained brain response. In a follow-up paper, I show how the temporal generalization method can be used in a variety of context and provide a powerful tool to understand the mechanisms underlying complex neural dynamics.

These decoding methods are also applied to vegetative and minimally conscious state patients. The results demonstrate that early brain responses are partially preserved in both vegetative and minimally conscious state patients, but that late brain activity is only observed in minimally conscious state patients. While these results fit with several models of conscious processing (DEHAENE ET AL., 2006b; LAMME, 2006b, 2010; DEHAENE AND CHANGEUX, 2011), their relatively moderate statistical power suggests that, in practice, contrastive ERPs may not be suitable to detect consciousness in the clinics.

Consequently, I turned toward two other types of markers: functional connectivity and complexity. In collaboration with Jacobo Sitt, I first introduce a novel method to quantify the amount of information shared between distant brain regions, and demonstrate that this marker efficiently discriminates vegetative from minimally conscious state patients. Second, I show that the complexity of patients' EEG is strongly correlated with their state of consciousness. Third, I systematically compare these original measures to the traditional putative neural signatures of consciousness and isolate the best candidate markers. Finally, I demonstrate that combining these markers with multivariate analyses can usefully diagnose and predict the state of consciousness of individual patients. In particular, I show that patients clinically diagnosed to be in a vegetative state have greater chances of later presenting signs of conscious behaviour if their brain activity resembles those of conscious subjects.

I conclude this set of neuroimaging studies by going back to subjects' behaviour in response to conscious and unconscious stimuli. I show that multivariate methods can also provide a useful theoretical and empirical framework to tackle conscious and unconscious perception. In particular, I show how this approach formally integrates and clarifies the differences between confidence ratings, subjective visibility reports and objective discrimination performance. After deriving a number of original predictions from this framework, I successfully test one of them in a novel perceptual decision task.

Finally, I summarize the present findings, discuss their limits and relevance to current theories of consciousness, and briefly outline two perspectives for future research.

CHAPTER 3. SINGLE-TRIAL DECODING OF AUDITORY NOVELTY RESPONSES FACILITATES THE DETECTION OF RESIDUAL CONSCIOUSNESS

3.1. INTRODUCTION OF THE ARTICLE

As detailed in the literature review, event related potentials (ERPs) measured with electroencephalography (EEG) can be used to distinguish early processes (believed to be independent from conscious access) from late processes (believed to be correlated with conscious access). A critical test thus consists in isolating these early and late brain responses in vegetative and minimally conscious state patients. Such tests have already been performed and several teams have started to provide within-subject analyses (FISCHER ET AL., 2004, 2010; FISCHER AND LUAUTÉ, 2005; DALTROZZO ET AL., 2007; BEKINSCHTEIN ET AL., 2009; FAUGERAS ET AL., 2011), which provide useful complements to patients' diagnosis. These methods however face several challenges. First, vegetative and minimally conscious state patients generally present fluctuating vigilance and attention: a failure to identify the ERPs of interest may thus results from an inability to isolate the single trial responses. Second, patients often present dramatic brain and skull lesions. Consequently, the topographies and latencies of the EEG that are typically identified in healthy subjects may be dramatically transformed in these patients. Yet, systematically testing all EEG electrodes at all time samples increases the probability of identifying random effects, and therefore require more conservative statistical criteria.

These issues therefore call for developing a method that could, in principle, not only detect a particular brain activity in a given subject independently of its individual spatial and temporal characteristics, but also provide a way to extract this information at the single trial level to ultimately allow for real time monitoring of patients' brain activity.

In this first study, I implemented multivariate pattern analyses to maximize the detection of two putative neural signatures of conscious and unconscious processing: the MMN and the P3. After demonstrating that this approach provides accurate single trial prediction in normal subjects, I test its applicability in a large cohort of patients. As for the rest of the studies, the clinical recordings were acquired by Frédéric Faugeras, Benjamin Rohaut and Lionel Naccache.

3.2. ABSTRACT

Detecting residual consciousness in unresponsive patients is a major clinical concern and a challenge for theoretical neuroscience. We recently designed an experimental protocol that dissociates two electro-encephalographic (EEG) responses to auditory novelty. Whereas a local change in pitch automatically elicits a mismatch negativity (MMN), a change in global sound sequence leads to a late P300b response. The latter component is thought to be present only when subjects consciously perceive the global novelty. Unfortunately, it can be difficult to detect because individual variability is high, especially in clinical recordings. To optimize detection, the present study investigates the potential of multivariate pattern classifiers to extract subject-specific EEG patterns and predict single-trial local or global novelty responses. We first validate our method with 38 high-density EEG, MEG and intracranial EEG recordings. We demonstrate the high sensitivity of our approach in control subjects and confirm that local responses are robust to distraction whereas global responses depend on attention. We then investigate 158 clinical EEG recordings from vegetative state (VS), minimally conscious state (MCS) and conscious state (CS) patients. For the local response, the proportion of patients with significant classifications scores (M=60%) does not vary with the state of consciousness. By contrast, for the global response, only 14% of VS patients present a significant effect, compared to 31% of MCS and 52% of CS patients. In conclusion, single-trial multivariate decoding of novelty responses provides valuable information in unresponsive patients and paves the way towards real-time monitoring of the state of consciousness.

3.3. INTRODUCTION

Despite a recent flurry of experimental discoveries, the neuronal mechanisms that support conscious perception remain a major challenge for theoretical neuroscience. Numerous studies have associated conscious perception with macroscopic neurophysiological phenomena such as synchronous activity across distant cortical regions and sustained fronto-parietal activations (SERGENT ET AL., 2005; FAHRENFORT ET AL., 2007, 2012; MELLONI ET AL., 2007; GAILLARD ET AL., 2009) which are thought to reflect global information integration (TONONI AND EDELMAN, 1998; REES ET AL., 2002; TONONI AND SPORNS, 2003; LAMME, 2006B; FISCH ET AL., 2009; DEHAENE AND CHANGEUX, 2011; MELLONI ET AL., 2011; SETH ET AL., 2011). However, identifying the neuronal signatures of conscious processing is not just a theoretical exercise. Every year, severe brain injuries lead thousands of patients to lose their communication abilities and fall into a variety of clinical conditions ranging from coma, to vegetative state (VS), minimally conscious state (MCS) or conscious but paralyzed patients (locked-in syndrome). Clinically, separating disorders of consciousness (DOC) from communication deficits can be difficult. In particular, patients in vegetative states (VS) present moments of arousal, during which they open their eyes and produce complex behavioral reflexes. Yet, they show no clear signs of intentional behavior, even after careful clinical examination performed by experienced teams (BRUNO ET AL., 2011A). Slightly more functional patients, referred to as being in a "minimally conscious state" (MCS), present some intentional behaviors but seem unable to establish any long-lasting communication (GIACINO ET AL., 2002).

To facilitate clinical diagnosis, brain imaging techniques may play an important role (LAUREYS ET AL., 2004; OWEN ET AL., 2006; OWEN, 2008; BYRNE ET AL., 2010; LAUREYS AND SCHIFF, 2011). By directly detecting the neural activity associated with conscious processing, they could be used to circumvent communication deficits and thus provide crucial information for the diagnosis of these patients. The Local Global protocol (BEKINSCHTEIN ET AL., 2009) was designed for this purpose (FIGURE 3.1). This experimental setup

allows the isolation of two event related potentials (ERPs) elicited by two types of auditory novelty. First, a change in pitch within a five-sound sequence (hereafter referred to as local deviancy) typically leads to a frontal mismatch negativity (MMN) ~150ms after stimulus onset. Second, a change in auditory sequence in a fixed global context generates a late P300b response over centro-posterior electrodes. Crucially, these auditory changes can be arranged to create a 2x2 design in which local deviancy and global deviancy are orthogonally manipulated (BEKINSCHTEIN ET AL., 2009).
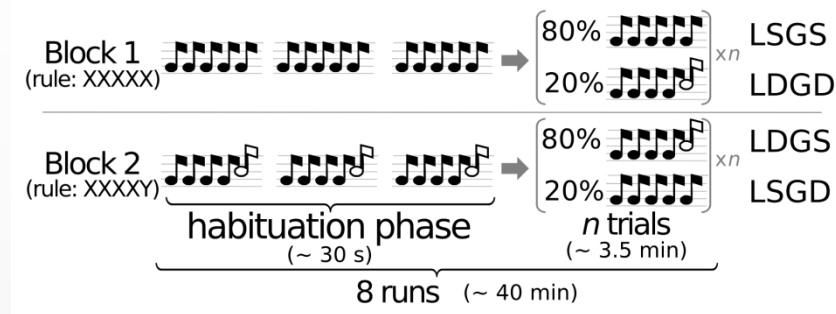
FIGURE 3.1 THE LOCAL GLOBAL PROTOCOL

The Local Global paradigm (BEKINSCHTEIN ET AL., 2009) is an auditory odd-ball experimental setup that implicitly tests subjects on their ability to detect two orthogonal types of auditory novelty. Each trial is composed of five successive tones (SOA=150 ms). The first four sounds are always identical. Local-deviant (LD) trials differ from local-standard trials (LS) because their fifth sound deviates in pitch. Global-deviant (GD) trials correspond to the presentation of a sequence of five sounds which is rare in a given block, compared to the frequent "global standard" sequence (GS). Both local and global novelties depend entirely on the fifth sound, which therefore serves as the origin of time scales in all subsequent graphs.

There is now growing evidence that the MMN reflects a prediction error signal elicited whenever the incoming sound does not fit with a prediction constructed on the basis of previous local auditory regularities (NÄÄTÄNEN ET AL., 1978, 2010; GARRIDO ET AL., 2007, 2008; WINKLER, 2007; WACONGNE ET AL., 2011, 2012). Moreover, manipulations of attention, sleep and anaesthesia show that the MMN may persist even in unconscious states (ATIENZA ET AL., 1997; BRÁZDIL ET AL., 2001; HEINKE ET AL., 2004; MULLER-GASS ET AL., 2007; GARRIDO ET AL., 2008; BEKINSCHTEIN ET AL., 2009; ROHAUT ET AL., 2009; NÄÄTÄNEN ET AL., 2010; TZOVARA ET AL., 2012). By contrast, the P300b is thought to reflect a higher-order violation of subjects' expectations of a given rule, constructed over a longer time period and has thus been closely linked to working memory (GOLDSTEIN ET AL., 2002; POLICH, 2007) and conscious access (DEHAENE ET AL., 2006B; DEHAENE AND CHANGEUX, 2011). Converging lines of evidence suggest that the dissociation between these two neural signatures could discriminate patients in vegetative state (VS) from those in conscious (CS) or minimally conscious states (MCS) patients (NACCACHE ET AL., 2005; WIJNEN ET AL., 2007; ROHAUT ET AL., 2009; FISCHER ET AL., 2010; FAUGERAS ET AL., 2011, 2012).

However, isolating these event-related responses in single patients can unfortunately be difficult for several reasons. First, clinical recordings often present a low signal-to-noise ratio (SNR) because of numerous physiological (movements, eye blinks, *etc.*) and environmental (presence of auditory noise, no Faraday cage, *etc.*) artefacts. Moreover, patients often present severe brain and even skull damages which can alter the scalp electrical projections of their cortical activity. This topographical variability can be made worse by temporal delays and inter-trial variability caused by processing impairments or white matter damage (TSHIBANDA ET AL., 2009; NEWCOMBE ET AL., 2010). In other words, unlike control recordings, a patient's MMN and P300b may not be optimally observed over the frontal and parietal channels at ~150 and ~350ms respectively. While more liberal analyses testing a greater number of EEG channels and time

samples could be implemented, correction for multiple comparisons would largely diminish either sensitivity or confidence in the presence of a given brain response.

To overcome these issues, we evaluate in the present research the potential of a single-trial multivariate pattern (MVP) analysis. We implemented, separately for each subject, a MVP classifier that aims at maximally extracting information from each trial by combining evidence from multiple EEG channels and multiple time samples. After training on an independent dataset, the classifier estimates the probability that each trial contains a local or a global response to auditory novelty. This prediction can be compared to trials' effective classes. Classification scores can thus indicate whether a given subject is able to detect the corresponding type of novelty.

We first apply our method to EEG, MEG and intracranial EEG recordings acquired from control subjects, then to high-density EEG recordings from 158 DOC patients. We consider three successive questions: (1) What level of *accuracy* can be achieved from each type of recordings? (2) Can decoders be formed to *generalize* the detection of novelty from one experimental context to another? (3) Is our method sensitive enough to be applied to the detection of residual novelty processing in DOC patients?

3.4. METHODS

3.4.1. PROCEDURE, MATERIAL & APPARATUS

The data analyzed here come from four different experimental settings, using either scalp EEG, MEG, or intracranial EEG, which together enables the direct comparison of the utility of each approach with regard to single trial decoding. Events Related Potentials (ERPs) and Events Related Fields (ERFs) have been partially reported elsewhere (BEKINSCHTEIN ET AL., 2009; WACONGNE ET AL., 2011; FAUGERAS ET AL., 2012). All experiments were approved by the relevant regional ethical committees (Comité pour la Protection des Personnes Pitié-Salpêtrière and Bicêtre hospitals). Healthy volunteers received a financial compensation for their participation. Unless specified otherwise, the procedure used in our experiments exactly followed the Local Global protocol (BEKINSCHTEIN ET AL., 2009) which enables the comparison of effects engendered by physically identical but contextually different auditory stimuli. In the standard design, subjects are required to count the global deviant trials and report this number at the end of each block, in order to ensure that they pay attention to the task.

The auditory stimuli were 50 ms-duration sounds composed of 3 sinusoidal tones (either 350, 700, and 1400 Hz, hereafter sound A; or 500 Hz, 1000 Hz, and 2000 Hz, hereafter sound B), with 7-ms rise and 7-ms fall times. Sequences were composed of five stimuli presented at a Stimulus Onset Asynchrony (SOA) of 150 ms, and were separated by a variable silent interval of 1350 to 1650 ms (50 ms steps). The sequences could comprise five identical tones (xxxxx) or four identical tones followed by a distinct one (xxxxY, where X can be sound A or sound B and Y the other sound). Following the original design, in a given block, 80% of trials consisted in one type of sequence (*e.g.* aaaaB) and 20% of trials were global deviants (aaaaa in this example), pseudo randomly distributed at least one and at most six global-standard trials apart (FIGURE 3.1). In all experiments, trials immediately following a global deviant were removed from the analyses. Each block started with a 30s habituation phase during which the frequent sound sequences were repeatedly presented to establish the global regularity, before the first infrequent stimulus was heard. In experiments 1, 3-5 , sounds were presented via headphones with an intensity of 70 dB, using E-prime v1.2 (Psychology Software Tools Inc.). In experiment 2, the intracranial recording ap-

paratus being incompatible with headphones, sounds were directly presented from the computer's speakers.

3.4.1.1.   Experiment 1: counting task (EEG)

In the first experiment (reported in (FAUGERAS ET AL., 2012)), ten healthy adults (Age M = 23.0 years old, SD = 0.67 years, 3 females) performed the standard Local Global protocol, while EEG was continuously recorded using a 256-channel EEG geodesic net (EGI).

Each subject was recorded for approximately 45 min, comprising 8 blocks of 3-4 min duration, each beginning with a 30 s habituation phase in which the global standard stimuli were repeatedly presented. As for all experiments, trials from these habituation phases were not included in the analyses. Each block was interleaved with resting periods of a few minutes. In each block, subjects were instructed to mentally count the global deviant trials. This experiment will therefore be referred to as 'counting EEG'.

Bad sensors, defined as those showing no signal at all, constant white noise, or presenting intermittent signals, were interpolated. Trials during which more than 20% of the sensors were bad, the EEG voltages exceeded $\pm$ 150 μV, EEG transients exceeded $\pm$ 100 μV or electro-oculogram activity exceeded $\pm$ 80 μV were excluded from the analyses. All signals were digitally low-pass filtered at 40 Hz, downsampled to 250 Hz, and referenced with a common average. Trials were then segmented from -800 ms to 736 ms after the critical stimulus onset, and were baseline corrected over a 200 ms window before the onset of the first of the five sounds. All EEG processing stages were performed in the EGI Waveform Tools Package and with the Fieldtrip toolbox (OOSTENVELD ET AL., 2011) and Matlab 2009b.

3.4.1.2.   Experiment 2: counting task (iEEG)

In the second experiment, nine patients (Age: M=33 years old, SD=11 years, 5 women) suffering from drug-resistant epilepsy, and who had consequently undergone electrode implantation for pre-surgical purposes, performed a standard Local Global protocol (two patients were already reported in (BEKINSCHTEIN ET AL., 2009)) in 8 consecutive blocks. It should be noted that, although epileptic patients cannot be considered as healthy controls, their attention and their state of consciousness were relatively comparable to healthy subjects'. On average, 56 (SD=9) intracranial electrodes (IEEG) sampled at 400 Hz and 1kHz (depending on the system) recorded their brain activity from various cortical areas mainly within the temporal, the occipital, and the frontal lobes. Electrode locations are reported in SUPPLEMENTARY FIGURE 3.7. The task here was exactly as in Experiment 1.

After removing channels showing inter-ictal activity, analyses were performed on 401 channels. All signals were digitally low-pass filtered at 40 Hz. Trials were then segmented from -800 ms to 700 ms after the critical stimulus onset, and were corrected for baseline over a 200 ms window before the onset of the first of the five sounds. All EEG processing stages were performed with Matlab 2009b and the Fieldtrip toolbox (OOSTENVELD ET AL., 2011).

3.4.1.3.   Experiment 3: attentive task (MEG)

In the third experiment (reported in (WACONGNE ET AL., 2011)), ten healthy adults (Age M=25 years old, SD=4.7 years, 5 females) performed a modified version of the Local Global protocol (see below) while their brain activity was measured with MEG (Elekta Neuromag® MEG system, Helsinki, Finland, comprising 204 planar gradiometers and 102 magnetometers in a helmet-shaped array) and EEG (built-in 64 electrodes system). Scalp EEG electrodes were not analyzed in the present study. Data were sampled at 1 KHz with on-line analog low-pass filtering at 330 Hz, and on-line analog high-pass filtering at 0.1 Hz. The head position with respect to the sensor array was determined by four head position indica-

tor coils attached to the scalp. The locations of the coils and EEG electrode positions were digitized with respect to three anatomical landmarks (nasion and preauricular points) with a 3D digitizer (Polhemus Isotrak system®). Then, head position with respect to the device origin was acquired before each 3 - 4 minute block of MEG/EEG recording.

Each recording session lasted 1 hour, comprising 14 blocks of 3 - 4 min duration with resting periods between each block. Subjects were asked to keep their eyes open and to avoid eye movements by focusing on a fixation cross displayed in the center of the screen. Subjects were instructed to pay attention to the auditory stimuli.

The MEG task differed from experiment 1 in the following respects: First, in most (n=12) blocks, 10% of the trials were omission trials composed of only four sounds; in the remaining two blocks, the frequent auditory sequence was also made of only four sounds. These conditions were applied in order to test the brain responses to expected and unexpected omissions. The corresponding trials were excluded from the present analyses, but are reported in detail in (WACONGNE ET AL., 2011). Second, subjects performed more trials than in the previous experiment (780 trials instead of 500). Third, subjects were not asked to count the number of globally deviant trials, but were only required to pay attention to the auditory stimuli. This 'attentive MEG' experiment aimed at demonstrating that the previously identified neurophysiological signatures associated with local and global deviant trials were independent of the counting task. This control can thus validate the applicability of the Local Global protocol in a clinical setup, in which patients may not be able to perform complex instructions such as counting global deviant trials. At the end of the recording, a list of questions was submitted to the subject to check that they had detected the various auditory regularities.

Artefacts arising from outside the sensor array, such as those stemming from limb movement or other ambient magnetic disturbances, were reduced by the signal space separation method (SSS) (TAULU ET AL., 2004). Additionally, and for each subject separately, a linear transform of the MEG data into harmonic function amplitudes via the SSS method was used to estimate the MEG signals corresponding to different head positions and to convert the data acquired from several blocks into one common head-centered reference frame. This reference head position was determined from all head position measurements done at the beginning of each recording session. This data transformation helps the direct comparisons of MEG data between conditions and blocks.

Except if explained otherwise, eye blinks and cardiac artefact were corrected for each type of channel (gradiometer, magnetometers and EEG sensors) separately by decomposing the average artefacts into principal components, and regressing out those principal components from the continuous recording – a technique known as signal space projection (SSP). Noisy MEG sensors were removed with Maxfilter in the SSS preprocessing step. All signals were digitally low-pass filtered at 40 Hz and down-sampled to 256 Hz. Trials were then segmented from -800 ms to 736 ms after the critical stimulus onset, and were corrected for baseline over a 200 ms window before the onset of the first of the five sounds. Segmentation was done with Fieldtrip(OOSTENVELD ET AL., 2011). Trials with more than 20% of bad sensors were rejected.

3.4.1.4.   Experiment 4: distracting task (EEG)

In the fourth experiment (reported in (BEKINSCHTEIN ET AL., 2009)), subjects were actively distracted by a continuous speeded visual detection task simultaneous with the presentation of the Local Global auditory stimuli, while EEG was continuously recorded at 250 Hz using a 128-channel EEG geodesic net (EGI) referenced to the vertex. Participants were instructed to detect a visual target in a rapid stream of successive letters presented at the fovea and were explicitly asked to neglect the unrelated auditory stimuli. The visual stimuli were twelve 1° x 1° colored upper or lower case letters, and were maximally

presented for 1000 ms, using E-prime v1.1 (Psychology Software Tools Inc.). To check that subjects did not consciously perceived the global structure of the auditory stimuli, they were asked at the end of the experiment whether they had perceived any global regularity or novelty. EEG preprocessing was identical to Experiment 1.

3.4.1.5.   Experiment 5: DOC patients (EEG)

One hundred and fifty eight (158) EEG recordings were acquired from 104 distinct patients suffering or recovering from variably severe disorders of consciousness and/or communication (DOC) while they performed the Local Global protocol. The ERPs analyses from 65 recordings have been reported in (FAUGERAS ET AL., 2012). As can be observed in Supplementary Table 1, some patients were recorded several times. These sessions were performed several days apart, in order to identify a potential recovery of consciousness. In most cases, patients' states of consciousness vary between different EEG recordings and can thus be treated as different samples. Hereafter "patients" refer to distinct EEG recordings. The clinical definition of CS, MCS and VS was based on the French version of the Coma Recovery Scale Revised (CRS-R) (SCHNAKERS ET AL., 2008B), and careful neurological examination by trained neurologists (FF, LN) immediately before EEG recording. All patients had been without sedation for at least 24 hours prior to the recording session. All clinical details are available in table S1.

After clinical examination, each participant was asked to perform a task identical to Experiment 1 (count the global deviants). Patients were verbally stimulated between each block (~4 min) to ensure stable arousal, and instructions were explicitly repeated by the experimenter before each run. Although we present results demonstrating that global effects are independent of counting global deviant trials, we reasoned that such instructions could help patients paying attention to the auditory stimulations.

Recording high-density scalp ERPs from non-communicating patients in the intensive care unit or a similar environment is very challenging for technical reasons. First, the electro-magnetic environment is noisy, and patients were not recorded in a shielded room but at bedside. Second, many patients presented physiological artefacts such as EMG, eye-movements and blinks, or other involuntary movements. Therefore, it is particularly important to systematically evaluate the technical quality of data before statistical analysis. Recordings including at least one block with more than 50% of rejected trials were discarded from further analyses in order to avoid possible biases across experimental conditions. EEG preprocessing was identical to Experiment 1.

3.4.2.   ANALYSES

3.4.2.1.   Classification

In the following experiments, we aimed at evaluating, for each subject, the number of trials that could be accurately classified in two distinct and orthogonal types of classes: (1) as locally standard (*LS, i.e.* following an aaaaa sequence) versus locally deviant (*LD, i.e.* following an aaaaB sequence) ('local classification'); (2) as globally standard (*GS* =frequent sequence) versus globally deviant (*GD* =rare sequence in a given block) ('global classification') (see FIGURE 3.1). The Local Standard class corresponds to the union of *LSGS* and *LSGD* trials, and the Local Deviant class corresponds to the union of *LDGS* and *LDGD* trials. Similarly, the Global Standard class corresponds to *LSGS* and *LDGS* trials, and the Global Deviant class corresponds to *LSGD* and *LDGD* trials. For each subject, all data were normalized across all artefact-free trials in each sample of each sensor.

A ten-fold stratified cross-validation was implemented for each analysis. Stratified cross-validation balances the proportion of each class across folds in order to maximize the classifiers' ability to generalize

to unknown data. A support vector classifier (SVC) (CHANG AND LIN, 2001). Was supplemented with a continuous output method providing, for each trial, an estimate of the probability of belonging to a given class (PLATT, 1999). Among the several advantages of this continuous method, we note that it allows across-trial rank statistics and hence avoids the computationally expensive permutation analysis generally required with discrete and/or imbalanced classifiers. After training on a random subset of trials, classification scores were estimated only from the complement of the training set in the set of all trials (later referred to as test set).

Classification scores were estimated with a receiver-operative curve (ROC) analysis applied on trials' predicted probabilities and are summarized using the area under the curve (AUC). The ROC analysis is a standard 2-class (positive and negative) non-parametric statistical method. It is based on the plotting of true positive rate as a function of false positive rate. The result of this function can be summarized by the area under its curve (AUC). An AUC of 50% implies that true positive predictions (*e.g.* trial predicted deviant and is deviant) and false positive predictions (*e.g.* trial predicted as deviant but is standard) are, on average, equally probable; an AUC of 100% indicates a perfect positive prediction with no false positive. Amongst the advantages of the ROC analysis, we note that, unlike mean accuracy, it is robust to imbalanced problems (unlike average accuracy) and remains independent from classes' distributions.

3.4.2.2.   Generalization across context

We implemented a set of generalization analyses which aimed at testing the invariance of the neurophysiological signatures of local and global novelty detection. These generalization analyses consisted in training the classifier using data from a fixed context, and subsequently testing it in a different context (see FIGURE 3.1 & FIGURE 3.2). Classifiers were for instance trained to discriminate local standards trials from local deviant trials using only global standard trials (LS**GS** *versus* LD**GS**). The discriminative hyper-plane (*w*) found was subsequently applied to trials from a different global context, in this case the global deviants (LS**GD** *versus* LD**GD**). This approach was also adapted to the contextual generalization of global effects. In this case, the classifier was first trained, for instance, to discriminate global effects in a fixed local context (**LS**GS *versus* **LS**GD), and then tested on a different local context (**LD**GS *versus* **LD**GD). This procedure was systematically applied in a symmetrical manner: a classifier was either trained in standard contexts and tested in deviant ones, or trained in deviant contexts and tested in standard ones, and the results were then averaged over both directions of generalization. Note that, in addition to presenting the difficult challenge of identifying neural signatures capable of generalizing across different contexts, this procedure divides the number of trials available for training the multivariate classifier in half.

3.4.2.3.   Time-windows of interest

The selection of temporal windows of interest was based on two conceptually different approaches. First, a unique classifier was implemented at each time point. This approach repeatedly combines the evidence from different sensors at a fixed time point. Second, we implemented a set of classifiers using multiple time samples. These classifiers combined either all or a sub-selection of the time samples following the onset of the last sound (t=[0,736] ms): the early time-window refers to t=[0, 367] ms, and the late time window refers to t=[367,736] ms.

3.4.2.4.   Classifier

Each trial was transformed into a *p*-dimensional vector *x*, in which each coordinate corresponds to a single data sample at a given sensor ($p = n_{sensors} \cdot n_{samples}$). The entire dataset can hence be represented as a matrix X in which each row *i* corresponds to one trial x_i, and each column corresponds to an attribute. Moreover, trial classes (standard or deviant) can also be represented as a binary vector *y*, in which standard trials are labeled as 1, and deviant trials as -1. As for all linear classification analyses, the aim is to find a

hyperplane (materialized by a *p*-dimensional vector of weights *w*) that discriminates the two classes ($y_{standard}$ and $y_{deviant}$). For a new trial x_{new}, the sign of the dot product $x_{new} . w$ is then generally used to predict its class. In the present case, a cumulative probability distribution function was fitted to the training set using Platt's method (PLATT, 1999). The signed distance computed from the dot product $x_{new} . w$ could thus be transformed into a continuous value bounded between 0 and 1. This value is directly representative of the probability of belonging to one of the two classes. Note that rank statistics are not affected by the transformation of the signed distance between a given trial and w by a monotonous function, such as a cumulative distribution function. When the number of trials is small compared to the number of attributes (here up to 56000), there are infinitely many *w* that can fit the training data equally well. To limit this issue, we implemented within the cross-validation, a dimensionality reduction based on a univariate feature-selection step that selects a subset of attributes prior to the classification analysis. Feature selection was performed with an ANOVA nested within the cross-validation step. Various levels of the ANOVA p value threshold were explored in Experiment 1 (1%, 5%, 10%, 30% 50%, 100%), and on this basis a fixed value of 10% was chosen for all other experiments. No feature selection was used for the decoding of each time point as dimensionality was relatively small (*e.g.* from 40 channels to 306 channels depending on the type of recording). SVC's regularization parameter was calibrated by nested cross-validation in Experiment 1 (.01, .1, .3, .5, 1, 2) and remained arbitrarily fixed (1) for all other experiments as its values did not dramatically affect classification scores. Finally, sample weights were applied in proportion of the trial classes (LSGS, LSGD, LDGS, LDGD) so that each of the category would equally contribute to the definition of the *w*, and this independently of the contrast of interest (local or global). This step is known to contribute to the minimization of imbalanced dataset artefacts and thus maximizes the number of trials that can be considered in the training process. In practice this step did not lead to a strong improvement of classification performance. All multivariate analyses were performed with the Scikit-learn toolbox (PEDREGOSA ET AL., 2011).

3.4.2.5.   Statistics

ROC analyses and AUC are methods to estimate the size of a given effect, and in our case, the classifiers' ability to discriminate two types of trials. To test for statistical significance within subjects, we performed Mann-U-Whitney analyses across trials. Because the classifier attributes a continuous estimate to each trial (its predicted probability of belonging to a given class C), we can indeed efficiently compare those predicted probabilities across the two levels of the trials' true classes. For instance, for each trial, the classifier outputs a predicted probability of belonging to the standard class (S). Note that the probability of belonging to the other, deviant class (D) can be calculated as $P(D) = 1 - P(S)$. We can then compare the predicted probability of belonging to S depending on whether the trials truly are standard (y=S) or not (y=D) and thus apply a traditional Mann-U-Whitney between $P(S|y=S)$ and $P(S|(y=D)$.

Similarly, across-subjects statistics were performed using Wilcoxon Signed Ranks Tests based the mean predicted probability conditional of trials' true classes. For each subject, the predicted probability of belonging to the standard class (S) is averaged across standard trials (y=S) and, separately, over deviant trials (y=D), yielding $P(S|y=S)$ and $P(S|y=D)$. For each subject *i*, we can thus compute the sum of positive ranks and perform a Wilcoxon test.

A correction for multiple comparisons was performed using the standard False Discovery Rate (FDR) correction, and is referred to as p_{FDR}. Statistical analyses were performed with R and Matlab 2009b.

3.5. RESULTS

The Local Global protocol enables the isolation of two types of neurophysiological activity: either the response to a change in pitch within a five-sound sequence (local effect), or the response to a rare auditory sequence within a block dominated by another frequently repeated sequence (global effect, FIGURE 3.1).
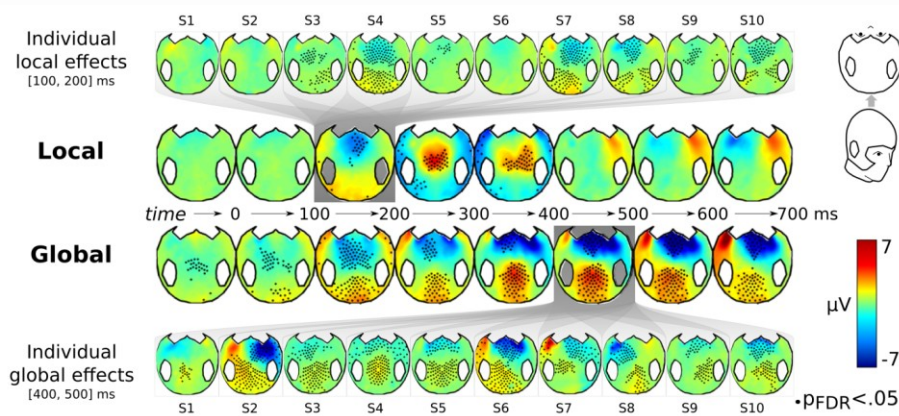
FIGURE 3.2 INTER-INDIVIDUAL VARIABILITY IN THE TOPOGRAPHY OF EEG EFFECTS IN EXPERIMENT 1.

In the two central rows, control EEG topographies of the mean local effect (LD>LS) and of mean the global effect (GD>GS) are plotted as a function of time following the onset of the fifth sound. Black dots correspond to EEG channels presenting significant differences between standard and deviant conditions, corrected for multiple comparisons with FDR. The top and bottom rows show the topography in individual subjects, separately for the local and global effects in their respective time windows of interest. Local deviant trials elicit significant differences over anterior regions with an initial negativity peaking around 150 ms followed by a short central positivity between 200 and 300 ms. Global deviant trials elicit a centro-posterior sustained positivity mainly from 300 ms onwards. While the group statistics replicate the traditional MMN and P3b associated with the Local Global paradigm (BEKINSCHTEIN ET AL., 2009), individual analyses reveal substantial topographical variability in healthy subjects, and thus highlight the usefulness of tailoring the analyses to each subject.

3.5.1. TOPOGRAPHICAL ANALYSES

Traditional ERP analyses revealed topographies and time courses similar to the ones observed in previous studies (BEKINSCHTEIN ET AL., 2009; KING ET AL., 2011; WACONGNE ET AL., 2011; FAUGERAS ET AL., 2012). EEG results, summarized in FIGURE 3.2, showed that local effects arose between approximately 130 ms and 350 ms and mainly evoked a frontal negativity (MMN) followed by a central positivity (P300a). In contrast, global effects were mainly observed from 200 ms onwards, and were characterized by a sustained centro-posterior positivity (P300b) peaking between 300 ms and 500 ms. These two effects replicate the EEG components previously reported in this type of experimental protocol. Interestingly, and as can be seen on FIGURE 3.2, a vast amount of inter-individual variability can be observed in the single-subject data. This variability thus highlights the potential usefulness of tailoring the analyses to each subject.

3.5.2. DECODING ACROSS TIME

To maximize the detection of the neurophysiological responses elicited by local and global novelties, we applied, to each subject separately, a multivariate pattern (MVP) classifier. The classifications

scores of each classifier reported below refer to the area under the curve (AUC) estimated from a receiver operative curve analysis (see methods).

We first aimed at characterizing the dynamics of classifications scores across time, and thus trained a different classifier for each time sample. As expected, during the time period preceding the onset of the last sound, both local and global decoding remained at chance level (AUC did not differ from 50%). Accuracy of the local decoder exceeded chance level earlier in the epoch than did the accuracy of the global decoder. As can be seen on FIGURE 3.3.A., two peaks of local decoding were observed in each experiment between 150 ms and 300 ms after stimulus onset. Mean single-trial local classification scores across subjects varied from 62.0% to 77.8% of trials depending on the experimental apparatus (all p_{FDR}<.05).

The dynamics of global effects were more variable across experiments. Experiment 1, in which subjects were instructed to count rare global deviant trials, revealed a quick rise of EEG-based classifications scores around ~130 ms, followed by a sustained period during which global classification remained above chance almost throughout the epoch (between 300 ms and 730 ms). However, in intracranial EEG (Experiment 2), despite similar instructions, only a transient period of global decoding was seen, peaking at ~260 ms, then dropping back to chance level. Finally, Experiment 3, in which subjects were recorded with MEG and were instructed to merely pay attention to the sounds, demonstrated sustained global classifications scores from 200 ms onwards (AUC=66%). These results suggest that the neurophysiological signatures of novelty detection seem relatively independent from task instructions.

Interestingly, a sharp increase in global classifications scores was observed as early as 150 ms in the attentive MEG condition (Experiment 3). Although much smaller (AUC=55.0%, p_{FDR}<.05) a similar trend was also apparent in the counting EEG condition (Experiment 1). Finally, intracranial recordings, mainly taken from the temporal cortices (SUPPLEMENTARY FIGURE 3.7) presented significant global classification performance between 100 ms and 300 ms (max AUC=66.1%, p_{FDR}<.05). Taken together, these results suggest, contrary to what was previously suggested (BEKINSCHTEIN ET AL., 2009), that global novelty can affect early processes too.

Finally, subjects who were distracted by a concurrent visual task (Exp 4.) presented lower but still significant local classifications scores (AUC=63.7%, p_{FDR} < .05). Moreover, distraction dramatically impaired global classifications scores, which consequently failed to reach significance across subjects (AUC=54.0%, p_{FDR}>.05).

Overall decoding local and global effects across time showed that multivariate pattern classifiers could extract qualitatively similar effects as the ones observed from ERPs (for ERFs see (WACONGNE ET AL., 2011)) but could also reveal subtle effects such as an early global effect unreported in previous studies.
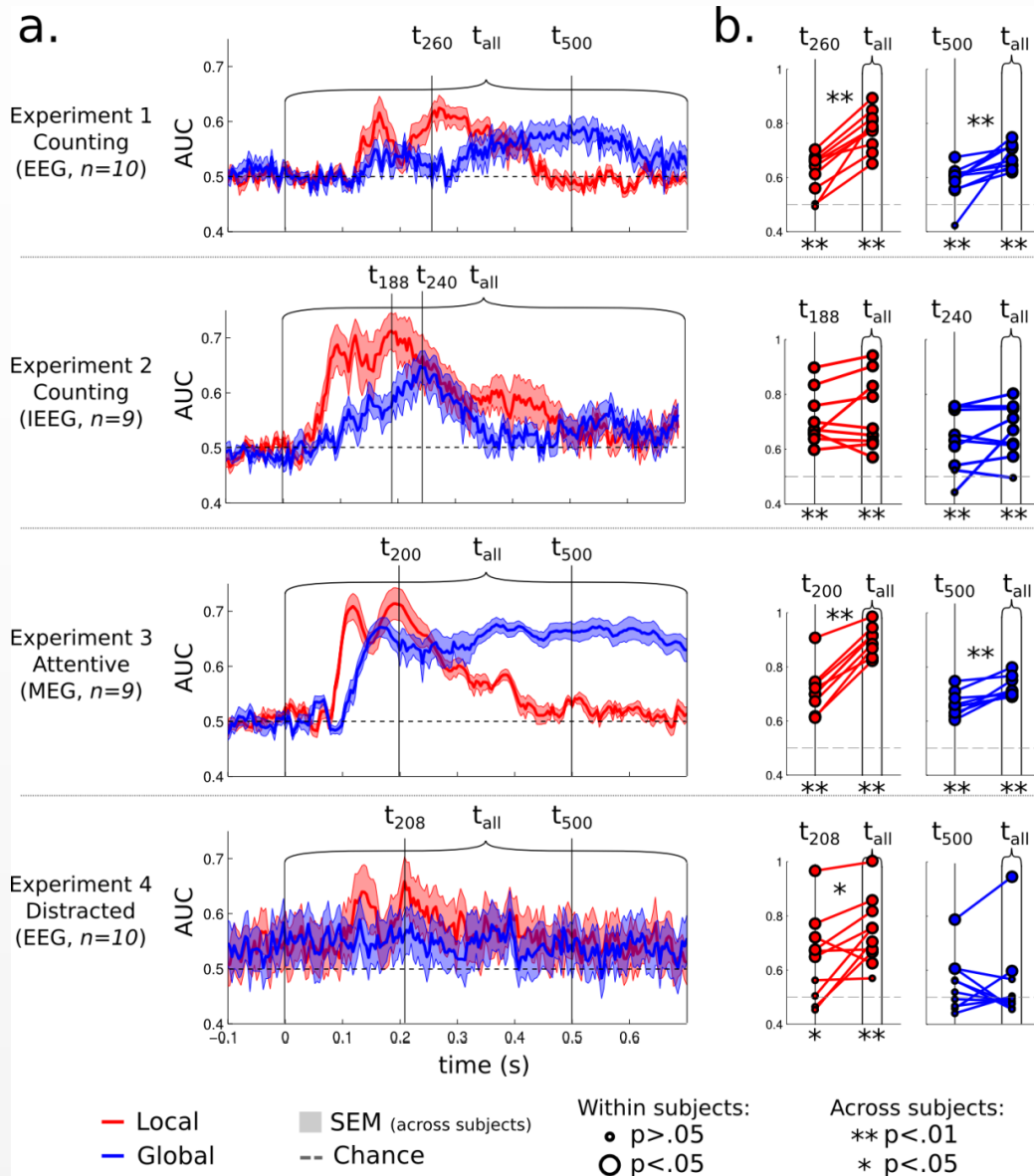
FIGURE 3.3 LOCAL AND GLOBAL MULTIVARIATE DECODING SCORES.

a. Decoding of the local effect (red) and of the global effect (blue) was applied successively to each time sample of the scalp EEG, MEG and intracranial EEG recordings obtained under different experimental conditions: subjects either counted the global deviant trials (Experiments 1-2), were attentive to the sounds (Experiment 3), or were distracted by a visual task (Experiment 4). Results demonstrate a non-sustained decoding of the local effect (~130-400 ms), with above-chance performance regardless of recording apparatus and experimental condition. Decoding of the global effect appeared later and was more sustained in time, but was absent in the distracted condition.

b. Comparison of the decoding scores based on the best time point (left dot in each graph) or the full trial dynamics (right dot). Each dot represents the decoding score of an individual subject. All subjects but one presented significant local decoding scores. All experiments led to significant global decoding scores, except for the distracted condition. Local and global decoding scores based on the dynamics of the electrophysiological signal across multiple time samples (t_{all}) led to a significant improvement of decoding scores in most scalp recordings.

3.5.3.   USING DYNAMICS TO FACILITATE DECODING

Decoding a spatial topography at each time sample, as was done in the previous section, can overcome individual topographical variability but remains dependent on the precise timing of a given effect. To maximize the extraction of local and global effects, we thus trained another decoder using the full dynamics of brain signals on a given trial. For each subject separately, and for local and global effects, this decoder was trained to distinguish the standard and deviant trials based on all the information available on a given trial (*all channels* x *all time samples*). Results are presented in FIGURE 3.3.B.

Overall, this dynamic approach provided better classifications scores than in the previous section. To prove this, we compared it to the performance of the best time sample of the previous section. Note that is a very conservative test. Indeed, the a posteriori selection of the best time sample is not cross-validated, and thus likely overestimates the actual scores one could hope to obtain if an independent data sample was available (see *e.g.* (VUL ET AL., 2009B)). Still, an ANOVA across subjects, contrasts (local and global) and type of classifier (dynamic versus best single time point) revealed a significant main effect of classifier type, $F(1,37) = 47.9$, $p<10^{-10}$, indicating better classification overall with the dynamic approach (mean AUC =72.0%) than with the previous approach (63.7%). This improvement was robust across recording methods (all $p<.05$) except for intracranial EEG ($p>.33$), and therefore suggests that the classifier manages to exploit the time course of brain signals to provide information at the single-trial level (See SUPPLEMENTARY FIGURE 3.6 for a depiction of single trials' local and global prediction in Experiment 3).

In more detail, using the dynamic approach, the local classifications scores reached an average AUC of 77.8% ($p<.01$) in the counting EEG condition (Experiment 1), 73.2% ($p<.01$) in the counting intracranial condition (Experiment 2), 73.5% ($p<.01$) in the distracted EEG condition (Experiment 4) and 89.8% ($p<.01$) in the attentive MEG condition (Experiment 3). The latter performance, interestingly, was higher than the one obtained from high-density EEG (all $p<.01$) and even than intracranial recordings ($p<.05$). Importantly, across four experiments, all but one subject (from the distracted group) presented significantly above chance local classifications scores.

Similar results were obtained for global classifications scores across experiments 1-3. The counting EEG condition (Experiment 1) led to an average AUC of 67.9% ($p<.01$), the counting intracranial condition (Experiment 2) led to an average AUC of 66.1% ($p<.01$) and the attentive MEG condition (Experiment 3) led to an average AUC of 72.3% ($p<.01$). Amongst the 28 subjects who were paying attention to the sounds, only one subject failed to present a significant global decoding score.

Crucially, global classifications scores were dramatically reduced in distracted subjects ($p<.01$ as compared to EEG and MEG recordings (Experiments 1 and 3); $p<.05$ as compared to intracranial recordings (Experiment2)). Not only was the global decoding score not-significantly different from chance for distracted subjects (AUC=55.0%, $p>.05$), but 8 out of 10 subjects did not present any significant global decoding.

In summary, by maximizing the extraction of information from individual recordings, these results demonstrate that the human brain response to auditory deviancy, both local and global, can be detected in single trials and a fortiori in individual subjects. It also confirm that this information is not entirely dependent on the fact that subjects are asked to count the rare global deviant trials, but remains present under the instruction to merely attend to the sounds. Finally, the comparison between the active and the distracted conditions confirms the automaticity of processes underlying local novelty detection, and the necessity of attention in the detection of global novelty.

3.5.4. GENERALIZATION OF EFFECTS ACROSS CONTEXTS

The above analysis, while sensitive, could be partially affected by a contextual modulation of the local mismatch effects (MMN). The MMN elicited by an AAAAB sequence, indeed, is stronger when this sequence is rare than when it is frequent (WACONGNE ET AL., 2012). This effect could be used by the global decoder to provide early above-chance classification of global deviants from global standards, even though it does not reflect a genuine response to global novelty. To address this issue, we reasoned that cross-context generalization would provide a stricter criterion for a physiological signature of the brain's response to global novelty. For instance, a neuronal process responding to rare sequences, if generic, should be found whenever a rare global deviant sequence is presented, whether this sequence is aaaaB (in blocks where aaaaa is the frequent stimulus) or aaaaa (in blocks when aaaaB is the frequent stimulus). Such a generalization analysis could sort out the genuine signatures of global effects from the modulations of local novelty effects. With this idea in mind, we investigated the generalization of global classification across different local contexts (and vice-versa see methods), and restricted the local and the global analyses to the early (0-368 ms) and to the late (368-736 ms) time windows respectively. As intracranial classifications scores were not significant in the late time window (FIGURE 3.3), we tested this analysis on experiments 1, 3 and 4. Results are presented in FIGURE 3.4.

An ANOVA across subjects, contrasts (local or global) and type of classifier (using both contexts or within-context decoding) showed that classifications scores resulting from within-context decoders were smaller than those obtained from decoders using all trials (section I): $F_{(2,28)}=26.56$, $p<10^{-6}$. This is expected as restricting the decoder to trials performed in a given context automatically reduces the number of trials available for the training set. Note however that the within-context classifications scores remained significantly above chance in all experimental conditions: Local: Experiment 1: 69.1% ($p<.01$), Experiment 3: (71.2 % $p < .01$), Experiment 4: 68.8% ($p<.01$); Global: Experiment 1: 66.0% ($p<.01$), Experiment 3: 63.2% ($p<.01$), Experiment 4: 56.7% ($p < .05$).

Cross-contexts generalization scores appeared significantly worse than within-context classifications scores (Local: Experiment 1: $p<.01$, Experiment 3-4: $p<.05$), Global: Experiment 1: $p<.01$, Experiment 3-4: $p<.1$). As can be seen in FIGURE 3.4.A. presenting the MEG generalization scores across time, the differences between within-context and across-contexts scores were mainly visible i) in early time windows; and ii) in the global contrast. This result suggests that part of the early global effect observed in section I was due to an early modulation of novelty responses that did not generalize across contexts. However, the overall reduction of cross-context generalizations suggests that this conceptually more suitable analysis may, in practice, be less appropriate when the signal-to-noise ratio is low.

Crucially, whereas all local generalization scores remained significantly above chance (Experiment 1: 57.1%, Experiment 3: MEG: 66.3%, Experiment 4: 61.5%, all $p<.01$), global generalization scores were now exclusively significant in subjects who were paying attention to the sounds (Experiment 1: 57.9%, Experiment 3: 60.2%, both $p < .01$). Distracted subjects did not present any significant global generalization scores (48.1%, $p>.1$), and the latter were significantly smaller than the ones obtained in the counting (Experiment 1: $p< .001$) and the attentive (Experiment 3: $p<.0001$) conditions.

Finally, it is interesting to note that global generalization scores steadily increased from 180 ms after stimulus onset, until they eventually reached, at the end of the epoch, scores that resembled those obtained with the within-context decoding analysis in MEG (FIGURE 3.4.A). This pattern of results suggests that distinct neurophysiological signatures were initially elicited by the two forms of global deviancy tested here. Most likely, the rare xxxxY sequence was easily detected in an xxxxx context, whereas, conversely, the rare xxxxx sequence took a longer time to be detected in an xxxxY context. Late in the epoch, however, the neuronal activity that they evoked eventually converges to the same state, thus permitting similar levels of within-block classification and cross-block generalization.
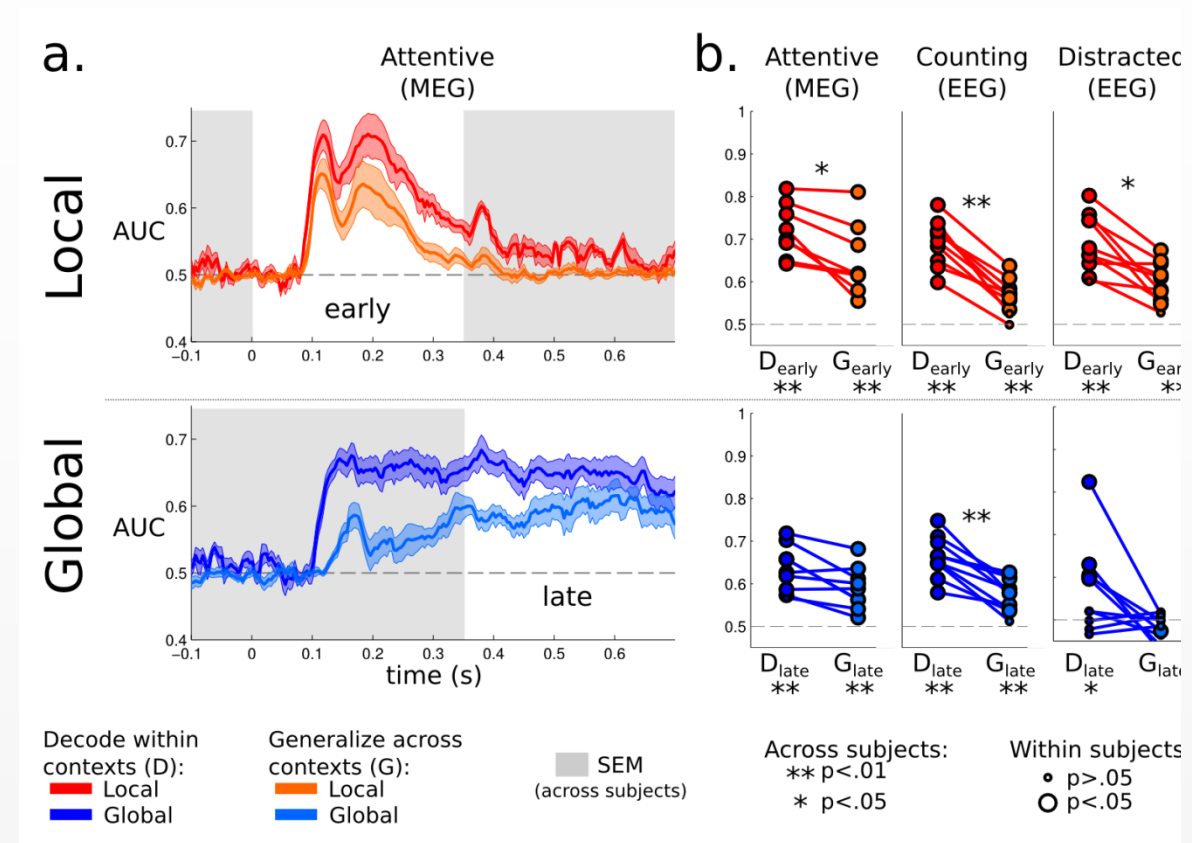
FIGURE 3.4 GENERALIZATION OF THE MULTIVARIATE DECODING ACROSS EXPERIMENTAL CONTEXTS.

Generalization analyses consist in training the classifier in a given context (e.g. local standard trials only) and testing the ability of the classifier to generalize to another context (e.g. local deviant trials only). For example, we train the classifier to discriminate global deviants from global standards, within the context of local standard trials, and then we test the performance of the classifier on the same task, but within the context of local deviant trials.

a. Local (red) and global (blue) scores obtained from within-context (D) and cross-context (G) generalization analyses are plotted as a function of time. Local effects generalized early on (orange) and rapidly vanished. Global effects generalized increasingly well over time (cyan) until generalization performance did not differ significantly from decoding performance (blue).

b. Each dot represents the decoding and generalization score of an individual subject. Although the generalization of local effects was significantly smaller than decoding performance, it remains above chance in all experiments. Generalization of global effects was however only significant in the attentive and counting condition.

3.5.5.   PATIENTS: DECODING ACROSS TIME AND DYNAMICS

The above results demonstrate that multivariate classifiers efficiently capture the dynamics of the brain responses to local and global deviancy. In particular, we confirmed that the processing of local novelty was relatively independent of attention, while the late effects elicited by global novelty only emerged and generalized across contexts in attentive subjects. These analyses allowed us to formulate a simple hypothesis: in patients with communication disorders, cerebral activity in the early and late time windows, respectively, could provide useful markers of automatic versus conscious processing of auditory regularities. We thus applied the present method to 158 EEG recordings acquired from patients suffering from disorders of consciousness (DOC). Individual and group results are summarized in FIGURE 3.5.
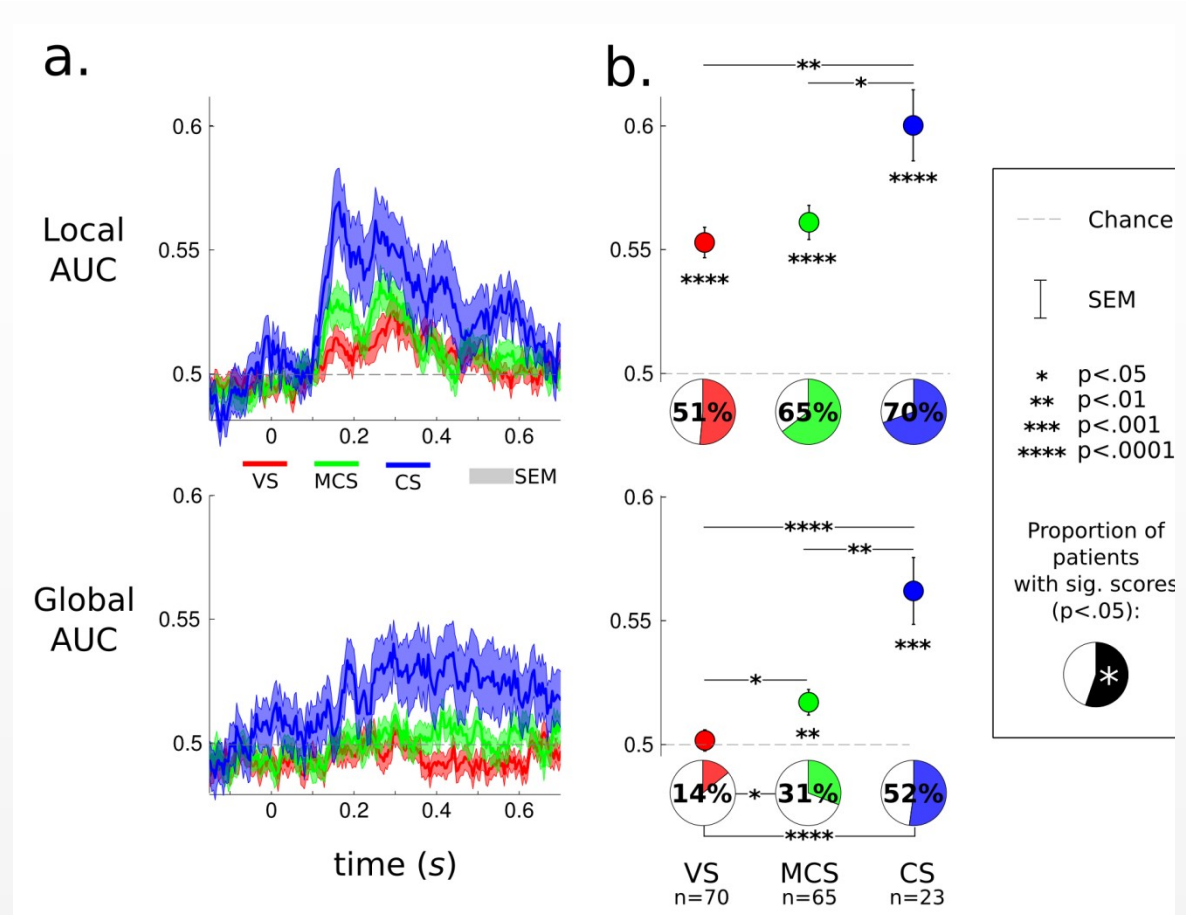
FIGURE 3.5 LOCAL AND GLOBAL DECODING IN PATIENTS WHOSE STATE WAS DIAGNOSED AS VEGETATIVE (VS), MINIMALLY CONSCIOUS (MCS) AND CONSCIOUS (CS).

a. Local (top) and global (bottom) decoding scores are plotted as a function of time. Overall, local and global decoding scores follow the same qualitative trends as the ones observed in healthy subjects (Figure 2). CS patients (blue) presented higher local and global decoding scores over time than either MCS (green) or VS (red) patients.

b. Decoding scores obtained from the EEG dynamics of each trial are summarized for each state of consciousness. The graphs give the mean and standard error of the decoding scores in each group, its significance relative to chance level, and the significance of pair-wise group comparisons. Pie charts summarize the proportion of patients who presented significant decoding scores.

First, it appeared that the decoding of the EEG dynamics of DOC patients was qualitatively similar to what was observed in healthy controls: local classifications scores were maximal between 150 ms and 300 ms after stimulus onset, whereas global effects, if present, appeared later and were relatively sustained between 250 ms and 700 ms (see FIGURE 3.5.A). Classifiers based on the full dynamics of the EEG signals (see methods) were again superior to selecting the best time point obtained from healthy controls (local: $p<.10^{-5}$, global: $p<.01$) or directly from DOC patients (local: $p<.0001$, Global: positive trend n.s.). These results therefore confirm the utility of our decoding approach.

Despite similar qualitative results, quantitative comparisons with healthy controls (Experiment 1) showed that DOC patients presented lower local classifications scores (AUC=56.3%, $p<10^{-5}$) and lower global classifications scores (AUC=51.7%, $p < 10^{-5}$). Interestingly, when comparing DOC patients to healthy distracted subjects (Experiment 4), results demonstrated significant differences only in local classifications scores ($p<10^{-4}$) but not in global classifications scores ($p>.1$).

Despite being reduced, the patients' classifications scores were not at chance. Local AUCs were ranged on average from 55.3% amongst VS patients, 56.1% amongst MCS patients, to 60.0% amongst CS patients. These values were above chance within each group of patients (all p<.0001). Local classifications scores of VS and MCS patients were not significantly different from one another (p>.1). However, CS patients presented significantly higher local classifications scores than both MCS (p<.05) and VS (p<.01) patients.

Crucially, for global decoding, the scores were above chance for MCS (AUC=51.7%, p<.01) and CS (AUC=56.2%, p<.001) patients, but VS patients, on average, did not present any significant global decoding effects: AUC=50.2%, p>.1. Moreover, the global decoding AUCs of VS patients were significantly smaller than both those of CS patients (p<.0001) and those of MCS patients (p<.05). Note that the latter also presented lower global classifications scores than CS patients (p<.01).

The above group differences could be due to a minority of subjects, or to an overall group effect. An advantage of the present single-trial MVP analysis is that it provides within-subject significance. We thus quantified the proportion of patients who presented significant local and global classifications scores. The results, summarized in FIGURE 3.5.B. showed that 51% of the VS patients, 65% of the MCS patients and 70% of the CS patients presented significant local classifications scores. This suggests the presence of an MMN amongst these subjects. The proportions of patients with significant Local classifications scores did not differ across groups, neither with full (VS *versus* MCS *versus* CS) nor with pair-wise (VS *versus* MCS, MCS *versus* CS, and CS *versus* VS) chi-square tests (all p>.1).

The results were quite different for global decoding, as the proportion of patients presenting significant global classifications scores nearly doubled across states of consciousness. First, only 14% of VS subjects showed significant global decoding. Amongst these 14%, half presented scores which resisted a FDR correction for multiple comparisons across subjects. Like other studies, this result suggests that a small proportion of carefully diagnosed VS patients may still have residual consciousness (BYRNE ET AL., 2010). Second, in contrast, 31% of the MCS patients and 52% of the conscious patients presented significant global scores. The proportions of significant global scores across the three states of consciousness were significantly different from one another: $\chi^2(2, N=158)=13.73$, p<.001. Pair-wise chi-square tests confirmed this finding by showing a smaller proportion of patients with global decoding in VS relative to MCS ($\chi^2(1, N=135)=4.39$, p=.036) and to CS ($\chi^2(1, N=93)=11.74$, p=.0001). No differences were observed between the proportions of CS and MCS patients with significant global decoding ($\chi^2(1, N=88)=2.50$, p=.113).

To increase the specificity of the present results, we also applied the generalization method detailed above. Scores obtained from within-context classification were similar to but lower than the classifications scores obtained from the joint analysis of both contexts (unsurprisingly given that the number of training trials was halved). For the local effect, while not differing from one another (VS-MCS: p=.252), local scores from VS (AUC=56%, p<.0001) and MCS (AUC=57%, p<.0001) were significantly smaller than those obtained than CS patients (AUC=61%, p<.0001, CS-VS: p=.005, CS-MCS: p=.039). Global within-context classifications scores presented a similar pattern: VS (AUC=54%, p<.0001) and MCS (54%, p<.0001) scores did not differ from each other (p=.969), but were significantly smaller from CS (59%; both p=.001). Finally, cross-context generalization scores were low (all below 53%). Local cross-context generalization performance was lower for VS patients than for MCS (p=.038) and CS (p=.003) patients, but none of the global cross-context generalization scores differed from one another (all p>.287).

In summary, by quantifying the proportion of patients with significant local and global effects, we confirmed the earlier finding that DOC patients may still exhibit similar local mismatch effects, relatively independently of their conditions (FISCHER ET AL., 1999; NACCACHE ET AL., 2005; BEKINSCHTEIN ET AL., 2009;

FAUGERAS ET AL., 2012; TZOVARA ET AL., 2012), and found that the capacity to show global effects was strongly modulated by the state of consciousness. A classifier based on the whole set of trials and their temporal dynamics proved the most sensitive tool to detect these local and global effects. Cross context generalization was unable to dissociate the three types of patients, presumably because of a halving of the number of training trials.

3.6. DISCUSSION

In this study, we investigated, at the single trial level, the neuronal response following the violation of two embedded auditory regularities structured across two different time ranges ("local" and "global"). We implemented, for this purpose, a series of multivariate pattern (MVP) analyses extracting this information from the temporal dynamics of the neurophysiological activity recorded with high-density EEG (Experiment 1 and 4, n=19), intracranial EEG (Experiment 2, n=9) or MEG (Experiment 3, n=10). Analyses were performed on attentive and distracted healthy control subjects, as well as on three types of patients suffering from disorders of consciousness (DOC), namely patients in vegetative state (VS, n=70), minimally conscious state (MCS, n=65) and conscious state (CS, n=23), all recorded with high-density EEG for clinical purposes.

Results from control experiments revealed that when subjects were attentive, single-trial classification could lead to AUCs between 73% and 90% for local novelty, and between 66% and 72% for global novelty, depending on the recording apparatus (Experiment 1-3). Remarkably, MEG recordings achieved classification scores comparable to, or even higher than, intracranial EEG data. Moreover, we showed that providing the decoder with multiple time samples systematically improved classification as compared to a decoder trained on the single best time sample. This result therefore demonstrates the utility of MVP classifiers in the present context, and confirms that this method can reliably and automatically extract neuronal dynamics specific to each subject in order to efficiently classify each trial.

It should be noted that our method, although different in technical details, follows a similar approach to that taken in a recent study (TZOVARA ET AL., 2012). Tzovara and collaborators decoded, from EEG recordings of coma patients, the difference between regular and irregular trials, that is, the equivalent of the local effect in the present study. To classify each trial, the authors used a different type of classifier which modeled the ERPs with a mixture of Gaussians. Advantages and disadvantages can be identified in each of these classification methods. Our approach does not make any Gaussian assumptions, can make use of imbalanced training dataset and can extract a large number of different types of topographies by searching across all channels – which therefore are not restricted to EEG. In contrast, de Lucia and collaborators first transform the ERPs into components. This computational step reduces the dimensionality of the data, and thus likely improves the efficiency of the ensuing classification process. However, their classifier is unable to optimally use imbalanced datasets, which are necessarily encountered in this type of novelty experiment. Taken together, these differences may explain why our approach provided slightly better classifications scores (AUC=77.8%) than theirs (AUC=71%) in similar control subjects recorded with EEG. Future efforts should capitalize on a combination of these methodological technicalities.

Crucially, our MVP classifiers replicated and extended previous observations on the key electrophysiological properties of local and global effects (BEKINSCHTEIN ET AL., 2009). As expected, local novelty mainly affected the early part of the neural signal (< 300 ms) and remained unaffected by visual distraction. In sharp contrast, global novelty elicited late and stable effects in both counting and attentive sub-

jects, but most distracted subjects presented dramatically reduced, and in fact, non significant global classifications scores.

The present decoding approach allowed us to investigate whether the neuronal activities elicited by local and global novelty are specific and reproducible enough to generalize from one context to the other. Specifically, we asked which aspects of the neuronal response to global novelty could generalize from a context in which the AAAAB sequence was rare (in AAAAA blocks) to another in which the AAAAA sequence was rare (in AAAAB blocks), and *vice-versa*. Generalizations of the global effects confirmed a progressive increase in the similarity of these two types of global novelty responses from 180 ms onwards, until they eventually fully resembled each other at the end of the trial. Conversely, local novelty detection showed a significant generalization across contexts only in the early part of the event-related response. Taken together, these results reveal a double dissociation. Local effects are attention independent, context dependent and are not maintained across time. By contrast, late global effects are attention dependent, context independent and stable for a prolonged temporal duration.

One of the major motivations of the Local Global protocol is to provide a minimal design that dissociates two types of auditory novelty processing – one generating the MMN followed by a P300a, both likely being automatic, and the other generating the P3b which depends on working memory and conscious access. This goal is of particular importance for DOC patients. Despite an increasing interest for this clinical population (LAUREYS ET AL., 2004; OWEN ET AL., 2009B), unambiguously distinguishing patients suffering from communication disorders from those with a genuine loss of conscious processing remains a challenging task (OWEN ET AL., 2006; LAUREYS AND SCHIFF, 2011). In this context, our present capacity to dissociate, from EEG alone, an automatic process of local novelty detection from a later process that depends on conscious processing thus opens up the possibility of detecting states of consciousness independently of the patient's ability to communicate.

We applied our MVP classifier to 158 EEG recordings acquired at bedside from patients suffering, or recovering from a DOC. The results demonstrated that, at the group level, our method could accurately distinguish neuronal responses elicited by local deviants relative to local standard sounds: 51 % of VS, 65% of MCS and 70% of CS patients presented significant local classifications scores. Moreover, whereas CS patients presented significantly higher classifications scores, VS and MCS patients did not differ from one another, suggesting that the cerebral processes that detect local novelty are not unique to conscious processing and can remain functional in all states of consciousness. These results are in line with a series of studies demonstrating the presence of the MMN in many DOC patients (WIJNEN ET AL., 2007; BEKINSCHTEIN ET AL., 2009; FISCHER ET AL., 2010; FAUGERAS ET AL., 2012), including coma patients (KANE ET AL., 1996, 2000; TZOVARA ET AL., 2012). Indeed, they confirm that the effects elicited by local changes in pitch, as observed in the auditory odd-ball experiment, are poor predictors of the state of consciousness (BEKINSCHTEIN ET AL., 2009; TZOVARA ET AL., 2012). The lack of a detectable local effect in some patients could be due to a variety of causes, including poor signal-to-noise, excessive number of artefacted trials, or an impairment to auditory pathways.

The situation was quite different for the global effect. Crucially, the detection of global deviants was considerably reduced in DOC patients as compared to healthy controls. As a group, VS patients did not present any significant global effects, and their classifications scores were smaller than those of MCS and CS patients. Taking advantage of the fact that the present analyses allow for single-subject predictions, we showed that only a small proportion (14%) of VS patients exhibited a significant global decoding score, and that this proportion was significantly smaller than the proportions of MCS (31%) and CS (52%) patients in whom a global effect could be significantly detected. This finding confirms that global effects provide a reliable, although partial, index of the state of consciousness.

Further studies will need to assess the sensitivity and specificity of the global effect as a test of consciousness. Although a small fraction of VS patients still showed a significant global effect, note that this need not necessarily imply a failure of our test, but rather may indicate that the clinical label of VS may not be fully reliable. Indeed, fMRI studies also reveal that a fraction of VS patients, continue to present complex cortical responses that suggest preserved consciousness (BYRNE ET AL., 2010). We have previously reported that two VS patients with a significant global effect moved to the MCS category within the next few days (FAUGERAS ET AL., 2011).

In the converse direction, unfortunately, our test clearly lacks sensitivity since about half of CS patients and two-third of MCS patients did not present any significant global classifications scores. Further research should determine if this problem can be remedied, for instance using a larger number of trials, different days of testing, or better noise reduction techniques, or if it reflects a genuine cognitive limit, whereby patients are conscious but too cognitively impaired to successfully detect global novelties. An important issue is that the global effect is known to vanish under conditions of inattention (BEKINSCHTEIN ET AL., 2009). However, our auditory stimuli are monotonous and devoid of interest, and some patients are likely to lose focus during the 40 min recording session. In the future, special efforts should thus be dedicated to enhance the patients' motivation and attention towards the stimuli, as well as to improve the quality of EEG recordings.

These difficulties are not unique to our test. Most other tests of consciousness currently require patients to understand and maintain, for several minutes, a complex instruction such as imagining playing tennis (OWEN ET AL. 2006B), or retrieving the answer to a spoken question (MONTI ET AL. 2010). These tests, like ours, are therefore asymmetrical: when positive, they are highly indicative of preserved consciousness, but they may also fail to detect residual consciousness if the patient suffers from hearing, linguistic, attentional or working memory deficits. For instance, in the Monti et al (BYRNE ET AL., 2010)'s study, 30 out of 31 MCS patients, who therefore gave occasional behavioral signs of consciousness upon clinical examination, showed no signs of communication via imagined tennis playing or spatial navigation. Relative to these fMRI studies, the current approach presents at least two advantages. First, it relies on a method (EEG) which is easy to implement, available in all clinics and applicable at bedside. Second, it only depends on subjects' attention to the stimuli and does not require complex task instructions.

Alternative ways of investigating consciousness, which bypass entirely the need to attend to external stimuli, are also being developed. For instance, Massimini and collaborators have developed a TMS-EEG apparatus that tests the complexity and the functional connectivity of brain responses to TMS pulses. The results demonstrate that this artificial probe differentiates the states of consciousness in sleep (MASSIMINI ET AL., 2010), anaesthesia (FERRARELLI ET AL., 2010) and DOC patients (ROSANOVA ET AL., 2012). Our own research, again using only high-density EEG, also suggests that the intrinsic complexity of the EEG and, especially, the amount of information shared across distant electrode sites, provides an index that usefully complements the present approach (King, Sitt et al, *submitted*; Sitt, King, et al, *in prep*). Ultimately, a combination of simple experimental protocols with sophisticated signal post-processing, as attempted here, may prove crucial for the automatic diagnosis of non-communicating subjects.

3.7. ACKNOWLEDGMENTS

3.8. SUPPLEMENTARY MATERIALS

FIGURE 3.6 SINGLE TRIAL PROBABILITIES FOR EACH SUBJECT IN EXPERIMENT 3 (ATTENTIVE MEG).

Each graph represents the decoding results for a single subject, in either local decoding (top row) or global decoding (bottom row). Each dot shows the predicted probability of being standard for a given trial, as estimated from an independent classifier using the full time window ([0 736] ms). Red and blue histograms indicate the distributions of these probabilities over trials, separately for trials with a deviant (red) or a standard sequence (blue). The separation of these distributions therefore indicates a good decoding performance, while their overlap indicates inter-trial variability that could not be resolved by the decoder.

FIGURE 3.7 . INTRACRANIAL ELECTRODE LOCATIONS AND DECODING SCORES FOR EACH ELECTRODE.

Each dot represents one of the 401 electrodes implanted in 9 epileptic patients. Large circles indicate significant decoding scores (p_{FDR}<.05). Dots' color codes for the decoding AUC obtained from classifier using all time samples following stimulus onset.
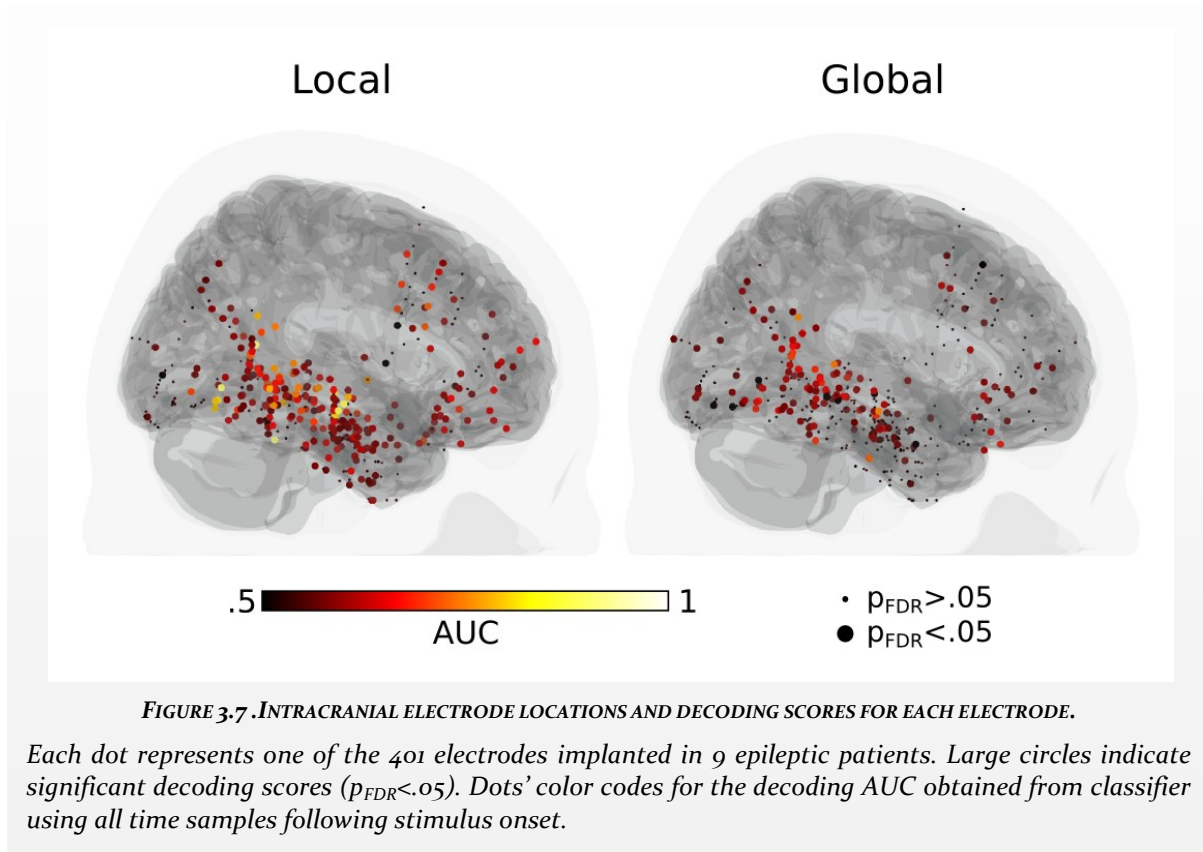
MVPAs extract the dynamics of the brain signals

We show that a single classifier using a large time window outperforms the best classifier using single time points (FIGURE 3.3.B). Two non-exclusive hypotheses could account for the improved classification performances obtained with a single classifier:

H_0) *The slow-frequency nature of ERPs/ERFs account*: consecutive time sample contain the same information but are affected by different noises.

H_1) *The extraction of ERPs/ERFs dynamics account*: consecutive time sample contain different information.

If H_0 entirely explains the present findings, providing the average of consecutive time samples to a classifier should lead to similar decoding performances as a single classifier using the very same time samples separately. We thus compared the results obtained from:

- a unique classifier using the dynamics of all time points between 0 and 700 ms (red)
- distinct classifiers tested at each time point (purple)
- distinct classifiers tested on the average time course of the ERFs over a time window of 16 ms (yellow), 32 ms (green) and 64 ms (turquoise).

FIGURE 3.8 MVPAS CAPTURE THE SIGNAL DYNAMICS
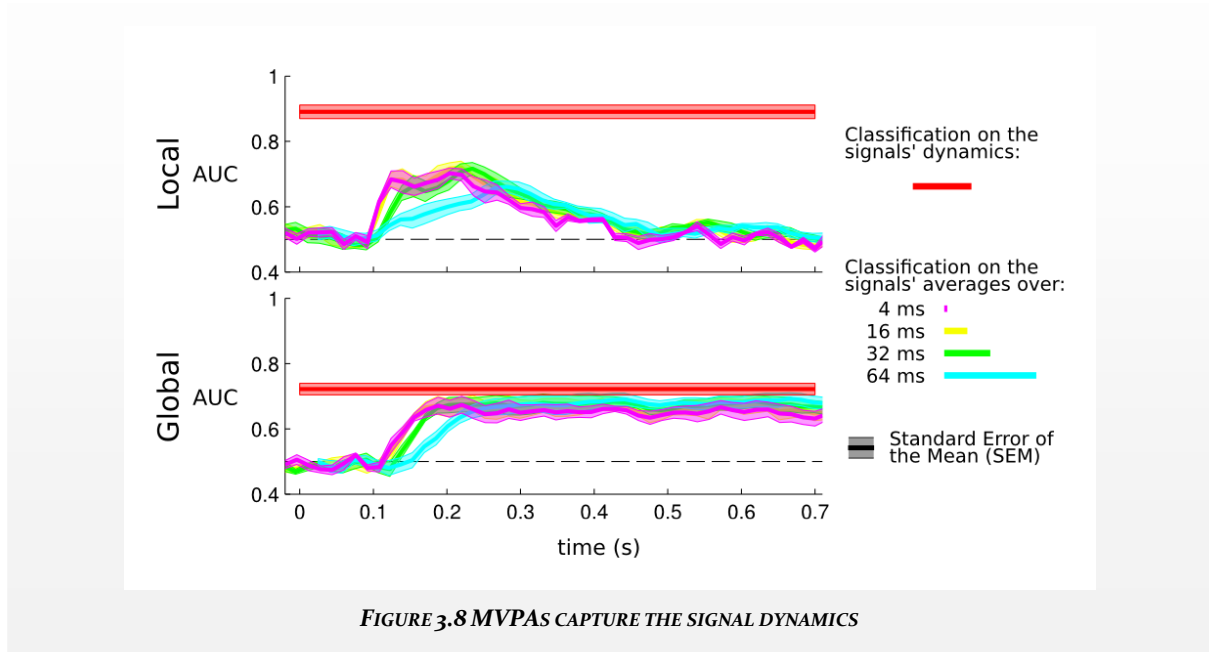
The results appear in SUPPLEMENTARY FIGURE 3.8. The AUC of different classifiers applied to Experiment 3 is plotted as a function of time. The purple line depicts the decoding scores obtained with distinct classifiers tested at each time point. The red line depicts the decoding scores obtained with a unique classifier based on the entire signal dynamics between 0 and 700 ms. The yellow, green and turquoise lines refers to the performance obtained with distinct classifier based on the averaged time course of a sliding 16 ms, 32 ms or 64 ms window.

The results show that, at best, averaging the brain signals across consecutive time-samples did not improve classification performances. Importantly, the classifiers using the dynamics of the signals remained systematically better than the classifier using averaged ERF signals. These results demonstrate that the present approach enables the extraction of the ERF dynamics and thus outperforms a traditional averaging approach.
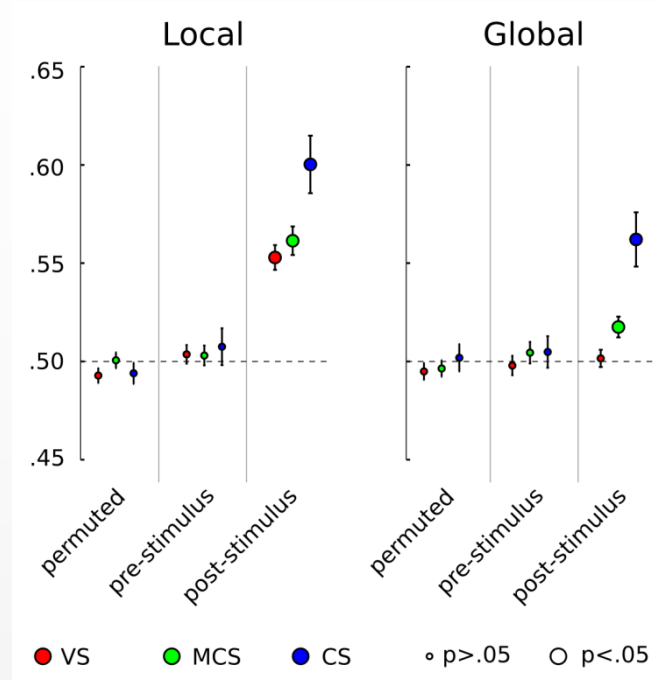
FIGURE 3.9 EXPERIMENT 5: SUPPLEMENTARY STATISTICS.

Mean local and global AUCs are plotted effects for each group of patients. Error bars indicate the SEMs across subjects. Two additional statistical analyses were implemented to i) show statistical robustness and ii) test whether the classification performance could result from block-specific artefacts such as muscle contraction and eye movements. Both shuffling the trial labels("permuted") and applying the classifier to the time period preceding the onset of the last sound ("pre-stimulus") led to chance-level AUCs. These results contrast with the significant classification of post-stimulus onset, and therefore strongly suggest that the present results are not imputable to movement artefacts or issues related to the block design (GOLDFINE ET AL., 2012B).
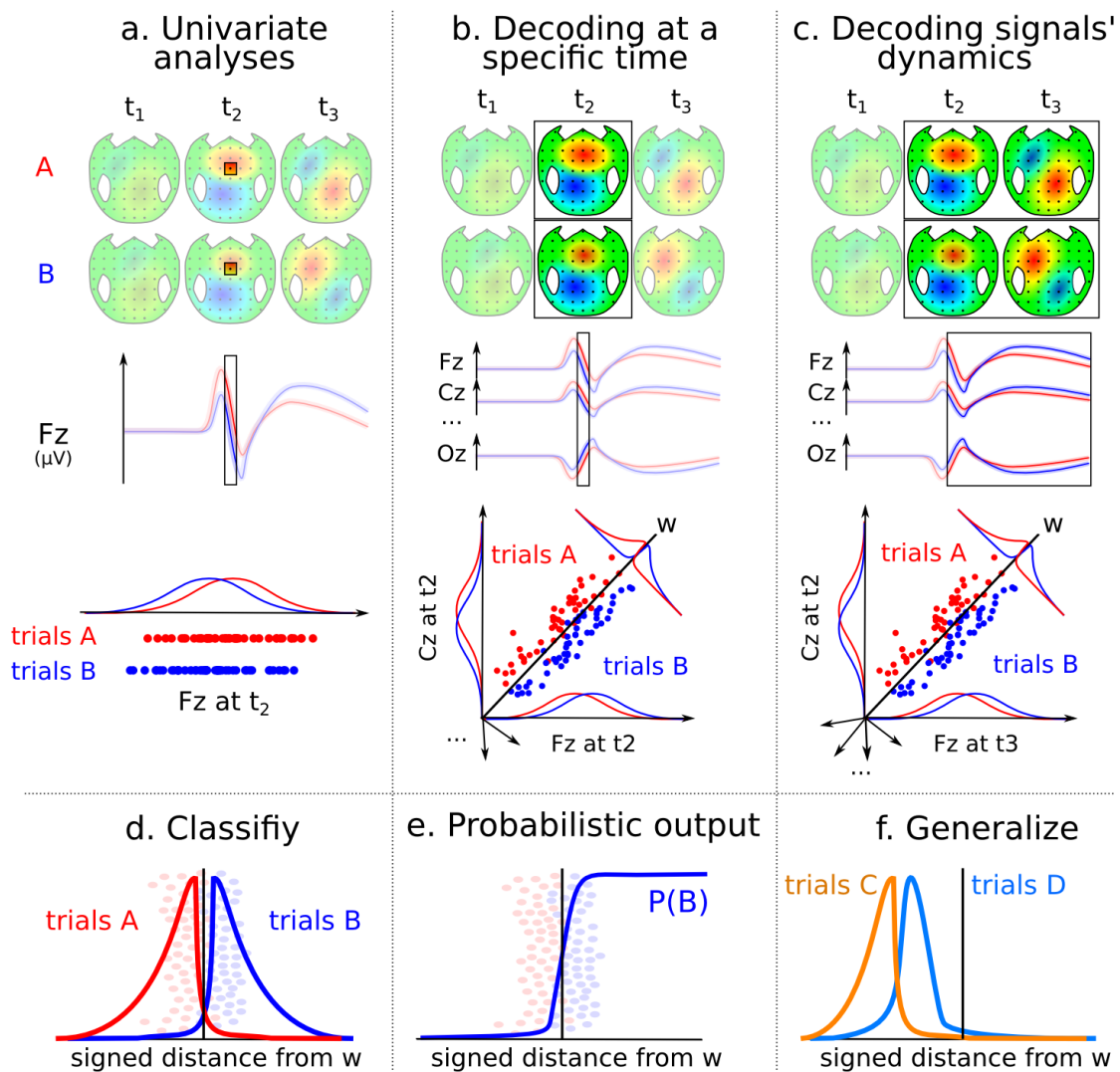
FIGURE 3.10 SCHEMA OF THE DECODING METHODS.

a. Univariate analyses compare the distributions of the signals recorded in a single EEG channel at a single time point (e.g. t_2) in two conditions (A and B). By contrast, the present multivariate pattern analyses compare A and B trials in an n-dimensional space.

b. A multivariate classifier using all channels at a given time can be used to extract the information present in the topography (i.e. the information contained across all channels recorded at t_2). The linear classifier aims at finding the linear function (w) that separates the two sets of trials in the resulting n-dimensional space.

c. A multivariate classifier using all channels across multiple time samples can extract both the topography and the dynamics of the signal.

d. Decoding techniques are traditionally based on a discrete classification: each trial is classified depending on the sign of its signed distance from w.

e. Here, using Platt's method (PLATT, 1999), we provide a continuous decoding output , which estimates the actual probability of belonging to a given class depending on the signed distance from w.

f. This continuous approach can be particularly useful for generalization analyses: if the classifier is trained/fitted to discriminate A from B, and tested on its ability to discriminate C from D, then a continuous output will be robust to overall biases toward a given class.
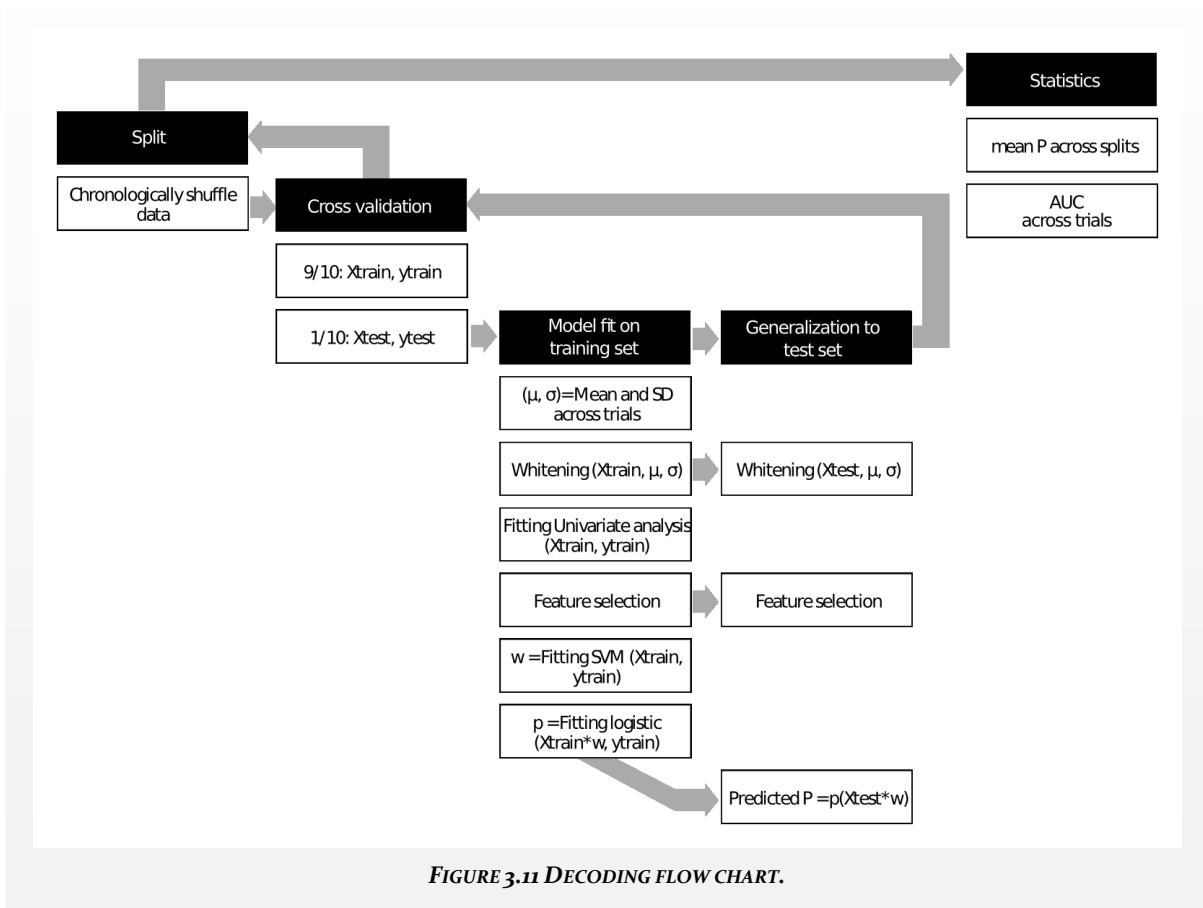
FIGURE 3.11 DECODING FLOW CHART.

Patients' complete details are available online (Table S1).

Chapter 4. Two Distinct Dynamic Modes Subtend the Detection of Unexpected Sounds

4.1. Introduction of the Article

In the first study, the decoding approach was essentially used in order to maximize the signal to noise ratio and provide within subjects statistics. One of the putative neuronal signature of consciousness (the presence of a late P300b following a rare auditory sequence), especially emphasized in the global neuronal workspace theory (Dehaene and Naccache, 2001; Dehaene et al., 2006b; Dehaene and Changeux, 2011), was isolated in each subject and patient as a result of this method. However, the global neuronal workspace theory makes a more specific prediction about the P300b. This component, according to the model, reflects conscious access because it indexes the ignition of the global workspace which itself allows relevant information to be maintained over time, and thus be integrated by the various parallel processors that constitute the cortex. In other words, not only should conscious access be marked by the presence of the late event relate potential mark, but this brain activity should be sustained over time.

In the present article, a variation of the decoding technique described in Chapter 3. is presented in order to test this idea. As detailed in the following article, this technique simply consists in training a distinct classifier at each time point and systematically testing its ability to discriminate all other time points. Interestingly, this method revealed fundamentally different patterns of results when it decoded a local change of tone (local effect) and when it decoded a global change of auditory sequence (global effect). This simple method turned out to highlight a feature that is generally left out in traditional time-resolved analyses - the extent to which a particular process is implemented by the sequential activation of different brain regions, or the maintenance of a single (set of) brain area(s). In other words, this simple technique characterizes the dynamics elicited by a particular stimulus.

4.2. Abstract

The brain response to auditory novelty comprises two main EEG components: an early mismatch negativity and a late P300. Whereas the former has been proposed to reflect a prediction error, the latter is often associated with working memory updating. Interestingly, these two proposals predict fundamentally different dynamics: prediction errors are thought to propagate serially through several distinct brain areas, while working memory supposes that activity is maintained over time within a stable set of brain areas. Here we test this temporal dissociation by showing how a new method, generalization across time, can characterize the dynamics of the brain activity. We apply this method to magnetoencephalography (MEG) recordings acquired from healthy participants who were presented with two types of auditory novelty. Following our predictions, the results show that the mismatch evoked by a local novelty leads to the se-

quential recruitment of distinct and short-lived neuronal assemblies. In sharp contrast, the global novelty evoked by an unexpected sequence of five sounds elicits a sustained state of brain activity that lasts for several hundreds of milliseconds. The present results highlight how MEG combined with multivariate pattern analyses can characterize the dynamic of human cortical processes.

4.3. INTRODUCTION

When faced with an unexpected sensory event, the brain must perform two major computations: i) identify the most probable reason for the novelty and ii) determine whether this novel information is relevant to future decisions. Indeed, when comparing the brain response elicited by expected sounds ("standard") and unexpected sounds ("deviant"), two radically different electro-enphalography (EEG) components are observed: the mismatch negativity (MMN), peaking over centro-anterior EEG sites between ~100 and 150 ms (NÄÄTÄNEN ET AL., 2010), and the P300 over centro-posterior electrodes (GOLDSTEIN ET AL., 2002). The MMN is primarily generated within superior temporal areas (HARI ET AL., 1984; HALGREN ET AL., 1995; NÄÄTÄNEN ET AL., 2007; GARRIDO ET AL., 2009), whereas the P300 involves distributed areas of the frontal, parietal and temporal lobes (POLICH, 2007; BEKINSCHTEIN ET AL., 2009). The MMN and P300 are also functionally dissociable. The MMN is robust to instructions, subjects' attention, and the subjects' state of consciousness (TIITINEN ET AL., 1994; NÄÄTÄNEN ET AL., 2007; BEKINSCHTEIN ET AL., 2009; GARRIDO ET AL., 2009; FISCHER ET AL., 2010; FAUGERAS ET AL., 2011, 2012; WACONGNE ET AL., 2011; CHENNU ET AL., 2013; KING ET AL., 2013A). Conversely, the full-scale P300 is highly sensitive to whether or not subjects consciously detect the novelty (POLICH, 2007; BEKINSCHTEIN ET AL., 2009; KING ET AL., 2013A). Finally, any low-level novelty in pitch, duration, identity, triggers an MMN (GARRIDO ET AL., 2009; NÄÄTÄNEN ET AL., 2010) whereas the P300 requires the violation of relevant rules constructed over several seconds (POLICH AND MARGALA, 1997; BEKINSCHTEIN ET AL., 2009; WACONGNE ET AL., 2011; KING ET AL., 2013A).

The two components may thus reflect two different computations: the P300 is thought to index a working memory update, passing relevant information to the next trial (SQUIRES ET AL., 1975B; DEHAENE ET AL., 2006B; POLICH, 2007), whereas the MMN would reflect a prediction error signal (GARRIDO ET AL., 2007, 2009; WACONGNE ET AL., 2012), elicited whenever an incoming stimulus differs from its internally generated prediction (RAO AND BALLARD, 1999; POUGET ET AL., 2002; FRISTON, 2005).

Crucially, working memory and predictive coding imply fundamentally different dynamics: fast serial for MMN, and slow and stable for P300. Predictive coding stipulates that errors propagate through a series of different areas until the appropriate internal model cancel the prediction error (RAO AND BALLARD, 1999; POUGET ET AL., 2002; FRISTON, 2005), while working memory implies an active maintenance of information in a stable activity pattern.

Here, we put these predictions to a test using magnetoencephalography (MEG) recordings and multivariate decoding. To characterize the two predicted dynamic patterns, we first trained a multivariate pattern classifier to discriminate standard from deviant trials at each time sample, and then examined their ability to generalize to new time samples. We thus obtained a *temporal generalization matrix* that can distinguish two types of dynamics (FIGURE 4.2). We applied this approach to two different violations of auditory regularities originally designed to isolate the MMN and the P300 components (FIGURE 4.1) (BEKINSCHTEIN ET AL., 2009).

4.4. METHODS

4.4.1.   PROCEDURE, MATERIAL & APPARATUS

The Local Global protocol (BEKINSCHTEIN ET AL., 2009) enables the comparison of effects engendered by physically identical but contextually different auditory stimuli (FIGURE 4.1). Traditional analyses (topography, sources, *etc.*) of the present MEG have been partially reported elsewhere (WACONGNE ET AL., 2011; KING ET AL., 2013A). Each recording session comprised 14 blocks (780 trials) of ~3.5 minutes duration. Nine healthy volunteers (Age M = 25 years old, SD = 4.7 years, 5 females) were asked to pay attention to the auditory stimuli while keeping their eyes opened and fixated at a central cross. All subjects gave written informed consent to participate to this study, which was approved by the local Ethics Committee (Comité de protection des personnes "Ile-de-France VII", hôpital de Bicêtre, 78 rue du Général-Leclerc, 94270 Le Kremlin-Bicêtre).

Signal space separation (SSS, TAULU ET AL., 2004) was applied to suppress external magnetic interference, interpolate noisy MEG sensors and realign MEG data into a subject-specific head position. This reference head position was determined from head position measurements acquired at the beginning of each recording session. Eye blink and cardiac artefacts were corrected separately for each type of channel (gradiometer and magnetometers) using signal space projection (SSP, UUSITALO AND ILMONIEMI, 1997). Noisy MEG sensors were removed with Maxfilter software application (Elekta Neuromag®) in the SSS preprocessing step. All signals were digitally low-pass filtered at 40 Hz and down-sampled to 256 Hz. Trials were then segmented from -800 ms to 700 ms after the critical stimulus onset, and were corrected for baseline over a 200 ms window before the onset of the first of the five sounds. Trials with large artefacts remaining after correction for ocular and cardiac artefacts were identified manually and excluded from the present analyses.
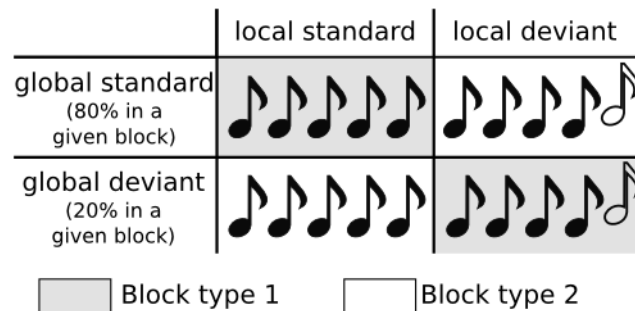
FIGURE 4.1 VIOLATING TWO TYPES OF AUDITORY REGULARITIES.

The Local Global experimental design (BEKINSCHTEIN ET AL., 2009) is a variation of the auditory oddball paradigm. It consists in presented series of 5-sound sequences which are composed of five identical tones (local standard) or four identical tones followed by a deviant one (local deviant). The global regularity is established across trials by making 80% of the trials identical (global standard). The design thus dissociates the violation of local predictions (change of tone) and global predictions (change of sequence).

4.4.2.   CONTRASTS AND CLASSES

Two classifications were attempted (FIGURE 4.1): (1) local standard (*LS, i.e.* an xxxxx sequence) versus local deviant (*LD, i.e.* an xxxxY sequence); (2) global standard (*GS*, frequent sequences) versus

global deviant (*GD,* rare sequences). Both of these analyses contrast trials that are evenly distributed across blocks and are therefore free of potential block-design artefacts (LEMM ET AL., 2011).

4.4.3.   MULTIVARIATE PATTERN ANALYSIS (MVPA)

Multivariate pattern analyses (MVPA) were implemented to systematically track the dynamics of neuronal processes. Our method is based on the principle that when a brain area – or set of areas – is activated, its electric and magnetic fields project to the MEG sensors in a specific spatial pattern. This specificity is obviously limited by the spatial resolution of the MEG: if two distinct areas are very close to one another or too far from the scalp, the resulting pattern will be indistinguishable. MVPA identifies each of these projections directly at the sensor level and for each subject separately.

4.4.3.1.   SVM & cross validation

The detailed procedure of the multivariate pattern analysis is reported in KING ET AL. (2013). A ten-fold stratified cross-validation was implemented for each within-subject analysis. For each fold and at each time sample, a linear support vector machine (SVM, (CHANG AND LIN, 2001)) was fit on 9/10 of the trials (training set) to find the hyperplan (w) that best discriminated standard and deviant trials. Classification performance was then computed with a Received Operative Curve (ROC), based on the signed distance separating w and the trials from an independent test set (1/10). All multivariate analyses were performed with the Scikit-Learn toolbox (PEDREGOSA ET AL., 2011).

4.4.3.2.   Time generalization

Crucially, once we have fitted t linear classifiers (where t is the duration of a trial expressed in time samples), each of these classifiers is tested on its ability to discriminate the two types of trials at any time t'. This method thus leads to a *temporal generalization matrix* of training time x testing time. In each cell of the matrix, decoding performance is summarized by the Area Under the Curve (AUC). Classifiers trained and tested at the same time point correspond to the diagonal of this t^2 matrix, and are thus referred to as "diagonal" decoding. The decoding performance obtained when t' differ from t is referred to as "off-diagonal" decoding. Note that the cross-validation was applied independently of the temporal generalization analyses: the trials used in the training set at time t were never included in the generalization at time t' as consecutive time samples are not independent.

To compute the average duration over which temporal generalization remained significant, we computed the number of time samples during which each classifier could significantly predict the trials' classes, using false discovery rate (FDR) to correct for multiple comparison. To avoid underestimating the mean generalization-time, we only considered the time window during which the diagonal classifiers performed above chance (~82 ms – 450 ms).

4.4.3.3.   Statistics & effect sizes

To test for statistical significance within subjects, we performed Mann-Whitney U tests on the signed distance to w depending on the trials classes (standard or deviant), with trials as the random variable. Similarly, across-subjects statistics were performed using Wilcoxon Signed Rank Tests based on the mean signed distance within each of the true trial classes. Effect sizes are summarized with the AUC computed from empirical ROC analyses. An AUC of 50% implies that true positive predictions (*e.g.* trial was correctly predicted to belong to class α) and false positive predictions (*e.g.* trial was erroneously predicted to belong to class α) are, on average, equally probable; an AUC of 100% indicates a perfect prediction with no false positives. In principle, for the diagonal decoding, classification performance should not systematically yield AUCs that are significantly below 50%. However, decoding performance during generali-

zation to a time sample different from the classifier's fitting time can be significantly below 50%, as the pattern of brain activation carrying the discriminative information can be flipped in sign between *t* and *t'*. Statistical analyses were performed with MATLAB 2009b.

4.4.3.4.   Modelling

To test our method, we ran a series of simulations. For each class, 50 trials (50% in each class) were generated across 20 simulated sensors and 80 time-samples (t). Each generator (g), simulating one or several brain areas, projected on a random combination of sensors (C), and was activated (A) with a temporal profile specific to each simulation. Each generator was thus defined by a vector of 20x1 features of normally distributed values, as well as by a second vector of t time-samples indicative of its activity. Each trial (S(c,t)) corresponded to the sum of the generators' activities in the direction of the class (class y=[-1, 1]):

$$S(c,t) = y \sum_{g} C(g)A(t)$$

Subsequently, Gaussian white noise was added to all signals. Signal-to-noise ratio was set to 0.5. Finally, each simulation was repeated ten times to simulate a group of subjects. In the simulation of a sequential pattern, 10 generators were successively active for 6 time samples each. In the simulation of sustained brain activity, a single generator was active for 60 time samples (FIGURE 4.2).
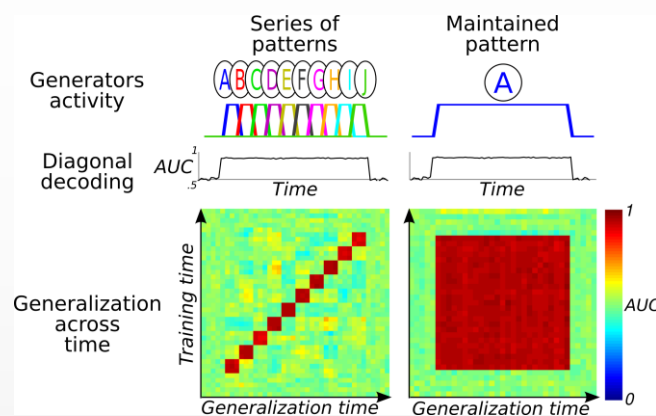
FIGURE 4.2 DETECTING TWO TYPES OF BRAIN DYNAMICS BY GENERALIZING ACROSS TIME MULTIVARIATE CLASSIFICATION PATTERNS

Multivariate decoding leads to temporal generalization matrices that reflect the underlying pattern of brain activity. (left) When the stimulus evokes a serial chain of brain activations, a classifier can extract stimulus information at each time point, but cannot generalize across time samples because the underlying active regions keep changing. The result is a diagonal generalization matrix. (right) In contrast, a decoder trained on sustained brain activity at one time point generalizes to others, leading to a square generalization matrix.

4.5. RESULTS

We applied the generalization across time analyses to nine subjects who performed the Local Global protocol while their brain activity was recorded with MEG. Traditional analyses, including source reconstruction, are reported in WACONGNE ET AL. (2011) AND KING ET AL. (2013).

A traditional "diagonal" decoding method, consisting in repeatedly training and testing a classifier with the MEG sensor data recorded at each time point, revealed the presence of decodable information between approximately 100 ms and 450 ms following the onset of the fifth sound (all $p_{FDR} < .05$). Local auditory violations lead to a decoding peak at 120 ms (AUC = 69.6% ± 7.9, p = .003) whereas global violations lead to a stable decoding performance from ~150 ms to 700 ms (*e.g.* t = 350ms: AUC = 66.3% ± 4.0, p = .003). This result confirms previous analyses showing a mismatch response around 120 ms (HARI ET AL., 1984; WACONGNE ET AL., 2011) and significant local and global effects ranging from 200 ms to 700 ms (BEKINSCHTEIN ET AL., 2009; WACONGNE ET AL., 2011; FAUGERAS ET AL., 2012; KING ET AL., 2013A).

Crucially, generalization across time demonstrated remarkably different dynamics for the local and for the global effects (FIGURE 4.3). In the local contrast (decoding of local standards versus local deviants, corresponding to the classical mismatch response), none of the classifiers generalized to the full time window. Although the traditional diagonal decoding indicated the presence of decodable information about local auditory novelty within a long time interval of approximately 400 ms, each classifier significantly generalized for only ~100 ms on average ($p_{FDR} < .05$), and was not significantly different from the diagonal decoder over a time window of only ~50 ms ($p_{FDR} < .05$). Six of the classifiers, trained between 100 and 600 ms and the full temporal generalization matrix for all classifiers is presented in FIGURE 4.3 (top). The results show a clear diagonal pattern of temporal generalization and thus indicate that each classifier only generalizes for a limited amount of time: each time sample is thus associated with a slightly different pattern of MEG activity. This result suggests that different brain regions are serially recruited, each for a short-lived time period, in response to a local auditory violation.

Interestingly, the classifiers trained around 120 ms generalized in the opposite direction around 200 ms. For example, a classifier trained at 114 ms led to a high AUC at this time point (AUC = 70.7% ± 7.2, p = .003), but generalized to an AUC below 50% at 200 ms (AUC = 34.3% ± 11.3, p = .003). This result means that trials were predicted to belong to the opposite class (*e.g.* standard trials were systematically predicted as deviant). This below-chance performance suggests that the pattern of brain activity is inverted between these two time points. To test whether this reversal reflects the polarity reversal of a single pattern, we compared the initial peak of diagonal decoding performance to the peak of anti-generalization performance (*i.e.* AUC(t,t) versus (1-AUC(t,t')) and *vice versa*. The results showed that diagonal performance was significantly higher than anti-generalization performance (F(8,1) = 5.75, p = .024). This result thus suggests that this reversal is only partial, and that a qualitatively different pattern of brain activity is elicited at 110 and 200 ms respectively. This result is further supported by the fact the diagonal decoding performance is always significantly above chance between these two time samples (all p < .004) whereas a simple polarity inversion would lead the diagonal decoding performance to drop to chance in the middle part of the reversal. However, as this pattern remains more complex than what we initially predicted, we would argue that only the late part of the diagonal (150 – 450 ms) unambiguously follows the prediction of a serial processing (FIGURE 4.2).
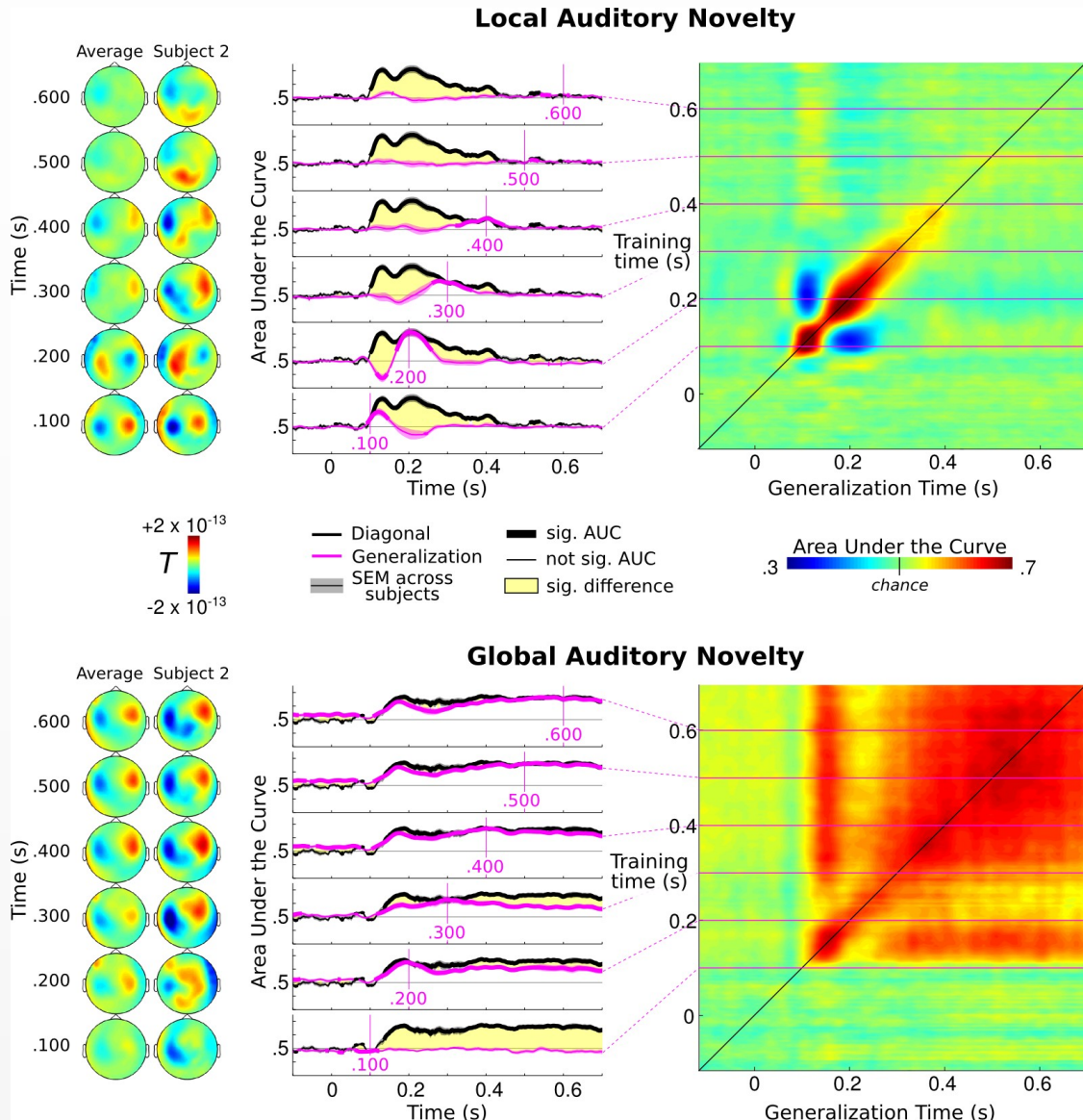
FIGURE 4.3 GENERALIZATION ACROSS TIME OF THE LOCAL AND GLOBAL RESPONSES TO AUDITORY NOVELTY

At each time point, a classifier was trained to extract the pattern of neuronal activity that distinguishes local-standard from local-deviant trials ("oddball" or mismatch effect top) or to contrast global-standard from global-deviant trials (bottom). Each classifier was subsequently tested on its ability to generalize this discrimination to all other time samples.

(left) Differential pattern of brain activity of a single representative subject (standard – deviant). For simplicity purposes, only the magnetometers are plotted (n=102/306 channels).

(middle) Generalization of six different classifiers trained at regularly spaced times between 100 ms and 600 ms (purple), compared to the traditional "diagonal" decoding method where a different classifier is trained and tested at the same time point (black). The thick lines indicate significant decoding scores. The yellow areas indicate when the diagonal performance was significantly different from the generalization across time.

(right) Generalization matrix. Decoding performance is plotted as a function of training time (y axis) and testing time (x axis) for all classifiers. Decoding of the local-violation effect leads to a diagonal-shaped decoding performance from 82 ms to 508 ms (AUC over 50% in red), demonstrating that each classifier was only able to predict trials' classes for a short amount of time. Decoding of the global-violation effect leads to a square generalization matrix, suggesting that the underlying brain activity is essentially stable during this time period. Early classifiers (< 350 ms) are slightly lower than the traditional "diagonal" decoding performance, thus suggesting only a small change in the underlying pattern of activity.

Applying these analyses to the global contrast (global standard – global deviant) led to a strikingly different pattern of decoding performance. Within a broad temporal window, a nearly "square" pattern of temporal generalization indicated that most classifiers, regardless of their training time, produced very similar decoding performance across all testing times. Decoding performance was statistically significant from approximately 125 ms until the end of the trial (700 ms). Sample classifiers trained between 100 ms and 600 ms and the full temporal generalization matrix is presented in FIGURE 4.3 (bottom). Overall, these findings show that a similar combination of MEG sensors can discriminate frequent auditory sequences from rare auditory sequences across many different time points. These results thus suggest that the underlying patterns of brain activity are sustained in a stable form for several hundreds of milliseconds. We only observed a small but significant difference between the temporal generalization of the early classifiers (< 350 ms, all p_{FDR} < .05) and the traditional "diagonal" classifiers. This suggests that the early brain response to a global violation was partly changing over time, and became fully stable from 350 ms on.

4.6. DISCUSSION

We characterized the dynamics of the brain response to two types of auditory novelty detection. We predicted that i) local novelties should elicit a serial propagation of prediction error in successive brain areas whereas ii) global novelties should lead to an active maintenance of a particular pattern of brain activity. Traditionally, multivariate pattern classifiers are trained and tested at a given time point – an approach hereafter referred to as "diagonal decoding". Here, by contrast, we trained a classifier to distinguish standard from deviant trials at each time sample, and evaluated its ability to generalize to different time samples. The results showed that the two types of auditory violations are characterized by strikingly distinct dynamics.

4.6.1. VIOLATION OF A LOCAL AUDITORY EXPECTATION LEADS TO THE SERIAL RECRUITMENT OF SHORT-LIVED NEURONAL ASSEMBLIES

Decoding local-standard versus local-deviant trials revealed a diagonally-shaped pattern of temporal generalization, together with a partial reversal of decoding performance in an early time window.

The diagonally-shaped decoding performance suggests that the pattern of neuronal activity changes continuously over time. This result therefore shows that the violation of a low-level auditory regularity recruits a series of different areas for a short time period. This novel result supports the early proposal that the brain response to low-level auditory novelties is generated by several different generators (NÄÄTÄNEN AND PICTON, 1987). More generally, it also fits predictive-coding theories, which postulate that distinct brain regions compare internally generated predictions to the incoming bottom-up evidence (RAO AND BALLARD, 1999; POUGET ET AL., 2002; FRISTON, 2005). Subtracting the sensory evidence and the prediction leads to a "prediction error" signal, which is passed on to higher areas that iteratively search for an internal model making sense of the incoming data. Empirical and modeling studies have shown that the MMN could reflect a prediction error (WACONGNE ET AL., 2011, 2012). The results supplements this proposal by confirming that unexpected sounds lead to a serial propagation of neuronal activity.

Furthermore, the early reversal of decoding performance ("worse-than-chance" generalization between 120 ms and 200 ms) implies that the pattern of brain activity that distinguishes between standard and deviant tones partly reverses between these time points. One interpretation is that the neuronal assembly which is initially activated is subsequently inhibited (or vice versa). This interpretation fits with

intracranial recordings (HALGREN ET AL., 1995; BEKINSCHTEIN ET AL., 2009) and source reconstruction analyses (HARI ET AL., 1984; WACONGNE ET AL., 2011) which typically show a similar reversal in the primary auditory cortex. However, the physiological interpretation of this pattern remains ambiguous. For example, the above excitation/inhibition hypothesis is indistinguishable from a reversal of the current flow hypothesis. Indeed, if the neural currents first flow out the cortex (bottom-up) and then flow back in (top-down), the magnetic field would also reverse. Such a reversal may occur if an early feedforward prediction error signal is followed, in the same region, by a later top-down cancellation signal.

4.6.2. VIOLATION OF A GLOBAL AUDITORY REGULARITY LEADS TO A SINGLE SUSTAINED ACTIVITY PATTERN

In sharp contrast with the local-violation results, decoding global standard versus global deviant trials leads to a nearly square-shaped temporal generalization matrix. This pattern results from the fact that whenever a classifier is trained at a given time sample, it generalizes almost perfectly to any other informative time sample. This result thus suggests that the underlying neuronal activity is essentially stable from 200 to 700 ms approximately. In other words, a single sustained neuronal assembly appears to be recruited and maintained during this time window.

Although temporal stability is the dominant feature of this temporal generalization, we also observed, between 200 and 350 ms, a small but significant advantage along the diagonal compared with off-diagonal decoding performance (*i.e.* generalizing over time). This pattern suggests that, during this period, a small temporal evolution of brain activity coexists with the main effect of stable maintenance. Interestingly, the global effect rises slightly later than the local violation one, and thus fits with the idea that this more abstract violation recruits higher levels of processing than the local novelties. Together with fMRI (BEKINSCHTEIN ET AL., 2009) and source analyses (WACONGNE ET AL., 2011), these results fit with the idea that this type of violations durably engages working memory resources allocated by the prefrontal, parieto-temporal cortex (KOJIMA AND GOLDMAN-RAKIC, 1982; ROMO ET AL., 1999; FUSTER, 2008). The meta-stable activity of this network has also been proposed as a hallmark of information broadcasting and conscious access (DEHAENE AND CHANGEUX, 2011). It is unclear, however, whether the present activity corresponds to the content of working memory or to a more transient updating process.

4.6.3. A SYSTEMATIC METHOD TO CHARACTERIZE THE TEMPORAL DYNAMICS OF BRAIN ACTIVITY

The present method, generalization across time, presents several advantages for the systematic analysis of the dynamics of brain signals. With advances in neuroimaging, the number of brain signals that are simultaneously recorded increases rapidly and it becomes difficult to embrace all of the data at once. The present recordings were, for instance, obtained from 206 gradiometers and 102 magnetometers, each capturing different directions of the magnetic fields. Yet, the relationship between MEG sensors and brain areas dramatically varies as a function of subjects' anatomy and position in the scanner. Source analysis provides a way to put these different signals in a common space across subjects but suffers from strong methodological difficulties and often generates an even larger dimensionality problem than scalp analyses. Given these issues, the method of multivariate decoding followed by temporal generalization presents several major advantages. First, it combines all simultaneous recordings into a unique information estimate. Second, each classifier is fitted on a single subject separately, which maximizes sensitivity. Third, we have shown here how decoding can be used to identify the sequence of cortical activity patterns without relying on the strong hypotheses associated with source reconstruction. Generalization across time analyses therefore provides a powerful supplement to source reconstruction and paves the way to a systematic characterization of the dynamics subtending cognitive processes.

4.7. ACKNOWLEDGMENTS

Chapter 5. Characterizing the Dynamics of Mental Representations: the Temporal Generalization Method

5.1. Introduction of the article

In Chapter 4. , I showed how a slight adaptation of classic decoding techniques could characterize and discriminate the neural dynamics elicited by two different types of auditory novelties. A specific search across the literature later revealed that similar techniques to the temporal generalization method had employed sporadically across the literature. Consequently, in the following opinion paper, I formalize the generic principles and the specific advantages of the temporal generalization method. I show, from a series of simulations and empirical examples, that a limited number of canonical dynamics can be evidenced thanks to this simple method. Beyond the specific questions of conscious and unconscious processing, I argue that this technique may prove helpful to a broad audience of cognitive neuroscientists.

5.2. Abstract

Parsing a cognitive task into a sequence of operations is a central problem in cognitive neuroscience. We argue that a major advance is now possible thanks to the application of pattern classifiers to time-resolved recordings of brain activity (electroencephalography, magneto-encephalography, or intracranial recordings). By testing at which moment a specific mental content becomes explicitly decodable in brain activity, we can characterize the time course of cognitive codes. Most importantly, the manner in which the trained classifiers generalize across time, and from one experimental condition to another, sheds light on the temporal organization of information-processing stages. This method identifies a repertoire of canonical dynamical patterns that recur across various experiments and brain regions.

5.3. Introduction: isolating a sequence of processing stages

Understanding how mental representations unfold in time during the performance of a task is a central goal for cognitive psychology. Donders (Donders, 1969) first suggested that mental operations

could be timed by comparing the subjects' response times in different experimental conditions. This "mental chronometry" was later enriched with several methodological inventions, including the additive-factors method (STERNBERG, 1969) and the psychological refractory period method (PASHLER, 1994). While these behavioral techniques can provide considerable information on the temporal organization of computations, they remain fraught with ambiguities. For instance, they cannot fully separate serial from parallel processes (TOWNSEND, 1990), or processes organized into a discrete series of steps from those operating as a continuous flow or "cascade" of overlapping stages (MCCLELLAND, 1979).

More recently, the advent of brain-imaging techniques has provided unprecedented access into the content and the dynamics of mental representations. Electro-encephalography, magneto-encephalography, local field potentials and neuronal recordings can provide a fine-grained dissection of the sequence of brain activations (see e.g. (DEHAENE, 1996; NISHITANI AND HARI, 2002)). Here, we show how the analysis of these time-resolved signals can be enhanced using multivariate pattern analysis (MVPA), also known informally as "decoding". We argue that temporal decoding methods offer a vast and largely untapped potential for the determination of how mental representations unfold over time.

5.4. DECODING MENTAL CONTENTS FROM BRAIN ACTIVITY: FMRI.

MVPA was first introduced to brain imaging in order to refine the analysis of functional magnetic resonance imaging signals (fMRI). Temporal resolution aside, functional Magnetic Resonance Imaging (fMRI) is an efficient tool to isolate and localize the brain mechanisms underlying specific mental representations. Initially, fMRI was primarily used with binary contrasts that revealed major differences in regional brain activity (e.g. faces *versus* non-faces in the fusiform cortex (KANWISHER ET AL., 1997)). MVPA, however, led to a considerable refinement of such inferences, because it proved able to resolve, inside an area, the fine-grained patterns of brain activity that contain detailed information about the stimulus or the ongoing behavior (for review, see (HAYNES AND REES, 2006; QUIAN QUIROGA AND PANZERI, 2009; KRIEGESKORTE AND KIEVIT, 2013)).

Using MVPA, subtle details of mental representations can be decoded from fMRI activity patterns. It is now possible to decode low-level visual features such as orientation (KAMITANI AND TONG, 2005; HARRISON AND TONG, 2009; FREEMAN ET AL., 2011; KOK ET AL., 2012) or color (BROUWER AND HEEGER, 2009), and determine how their cortical representation is changed, tuned or suppressed according to subjects' goals (HARRISON AND TONG, 2009) and prior knowledge (KOK ET AL., 2012). Using distributed activity over the ventral visual pathway, it is possible to reconstruct which static images (THIRION ET AL., 2006; MIYAWAKI ET AL., 2008; GALLANT ET AL., 2009; KAY AND GALLANT, 2009; GRAMFORT ET AL., 2012), moving objects (VAN GERVEN ET AL., 2011) or movies (NISHIMOTO ET AL., 2011) the subject is watching. The identification of these mental contents is not limited to sensory information: in the absence of any stimulus, purely mental objects can still be decoded, for instance during mental imagery (LEE ET AL., 2012; ALBERS ET AL., 2013), working memory (CHRISTOPHEL ET AL., 2012; ALBERS ET AL., 2013), or even dreams (HORIKAWA ET AL., 2013). More recently, MPVA has also been used to decode non-visual representations, including auditory (FORMISANO ET AL., 2008; GIORDANO ET AL., 2013), mnemonic (RISSMAN ET AL., 2010), numerical (KNOPS ET AL., 2009), and executive information (COLE ET AL., 2013; ZHANG ET AL., 2013).

BOX 5.1 METHODOLOGICAL ISSUES IN DECODING FROM TIME-RESOLVED BRAIN-IMAGING DATA

The ability of multivariate pattern analysis (MVPA) to extract information from a complex multidimensional dataset has rendered this statistical technique indispensable to the neuroimaging community (KRIEGESKORTE AND KIEVIT, 2013). By concentrating the information distributed in several data points, MVPA increases the signal-to-noise ratio and facilitates single-trial decoding. These advantages are particularly useful when signals present a high inter-individual variability that prevents spatial averaging. MVPA simplifies such complex dataset by presenting the results in an information space of direct relevance (SHEPARD, 1987; KRIEGESKORTE AND KIEVIT, 2013), in which data from multiple subjects can readily be averaged.

Here we specifically emphasize the usefulness of MVPA applied to time-resolved intracranial, MEG and EEG recordings. MVPA projects such multidimensional data into a smaller-dimensionality space whose axes are the cognitive codes of interest (e.g. stimulus features, subject response, etc.). The output axes are shared across individuals, but the projection is optimized for each subject and each time point. In MEG for example, this approach allows maximizing the spatial resolution of the signals without necessarily addressing the difficult issue of source localization.

In fMRI, MVPA is often used in combination with a search light method (KRIEGESKORTE ET AL., 2006; HAYNES ET AL., 2007), which consists in sliding a small spatial window over the data in order to detect which segments contain decodable information. By analogy, with time-resolved signals, a sliding time window can be used to detect periods of optimal decodability. Furthermore, this approach can be extended by testing whether a classifier is able to generalize to other moments in time. Not only can decoding determine when and for how long a given piece of information is explicitly present in brain activity, but with generalization, it becomes able to characterize whether this information recurs in time, and when.

*When applied systematically, the method yields a full **temporal generalization matrix** where classifiers are trained and tested at all available time points (Figure 1). A variety of methods can be used to build such a matrix, including support vector machines (e.g. (KING ET AL., N.D.; NIKOLIĆ ET AL., 2009)), linear discriminant analyses (e.g. (CARLSON, 2011; CARLSON ET AL., 2013)), or even simple linear regression (e.g. (MEYERS ET AL., 2008; ZHANG ET AL., 2011; SCHURGER ET AL., 2013)). To avoid data over-fitting, MVPA must be nested inside a cross-validation loop, such that performance is only measured on novel left-out data samples (for both diagonal and off-diagonal time points). To evaluate classifier performance, "criterion free" estimates should be preferred over mean accuracy, because the latter may lead to systematic biases during generalization (i.e. all trials may be classified in the same category). We favor using the area-under-the-curve (AUC), a sensitive non-parametric criterion-free measure of generalization.*

5.5. DECODING THE DYNAMICS OF INFORMATION PROCESSING

MVPA applied to fMRI signals does not reveal much about the dynamics with which mental representations are activated and manipulated (although some slow processes can be tracked with fMRI: *e.g.* (KAMITANI AND TONG, 2005; HARRISON AND TONG, 2009; ALBERS ET AL., 2013)). Here, we focus specifically on the less explored question of what MVPA may bring to our understanding of the dynamics of information processing in the brain.

Methodologically, MVPA readily applies to EEG, MEG or intracranial recording data where time can be considered as an additional dimension, besides the spatial information provided by the sensors. In order to obtain time-course information, a series of classifiers can be trained, each using as an input a

specific time slice of the original data (see BOX 5.1). The output is a curve representing decoding performance as a function of time, which specifies the time window(s) when a certain piece of information becomes explicitly encoded in brain activity. Multiple such classifiers can be trained to decode distinct features of the trial, thus dissecting a trial into a series of overlapping stages. Recently, for instance, in a simple response-time task, we decoded successively the location of the stimulus, the subject's required response, his actual motor response (which differed on error trials), and whether the brain detected whether the response was correct or erroneous (CHARLES ET AL., N.D.).
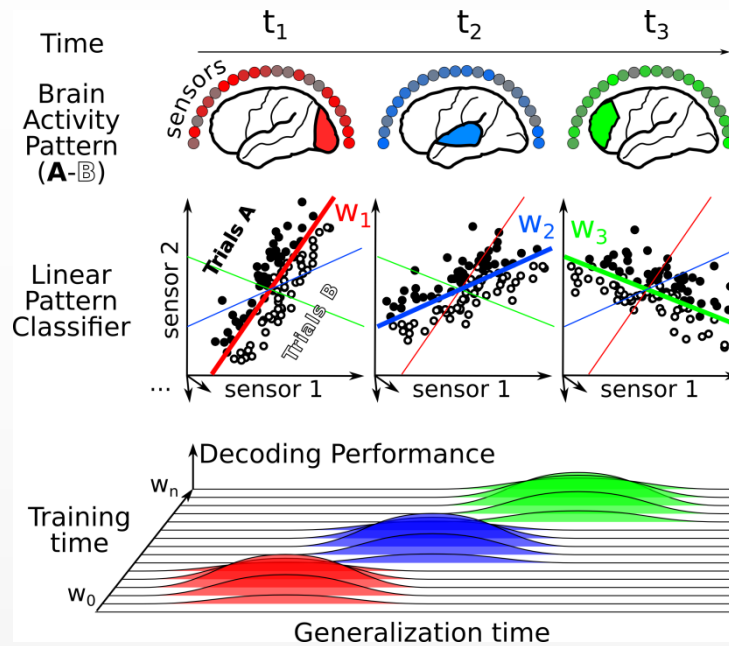
FIGURE 5.2 THE PRINCIPLES UNDERLYING TEMPORAL DECODING AND TEMPORAL GENERALIZATION

*At each time point t, a multivariate pattern classifier w(t) is trained to identify the linear combination of measurements (weights of EEG electrodes, MEG sensors, individual neurons, etc.) that best discriminates two experimental conditions (A and B). This combination may vary with time, as the underlying pattern of activity changes. Classifier performance is assessed, not only at the time used for training (e.g. classifier w(t₁) tested at t₁, w(t₂) tested t₂ ..., hereafter referred to as "diagonal decoding"), but also on data from other time samples (e.g. classifier w(t₁) is tested at all times t₁, t₂, t₃...; hereafter referred to as "off-diagonal decoding"). The outcome is a **temporal generalization matrix** representing the decoding performance of each classifier at each time point. By convention, we depict this matrix with training time on the y axis and generalization time on the x axis. With this convention, horizontal "slices" through the matrix show the time course of activation of the brain systems identified by a given classifier.*

Even scalp EEG recordings contain a lot of information sufficient to discriminate a variety of processing stages. Duncan et al. (DUNCAN ET AL., 2010), for instance, showed that the orientation of a large visual grating can be reconstructed from EEG signals – a result recently replicated with MEG (GARCIA ET AL., 2013; RAMKUMAR ET AL., 2013). EEG even permits decoding the covert production of imagined syllables (DENG ET AL., 2010). Auditory information (KING ET AL., 2013A), including conceptual and semantic information (CHAN ET AL., 2011; SUDRE ET AL., 2012) and even music samples (SCHAEFER ET AL., 2010) have also been decoded from EEG and MEG recordings.

Decoding is typically performed on raw signals in the time domain. However, the expansion of brain signals through a time-frequency transform may increase their decodability and reveal information spread over both frequency and time (DENG ET AL., 2010; FUENTEMILLA ET AL., 2010; SCHYNS ET AL., 2011).

Two approaches can be used to simultaneously obtain a high spatial and temporal resolution. First, source reconstruction analyses may provide an approximate location of the neural generators underlying scalp recordings. Second, intracranial recordings can now be acquired from dozens or even hundreds of different cortical and subcortical sites. Decoding intracranial recordings has revealed a rich temporal dynamics of fine-grained codes. For example, in the olfactory bulb of the zebra fish, decoding identified a sequence of neuronal responses to odors, revealing that ambiguous mixtures of odors are initially coded continuously and become categorically represented later in time (NIESSING AND FRIEDRICH, 2010). In humans, decoding has been used to show that perceived phonemes are categorically represented in the posterior superior temporal gyrus, with a peak as early as 110 ms following sound onset (CHANG ET AL., 2010). Similarly, the production of spoken syllables can be deciphered from sensori-motor somatotopic cortex, with a sequential activation of distinct codes for the initial consonant and the subsequent vowel (BOUCHARD ET AL., 2013).

5.6. GENERALIZATION ACROSS TIME

Applying decoding techniques to successive time slices can identify when, and for how long, a specific piece of information is represented in the brain. However, the underlying neuronal code may change with time. The MVPA approach can be extended to ask whether the neuronal code is stable or dynamically evolving (BOX 5.1 & FIGURE 5.2). The principle is simple: instead of applying a different classifier at each time point, the classifier trained at time t can be tested on its ability to generalize to time t'. Generalization implies that the neuronal code that was identified at time t recurred at time t'.
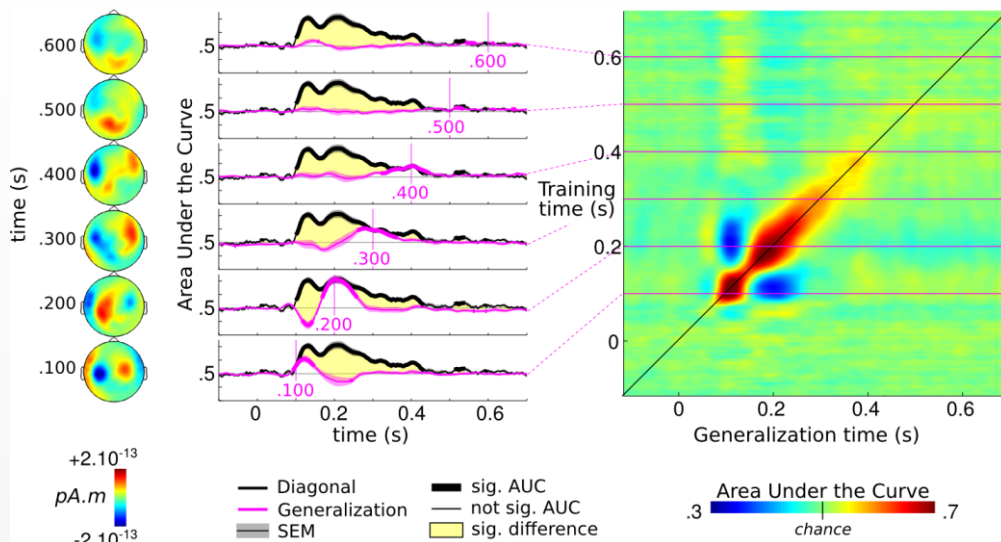
FIGURE 5.3 EXAMPLE OF GENERALIZATION ACROSS TIME (ADAPTED FROM KING ET AL, UNDER REVISION).

In this auditory mismatch MEG paradigm, classifiers are trained to determine whether the last sound of a sequence is identical to the four preceding tones or different from them, thus generating a mismatch response. Each classifier only generalizes over a transient time period, as indicated by the diagonal generalization matrix (right) and the fact that diagonal performance (black line) is systematically superior to off-diagonal temporal generalization (6 pink lines, each indicating a classifier trained at the indicated time). The changing topographies (left) confirm that the difference in magnetic field evolves over time. These findings suggest that the same stimulus (an unexpected sound) elicits a series of distinct patterns of brain activity over time.

Systematically adopting this approach leads to a two-dimensional temporal generalization matrix, in which each row corresponds to the time at which the classifier was trained, and each column to the time at which it was tested. For instance, when we apply this method to the decoding of novel versus habitual sounds (KING ET AL., 2014), we find that mismatch signals, classically assigned to a single "mismatch response", actually correspond to an extended sequence of distinct brain activation patterns (FIGURE 5.4). Although sound novelty can be decoded over a long time window, each of the classifiers is time specific and does not generalize over a long time period. All of this information is apparent in the temporal generalization matrix, which takes a diagonal form.

The simulations presented in FIGURE 5.4 exemplify how the temporal generalization method may distinguish fundamentally different dynamics of brain activity to which traditional sliding-window classifiers can be blind (FIGURE 5.4). So far, this capacity has only been used sporadically in the literature. The few available examples suggest that the diagonal pattern, indicative of a series of processing stages, is only one of several canonical dynamics modes of brain activity (FIGURE 5.5). For instance, when we analyze a slightly different response to auditory novelty, the late brain response to frequent *versus* rare auditory melodies (KING ET AL., 2014), we find that it obeys a strikingly different dynamics from the mismatch response, with a square generalization matrix indicating a stable neural code (compare FIGURE 5.5.G and FIGURE 5.5.H). A similar square matrix was observed for categories of visual pictures in infero-temporal cortex during a simple attention task (ZHANG ET AL., 2011). Interestingly, other experiments (MEYERS ET AL., 2008; STOKES ET AL., 2013) find that the same area, as well as the prefrontal cortex, may switch to a diagonal pattern during a delayed match-to-sample task (FIGURE 5.5.A and FIGURE 5.5.B). These examples suggest that, in different contexts, either a stable state or a time-changing code is used by the brain to bridge across a long temporal delay.
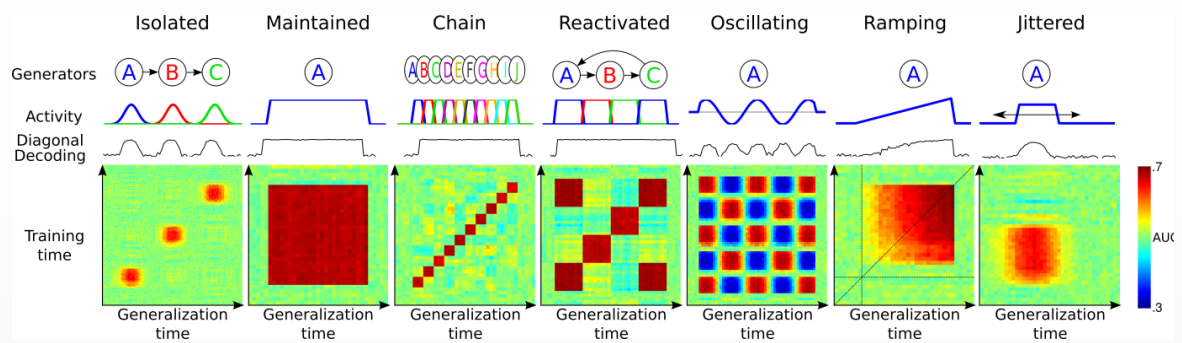
FIGURE 5.4 GENERALIZATION ACROSS TIME: PRINCIPLES AND POSSIBILITIES.

The temporal generalization matrix contains detailed information about the underlying brain processes. For illustration, we simulated seven different temporal structures. For each of them, the generators, their time course, the diagonal decoding performance and the full temporal generalization matrix are displayed. **Isolated**: *Three simulated brain regions are differentially activated at three distinct times, leading to three isolated patterns of above-chance decoding performance.* **Sustained**: *Analysis of a single process maintained over time leads to a square-shaped decoding performance.* **Chain**: *Decoding a chain of distinct generators leads to a diagonal-shaped decoding performance, as each component generalizes over a brief amount of time only.* **Reactivated**: *A given generator reactivates at a later time, leading to transient off-diagonal generalization. Note that the maintained, chain and reactivated conditions are indistinguishable from their diagonal performance, but are easily separated by their matrices.* **Oscillating**: *An oscillatory or reversing component leads to transient below-change performance.* **Ramping**: *Slowly increasing activity leads to a subtle asymmetry: temporal generalization is higher when the classifier is trained with high signal-to-noise data and tested with noisier signals, than in the converse condition.* **Jittered**: *Temporal jitter in activation onset smoothes the generalization matrices both horizontally and vertically.*

Other types of dynamics may exist. Fuentemilla and collaborators (FUENTEMILLA ET AL., 2010) trained a multivariate pattern classifier during the presentation of indoor or outdoor stimuli. When testing during the delay period of a working memory task, they obtained above-chance performance which, interestingly, oscillated at the theta rhythm (4-8 Hz), indicating that a working-memory code recurred cyclically. Carlson *et al.* trained a classifier to decode the position of a visual stimulus. They showed that, after training a classifier at the onset of the image, the classifier led to *below*-chance predictions at the time of stimulus offset, suggesting that the neural activity pattern recurred with a reversed polarity (CARLSON, 2011). Similar off-diagonal below-chance generalization has been observed by others (NIKOLIĆ ET AL., 2009; CARLSON, 2011; CARLSON ET AL., 2013; KING ET AL., 2014). Understanding when and why such reversals occur is an interesting question for further research.
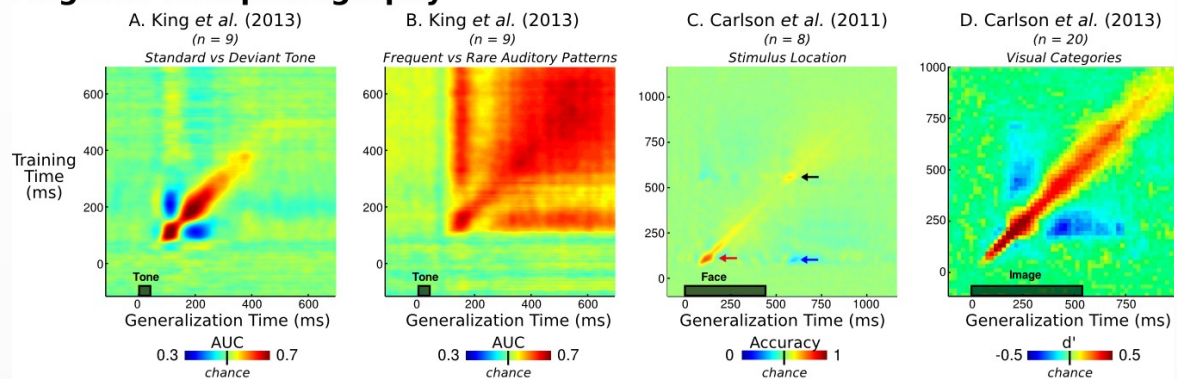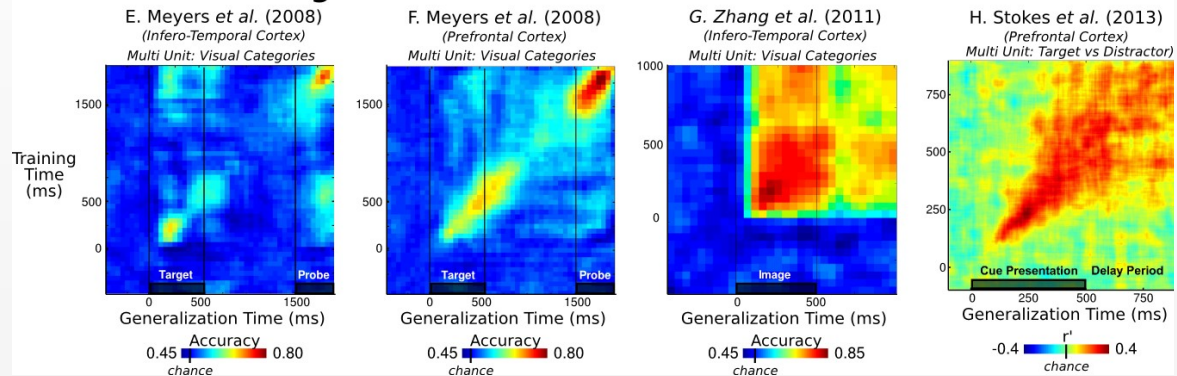
FIGURE 5.5 EXAMPLES OF EMPIRICAL FINDINGS.

Temporal generalization has been used with both invasive neuronal recordings and non-invasive MEG data. Although the classifier (Support Vector Machine, Linear Discriminant Analysis, etc.) and performance measure varied (accuracy, d', area-under-the-curve (AUC) or correlation index r'), the results illustrate some of the major dynamic structures postulated in figure 3: diagonal chain (e.g. A, C, D, F), reactivation at the time of a second stimulus (E, F) or at stimulus offset (C), sustained activity (B, G) or transition from diagonal to sustained (H). Reversing brain patterns are visible as below-chance generalization performance (blue patches in panels A, C, D). Note that across studies, the same region (e.g. infero-temporal cortex) seems capable of generating very distinct dynamics (compare panels E and G).

5.7. GENERALIZATION ACROSS TIME AND CONDITIONS

The principle of generalization across time can be further extended to generalization across experimental conditions. Ever since Donders and Sternberg, the manipulation of various experimental factors (*e.g.* attention, expectation, picture contrast, *etc.*) has been used to selectively accelerate, slow down, remove, insert, or reorder specific processing stages. The temporal generalization matrix may directly reveal such changes in processing architecture (FIGURE 5.6). The logic consists in training at time t in condition c and testing at time t' in condition c'. An acceleration of some stages will then be perceptible as a displacement of the generalization window outside of the diagonal. The method can identify at what time, and for how long, the acceleration occurred. Other changes, such as the deletion or insertion of processing stages or their temporal reordering, can be similarly characterized.
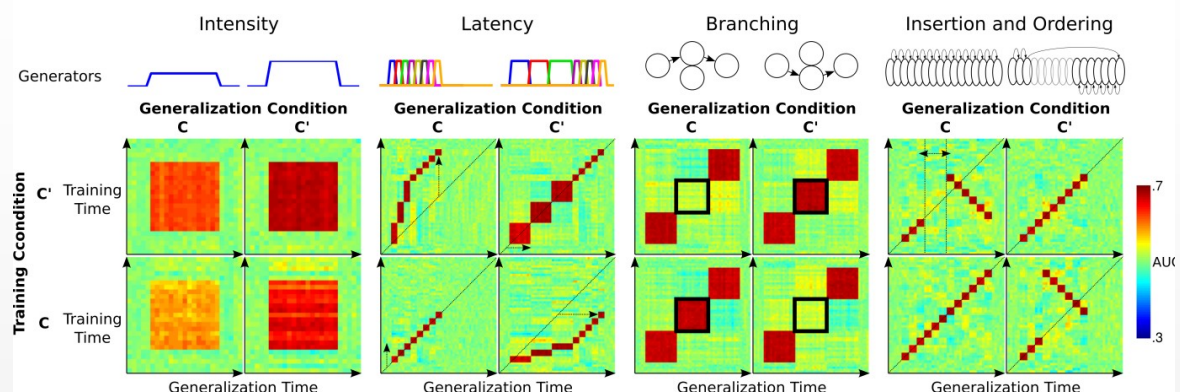
FIGURE 5.6 GENERALIZATION ACROSS TIME AND EXPERIMENTAL CONDITIONS

When data is available from two experimental conditions (c and c'), the pattern of generalization across time and conditions provides diagnostic information about the organization of brain processes. The four simulations shown indicate how changes in activation intensity, latency, branching, or ordering each lead to a distinct cross-condition generalization matrix.

A striking example of temporal reorganization is provided by the decoding of spatial location from single-cell recordings. Capitalizing on the earlier demonstration that rat location could be accurately decoded from hippocampal place-cell activity (WILSON AND MCNAUGHTON, 1994), Louie and Wilson (LOUIE AND WILSON, 2001) identified a sequence of place-cell firing that reproducibly tagged the animal's movement through a circular track. They then showed that the same sequence was replayed during REM sleep, at approximately the same speed or slower (see also (POE ET AL., 2000)). Subsequently, Lee and Wilson (LEE AND WILSON, 2002) showed that place-cell activity, which could be used to detect the location and direction of actual animal movement, was also replayed at 20-times faster speed during slow wave sleep, while the animal was, of course, immobile. Accelerated replay was also observed in the awake state (DAVIDSON ET AL., 2009). Recently, Pfeiffer and Foster (PFEIFFER AND FOSTER, 2013) found that brief bouts of place-cell activity could be decoded into single-trial goal-directed trajectories that anticipated, at an accelerated pace, the subsequent movement of the rat on the very same trial. Place-cell firing may also recur in reverse order (FOSTER AND WILSON, 2006), perhaps reflecting a form of goal-based problem solved by means-ends analysis. Those examples prove that temporal accelerations and reversals do occur in brain activity, and invite a search for their occurrence in other cognitive domains (*e.g.* bird song (DAVE AND MARGOLIASH, 2000)), using the temporal generalization matrix as a telling signature.

5.8. CONCLUSION

In the brain-imaging community, multivariate pattern classifiers are primarily used to analyze brain-imaging data at a fine *spatial* scale. Here, we summarized a number of ideas and empirical studies which suggest that it can also be used to probe the fine *temporal* organization of brain activity. Characterize the building blocks of cognitive processes in time, rather than in space, presents many challenges and open issues (see BOX 5.8), for which we hope that the temporal generalization method may prove useful.

BOX 5.7 *DOES THE BRAIN OPERATE AS A DECODER OF ITS OWN SIGNALS?*

Multivariate pattern analysis is a powerful method. Could it also be considered as a metaphor for some brain operations? Consider the problem of identifying a face from retinal inputs. The primary visual area contains all the information needed to identify a flashed face, yet this information is "entangled" in a complex manifold of firing rates (DICARLO ET AL., 2012). The hierarchy of areas in the ventral visual stream may "disentangle" the information until it is no longer implicit in distributed activity, but is explicitly coded in the firing rate of a small neuronal population. For IT neurons, learning to become sensitive to a specific face may consist in learning a classification function that, given the input firing rates, separates instances of this face from any other stimulus. Similarly, training on a psychophysical experiment implies that the prefrontal and parietal areas learn to weigh evidence from the relevant sensory neurons and disregard uninformative cells. Each brain area may thus be confronted with a multivariate classification problem similar to that of the neuroscientist attempting to sift through a pile of recorded data.

Asking whether a brain area acts as a decoder of its afferent inputs leads to interesting questions. For instance, is the brain confronted with issues of over-fitting and, if so, does it use regularization or penalization schemes, as some pattern classification algorithms do (e.g. SVM (CHANG AND LIN, 2001))? Does it reject outlier data? Does it suffer from a "curse of dimensionality", and if so, does the pyramidal neuron's limited dendritic span provide a solution by drastically reducing the data under consideration? Does every single neurons operate as a high-level decoder, as in the classical "grand-mother cell" scheme? Or is information decodable only at the population level, with neurons failing to provide invariant information individually, yet collectively providing a linearly separable code to the next hierarchical level (LI AND DICARLO, 2010)?

The brain-as-a-decoder metaphor suggests novel experiments. It implies that the activity of a neuron, voxel or brain region could be modeled as a linear combination of other brain signals (a cortico-cortical extension of the concept of "receptive field") (HEINZLE ET AL., 2011). Furthermore, the metaphor justifies the use of linear MVPA, such as linear discriminant analysis or linear support machine, in order to analyze brain signals. A non-linear MVPA would exceed the power available to a typical single-layer neural network (MINSKY AND PAPERT, 1988) and would therefore decode implicit information which is probably not available to the brain itself (e.g. faces from V1). Identifying a temporal sequence of neuronal codes, as proposed here, would not be possible if an exceedingly powerful non-linear MVPA was used, because even abstract information could then be extracted from early areas. Ideally, MVPA should aim to decipher precisely those signals that the brain uses for its internal computations, no more, no less. Thus, MVPA should attain the same performance as the behavior or brain system of interest (e.g. (LI AND DICARLO, 2010; RUST AND DICARLO, 2010)), and should fail on exactly the same trials (WILLIAMS ET AL., 2007).

BOX 5.8 OUTSTANDING QUESTIONS

- *What factors make certain cerebral operations appear as "diagonal" and others as "square" in temporal generalization matrices?*

- *What other dynamical patterns may appear in brain activity? Does the brain rely on a limited repertoire of canonical dynamical patterns that recur in very different types of computations?*

- *Does each brain region possess a characteristic repertoire of dynamical patterns (e.g. serial flow in the ventral stream, evidence accumulation in parietal cortex, all-or-none maintenance in prefrontal cortex…)?*

- *Is there a systematic correspondence between dynamical patterns at the microscopic (single-neuron) and macroscopic (neuronal population) levels?*

- *Does sensory processing consist in a discrete series of stages (as suggested by the labels of EEG components P_1, N_1, P_2, etc), or does it involve a continuous cascade of events?*

- *Why do we often see a reversal of generalization, leading classifiers to worse-than-chance performance when tested away from their initial training time?*

- *How do experimental factors such as expectation, task relevance or task difficulty affect the dynamics of neuronal encoding and decoding? Do they systematically modulate, delay, or reorganize brain activity?*

CHAPTER 6. INFORMATION SHARING IN THE BRAIN INDEXES CONSCIOUSNESS IN NON-COMMUNICATING PATIENTS

6.1. INTRODUCTION OF THE ARTICLE

Event related potential only reflect one of the putative neuronal signatures of conscious processing. As detailed in the literature review, a series of other electrophysiological markers have been proposed by neural theories of conscious access. In particular, several models converge on the idea that the amount of information shared across brain regions should particularly well index subjects' state of consciousness.

Assessing information sharing across brain solely with EEG can be particularly difficult. Indeed, each EEG electrode is not influenced by a unique and specific brain region but captures a mixture of different brain areas. Furthermore, several scalp electrodes can record a signal generated by a single brain area. As a consequence, correlating the signals across EEG channels is very different from correlating signals across brain regions. Finally, clinical data is terribly noisy and thus makes functional connectivity analyses difficult for two main issues. First, ocular and muscle movements introduce a common signal to most EEG channels. Second, patients often present important brain and even skull lesions, which drastically limits the possibility of solving the inverse problem and compute functional connectivity in the source space.

In the present paper, I developed, together with Jacobo Sitt, a novel method to overcome these issues. We propose a simple analysis to compute the mutual information across qualitatively distinct patterns of EEG signals. The logic is simple: if the patterns of two EEG signals are qualitatively different, then they cannot be generated by a common source – should it be cortical, ocular or muscular. If these two patterns systematically co-occur, then it indicates that their respective generators are functionally connected. The analysis therefore consists in i) transforming the EEG signals into different qualitative dynamical patterns ("symbols") , ii) masking the pairs of patterns that can be trivially explained by common sources and iii) computing the mutual information across the remaining pairs of symbols.

It may be interesting to note that the present finding beneficiated from serendipity. In the initial submission of the present work, the analysis did not include the weighing step. Although this first measure significantly discriminated vegetative from minimally conscious state patients, we imagined and implemented the weighing feature during the revision of the manuscript. The subsequent results were particularly striking, as they not only reached significance and thus validated our first finding, but they largely outperformed the initial measure.

6.2. ABSTRACT

Neuronal theories of conscious access tentatively relate conscious perception to the integration and global broadcasting of information across distant cortical and thalamic areas (TONONI AND EDELMAN, 1998; REES ET AL., 2002; DEHAENE ET AL., 2006B; TONONI AND KOCH, 2008; LAMME, 2010; DEHAENE AND CHANGEUX, 2011). Experiments contrasting visible and invisible stimuli support this view and suggest that global neuronal communication may be detectable using scalp electro-encephalography (EEG) (REES ET AL., 2002; SERGENT ET AL., 2005; DEHAENE ET AL., 2006B; DEL CUL ET AL., 2007; FISCH ET AL., 2009; GAILLARD ET AL., 2009; DEHAENE AND CHANGEUX, 2011; MELLONI ET AL., 2011). However, whether global information sharing across brain areas also provides a specific signature of conscious state in awake but non-communicating patients remains an active topic of research (FAUGERAS ET AL., 2012; FINGELKURTS ET AL., 2012A; LEHEMBRE ET AL., 2012; ROSANOVA ET AL., 2012). We designed a novel measure termed "weighted symbolic mutual information" (wSMI) and applied it to 181 high-density EEG recordings of awake patients recovering from coma and diagnosed in various states of consciousness. The results demonstrate that this measure of information sharing systematically increases with consciousness state, particularly across distant sites. This effect sharply distinguishes patients in vegetative state (VS), minimally conscious state (MCS) and conscious state (CS) and is observed regardless of etiology and delay since insult. The present findings support distributed theories of conscious processing and open up the possibility of an automatic detection of conscious states, which may be particularly important for the diagnosis of awake but non-communicating patients.

6.3. INTRODUCTION

We evaluated whether measures of brain-scale information sharing, derived from 181 high-density electro-encephalography (EEG) recordings, could discriminate, within awake patients, those showing clinical signs of consciousness from those who do not. Our research capitalizes on experimental studies in normal subjects showing that consciously perceived stimuli, relative to subliminal stimuli, lead to a late ignition of fronto-parietal networks and to an increased sharing of information in the brain (DEHAENE AND CHANGEUX, 2011). Several theories share the hypothesis that this global communication between distant cortical areas defines what we experience as a conscious content (BAARS, 1989; TONONI AND EDELMAN, 1998; LAMME AND ROELFSEMA, 2000; REES ET AL., 2002; DEHAENE ET AL., 2006b; TONONI AND KOCH, 2008; LAMME, 2010; DEHAENE AND CHANGEUX, 2011; SETH ET AL., 2011).

To quantify global information sharing, we introduced a novel measure, weighted Symbolic Mutual Information (wSMI), which evaluates the extent to which two EEG signals present non-random joint fluctuations, suggesting that they share information (FIGURE 6.1). This method presents three main advantages. First, it looks for qualitative or "symbolic" patterns of increase or decrease in the signal which allows a fast and robust estimation of the signals' entropies. The symbolic transformation depends on the length of the symbols (here, k = 3) and their temporal separation (here, τ = 4, 8, 16 or 32 ms, see methods and (BANDT AND POMPE, 2002)). Second, wSMI makes few hypotheses on the type of interactions and provides an efficient way to detect non-linear coupling. Third, the wSMI weights discard the spurious correlations between EEG signals arising from common sources and favor non-trivial pairs of symbols, as confirmed by simulations (SUPPLEMENTARY FIGURE 6.5).
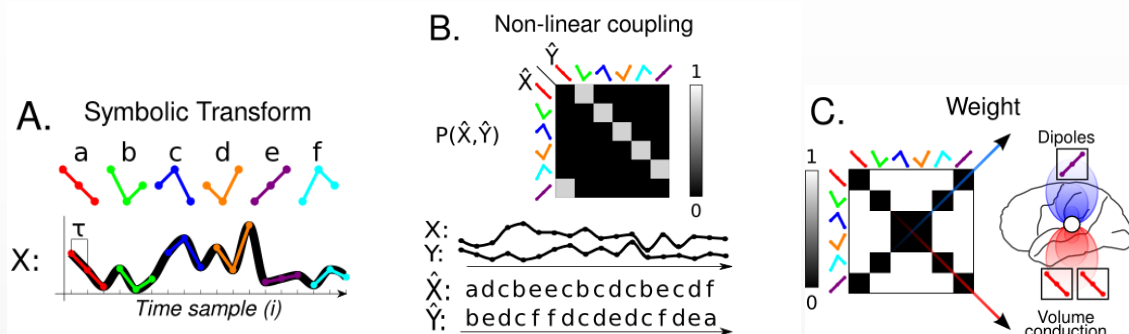
FIGURE 6.1 WEIGHTED SYMBOLIC MUTUAL INFORMATION (wSMI).

(a) The transformation of continuous signals (X) into sequences of discrete symbols (A, B ... F) enables an easy and robust estimation of the mutual information shared between two signals. The τ parameter refers to the temporal separation of the elements that constitute a symbol, composed of 3 elements. (b) By computing the joint probability of each pair of symbols, we can estimate the Symbolic Mutual Information (SMI) shared across two signals. (c) To compute wSMI, the SMI is weighted to disregard conjunctions of identical or opposite-sign symbols, which could potentially arise from common-source artefacts.

6.4. METHODS

Detailed experimental procedures and clinical details are provided in the Supplementary Materials and Table S1.

6.4.1.   PARTICIPANTS

181 EEG recordings (75 VS, 68 MCS, and 24 CS patients, as well as 14 Healthy controls) were obtained from 126 subjects (Age: M=47 years old, SD=18 years, males: 72 %) who performed an auditory experiment for clinical purposes (BEKINSCHTEIN ET AL., 2009). All patients had been without sedation for at least 24 hours prior to the recording session, which was performed to help assess their diagnosis and their state of consciousness. Before each EEG recording, trained neurologists (FF, BR, LN) performed a clinical evaluation of the patients with the Coma Recovery Scale Revised (CRS-R) from which patients' arousal and state of consciousness was derived (SCHNAKERS ET AL., 2008B). Note that CS patients differed from healthy subjects as they presented important brain lesions, were often recovering from a VS or an MCS, and were recorded at bedside. Data from healthy subjects were only used to verify the consistency of the proposed measure of consciousness.

6.4.2.   EXPERIMENTAL DESIGN & EEG PREPROCESSING

Analyses were based on 800 ms time-periods during which subjects were presented to 4 consecutive identical tones. EEG preprocessing is described in Supplementary Materials.

6.4.3.   WEIGHTED SYMBOLIC MUTUAL INFORMATION (wSMI)

EEG signals were first transformed in a series of discrete symbols defined by the ordering of k time samples separated by a temporal separation τ (FIGURE 6.1). Analysis was restricted to a fixed symbol size (k = 3) and four different values of τ (τ = 4, 8, 16 or 32 ms between time samples). To avoid aliasing artefacts, signals were low-pass filtered at corresponding frequencies (40, 20 and 10 Hz for τ = 8, 16 and 32 ms respectively). Then wSMI was estimated for each pair of transformed EEG signals by estimating the joint probability of each pair of symbols. To reduce spurious correlations between signals, the joint probability matrix was multiplied by binary weights. The weights were set to zero for pairs of identical symbols, which could be elicited by a unique common source, and for opposed symbols, which could reflect the two sides of a single electric dipole.

Cluster analyses were performed by averaging wSMI obtained across the 256*(256-1)/2 channel pairs within 16*(16-1)/2 manually selected regions. The distance separating EEG channels was calculated along a straight line using default electrode coordinates.

6.4.4.   STATISTICS

Except if stated otherwise, statistical analyses were performed with R and MATLAB (2009b) and non-parametric two-tail tests (Wilcoxon, Mann-Whitney U tests and MATLAB's robust and stepwise regressions). Effect sizes are reported using Receiver Operating Curve (ROC) and Area Under the Curve (AUC) analyses. False discovery rate (FDR) was used to correct for multiple comparisons (noted as p_{FDR}).

6.5. RESULTS

We focused our analyses on patients with preserved arousal abilities. Within this category, vegetative state (VS) patients present no clinical signs of conscious behavior, whereas minimally conscious state (MCS) patients demonstrate fluctuating but consistent deliberate responses (GIACINO ET AL., 2002).

6.5.1.   wSMI INDEXES THE STATE OF CONSCIOUSNESS

When considering the median wSMI across all channel pairs, analyses with τ = 32 ms revealed that VS patients (n = 75) presented significantly lower information sharing than MCS patients (n = 68; U = 3737, p < 10^{-5}, AUC = .73), conscious (CS) patients (n = 24; U = 1445, p<10^{-5}, AUC = .80), and healthy (H) controls (n = 14; U = 890, p < 10^{-4}, AUC = .85) (FIGURE 6.2.A). A robust regression confirmed that median wSMI predicted the clinical group to which the subjects belonged (1: VS, 2: MCS, 3: CS, 4: Healthy; p < 10^{-6}). These effects were observed for all temporal separation parameters τ, except the shortest value of τ = 4 ms (SUPPLEMENTARY FIGURE 6.6.A).
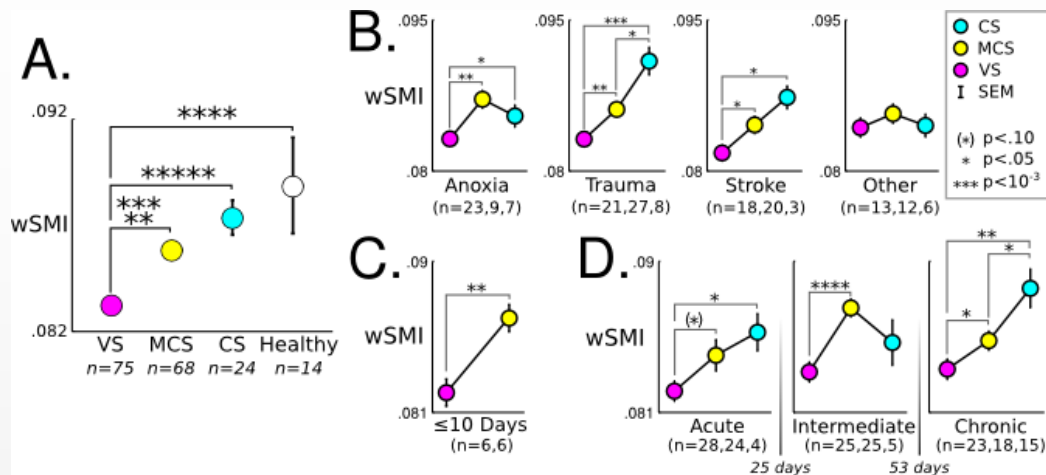
FIGURE 6.2 wSMI INDEXES CONSCIOUSNESS INDEPENDENTLY OF ETIOLOGY AND DELAY SINCE INSULT.

(a) The median wSMI across current sources is depicted for each state of consciousness. Error bar represent standard error of the mean (SEM). Significant pair-wise comparisons are denoted with stars. Analyses were reproduced for each (b) etiology and (c-d) delay since insult. The results showed that median wSMI is mainly affected by the state of consciousness, and does not vary significantly across etiology or delays.

6.5.2.   wSMI IS CONSISTENT ACROSS ETIOLOGIES AND DELAY SINCE INSULT

We tested the robustness of wSMI to variability in etiologies and delay since the initial insult. An ANOVA across patients, consciousness states and etiologies showed a main effect of consciousness state ($F_{(2,119)}$ = 11.96, p <10^{-4}), but no main effect of etiology ($F_{(3,119)}$ = 1.83, p = .145). The difference in median wSMI between VS and MCS patients remained significant within cases of anoxia (n = 23 VS, 9 MCS); U=181, p = .001, AUC = .87), traumatic brain injury (n = (21, 27); U = 126, p = .001, AUC = .78) and stroke (n= (18, 20); U = 102, p = .024, AUC = .72) (FIGURE 6.2.B).

Similarly, when we categorized the patients according to the time delay between disorder onset and EEG recording (acute [<25 days], intermediate [25-50 days] or chronic [>50 days]), we again found a main effect of consciousness state ($F_{(2,132)}$ = 10.01, p < 10^{-4}) but no main effect of delay ($F_{(2,132)}$ =

2.24, p = .110). The difference in median wSMI between VS and MCS patients remained significant within chronic (n = (23 VS, 18 MCS); U = 295, p = .022, AUC = .71) and intermediate (n = (25, 25); U = 98, p < 10^{-4}, AUC = .84) patients, and was marginal in acute subjects (n = (28, 24); U = 443, p = .054, AUC = .66) (FIGURE 6.2.D). Patients tested just after the insult (<10 days) presented a significant effect too (n = (6, 6); U = 36, p = .002, AUC = 1.00; FIGURE 6.2.C).

6.5.2.1.   Relationship between wSMI and other entropy or spectral measures

Does wSMI merely detect a difference which is also present in simpler measures? First, mutual information need not covary with the entropies of the two signals, but is bounded by them. Empirically, we found that permutation entropy significantly increased with consciousness states (SUPPLEMENTARY FIGURE 6.6.I). Crucially, the differences in wSMI between VS and MCS patients remained significant after normalizing the symbolic mutual information by local permutation entropy (SUPPLEMENTARY FIGURE 6.6.J). Thus, wSMI did not simply reflect changes in local entropies.

Similarly, the power in various frequency bands correlated partially with wSMI (Table S2) and was informative about the patients' state of consciousness (SUPPLEMENTARY FIGURE 6.6.G). Nevertheless, in a stepwise regression, median wSMI at τ = 16 and 32 ms systematically outperformed power spectrum measures in discriminating VS and MCS patients. Furthermore, once wSMI was entered in the model, spectral differences were no longer predictive. At shorter τ (4 or 8 ms), the converse pattern was observed: power spectrum measures contributed to the prediction of consciousness state whereas wSMI did not (Table S3). Therefore, for long τ, wSMI provides robust information about consciousness, over and above power spectral densities.

A distinct question is which frequency bands carry the effects detected by wSMI. Each selection of a τ value sensitizes wSMI to a different frequency range (~4-10 Hz for τ = 32 ms; ~8-20 Hz for τ = 16 ms; SUPPLEMENTARY FIGURE 6.6.H). Further band-pass filtering prior to wSMI computation suggested that the difference between VS and MCS was particularly driven by events in the q band (4–8 Hz). However, no consistent group differences were found in phase-locking value or phase-locking index at 4Hz or above, and phase-locking alone did not suffice to explain the difference in wSMI (Tables S4, S5).

6.5.3.   wSMI IMPAIRMENTS PREDOMINATE OVER CENTRO-POSTERIOR REGIONS

Topographies summarizing the amount of information that each EEG channel shares with others suggest that the information sharing deficit in VS patients was present over most scalp regions (p_{FDR}<.05 in more than 97% of the current sources, FIGURE 6.3.A). When comparing VS to MCS patients, the median wSMI over frontal areas was less impaired than over the posterior regions (Fz versus Pz EEG channels; U = 2035, p = .038, AUC = .60).

To facilitate the interpretation of the very large number of channel pairs (FIGURE 6.7.C-E), we reduced our data to 16 clusters composed of ~16 current sources each. The results confirmed that VS patients exhibited an overall reduction of information sharing mainly with centro-posterior areas (FIGURE 6.3.B): 48% of the 120 cluster pairs showed significantly smaller wSMI in VS than in MCS or in CS patients (p_{FDR} < 0.05).
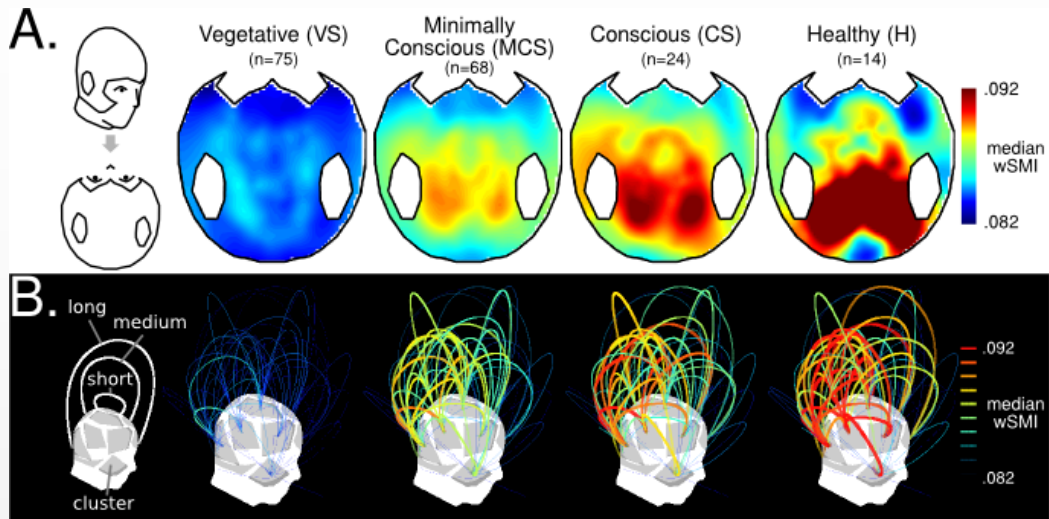
FIGURE 6.3 wSMI INCREASES WITH CONSCIOUSNESS PRIMARILY OVER CENTRO-POSTERIOR REGIONS.

(a) The median wSMI that each EEG channel shares with all other channels is depicted for each state of consciousness. (b) 120 pairs formed by 16 clusters of EEG channels are depicted as 3D arcs, whose height is proportional to the Euclidian distance separating the two clusters. Line color and thickness are proportional to the mean wSMI shared by the corresponding cluster pair.

6.5.4. VARIATIONS WITH INTER-CHANNEL DISTANCE
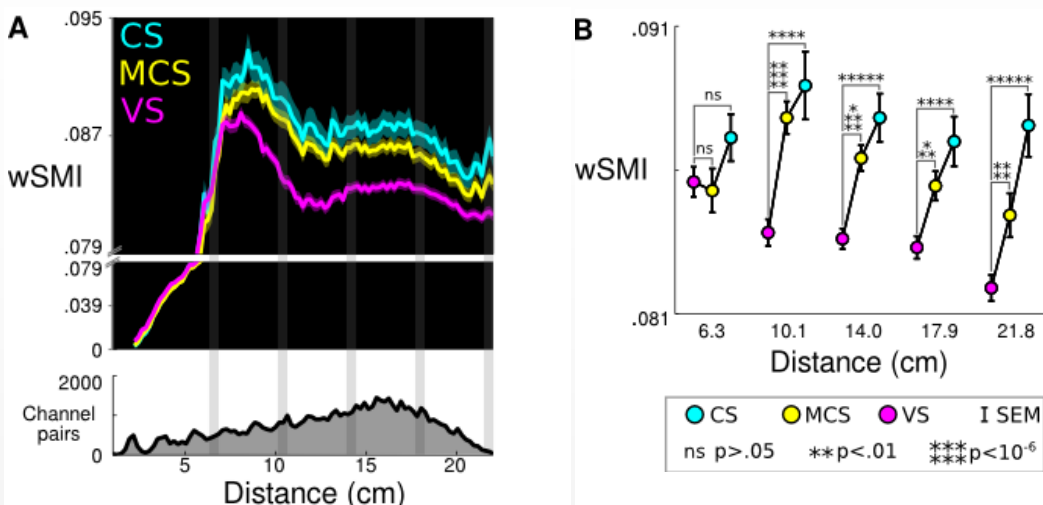
FIGURE 6.4 wSMI AS FUNCTION OF INTER-CHANNEL DISTANCE.

(A, top) wSMI is plotted as a function of the Euclidian distance separating each pair of EEG channels. While wSMI is relatively stable between 8 and 23 cm, it drops towards zero as inter-channel distances diminish, which thus confirms its robustness to common source artefacts. (bottom) Histogram plotting the density of channels pairs as a function of inter-channel distance. (B) VS patients presented lower wSMI than MCS and CS patients particularly over medium and long inter-channel distances (>10 cm).

To test the hypothesis of a change in brain-scale information sharing, we investigated the relationship between wSMI and the Euclidian distance separating the channels. For distances below 5 cm, wSMI quickly dropped towards zero, as expected given that this measure was designed to eliminate common source artefacts (FIGURE 6.4.A & SUPPLEMENTARY FIGURE 6.8.A). We therefore avoided these short distances

and restricted our analyses to five equally spaced distances for which the median wSMI was comparable at $\tau = 32$ ms. wSMI discriminated VS from MCS at all but the shortest inter-channel distance (FIGURE 6.4.C). The interaction of distance with consciousness state (VS versus MCS) was significant when pitting the shortest distance against any of the longer ones (all $p < 0.028$). Thus, wSMI is robust to variations in inter-channel distance, except in the very short range, suggesting that loss of consciousness is associated with an impairment in information sharing over medium to long distances. With non-weighted SMI, the difference between VS and MCS was weaker and was invariant to inter-channel distance (SUPPLEMENTARY FIGURE 6.8.C-D).

6.6. DISCUSSION

Several theoretical models of consciousness predict that brain-scale information sharing should provide a consistent signature of conscious processing (BAARS, 1989; TONONI AND EDELMAN, 1998; LAMME AND ROELFSEMA, 2000; REES ET AL., 2002; DEHAENE ET AL., 2006B; TONONI AND KOCH, 2008; LAMME, 2010; SLIGTE ET AL., 2010; DEHAENE AND CHANGEUX, 2011; SETH ET AL., 2011). In agreement with this prediction, we show that wSMI, which estimates the amount of information shared by two EEG signals, increases as a function of consciousness state and separates vegetative state (VS) from minimally conscious state (MCS) patients. This increase appears particularly prominent across centro-posterior areas and across medium and long inter-channel distances.

These results supplement recent EEG studies investigating the relationship between information sharing and loss of consciousness using spectral-based functional connectivity measures (FINGELKURTS ET AL., 2012B; LEHEMBRE ET AL., 2012). The present work relies on a large group of patients, which allowed us to demonstrate the independence of our findings from etiology and delay since insult. Moreover, our measure, unlike several traditional synchrony measures, minimizes common-source artefacts and improves the discriminability of consciousness states. Finally, we show that its changes cannot be simply reduced to local changes in entropy or power spectrum, but reflect a genuine change in information sharing particularly detectable over medium and long distances across the scalp. A similar change may also exist at shorter distances, but due to common-source artefacts, scalp EEG is unlikely to provide conclusive information on this point.

The observed change in brain-scale information sharing fits with earlier observations showing that the state of consciousness can be affected by diffuse anatomical lesions to the cortex and the underlying white matter, as well as to the thalamic and brain stem nuclei. In particular, several studies have underlined the prominent role of diffuse white matter lesions in persistent VS (AMMERMANN ET AL., 2007; NEWCOMBE ET AL., 2010; FERNÁNDEZ-ESPEJO ET AL., 2011; GALANAUD ET AL., 2012). These anatomical lesions may lead to functional deficits in thalamo-cortical (LAUREYS ET AL., 2000B; ZHOU ET AL., 2011) as well as cortico-cortical communication (LAUREYS ET AL., 1999A; CAUDA ET AL., 2009; VANHAUDENHUYSE ET AL., 2010; ROSANOVA ET AL., 2012) and to abnormal default mode network activity in VS patients (CAUDA ET AL., 2009; VANHAUDENHUYSE ET AL., 2010; BRUNO ET AL., 2011C; CRONE ET AL., 2011; FERNÁNDEZ-ESPEJO ET AL., 2011; SODDU ET AL., 2012), all of which would result in reduced mutual information over long cortico-cortical distances, as observed here.

wSMI could be computed after cortical source modeling, but this step remains fraught with inaccuracies, particularly given the patients' frequent brain and skull damage (KING ET AL., 2011). Instead, our analyses were performed after applying a current-source-density transform to EEG recordings, which coarsely focalizes the effects over the corresponding cortical regions. Topographically, the largest differ-

ences in information sharing between VS and MCS patients were found over centro-posterior regions. Although this effect may appear at odds with the preponderant role of the prefrontal cortex in conscious processing (DEHAENE ET AL., 2006B; LAU, 2008; DEHAENE AND CHANGEUX, 2011), it fits with the recent identification of posterior cingulate and precuneus as essential hubs of cortical networks (DEHAENE AND CHANGEUX, 2011) and the correlation of mesio-parietal activity with the state of consciousness (ALKIRE ET AL., 2008). In particular, numerous studies have highlighted a frequent hypoactivation of the precuneus and posterior cingulate in VS patients (LAUREYS AND SCHIFF, 2011). These areas participate in the default mode network and have been repeatedly associated with the representation of self and others, episodic memory and mental imagery (BUCKNER ET AL., 2008; NORTHOFF, 2012), *i.e.* processes which are characteristic of the conscious brain.

Our study could be criticized for pooling over a group of VS patients, while recent functional magnetic resonance imaging (fMRI) results suggest that some of them may actually show preserved consciousness undetectable by classical clinical examination (OWEN ET AL., 2006; MONTI ET AL., 2010). However, recent estimates suggest that this may concern ~15-20% of VS patients (MONTI ET AL., 2010). Although their presence in our data cannot be excluded, it would minimally affect our conclusions and would only reduce our effect sizes. Nevertheless, it would be interesting to measure wSMI separately in VS patients with versus without a capacity for fMRI-based communication. In the former, we predict that wSMI should remain quantitatively unimpaired.

Our findings are compatible with theories that associate consciousness with recurrent loops in posterior networks (LAMME, 2010), a distributed brain-scale global workspace (DEHAENE ET AL., 2006B; DEHAENE AND CHANGEUX, 2011), or a global "dynamic core" (TONONI AND KOCH, 2008). They add to the panoply of behavioral and neuroimaging tools available to diagnose disorders of consciousness (LAUREYS AND SCHIFF, 2011). Our measure has the advantage of using EEG, a measure available in all clinics, rather than the complex and costly method of fMRI combined with instructions such as imagining playing tennis (OWEN ET AL., 2006) or answering a spoken question (MONTI ET AL., 2010). In a recent fMRI study (MONTI ET AL., 2010), 28 out of 33 MCS patients with consistent behavioral signs of consciousness showed no fMRI markers of deliberate communication. Future research should investigate whether the present technique, which may detect any residual brain-scale information sharing, proves more sensitive. Ultimately, a combination of neuroimaging and behavioral measures is likely to prove most useful in the clinic.

6.7. ACKNOWLEDGEMENTS

6.8. SUPPLEMENTARY MATERIALS

6.8.1.   SUPPLEMENTARY FIGURES
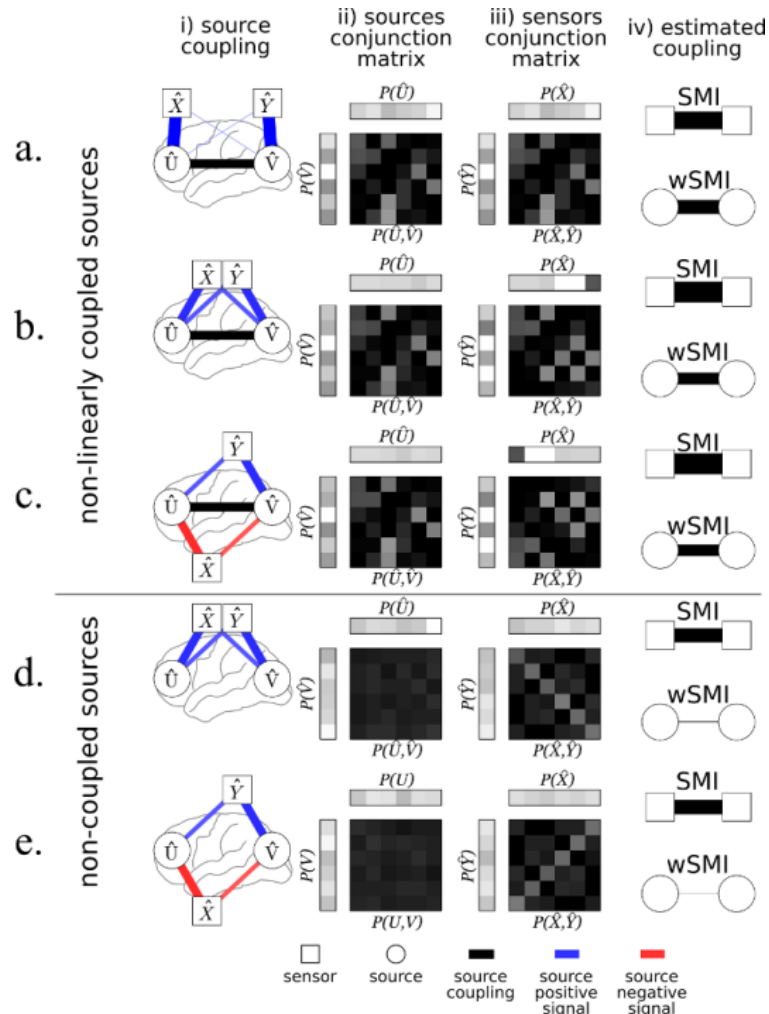
FIGURE 6.5 SIMULATIONS ESTABLISHING THE EFFICIENCY OF wSMI IN ESTIMATING THE COUPLING BETWEEN TWO DISTANT REGIONS WHILE MINIMIZING COMMON SOURCE ARTEFACTS.

Each horizontal set of graphs depicts the outcome of a simulation, using different hypotheses about source coupling. The figure depicts, for each simulation, the diagram of the simulation (i), the single and joint probabilities matrices at the source (ii) and at sensor level (iii), and the SMI and wSMI both estimated at the sensor level (X, Y) (iv).

(i), Circles represent two simulated sources (U, V) whose actual coupling strength is indicated by the width of the horizontal bar joining U and V. Squares represent sensors (X, Y), which may capture either a pure estimate or a heterogeneous mixture of signals from source U and V. The amount of signal they receive from U and V is represented by the width of the colored lines. Blue lines indicate a signal recorded on the positive side of the simulated "electric field" whereas red lines indicate recorded signals with the opposite sign. Line-width is proportional to the respective simulated values.

(ii) After transforming the continuous signals into symbolic sequences (U, V, X, Y), the single probability of each symbol can be computed for the time series corresponding to each source $(P(U), P(V))$. The joint probability matrix depicts the probability of each symbol v to occur in V if u is in U

(P(*U*, *V*)). (iii) Similar single probabilities and joint probabilities at the sensor level (P(*X*), P(*Y*), P(*X, Y*)) can be computed too.

(iv) Qualitative SMI and wSMI results as estimated from sensor signals (X, Y).

Five scenarios were explored: three scenarios in which there is a strong non-linear U-V coupling (a-c), and two in which there is a very small coupling (d, e). Note that wSMI, contrarily to SMI, recovers the correct nature of the source coupling (iv).

(a) In this scenario, sensors capture quasi pure signals (95%) from their respective source and only a small proportion of the other source (5%). In this trivial case, SMI and wSMI applied at the sensor level both provide good estimates of the U-V coupling.

(b) In this scenario, sensors capture heterogeneous signals (65%) from their respective source but are largely contaminated by the other source (35%). wSMI continues to correctly estimate the UV coupling.

(c) A similar case to (b), except that one of the sensors is located at the opposite side of U and V – mimicking the bipolar characteristics of electric fields.

(d) In this scenario, sensors capture a 65% mixture of U and V, although the UV coupling is close to zero. SMI thus overestimates the amount of UV coupling because it captures mutual information observed at the sensor level. Indeed, the sensor joint-probability matrix overestimates the downward diagonal. In contrast to SMI, wSMI remains robust to this common source artefact. In this difficult case, only wSMI indicates the genuine nature of the UV coupling.

(e) A similar case to (d), except that one of the sensor is located on the opposite side of the sources. Note that the joint probability matrix now overestimates the opposite diagonal. Again, in contrast to SMI, wSMI remains here robust to common source artefacts.
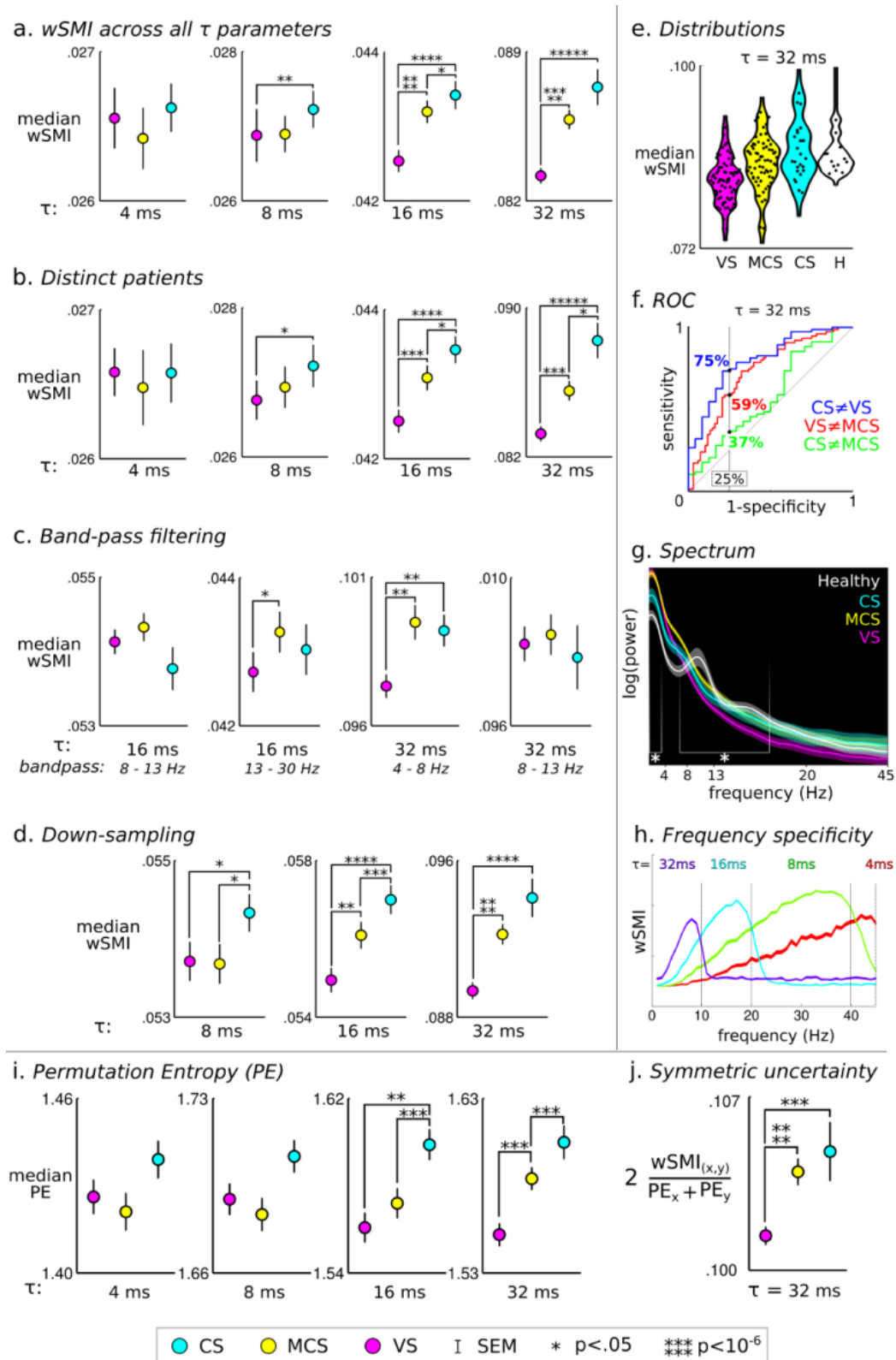
FIGURE 6.6 COMPLEMENTARY ANALYSES TESTING THE ROBUSTNESS AND THE SPECIFICITY OF wSMI.

a. The figure shows the median wSMI obtained for all tested τ values (4, 8, 16, or 32 ms). The main effect of consciousness state is robust across all τ values but $\tau = 4$ ms (all $p < .05$). Discrimination of VS and MCS patients is only significant for the higher values of τ (16 and 32 ms). At $\tau = 4$ ms, the analysis captures patterns of relatively high frequencies (panel h) and did not consistently vary across consciousness states.

124

b. *A few DOC patients were evaluated and recorded several times in order to assess potential improvements of their consciousness state (see Methods). Here we replicated the main analysis (shown in panel a) but using only a single EEG recording per patient diagnosed in a given state of consciousness. The obtained results closely match those observed in (a).*

c. *Median wSMI obtained for the discriminatory τ parameters (16 and 32 ms) after band-pass filtering the EEG signals (4-8, 8-13 or 13-30 Hz) to further isolate the frequencies responsible for the wSMI differences across consciousness states. The results suggest that wSMI variations are mainly due to events observed in the θ frequency range (4 – 8Hz).*

d. *Robustness to sampling rate. Median wSMI obtained for all tested time-scale parameters (τ = 8, 16, or 32 ms) after down-sampling the EEG recordings to 125 Hz. The results closely match those obtained from recordings sampled at 250 Hz (panel a). Note that at 125 Hz, it is not possible to compute wSMI with τ = 4 ms.*

e. *Distribution of wSMI values. The figure shows the median wSMI (τ = 32 ms) obtained in each individual EEG recording (black dot) as a function of consciousness state. Although wSMI differs across consciousness states, their respective distributions partially overlap.*

f. *Sensitivity – specificity analyses estimated with an empirical Receiver-Operating Curve. Sensitivity percentages are reported for all comparisons (red: VS-MCS, blue: VS-CS & green: MCS-CS) with a criterion fixed at a specificity of 75%.*

g. *Mean power spectrum densities (PSD, computed from non-facial EEG channels) for each state of consciousness. PSD in the δ, α and low β frequency bands significantly predict consciousness states.*

h. *Sensitivity of wSMI to pure-frequency signals. The results obtained from simulation analyses in which pairs of signals were constructed from phase-locked sinusoids (phase = $\pi/2$). wSMI is plotted for each temporal separation (τ) parameter, and for each frequency of the simulated signals. The results show that changing the value of τ makes the wSMI measure sensitive to different frequency ranges. To avoid aliasing artefacts, low-pass filtering is systematically applied as a function of τ (vertical lines, see Supplementary Method).*

i. *Permutation entropy (PE), computed for each channel separately, significantly indexes consciousness states for τ = 16 or 32 ms.*

j. *We calculated the symmetric uncertainty in order to test whether the changes in wSMI as a function of consciousness state were simply driven by local changes in entropy. The results for τ = 32 ms showed that symmetric uncertainty was significantly smaller in VS than in MCS and CS patients. Thus, wSMI discriminates consciousness states over and above PE.*
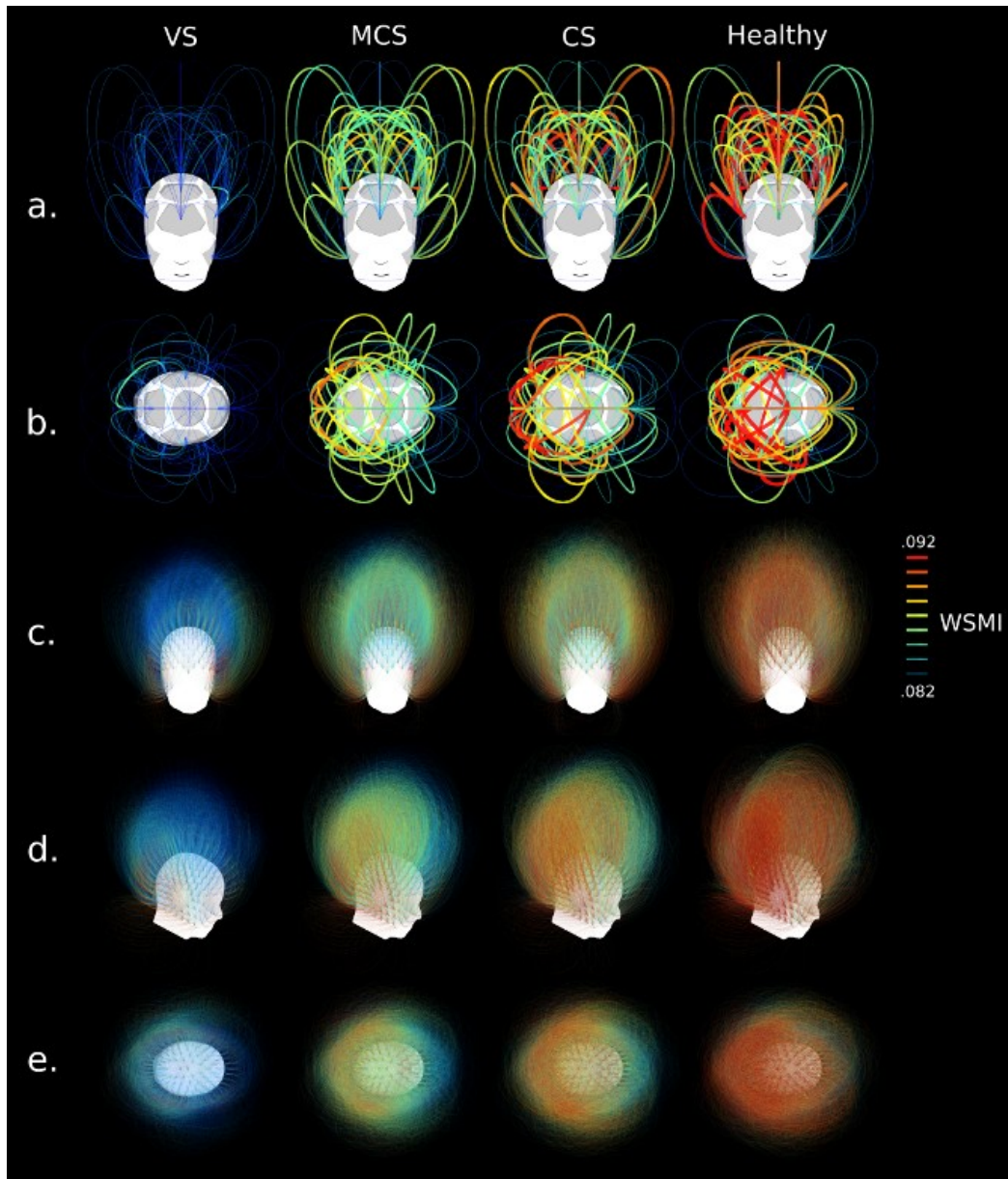
FIGURE 6.7 3D REPRESENTATION OF NON-CLUSTERIZED wSMI VALUES ACROSS STATES OF CONSCIOUSNESS.

*The color of each arc indicates the wSMI for each corresponding pair of channels or clusters. As in the cluster analysis (FIGURE 6.3), results show that the mutual information between a priori distinct cortical sources increases with the state of consciousness. (**a-b**) Front and top views corresponding to cluster analyses (FIGURE 6.3). (**c-e**) For each clinically defined state of consciousness, all 32,640 pairs of current sources are plotted in 3-dimensions following the principles described in FIGURE 6.3.*
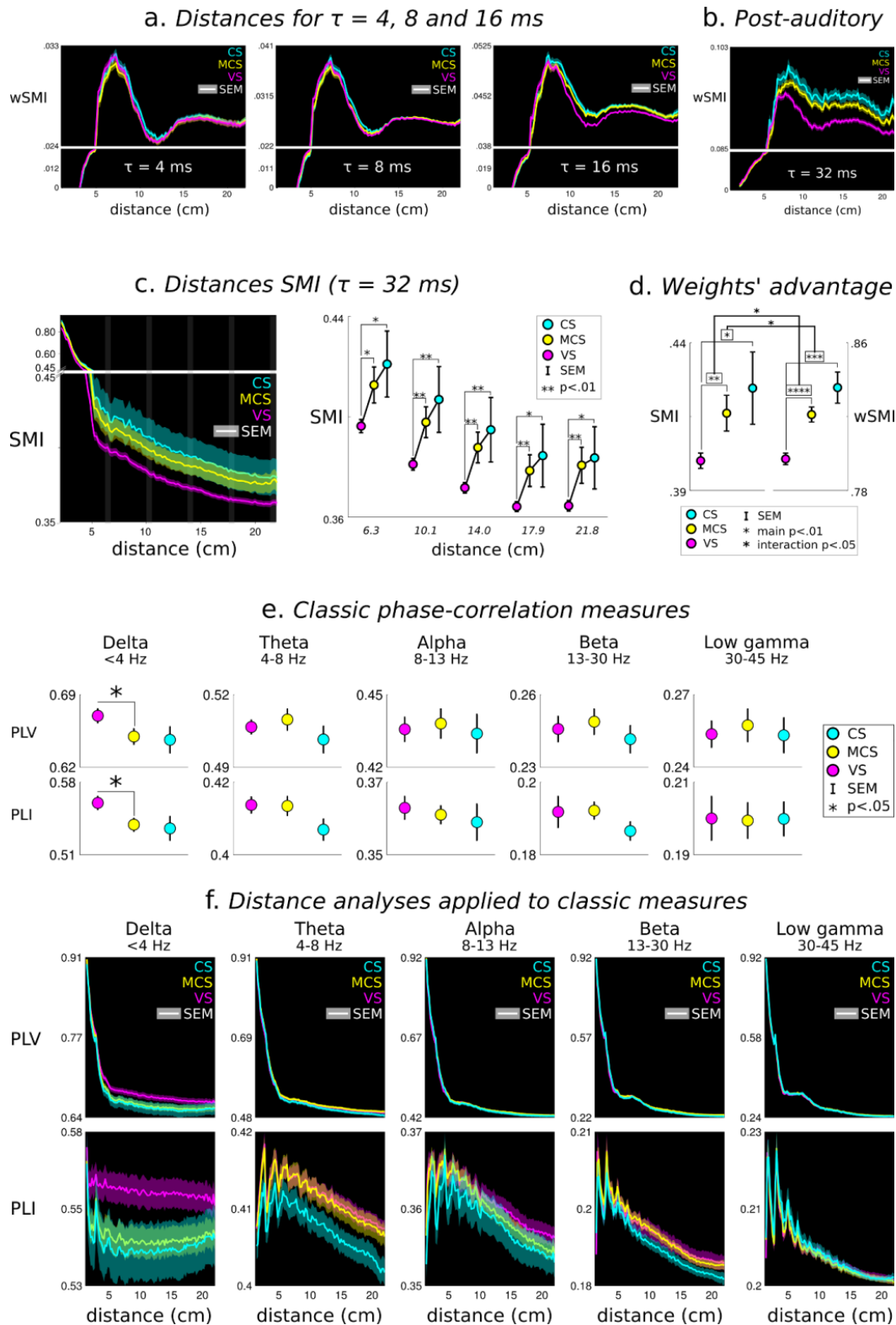
FIGURE 6.8 COMPLEMENTARY ANALYSES OF INTER-CHANNEL DISTANCE FOR EACH "FUNCTIONAL CONNECTIVITY" MEASURE.

a. *wSMI as a function of inter-channel distance is presented for all other tested temporal separation parameters (τ = 4, 8, or 16 ms).*

b. *Replication of the inter-channel distance analyses performed on wSMI (τ = 32 ms), but now using a different time period of the EEG recordings (post auditory stimulation). The obtained results closely match the ones obtained from signals acquired during the auditory stimulation.*

127

c. *Non-weighted SMI at τ = 32ms is displayed. The results show that contrarily to wSMI, SMI rapidly increases when the distance separating two EEG sensors drops towards zero, as expected given the sensitivity of SMI to common-source artefacts. Statistical analyses across the five distances (6.3 – 21.8 cm) revealed that VS had lower SMI than MCS and CS independently from inter-channel distance.*

d. *Analyses comparing the sensitivity of SMI (left) and wSMI (right) to consciousness states revealed that wSMI was a better predictor of consciousness state than SMI.*

e. *Traditional measures of "functional connectivity" / signal correlation such as Phase Locking Value (PLV) and Phase Lag Index (PLI) were also tested. The results are displayed as a function of inter-channel distance for each consciousness state and frequency of interest. Inter-channel distance is different from the previous analyses in order to plot the most representative values. Overall, none of these analyses was as powerful as wSMI in distinguishing the various states of consciousness. Statistical analyses of PLV and PLI suggest difference that VS have higher "functional connectivity" in the δ frequency band (0 – 4 Hz). None of these results significantly interacted with inter-channel distances.*

6.8.1.1.   Supplementary Tables

Table S1. Patients' clinical details

See online spreadsheet.

Table S2. Robust regression adjusted R² between wSMI and PSD

		Frequency (Hz)				
		0 - 4	*4 - 8*	*8 - 13*	*13 - 30*	*30 - 45*
τ (ms)	*4*	0.01	0.00	0.05	**0.30**	**0.42**
	8	**0.00**	**0.00**	**0.08**	**0.25**	**0.27**
	16	**0.14**	0.02	**0.12**	**0.08**	**0.04**
	32	**0.18**	**0.02**	**0.10**	**0.01**	0.00

Values correspond to the adjusted R² obtained with robust regressions. Bold values indicate a significant (uncorrected) correlation between wSMI at a given τ and the power in a given frequency band. wSMI at longer τ values mainly correlated with the power in low frequency-bands whereas at shorter τ wSMI mainly correlated with the power in higher frequency-bands.

Table S3. Stepwise regression: wSMI and PSD

		Frequency power (Hz)									
		0 - 4		*4 - 8*		*8 - 13*		*13 - 30*		*30 - 45*	
		PSD	*wSMI*	*PSD*	*wSMI*	*PSD*	*wSMI*	*PSD*	*wSMI*	*PSD*	*wSMI*
τ (ms)	*4*	****	-	-	-	***	-	**	*	-	-
	8	****	-	-	-	***	-	*	-	-	-
	16	*	****	-	****	-	****	-	****	-	****
	32	*	****	*	****	-	****	-	****	-	****

Stepwise regressions were applied to test whether PSD and wSMI independently predicted consciousness states. Stars indicate a significant contribution of the corresponding regressor (* $p < .05$, **** $p < 10^{-4}$, uncorrected) and dashes (-) indicate that the corresponding regressor was not selected by the stepwise regression. At $\tau = 16$ and 32 ms, wSMI ms always remained a significant predictor of consciousness states.

Table S4. Stepwise regression: wSMI and PLV

		Frequency power (Hz)									
		0 - 4		4 - 8		8 - 13		13 - 30		30 - 45	
		PLV	wSMI	PLV	wSMI	PLV	wSMI	PLV	wSMI	PLV	wSMI
	4	**	-	**	-	****	-	-	-	-	-
τ	8	**	-	**	-	****	-	-	-	-	-
(ms)	16	-	****	-	****	-	****	*	****	*	****
	32	-	****	***	****	*	****	-	****	-	****

Stepwise regressions were applied to test whether PLV and wSMI independently predicted consciousness states. At $\tau = 16$ and 32 ms, wSMI ms always remained a significant predictor of consciousness states.

Table S5. Stepwise regression: wSMI and PLI

		Frequency power (Hz)									
		0 - 4		4 - 8		8 - 13		13 - 30		30 - 45	
		PLI	wSMI	PLI	wSMI	PLI	wSMI	PLI	wSMI	PLI	wSMI
	4	**	-	****	*	****	-	-	-	-	-
τ	8	**	-	****	-	****	-	-	-	-	-
(ms)	16	-	****	*	****	-	****	**	****	**	****
	32	-	****	****	****	*	****	-	****	-	****

Stepwise regressions were applied to test whether PLI and wSMI independently predicted consciousness states. At $\tau = 16$ and 32 ms, wSMI ms always remained a significant predictor of consciousness states.

6.8.2. SUPPLEMENTARY METHODS

6.8.2.1. Participants

181 high-density EEG recordings (75 VS, 68 MCS, 24 Conscious patients (CS), and 14 Healthy (H) controls) were obtained from 126 distinct subjects (Age: M=47 years old, SD=18 years, males: 72 %). Another set of seven patients were excluded from the present study as they were diagnosed in a coma state or had less than 200 non-artifacted trials. As detailed in the Table S1, CS patients refer to patients with severe brain damage but who were still capable of functional communication and therefore did not belong to the MCS category. Note that 60% of CS patients had actually recovered from a VS or an MCS

state. 16 patients were recorded twice during their stay at the hospital, and 13 other were recorded between 4 and 6 times. Each of these subsequent recordings were performed between 1 and 673 days (mean = 74 days, SD = 157 days) following the initial EEG recording, and were aimed at tracking potential improvements in the patients' clinical state. We categorized each EEG recording in one of three types of delay (acute, intermediate and chronic) separating their accident from the time of EEG recording. Delay thresholds were determined from percentile analyses: the acute state refers to the third of patients with the shortest delays between the accident and the EEG recording (< 25 days) whereas the chronic state refers to the third of patients with the longest delays (> 50 days). We reasoned that 25 days was already away from a typical "acute" stage. We thus also report statistical analyses using patients examined and recorded within 10 days following their accident (n = 12).

Aetiologies were typical of DOC patients: 23% had gone through an anoxia or a hypoxia, 34% had had a stroke (either ischemic infarcts or intra-cerebral haemorrhages), and 25% suffered from a traumatic brain injury (TBI). The rest of the patients had suffered from other miscellaneous or mixed aetiologies. A chi-square testing the interaction between aetiology (hypoxia, stroke, TBI or other) and conscious state (VS, MCS or CS patients) revealed no significant result: $\chi(6, N=172) = 7.13$, $p > .308$, thus suggesting that our analyses looking at the correlations between EEG measures and patients' states of consciousness will not be confounded by aetiology. The delay separating the accident and our EEG study was variable (mean = 187 days, SD = 533 days), and mainly depended on the necessity for the patients to get an EEG to facilitate clinical diagnosis.

All patients had been without sedation for at least 24 hours prior to the recording session. Trained neurologists (FF, BR, LN) performed a careful clinical evaluation of patients' conscious state based on the French version of the Coma Recovery Scale Revised (CRS-R) (SCHNAKERS ET AL., 2008B) before each EEG recording. The CRS-R is a clinical examination that tests several abilities (arousal state, attentional orientation, communication etc) and allows a formal classification of DOC patients in comatose, vegetative, minimally conscious and conscious states (Table S1).

Note that EEG recordings of healthy subjects differed from the patients' in many respects that are irrelevant to conscious states: EEG recordings were performed in a quiet EEG room rather than at bedside, without any surrounding clinical equipment, subjects were fully attentive to instructions, clearly understood the task *etc*. Thus, we focus primarily on statistical comparisons between the clinical groups of VS, MCS and CS patients. The results from healthy subjects are nevertheless useful in the sense that they inform on the consistency of a given measure across consciousness states.

6.8.2.2. Experimental design

The EEG recordings were obtained during an auditory stimulation following Bekinschtein et al 's original design (BEKINSCHTEIN ET AL., 2009). Patients undertook this experiment for clinical purposes. The auditory stimuli were 50 ms-duration sounds composed of 3 sinusoidal tones (350, 700, and 1400 Hz, hereafter sound A; or 500 Hz, 1000 Hz, and 2000 Hz, hereafter sound B), with 7 ms rise and 7 ms fall times. Sequences were composed of five stimuli presented at a stimulus onset asynchrony of 150 ms, and were separated by a variable silent interval of 1350 to 1650 ms (50 ms steps). The sequences could comprise five identical tones (xxxxx, where X can be sound A or sound B) or four identical tones followed by a distinct one (xxxxY). In a given block, 80% of trials consisted in one type of sequence (frequent) and 20% of trials were of the other type (rare sequence), pseudo randomly distributed at least one and at most six frequent trials apart. Each block started with a 30s habituation phase during which the frequent sound sequences were repeatedly presented to establish the global regularity, before the first rare sequence was heard. Sounds were presented via disinfected headphones with an intensity of 70 dB, using E-prime v1.2 (Psychology Software Tools Inc.). At the beginning of each block, the experimenter gave a spoken instruc-

tion to count the rare sequences. The instructions attempted to motivate the patient to pay attention to the sounds, and patients were then systematically called by their first names. All subjects heard at least 8 blocks in a pseudo-random fixed-rule order (two runs of aaaaa, bbbbb, aaaaB, bbbbA as frequent sequences). Up to four additional blocks could be performed in case of highly noisy recordings.

Unlike previous studies (BEKINSCHTEIN ET AL., 2009; FAUGERAS ET AL., 2011, 2012), all trials were pooled independently of the condition of auditory stimulation, because our goal was to probe information exchanges in ongoing brain activity. Analyses were performed over 800 ms epochs, during the initial period of auditory stimulation (-200 ms before 1st sound until the beginning of last sound which could differ across conditions). This time period was identical across all trials. Further analyses were replicated on the time period following the beginning of the last sound (+600 ms to +1336 ms) for control purposes.

6.8.2.3.   EEG recording and preprocessing

EEG recordings were sampled at 250 Hz with a 256-electrode geodesic sensor net (EGI, Oregon, USA). Recordings were band-pass filtered (0.2-45 Hz). Trials were then segmented from −200 ms to +1336 ms relative to the onset of the first sound. Trials in which voltages exceeded ±150 μV, eye-movements activity exceeded ±80 μV or eye-blinks exceeded ±150 μV were rejected. All of these processing stages were performed in the EGI Waveform Tools Package. Trials were baseline-corrected over the first 200 ms window preceding the first sound onset. Channels with a rejection rate superior to 20% across trials were rejected. Bad channels were interpolated with non-artefacted neighboring channels. Trials with more than 20 bad channels were rejected. Current Source Density (CSD) estimates – also known as Laplacian transforms – were applied on each subject separately using Kayser & Tenke (KAYSER AND TENKE, 2006A)'s script. CSD is close to subtracting, from each channel, the activity of neighboring sensors; this technique thus coarsely diminishes volume conduction and increases the spatial focalization of EEG information.

Analyses specifically referring to Fz, Cz and Pz EEG channels were based on an average of six EEG channels surrounding each of them.

Finally, power spectral density (PSD) was estimated on each trial using the Welch method (WELCH, 1967). For each trial, each channel was divided in 500-ms sections with 400 ms of overlap. Sections were windowed with a Hamming window and zero padded to 2^{12} samples. The power in each frequency band of interested was calculated as the integral of the log-scaled power spectral density (PSD) within each frequency bands. Except if stated otherwise, frequency-bands of interest were: delta (δ: 1-4 Hz), theta (θ: 4-8 Hz), alpha (α: 8-13 Hz), beta (β: 13-30 Hz) and low gamma (γ: 30-45Hz). Higher frequencies were not estimated as they are generally difficult to measure in an artefact-free manner with scalp EEG.

6.8.2.4.   Computing indices of information sharing

In order to quantify the mutual information between sensors we introduce a novel marker: weighted symbolic mutual information (wSMI). wSMI is an extension of the permutation entropy analysis (BANDT AND POMPE, 2002) and is calculated between each pair of channels, and for each trial, after the transformation of the EEG time series into a string of discrete symbols. As explained below, the advantage of this measure is its ability to easily and efficiently detect non-linear coupling as well as its robustness to the traditional EEG artefacts.

Permutation Entropy (PE) and symbolic transform

Permutation entropy (PE), introduced by Bandt & Pompe (BANDT AND POMPE, 2002), is an effective method to compare time series and distinguish different types of behavior (*i.e.* periodic, chaotic or

random) in the signal (also see (STANIEK AND LEHNERTZ, 2008)). The main advantages of this method are (1) the identification of non-linear patterns in the signal (2) the reduction of the problem space to a limited set of discrete symbols and (3) its robustness to noise. The basic principle of this method consists in transforming a signal into a sequence of discrete symbols (FIGURE 6.1) and to quantify the entropy of the signal from the probability densities of those symbols. The transformation is performed by first extracting sub-vectors of the signal, each comprising k measures separated by a fixed time delay (τ). The parameter τ thus determines the broad frequency range to which the symbolic transform is sensitive. Because using τ values larger than 1 time sample can induce aliasing, we applied a low-pass filter to the continuous signal, before the symbolic transformation. The cut-off frequency of each low-pass filter was set according to the following formula: $f_{LowPass} = (80\ Hz)\ /\ (\tau\ time\ samples)$. Each sub-vector was then assigned a unique symbol, depending only on the order of its amplitudes. For a given symbol size (k) there are $k!$ possible orderings and thus $k!$ symbols. We calculated the symbolic transformation for every channel/trial with the following parameters: $k = 3$ time samples (sampled at 250 Hz) and $\tau = 4, 8, 16$ or 32 ms (*i.e.* 1, 2, 4 or 8 time samples). The parameter k determines the number of possible symbols ($k!$). k was fixed to 3, so as to robustly estimate the symbols probability densities. This value has been shown to be sufficient to detect dynamical changes in EEG during anaesthesia (OLOFSEN ET AL., 2008). Unfortunately, considering the trials' duration (~800ms), it was presently not possible to compute wSMI with $\tau > 32$ ms, and/or k > 3. Indeed, with $k = 4$, there exist $4! = 24$ distinct symbols, and thus $24^2 = 576$ combinations of symbols across two signals thus requiring much longer time series to robustly estimate wSMI. Symbolic transform of a signal will be hereafter referred to as X.

Symbolic Mutual Information (SMI)

A non-directional estimate of the coupling between two EEG recordings can be obtained by computing the mutual information between two time series (FIGURE 6.1). In our case, we computed the mutual information between each pair of electrodes after doing the previously described symbolic transformation. We refer to this measure as Symbolic Mutual Information (SMI), which is estimated as follow:

$$SMI(\hat{X}, \hat{Y}) = \frac{1}{log(k!)} \sum_{\hat{x} \in \hat{X}} \sum_{\hat{y} \in \hat{Y}} p(\hat{x}, \hat{y}) log \frac{p(\hat{x}, \hat{y})}{p(\hat{x})p(\hat{y})}$$

where x and y are all symbols present in signals X and Y respectively; $p(x, y)$ is the joint probability of co-occurrence of symbol x in signal X and symbol y in signal Y; $p(x)$ and $p(y)$ are the probabilities of those symbols in each respective signal and $k!$ the number of symbols – used to normalize the MI by the signals' maximal entropy.

For a directional estimate of symbolic transfer entropy (STE) across two signals see (STANIEK AND LEHNERTZ, 2008; MARTINI ET AL., 2011; LEE ET AL., 2013).

Weighted Symbolic Mutual Information (wSMI)

Weighted Symbolic Mutual Information (wSMI) is introduced in order to disregard trivial conjunction of symbols across two signals. Indeed, EEG is notorious for being subject to a series of artefacts, including muscle contraction, eye blinks and volume conduction, which may artificially inflate the similarity of EEG patterns recorded from two distinct EEG sensors. Notably, methods like phase locking value (PLV (LACHAUX ET AL., 1999)) and spectral coherence are highly affected by these various sources of common noise (STAM ET AL., 2007). The logic of wSMI consists in applying weights that emphasize conjunction of symbols which are less likely to be caused by common sources and, conversely, attribute a zero weight to conjunctions of symbols that may be due to common-source artefacts. With a symbol size of k = 3, the trivial conjunction patterns correspond to the conjunctions of identical items ($S_X = S_Y$), as well as to the conjunctions of opposed items ($S_X = -S_Y$). Opposed items could indeed be found if two EEG sensors

record each of the two sides of a common electric dipole. In FIGURE 6.1 & SUPPLEMENTARY FIGURE 6.5, these two sets of symbol pairs (identical and opposed) correspond to the two diagonals of the joint probability matrix. The computation of wSMI obeys the same formula as SMI, but with added weights (w) (GUIASU, 1977):

$$wSMI(\hat{X}, \hat{Y}) = \frac{1}{log(k!)} \sum_{\hat{x} \in \hat{X}} \sum_{\hat{y} \in \hat{Y}} w(\hat{x}, \hat{y}) p(\hat{x}, \hat{y}) log \frac{p(\hat{x}, \hat{y})}{p(\hat{x}) p(\hat{y})}$$

Note that because MI cannot be negative, it has a systematic positive bias. In the present case, we only compare the SMI and wSMI values between groups; the comparisons, always based on non-parametric statistics, are therefore not strongly affected by this bias. However, to estimate whether MI is significantly above chance in a given subject (or in a given group of subjects), one must build an estimate of the null distribution. Barrett and colleagues recently proposed an efficient method to achieve such estimate (BARRETT ET AL., 2012).

Symmetric uncertainty

Although MI need not be correlated with the entropy of the signals, it is bounded by them. To test whether the SMI and wSMI across channels predict consciousness state over and above any change in the local entropy, we computed the symmetric uncertainty, also known as redundancy, of each channel pair (PRESS ET AL., 2007). This measure basically normalizes MI by the entropy of the signals and is defined as follow:

$$SU(x,y) = 2 \; [MI(x,y) \; / \; (H(x) + H(y)]$$

where SU is the symmetric uncertainty, and H the entropy of the signal. In the present case we computed SU based on the wSMI and the PE values obtained for each pair of signal at the single trial level.

Phase Locking Value (PLV) and Phase Lag Index (PLI)

To confront our wSMI to already existing methods, we computed the phase locking value (PLV (LACHAUX ET AL., 1999)) and the phase lag index (PLI (STAM ET AL., 2007)) across each pair of channel. Both of these measures are based on the phase difference observed between signals ($\Delta\varphi_{i,j}$). PLV consists in computing the amplitude of the average vector of phase differences across time samples in a given trial whereas PLI measures the asymmetry of the distribution of phase differences in a given trial by computing the absolute value of the average of the sign of the phase differences. The advantage of PLI, as compared to traditional "functional connectivity" / correlation analyses such as cross-spectrum coherence and PLV, (as well as to the SMI method introduced above), is that it avoids spurious assignment of a high functional connectivity value to two EEG channels that both reflect the same underlying neural source. Indeed, whenever two channels record voltages arising from a shared source, their instantaneous phase difference is essentially $0 \pm \pi$, leading PLI to converge towards 0 (STAM ET AL., 2007).

To estimate PLI and PLV, signals were first band-passed filtered at a given frequency range and Hilbert transformed (in the present study: 0-4 Hz, 4-8Hz, 8-13Hz, 13-30Hz, 30-45Hz). The difference in instantaneous phase was then computed for each pair of CSD estimate, at each time point and for each trial.

Both PLV and PLI methods are affected by the number of time samples they consider. At the extreme, if only one time-sample is considered, PLV equals to 1 and PLI equals to 1 or -1, even if the two channels are fully independent. The more time samples are considered, the less PLV and PLI overestimate the correlation between two channels. As there was a variable amount of non-artefacted trials performed

by each patient, we first computed PLV and PLI estimate for each trial by averaging the vectors of phase differences (PLV) or the signs of the phase difference (PLI) across all time samples *within* each trial. Each trial had the same number of time samples; these values could therefore be compared with one another. For each subject, the value of these single-trial PLVs and PLIs were then averaged across trials to yield a final PLV and a final PLI estimate. As a consequence, trial number only affected the precision of the PLV and PLI estimates, and did not introduce a systematic bias related to the number of trials.

6.8.2.5. Topographical, cluster and distance analyses

Analyses were performed on each pair of CSD transform of EEG signals. As a result, we obtained 32,640 (256*(256-1)/2) values for each subject. As this huge dimensionality leads to an important multiple comparison issue, statistics were performed on summary measures (*e.g.* median across all pairs) or in smaller search spaces.

Except if stated otherwise, topographies represent the median wSMI each CSD estimate share with all other non-facial channels. It thus estimates the amount of information shared by a given area with other regions.

Fz and Pz refer to an averaged cluster of 6 EEG channel surrounding the EGI net's Fz and Pz channel.

Cluster analyses were performed in order to make the interpretation of our results more straightforward and minimize the issues associated with multiple comparisons. Once wSMI was estimated for each channel pair, the 256 channels were summarized to 16 regions (symmetric across the antero-posterior axis). We then calculated, within each of the cluster pairs, a summary measure by averaging the median connectivity that every channel of the first cluster shared with every channel of the second cluster.

Distance analyses were performed to estimate how wSMI varies with the spatial distance separating two channels. Distance between channels was calculated along a straight line in a 3-dimensional Euclidian space using the EGI default electrode coordinates.

6.8.2.6. Statistics

Statistical analyses were performed with R and MATLAB (2009b), and, except if stated otherwise with non-parametric methods and two-tail tests (based on Wilocoxon and Mann-Whitney U tests as well as MATLAB's robust regression methods). Significance level was set to $p < .05$, and false discovery rate (FDR) was used to correct for multiple comparisons (hereafter noted as p_{FDR}).

6.8.3. SUPPLEMENTAL RESULTS

6.8.3.1. Simulations

Effect of mixture of sources on SMI and wSMI

To test the validity of our measure, we ran a series of simulations in which we tested the ability of wSMI to detect the coupling of two distinct sources from two simulated scalp sensors capturing a heterogeneous mixture of these two sources. These simulations are presented in order to show i) how common source artefacts affect SMI and ii) why wSMI is robust to the latter. Because several signal and noise parameters were set arbitrarily, we only present results in a qualitative manner in SUPPLEMENTARY FIGURE 6.5.

We considered two main scenarios: i) the presence, and ii) the absence of coupling between two sources (U and V). First, in case of the presence of a coupling between U and V, we generated a random

joint probability matrix C ([k!, k!]) as well as a random prior probability vector P(U) ([1, k!]) of each symbol S to belong to U. From P(U), we then pseudo-randomly constructed a symbolic sequence U as a sequence of 1000 symbols. The Vsymbolic sequence was then constructed by pseudo-randomly generating 1000 consecutive symbols following the transformation of U by the joint probability matrix.

Finally, continuous signals U and V were generated from the symbolic sequences U and V, by generating two random (with a Gaussian distribution) numbers α and β for each time point. Each of the k ordinal elements of each symbol was then transformed into a continuous time point accordingly: $x = x * \alpha + \beta$, where x is a given symbol made of ordinal numbers, and α and β are two random variables generated from a normal distribution centered around 0, with a standard deviation of 1.

In the second scenario, U and V symbolic sequences were generated from a quasi homogeneous joint probability matrix indicative of very little coupling in the space of interest. Continuous signals U and V were then generated as in the first scenario.

In each scenario, two simulated EEG sensors were generated by creating more or less homogenous mixtures of the two continuous signals. Each simulated sensor captures γ% of the neighboring source – and thus (100-γ)% of the other source. White noises were independently added to each sensor with a signal to noise ratio of 10. Such setup mimics, two EEG sensors (X, Y) respectively located towards the electric fields' projections of U and V sources.

Effect of τ on the frequency-specificity of wSMI

Although SMI and wSMI cannot be fully expressed in terms of frequencies, it is useful to see the broad frequency range of information sharing to which wSMI can be sensitive. As mention in the Supplementary Methods, the temporal separation parameter of the symbols (τ) affects this frequency range. Sinusoidal signals were thus generated at each frequency ranging between 0 and 60 Hz and sampled at 250 Hz. Pairs of signals were synchronized at $\pi/2$ (90°). wSMI was estimated for each pair of signals at τ = [4, 8, 16, 32] ms. The results, presented in SUPPLEMENTARY FIGURE 6.6.H, show that none of the tested τ values captures very low frequency components (< 4Hz), and that the shorter τ, the wider and the higher the range of frequencies to which SMI is sensitive.

6.8.3.2.   Robustness of wSMI

Replication of wSMI results using different time periods of recordings

It is possible that our results are specific to the auditory stimulations presented during this experiment. We therefore replicated our analyses on different time periods following auditory stimulations (see Supplementary Methods). The obtained results were very similar to the ones reported in the main manuscript. At τ = 32 ms, wSMI was significantly lower in VS than in MCS (U = 3686, $p < 10^{-5}$, AUC = .72) and than in CS patients (U = 1437, $p < 10^{-4}$, AUC = .80) whereas MCS and CS patients did not present significantly different wSMI (U = 971, p = .169, AUC = .59). At τ = 16 ms, similar differences were observed (all p < .045, all AUC > .63) whereas shorter τ did not show consistent differences of wSMI with consciousness states. Similarly, distance analyses led to results closely matching the ones obtained from the auditory stimulation time periods (SUPPLEMENTARY FIGURE 6.8.B).

Together, these results show that VS patients' impairment in wSMI is not specific to a single type of auditory condition. To strengthen these results, future studies should however investigate the variation of wSMI in other conditions such as during sleep, resting state and other tasks requiring subjects' attention.

Effect of sampling frequency

To check that the present results are not solely dependent on the EEG sampling rate, we replicated the analyses after down-sampling the EEG recordings to 125 Hz. Analyses of the wSMI at τ = [8, 16, 32] ms revealed very similar patterns as the ones observed using a sampling frequency of 250 Hz SUPPLEMENTARY FIGURE 6.6.D). Note that because of the sampling rate, it was not possible to test τ = 4 ms. Overall, these results demonstrate that the present wSMI results are robust to sampling rates.

Frequency-range sensitivity of wSMI

By definition, wSMI can capture dynamics spread over a relatively large frequency range (SUPPLEMENTARY FIGURE 6.6.H). To further isolate the frequency ranges of interest, we replicated the wSMI analyses after band-pass filtering the EEG signals at more specific frequencies to which wSMI was sensitive (4-8, 8-13 and 13-30 Hz for τ = 32, 16 ms). The only robust difference found across consciousness states was obtained with τ = 32 ms in the θ frequency band (4-8 Hz, SUPPLEMENTARY FIGURE 6.6.C). VS also presented a lower wSMI computed from EEG signals band-pass filtered from $13 - 30$ Hz, however this difference was relatively weak (U = 3073, p = .022) and did not reach significance when comparing VS to CS patients (U = 764, p = .722). Together, these results suggest that the wSMI differences between VS and MCS are particularly driven by events in the θ band (4-8 Hz).

6.8.3.3.   Detailed results

Distance analyses: all temporal separation parameters (τ)

We replicated the distance analyses reported in the main manuscript using three other τ values [4, 8, 16 ms] (SUPPLEMENTARY FIGURE 6.8.A). At τ = 16 ms, the results were similar to those obtained with τ = 32 ms: wSMI was not different between VS, MCS, and CS at the short inter-channel distance (6.3 ± .3 cm, all p > .199) and VS had lower wSMI than MCS and CS patients at most longer distances (all p < .002). A noticeable difference with the main results (τ = 32 ms) was observed for the 21.8 cm distance at which VS and MCS did not show significantly different wSMI (p = .186). Note that because the number of channel pairs dramatically drops at this distance, the robustness of our analyses could be diminished. Finally, similar trends could be observed at τ = 8 ms, but did not consistently reach significance. No differences were observed for τ = 4 ms (all p > .05).

Together, these results show that the parameter τ changed the sensitivity of our test. However, when a difference of wSMI was observed across consciousness states, it was consistent with the main results obtained with τ = 32 ms: VS patients repeatedly showed lower wSMI over medium and long distances, and appeared to present non-significantly different wSMI at a short distance. These results therefore support the hypothesis that the loss of information-sharing characterizing the vegetative state is particularly easy to observe over medium- and long-distances.

SMI results

Symbolic mutual information (SMI) between two channels is a similar measure to wSMI, except that it equally considers all conjunction of symbols observed across two signals. SMI is however subject to multiple artefacts. Indeed, head movement, eye blinks, muscles contractions as well as the volume conduction of electric fields all tend to generate common signals in different EEG sensors. SMI is thus very likely to overestimate the amount of information sharing across distinct cortical sources.

Contrarily to wSMI, SMI rapidly increases as the distance between two EEG sensors diminishes (SUPPLEMENTARY FIGURE 6.8.C). Interestingly, VS patients appeared to present SMI values weakly but systematically lower than MCS and CS patients at all distances (all p < .05, uncorrected). Finally, SMI proved

to be less discriminative of consciousness states than wSMI (SUPPLEMENTARY FIGURE 6.8.D). This result empirically strengthens the utility of the weights in the MI computation.

6.8.3.4.   Relationships between wSMI and other measures indexing consciousness state

Permutation Entropy (PE) correlates with patients' states of consciousness

Do other simpler methods correlate with consciousness-states too? PE is an efficient method to estimate the entropy of a given signal and has proved to be a useful marker of consciousness states in anaesthesia (BANDT AND POMPE, 2002; JORDAN ET AL., 2008; OLOFSEN ET AL., 2008). We tested whether this local measure of entropy could also discriminate the state of consciousness of the present cohort.

The results demonstrated that at $\tau = 32$ms, the median PE across non-facial EEG channels was much lower in VS patients as compared to MCS (U = 3494, p < .001, AUC = .69) and CS patients (U = 1391, p < 10^{-4}, AUC = .77) (SUPPLEMENTARY FIGURE 6.6.I). MCS and CS patients' PE did not significantly differ from one another: U = 996, p = .111, AUC = .61). At $\tau = 16$ms, PE did not was not different between VS and MCS patients (U = 2841, p = .240, AUC = .56), but the latter had significantly smaller PE than CS (VS-CS: U = 1301, p = .001, AUC = .72; MCS-CS: U = 1119, p = .007, AUC = .69). For other τ values, none of the comparisons reached statistical significance.

These results show that PE can also be used to index the state of consciousness.

Symmetric Uncertainty demonstrates that wSMI indexes consciousness states independently of the signals' entropies.

The mutual information of two signals need not be related to the entropy of the signals but is bounded by them. Because PE also correlates with patients' states of consciousness, it is important to assess whether the present wSMI results are fully explainable by this simpler method. Symmetric uncertainty, also known as redundancy, can be used to tackle this issue. Symmetric uncertainty consists normalizing the mutual information observed across two signals by the sum of their respective entropy. Beyond its theoretical interpretation, symmetric uncertainty can thus be used to test whether MI discriminates consciousness states independently of PE.

The results demonstrated that at $\tau = 32$ms, the median symmetric uncertainty across non-facial channels was significantly lower in VS patients as compared to MCS (U = 3527, p < .001, AUC = .72) and CS patients (U = 1317, p < 10^{-4}, AUC = .73) (SUPPLEMENTARY FIGURE 6.6.J). MCS and CS patients' symmetric uncertainty did not significantly differ from one another: U = 845, p = .715, AUC = .53. The VS-MCS difference remained significant for all τ but $\tau = 4$ ms (all ps < .03) although the effect was smaller at shorter τ values ($\tau = 4$ ms: AUC = .51; 8 ms: AUC = .60; 16 ms: AUC = .61).

These results demonstrate that wSMI indexes the state of consciousness independently the entropy of the signals, computed from a similar decomposition of the EEG signals. They thus reinforce both the validity and the utility of wSMI in indexing patients' consciousness states. Taken together, PE and symmetric uncertainty analyses show that the conscious brain is characterized by more complex but also more integrated neuronal signals. This view particularly fits with an Integrated Information Theory of consciousness (TONONI AND KOCH, 2008).

Relationships between wSMI and the power spectral densities (PSD)

To further investigate the relationship between wSMI and frequency, we tested the extent to which the wSMI differences observed across consciousness states could be explained by simpler effects observable directly in the EEG power spectrum densities (PSD).

First, robust regression analyses revealed that the state of consciousness could be predicted by the power in the δ band (0 – 4 Hz: adjusted R^2 = .11, p < 10^{-5}), in the α band (8 – 13 Hz: adjusted R^2 = .06, p = .001), and in the β band (13 – 30 Hz: adjusted R^2 = .02, p .018) (SUPPLEMENTARY FIGURE 6.6.G). Furthermore, the power in multiple frequency bands correlated with the median wSMI (results summarized in Table S2). Overall, PSD in low frequency bands (δ, θ) correlated more with longer τ values (32 and 16 ms) whereas PSD in higher frequency bands (β: 13 – 30 Hz, low γ: 30 – 45 Hz) correlated with shorter τ values (8 and 4 ms). This set of results fits with the typical sensitivity of wSMI to various frequencies depending on its τ parameter (SUPPLEMENTARY FIGURE 6.6.H).

PSD and wSMI share common information and can both predict consciousness states. Are these two measures capturing the same phenomena? To compare the information carried by wSMI and PSD about the patients' states of consciousness, we applied multiple stepwise regression analyses. The results, reported in Table S3, demonstrated that for the discriminative τ (τ = 16 and 32 ms), wSMI systematically remained a significant predictor of patients' state of consciousness (all p < 10^{-4}) even after controlling for PSD; the predictive power of PSD barely reached significance (min p > .01). By contrast, for shorter τ (4 ms and 8 ms) which generally failed to discriminate patients' states of consciousness, nearly all the predictive power was captured by PSD. This analysis therefore suggests that the wSMI results obtained with short τ values could be simply explained by variation in frequency powers.

Together, these results show that while PSD and wSMI correlates with one another, wSMI (at the discriminative τ values: 16 and 32 ms) is a partially independent, and indeed a better predictor of the state of consciousness than the power spectrum.

PLV and PLI

We also analyzed the present data with more traditional indices of "functional connectivity" such as phase locking value (PLV) and phase lag index (PLI). The corresponding results are summarized in SUPPLEMENTARY FIGURE 6.8.E-F.

As expected, distance analyses showed that PLV presented a similar pattern to SMI: PLV rapidly increases towards 1 as the distance between two EEG channels approaches 0. Contrarily PLI did not, and either presented a similar pattern to wSMI or presented values in a similar range throughout all distances.

Comparison across states of consciousness and distances only revealed that low frequencies (< 4 Hz) phases were more synchronous in VS than in MCS patients. Note that SMI and wSMI were not here sensitive to these low frequencies (SUPPLEMENTARY FIGURE 6.6.H). Distance analyses applied to each frequency band did not show any significant pattern.

Could PLV and PLI nevertheless explain the wSMI differences across consciousness states? Following the method described in the PSD section, we applied a series of stepwise regressions to test whether wSMI was an independent predictor of consciousness states from PLV and PLI. The results, reported in Tables S4 and S5, demonstrated that for the discriminative τ (τ = 16 and 32 ms), wSMI systematically remained a significant predictor of subjects' state of consciousness (all p < 10^{-4}) even after controlling for PLI and PLV. At these τ values, the predictive power of the latter rarely reached statistical significance. Contrarily, for shorter τ values (4 ms and 8 ms) which, generally failed to discriminate patients' states of consciousness, wSMI was never used as a predictor of consciousness state by the stepwise regression. The latter selected the δ, θ and α bands, in both PLI and PLV analyses.

Together these results confirm that the wSMI is an independent and indeed better predictor of consciousness states than PLV and PLI.

CHAPTER 7. LARGE SCALE SCREENING OF THE NEURAL SIGNATURES OF CONSCIOUSNESS IN VEGETATIVE AND MINIMALLY CONSCIOUS STATE PATIENTS

7.1. INTRODUCTION OF THE ARTICLE

In the preceding chapter, I showed how a novel method, weighted symbolic mutual information (wSMI) could reliably quantify the amount of mutual information across different brain regions. This simple measure proved to significantly distinguish vegetative patients from minimally conscious and conscious patients. This result thus suggests that wSMI may reliably capture an important signature of consciousness.

However, finding a significant marker raises several questions. In particular, it remains to be determined whether wSMI is *i)* relevant to theories of consciousness *ii)* useful in the clinics, especially with regard to the already existing measures such as the MMN, the P300, the CNV etc. Indeed, and as outlined in the introduction of this thesis, one of the critical challenges of consciousness research is to sort the different markers in terms of their redundancy, theoretical relevance and clinical robustness.

In the present study carried out in close collaboration with Jacobo Sitt, I aimed at systematically implementing the various electrophysiological markers of consciousness proposed across the attention, subliminal, sleep and anesthetized literatures.

7.2. ABSTRACT

In recent years, numerous electrophysiological signatures of consciousness have been proposed. Here, we perform a systematic analysis of these EEG markers by quantifying their efficiency in differentiating vegetative state patients from those in a minimally conscious or in a conscious state. Based on a review of previous experiments we identified a total of 92 possible markers, which we organize based on current theories along four dimensions: (1) event-related potentials *versus* ongoing EEG activity; (2) local dynamics *versus* inter-electrode information exchange; (3) spectral patterns *versus* information complexity; (4) average *versus* fluctuations over the recording session. We analyzed a large set of 181 high-density EEG recordings from a 30-minute paradigm. We show that

low-frequency power, EEG complexity, and information exchange constitute the most effective signatures of conscious states. When combined, these measures synergize to enable an automatic classification of patients' state of consciousness.

7.3. INTRODUCTION

In spite of intense experimental and theoretical efforts, the neural signatures of conscious processing remain a highly debated issue: are they to be found in early (SUPÈR ET AL., 2001; PINS, 2003; KOIVISTO ET AL., 2006; MELLONI ET AL., 2007) or late (SERGENT ET AL., 2005; GAILLARD ET AL., 2009) responses to sensory stimulations? Is conscious processing systematically associated with reentrant top down processing (LAMME AND ROELFSEMA, 2000; PASCUAL-LEONE AND WALSH, 2001)? Does consciousness depends on a massive exchange of information across distant cortical sites (LUMER AND REES, 1999; VUILLEUMIER ET AL., 2001; REES ET AL., 2002; MAROIS ET AL., 2004; GAILLARD ET AL., 2009) with prefrontal cortex and cingulate cortices acting as critical communication hubs (SAHRAIE ET AL., 1997; DEHAENE AND NACCACHE, 2001; LAU AND PASSINGHAM, 2006)? Or, instead, can it emerge solely from localized reverberating activity (LAMME AND ROELFSEMA, 2000; PINS, 2003)? Does it simply require a global integration of information independently of any specific anatomical structure (TONONI, 2004)?

From a cognitive psychology perspective, it has proven equally difficult to identify operations unique to the conscious brain. Whereas a large variety of cognitive processes can unfold unconsciously, ranging from low-level perception to abstract semantic processing (KOUIDER AND DEHAENE, 2007), attention orienting (KENTRIDGE ET AL., 1999), motivation (PESSIGLIONE ET AL., 2007) and executive inhibition (VAN GAAL AND LAMME, 2011), the ability to actively maintain information in working memory and to flexibly distribute it to distant processors may be unique to conscious processing (BAARS, 1989; DEHAENE AND CHANGEUX, 2011). Several models thus share the view that long-distance information integration and coordination of distributed areas may be one of the specific properties of conscious processes (LAMME AND ROELFSEMA, 2000; TONONI, 2008; DEHAENE AND CHANGEUX, 2011).

The identification of reliable signatures of conscious processing goes beyond theoretical research, and has critical practical implications in the clinic. In particular, detecting these signatures is essential for patients with Disorders of Consciousness (DOC) who, even during wakefulness, are seemingly unable to communicate. To better describe these disorders, a distinction has been introduced between the vegetative state (VS) and the minimally conscious state (MCS). Both exhibit similarly preserved arousal, but MCS patients show signs of intentional behavior while VS patients remain largely unresponsive. Yet, even in the latter case, science and modern medicine remain hard-pressed to decide whether a patient diagnosed as VS may still be conscious but unable to communicate (LAUREYS, 2005B; SCHNAKERS ET AL., 2009B; LAUREYS AND SCHIFF, 2011). For instance, Owen and collaborators have shown that functional MRI could detect consciousness in some VS patients (OWEN ET AL., 2006) and, in a few cases even restore communication (BYRNE ET AL., 2010). Similar results may be obtained using scalp electroencephalography (EEG), a more economical and practical technique that can be easily applied at bedside (CRUSE ET AL., 2011; FAUGERAS ET AL., 2011; GOLDFINE ET AL., 2011). We recently introduced a measure (weighted symbolic mutual information, wSMI) which evaluates long-distance cortical information sharing from scalp EEG and discriminates VS and MCS patients (KING ET AL., 2013B). Another recent method based on the quantifica-

tion of the complexity in the EEG evoked responses to TMS pulses has also been shown to efficiently detect consciousness in DOC patients (CASALI ET AL., 2013). Nevertheless, there is still no consensus amongst clinicians as to which measure may be best suited to detect residual consciousness. Part of this results from the fact that the putative signatures of consciousness have been proposed and tested in independent studies, in distinct populations and with different criteria and methodologies.

The multiplicity of theoretical proposals and the practical need to improve the diagnosis of DOC patients call for a systematic assessment of the ability of each of these measures to index states of consciousness. To address this issue, we provide an extensive analysis of empirically and theoretically derived measures of conscious activity that can be extracted from a large database of EEG recordings in DOC patients. We show that local low-frequency power and complexity measures, together with information exchange, are privileged markers of conscious states. These measures and their respective fluctuations can be used in synergy in an automatic classification system in order to improve the diagnosis of VS patients.

7.4. METHODS

7.4.1. PATIENTS

Patients underwent EEG recording for clinical purposes. The auditory paradigm they were presented to (BEKINSCHTEIN ET AL., 2009) elicits event related potentials (ERPs) that help assessing patients' present and future state of consciousness (FISCHER ET AL., 2004; WIJNEN ET AL., 2007; BEKINSCHTEIN ET AL., 2009; SCHNAKERS ET AL., 2009A; FAUGERAS ET AL., 2011, 2012). Patients were recorded without sedation since at least 24 h in order to maximize their arousal and their cognitive abilities during the auditory stimulation. We performed a total of 173 patient recordings. Six recordings were discarded because they presented less than 200 non-artifacted trials (see below). The remaining 167 valid recordings were acquired from 113 distinct patients (79 males and 34 females, sex-ratio = 2.32), aged from 16 to 83 years (mean = 48 ± 17 years). Patients were recorded from one to six times. Their etiologies matched the one typically observed in DOC: anoxia (24%), intracranial hemorrhage (35%), traumatic brain injury (24%), and other etiologies (17%)(see supplementary Table 3 for details). Our cohort had variable delays separating the incident and the acquisition of the EEG (mean = 178 days since DOC onset; median = 35 days; SD = 532 days; earliest = 6 days; latest = 4383 days).

7.4.2. HEALTHY SUBJECTS

Experiments were approved by the Ethical Committee of the Salpêtrière hospital. All14 healthy subjects (mean age = 21.3 ± 2.9; sex-ratio (M/F) = 2.5) gave written informed consent.

7.4.3. BEHAVIORAL ASSESSMENT OF CONSCIOUSNESS

Clinical evaluation of consciousness was based on the French version of the Coma Recovery Scale Revised (CRS-R) scale (SCHNAKERS ET AL., 2009B), and careful neurological examination by trained neurologists (FF, BR, LN). This scale consists of 23 items forming six subscales addressing auditory, visual, motor, oromotor, communication and arousal functions. CRS-R subscales are

comprised of hierarchically arranged items. The scale enables a distinction between conscious (CS), minimally conscious (MCS) and vegetative (VS) states (SCHNAKERS ET AL., 2009B). Clinical examination and behavioral assessment were systematically performed right before EEG recording.

7.4.4. AUDITORY STIMULATION

Subjects were stimulated using the "Local Global" auditory protocol (BEKINSCHTEIN ET AL., 2009). Each trial was composed of a series of five 50-ms duration sounds presented via headphones with an intensity of 70 dB and a 100ms interval between each sound (stimulus onset asynchrony [SOA] = 150 ms). Each sound was composed of three superimposed sinusoidal tones (either a low-pitched sound composed with a mixture of 350, 700 and 1400 Hz tones, hereafter sound X; or a high pitched sound composed with a mixture of 500, 1000 and 2000 Hz tones, hereafter sound Y). Tones were prepared with 7ms rise and 7ms fall times. Four different series of sounds were used, the first two using the same five sounds: xxxxx or yyyyy (hereafter denoted as xx); and the other two with the final sound differing from the four other: xxxxY or yyyyX (hereafter denoted as XY). Trials were separated by a variable interval of 1350–1650ms (50ms steps). Blocks were arranged to contain the XY trials, either as a rare (block type 1: 80% XX & 20% XY); or as a frequent (block type 2: 80% XY & 20% XX) series of sounds. Both blocks presented a local (the fifth sound could be deviant or identical to previous sounds) and a global regularity (one of the series of sounds was rarer than the other). In order to unambiguously establish the global regularity, each block started with ~30-secondhabituation time period during which only trials with series of sounds of the frequent type were presented. Following the original design (BEKINSCHTEIN ET AL., 2009), habituation trials following a rare auditory sequence were discarded from the analyses. In each block the number of rare trials varied between 22 and 30. Auditory stimulations were presented with Eprime v1.1 (Psychology Software Tools Inc., Pittsburgh, PA). Instructions to pay attention to the stimuli and to count deviant stimuli were delivered verbally to all patients at the beginning of each block. All subjects performed eight blocks (3–4 min duration) in a fixed order (two runs of XX, YY, XY, YX frequent stimulation).

7.4.5. HIGH-DENSITY SCALP EEG RECORDINGS

EEG recordings were sampled at 250 Hz with a 256-electrode geodesic sensor net (EGI, Oregon, USA) referenced to the vertex. Recordings were band-pass filtered (form 0.2 to 45 Hz). Trials were then segmented from −200ms to +1336ms relative to the onset of the first sound. Trials with voltages exceeding ±150 V, eye-movements activity exceeding ±80 mV and eye-blinks exceeding ±150 mV were rejected. Trials were baseline corrected over the first 200 ms window preceding the onset of the first sound. Electrodes with a rejection rate superior to 20% across trials were rejected and were interpolated. Trials with more than 20 corrected electrodes were rejected. The remaining trials were digitally transformed to an average reference. All these processing stages were performed using the EGI Waveform Tools Package.

Connectivity measures were based on a spatial Laplacian transformation of the EEG - a computation also known as Current Source Density (CSD) estimate (KAYSER AND TENKE, 2006B). CSD consists, roughly, in subtracting, from each electrode, the activity of its neighboring electrodes. This has the main advantage of increasing spatial resolution and minimizing the influence of common sources on multiple distant electrodes.

7.4.6. CALCULATION OF PUTATIVE EEG MEASURES OF CONSCIOUSNESS

We calculated the entire set of EEG measures (m) independently for each individual subject, trial and for every electrode (n_e=256) or pair of electrodes (n_e=32640). Connectivity measures were summarized by calculating the median value from each electrode to all of the other scalp (non-facial) electrodes. Note that, given the spatial distribution of the electrodes, this procedure enhances the weight of long-distance connections on the computed measure. As a final result, all measure distributions ended up with the same number of values per subject and trial (n_e=256). Finally, for each subject, these values were again collapsed to two scalars by considering the mean and the standard deviation across trials.

Except for ERP measures, analyses were performed on EEG data recorded during the time period when subjects were presented with undifferentiated series of tones (from 200 ms prior to the onset of the first tone to the onset of the fifth tone). Thus, all trials were pooled independently of the condition of auditory stimulation.

See supplementary materials for a detailed description of each measure and its computation.

ERPs		"ONGOING" ACTIVITY			
		Single electrode		Across electrodes	
Early components	Late components	Spectrum	Information theory	Spectrum	Information theory
P1	P3a	Power in frequency bands	Permutation entropy	Phase lag index	weighted Symbolic Mutual Information
MMN	P3b	Spectral summaries	K complexity	Amplitude envelope correlation	
CNV		Spectral entropy		Imaginary coherence	

TABLE 1. EXPERIMENTAL PROTOCOL AND RELATED ELECTROPHYSIOLOGICAL MARKERS

Measures can be conceptually organized along several dimensions: First, we distinguish measures of stimulus processing from. The former (event-related potentials or ERPs) are further subdivided into early versus late components. The latter are classified according to the theoretical background used to derive the measure: (1) Local dynamics versus connectivity: some measures are computed within each electrode, while others index the interactions between electrodes; (2) Spectral (Fourier frequency analysis) versus Information Theory. Finally, for each measure, inter-trial average (computed as the mean across trials) or inter-trial fluctuations (computed as the standard deviation) were studied.

7.4.7. STATISTICS

7.4.7.1. Univariate ROC

Pair-wise comparisons were performed across the three clinical groups (VS, MCS and CS), leading, for each measure, to three statistical comparisons (1:VS-MCS, 2:MCS-CS, 3:VS-CS). We implemented a non-parametric statistical method (Mann-U Whitney test) and report the effect size as the empirical Area Under the Curve (AUC) from an empirical Receiver Operating Curve (ROC) analysis. The ROC plots the false positive rates (FPR) as a function of true positive rates (TPR).

For example, in a comparison of the alpha power between CS and VS patients, one can observe the percentage of CS patients (TPR) who show a higher alpha power than an arbitrarily setup criterion C, and the corresponding percentage of VS patients (FPR). By testing all possible empirical criteria, we can draw the ROC curve and compute the AUC (see SUPPLEMENTARY FIGURE 7.10). Values higher than 50% means that CS patients have on average higher alpha power than VS patients, and values lower than 50% implies that CS patients have lower alpha power than VS patients.

Note that the estimates of statistical effect size are intrinsically problematic in mass-univariate analyses, as one tends to look at the effect size of significant tests only. However, the effect size itself is an estimate and thus subject to error. We decided to make all values available to the reader, but we stress that it would be incorrect to pick the best measure as this may overestimate its effects size (KRIEGESKORTE ET AL., 2009; VUL ET AL., 2009B). Each measure is intrinsically high dimensional, as it was measured on each EEG electrode (n=256) or on each pair of EEG electrodes (n=32640). To sum up these large datasets, we thus summarized each multidimensional measure in a single value. ERP measures were summarized as the mean value observed in regions of interests traditionally used in the literature (see Supplementary Materials). Connectivity measures computed for each pair of EEG electrodes were summarized as follow: for each non-facial electrode, we computed the median value it shared with all other non-facial electrode. We then averaged these 224 values to summarize the amount of shared information across the scalp. All other measures were summarized by averaging the 224 values non-facial electrodes.

To account for the large number of statistical tests (n = 92 measures x 3 comparisons), statistical significance was systematically corrected for multiple comparison with a false discovery rate method (FDR at alpha=.05) across all measures and comparisons.

7.4.7.2. Topographical analysis

Topographical analyses were performed using a similar approach to the method above. Pair-wise comparisons across clinical states were performed with Mann-U Whitney tests on each electrode separately. Robust regression analyses were performed across the four groups (VS:1, MCS:2, CS:3, Healthy:4) to test for the monotony of the changes observed across states of consciousness. Statistical significance are reported after correction for multiple comparison across electrodes (FDR at alpha=.05).

7.4.7.3. Multivariate Pattern Analyses

In the present case, each analysis aimed at predicting the clinically-defined state of consciousness (VS, MCS or conscious) of each subject from the EEG-based measures of conscious processing. For this purpose, we used a Support Vector Classifier (SVC) (PEDREGOSA ET AL., 2011) with a probabilistic output calibration. See supplementary methods for a detailed description of the computational steps.

7.5. RESULTS

We analyzed a large set of 181 high-density 256-channel EEG recordings, corresponding to all 167 patients admitted at the Pitié-Salpêtrière Hospital and referred to us in the 2008-2010 period for a clinical evaluation of their state of consciousness. In total, 75 VS patients, 68 MCS patients,

and 24 brain-injured but conscious patients (CS) were recorded one to six times each (see methods for details). Fourteen additional recordings were obtained from healthy control subjects. Recordings were acquired in the "Local Global" protocol, a thirty-minute paradigm designed to probe the depth of processing of auditory regularities at two hierarchical levels (BEKINSCHTEIN ET AL., 2009) (FIGURE 7.1). This procedure allowed us to jointly quantify the event-related potentials (ERPs) evoked by exogenous stimuli and the presence of endogenous fluctuations in the EEG, while maximizing and homogenizing the patients' attention and vigilance. For each recording, we systematically extracted a set of measures organized according to a theory-driven taxonomy (Table 1). Full details and motivations for each measure can be found in the Supplementary Materials. Here we briefly describe the most relevant aspects of each measure.

We propose to organize EEG measures according to several major dimensions (Table 1). A first distinction separates measures of the processing of external stimuli (auditory ERPs) from measures which are not locked to the stimuli and rather reflect ongoing brain activity. Current theories of consciousness differ in their attribution of conscious awareness of an external stimulus to early or late brain responses (DEHAENE AND CHANGEUX, 2011). Therefore, we classified event related potentials according to their latency (early, < 250 ms, *versus* late, >300 ms). Measures of ongoing EEG activity were further classified based on: 1) dynamics of brain signals at a single electrode site *versus* assessment of functional connectivity between two brain sites; and 2) whether the measure is based on spectral frequency content or on information-theoretic estimates of signal complexity, which do not presume strong specific hypotheses about the frequency content of the signal. For each measure we computed, the inter-trial average, which reflects the overall mean value during the half-hour recording session, and the fluctuation of this measure (standard deviation) during the recording period, which tests the hypothesis that stability may be a hallmark of consciousness (SCHURGER ET AL., 2010).
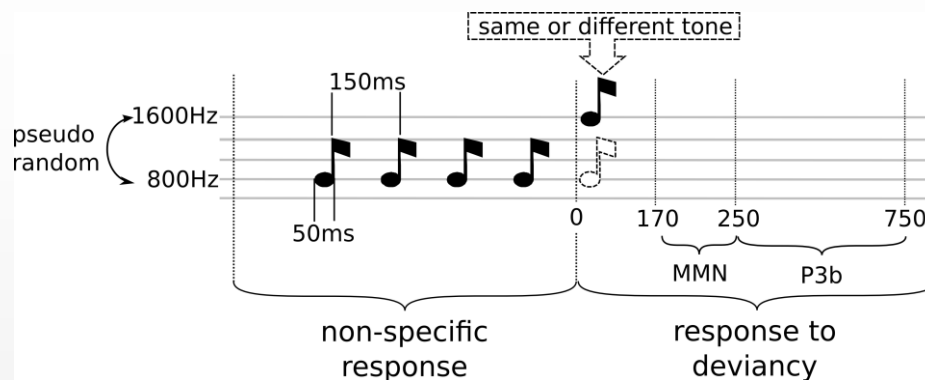
FIGURE 7.1 EXPERIMENTAL SETUP AND RELATED SIGNATURES OF CONSCIOUSNESS

Description of the paradigm used for patient auditory stimulation. Spectral and information-theory measures were computed in the early time window (which is identical for all trials), while event-related potentials (ERPs) were computed on the late window (response specific to the trial condition).

7.5.1. TOPOGRAPHICAL DIFFERENCES ACROSS MEASURES AND GROUPS

First we inspected whether differences in amplitude and spatial distribution of the computed measures could discriminate patients' state of consciousness. This analysis also aims at evaluating whether different measures present specific scalp topographies, and thus *i)* highlight optimal recording regions for clinical practice and *ii)* suggest different underlying neural systems. FIGURE 7.2

depicts a representative set of measures; the full set of topographies is presented in SUPPLEMENTARY FIGURE 7.6-.9. The specific results obtained for each marker is discussed below.
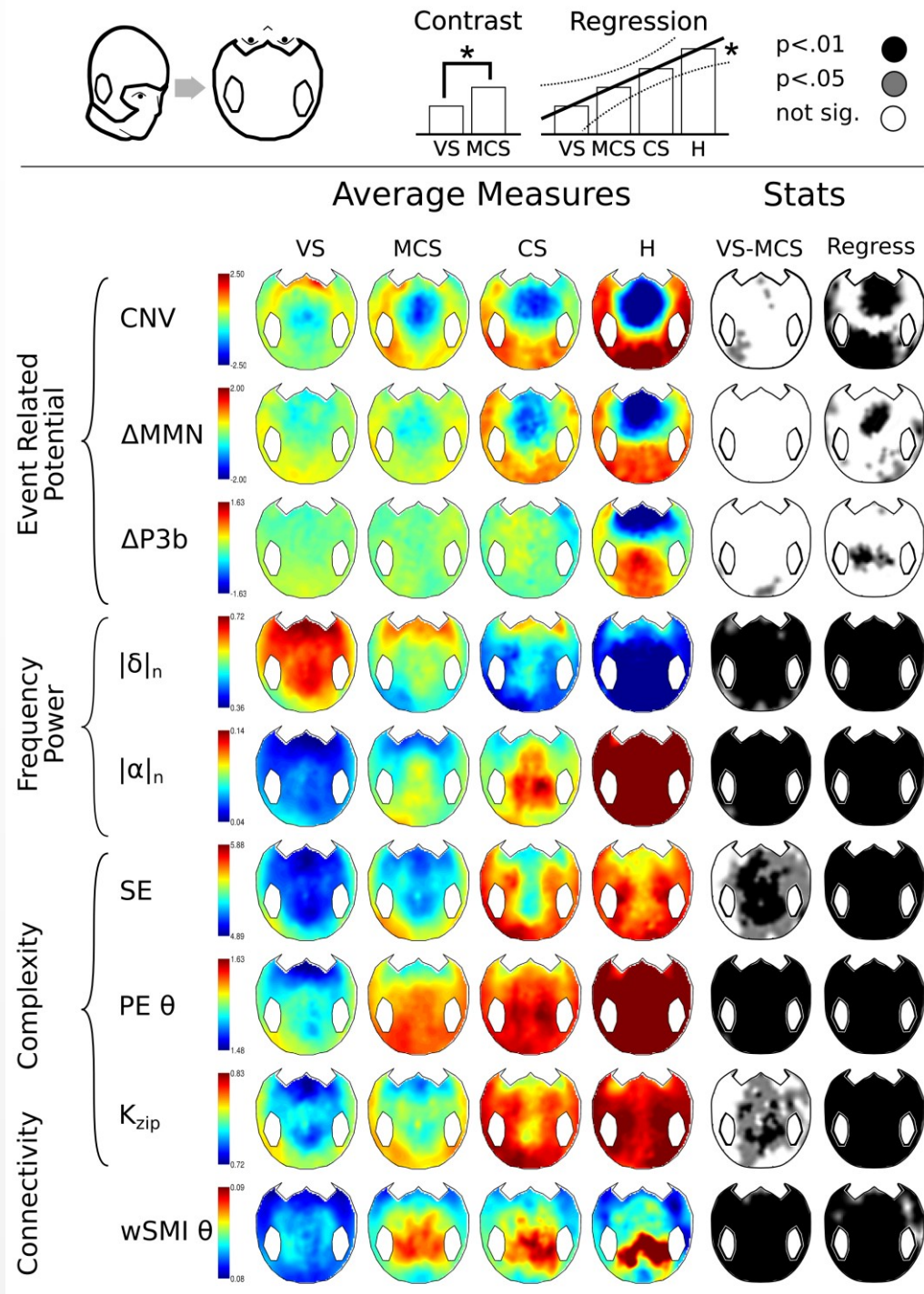
FIGURE 7.2 SCALP TOPOGRAPHY OF THE MOST DISCRIMINATORY MEASURES.

The topographical 2D projection (top = front) of each measure (contingent negative variation (CNV), mismatch negativity (MMN) and P300b (ΔP3b), normalized power in delta ($|\delta|_n$) and alpha ($|\alpha|_n$) bands, spectral entropy (SE), permutation entropy in theta band (PE$_\theta$), Komolgorov-Chaitin Complexity (Kzip) and weighted Symbolic Mutual information (wSMI$_\theta$)) is plotted in panel a for each state of consciousness (columns). The fifth column indicates whether the VS and MCS patients were significantly different from one another (light gray: p<.05, black: p<0.01, uncorrected). The sixth column shows the statistics of a regression analysis of the measure across the four states of consciousness (VS<MCS<CS<Healthy controls).

7.5.1.1. Event related topographies show low sensitivity to discriminate patients' groups

Only two out of seven sound-related potentials (BEKINSCHTEIN ET AL., 2009) differed significantly between VS and CS patients (SUPPLEMENTARY FIGURE 7.6). None of them could significantly discriminate VS and MCS patients. The MMN and the P300, two event related potentials which both signal the detection of violations of auditory regularities, only showed modest differences between the groups of patients. Although the MMN discriminated VS from CS and MCS from CS, confirming that it increases when consciousness recovers (WIJNEN ET AL., 2007), it did not discriminate VS from MCS. More surprisingly, univariate, electrode-by-electrode statistics of the P300 topography also failed to reveal any discrimination of VS from MCS. This finding, which partially contradicts earlier results with smaller patient samples (BEKINSCHTEIN ET AL., 2009), may be ascribed to large inter-individual variability in EEG topography (KING ET AL., 2013A), as discrimination improves when using multivariate decoding (see below).

7.5.1.2. Theta and alpha band power efficiently index the state of consciousness

Contrarily to ERPs, most of the power spectrum measures appeared to be efficient indexes of consciousness states. These measures appeared maximally informative for electrodes over the parietal region (SUPPLEMENTARY FIGURE 7.2). All spectral measures showed monotonic effects from VS to CS patients groups, and six out of ten succeeded in discriminating VS from MCS. Within the lower frequencies, normalized delta (1-4 Hz) showed decreasing power from VS to CS, significantly separating VS from non-VS patients. On the contrary, normalized theta (4-8 Hz) and normalized alpha power (8-13 Hz) increased significantly from VS to CS. Both frequency bands showed increasing power in parietal regions and significantly discriminated VS from the other groups of patients. Normalized beta power failed to discriminate between VS and MCS patients, but significantly discriminated CS from the other groups of patients.

Because of these opposing variations of low (delta) and higher (alpha and above) frequencies, spectral summaries such as the median spectral frequency (MSF), which summarize the relative distribution of power in the frequency spectrum, were particularly efficient. The spectral entropy (SE) analysis showed that CS and MCS patients presented a less predictable spectral structure (higher entropy) than VS patients.

7.5.1.3. EEG complexity increases with conscious state

Algorithmic (or Kolmogorov-Chaitin) complexity (K) estimates the complexity of a sequence based on its compressibility. Several theories predict that the complexity of information integration (TONONI, 2008) or distributed processing (DEHAENE AND CHANGEUX, 2011) is elevated during conscious states. In agreement with this prediction, we found that the computed measure of complexity, based on EEG compression, increased in patients with a higher clinical state of consciousness. This measure significantly discriminated VS from MCS patients, particularly for a set of electrodes over the parietal region (SUPPLEMENTARY FIGURE 7.8). A complementary mathematical approach is permutation entropy (*PE*) which evaluates the regularity of the probabilistic distributions of temporal patterns in the signal (BANDT AND POMPE, 2002). PE can be computed in distinct frequency bands; we found that PE-based measures were particularly efficient in the theta frequency range, discriminating VS from the other groups. Again, a greater value of PE, especially over centro-posterior regions (FIGURE 7.2), indicating a more complex and unpredictable distribution, indexed a higher state of consciousness.

7.5.1.4.   Information sharing across brain regions indexes conscious state

Similarly to the spectral measures at a single recording site, measures of functional connectivity between two recording sites proved particularly efficient at lower frequencies (SUPPLEMENTARY FIGURE 7.9). Amongst the spectral connectivity measures, only the phase-locking index (PLI) in the delta band was significant, progressive deficits in consciousness being accompanied by greater delta synchrony. Connectivity measures based on information theory, such as weighted symbolic mutual information (wSMI), demonstrated a higher sensitivity: as previously reported (KING ET AL., 2013B), inter-electrode information exchanges increased from VS to CS. VS patients presented significant lower wSMI than both MCS and CS patients in the theta and alpha bands, consistent with the theoretical notion that loss of consciousness in VS reflects an impaired exchange of information across brain areas, and particularly over medium-to-long cortico-cortical distances (KING ET AL., 2013B).

7.5.2.   QUANTIFYING THE EEG DIFFERENCES BETWEEN GROUPS OF DOC PATIENTS

While the above analysis evaluated the topographical differences across groups, judging discrimination capacity in sensor space, while correcting for multiple comparisons over the large number of available electrodes, poses a difficult statistical problem. To reduce dimensionality and quantify the discriminative power of each measure, we summarized spatial information by considering the average over predefined electrodes forming *a priori* regions of interest. All individual trial measures were summarized in their inter-trial average and in their fluctuation (standard deviation) during the recording period. In the case of event related measures, we also applied a systematic within-subject decoding approach for local and global responses to auditory novelty, following the procedure described in (KING ET AL., 2013A), which enhanced the discrimination of these conditions. This approach ultimately yielded a total of 92 measures per subject (see Supplementary Tables 1 and 2 for numerical summaries of each measure in each group).

In order to investigate which measures showed significant differences across groups of patients, we implemented receiver operator curves (ROC, SUPPLEMENTARY FIGURE 7.10) and quantified classification performance with the area under curve (AUC).A strict criterion based on false discovery rate (FDR) was applied to correct for multiple comparisons (92 values * 3 tests: VS-MCS, MCS-CS, and VS-CS). An AUC of 50% corresponds to chance classification. An AUC larger than 50% implies that the measure increases with conscious state (*i.e.* MCS > VS), while AUC < 50% implies a decrease with conscious state (*i.e.* MCS < VS).

7.5.2.1.   Average spectrum, complexity, connectivity, and global responses to novelty provide efficient signatures of consciousness

Analysis of the discrimination performance of the EEG measures revealed that the most discriminative measure was weighted symbolic mutual information, which separated VS from MCS ($wSMI_\theta$ AUC = 74%, p_{FDR}<.0001) and CS patients ($wSMI_\theta$: AUC = 78%, p_{FDR}<.001). Power spectrum measures also performed well: increased normalized delta power separated VS from MCS (AUC=31%, p_{FDR}<.001) and from CS patients (AUC=19%, p_{FDR}<.0002), while the converse occurred in higher frequency bands, with decreased normalized alpha power segregating VS from MCS (AUC= 72%, p_{FDR}<.0002) and from CS patients (AUC= 85%, p_{FDR}<10^{-4}). A third variable affording accurate classification was permutation entropy in theta frequency range, discriminating

VS from the other groups (PE_θ : MCS>VS, AUC=72%, p_{FDR}<.0002, CS>VS, AUC=83%, p_{FDR}<10^-4). Finally, the decoding of the global effect (the ERP response to deviant auditory sequences (BEKINSCHTEIN ET AL., 2009; KING ET AL., 2013A)) also separated VS from MCS (AUC = 62%, p_{FDR}<0.05) and CS patients (AUC = 81%, p_{FDR}<.0002).
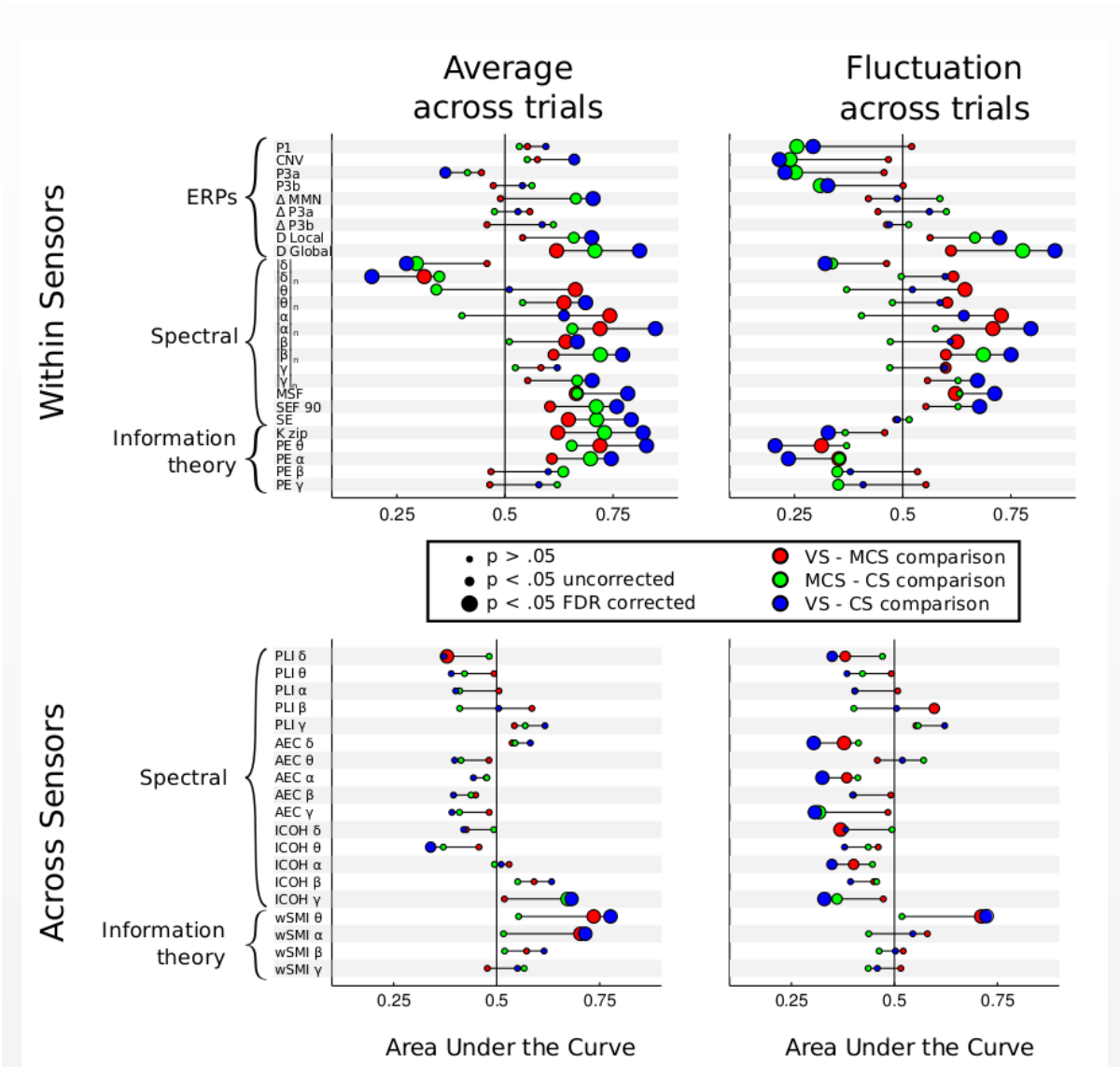
FIGURE 7.3 DISCRIMINATION POWER FOR ALL MEASURES.

Each line provides a summary report of its respective measure. The meaning of each acronym can be found in supplementary methods. The measures are ordered according to the taxonomy presented in Table 1. The location of each dot corresponds to the area under the curve (AUC) for a pair-wise comparison between two states of consciousness (see Methods). Chance level corresponds to AUC = 50% (central vertical line). An AUC bigger than 50% suggests that the corresponding measure is correlated with the state of consciousness (from VS to MCS and CS) whereas AUC < 50% suggests that the measure is anti-correlated with the state of consciousness. Dot color and size indicate the type and significance of the comparison (see Legend). The red color highlights the minimal contrast between the MCS and VS states of consciousness.

One issue is that the vigilance level can be confounded with VS-MCS differences. Indeed, the clinical assessment of the coma recovery scale-revised (CRS-R) subscore corresponding to the arousal level showed a small increase in the MCS group as compared to the VS group (mean ±

SEM, MCS: 1.53 ± 0.07, VS: 1.30 ± 0.05, p = 0.013). In order to rule out this potential confound and isolate the variations specifically due to consciousness, we replicated the previous analysis in the subset of VS and MCS patients with CRS-R arousal subscore of 1, corresponding to patients that presented eye opening only to stimulation (VS: 52 patients, MCS: 32 patients). Performance of the EEG measures was essentially unchanged in this vigilance-controlled subset of patients as compared to the overall comparison (SUPPLEMENTARY FIGURE 7.11 and SUPPLEMENTARY TABLES 3 AND 4).

7.5.2.2. Fluctuation of measures across trials convey independent information
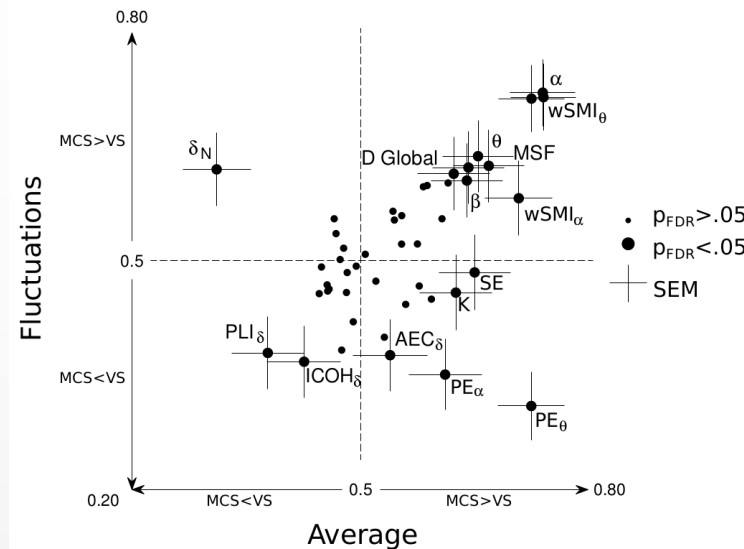
FIGURE 7.4 SUMMARY OF THE MEASURES DISCRIMINATING VS AND MCS PATIENTS.

Each measure is plotted in a two-dimensional graph. Acronyms meanings can be found in the supplementary methods. The x axis indicates discriminatory power for each measure's average across trials, while the y axis indicates discriminatory power for their respective fluctuations across trials. For instance, the Kolmogorov-Chaitin complexity (K) measure appears in the bottom right quadrant, suggesting that its average value is significantly higher in MCS than in VS, while its standard deviation, conversely, is higher in VS than in MCS. Large circles indicate significant measures ($p_{FDR}<0.05$). Non-significant measures are indicated with small dots.

The stability of evoked activity has been proposed as a marker of consciousness (SCHURGER ET AL., 2010). We then hypothesized that EEG variability over time, quantified as the fluctuations of a given measure across trials might add independent information about consciousness, relative to its mere average value. The results confirmed that EEG fluctuations add important discriminative information (FIGURE 7.3). Interestingly, we did not always observe a positive correlation between the classifying power of a given measure based on its average and on its fluctuations. FIGURE 7.4 provides a graphical comparison of discrimination power based on the mean or the fluctuation of each measure for the MCS-VS contrast. Different types of measures can be distinguished. Some simply fail to separate these two groups (*e.g.* low gamma power). Others show a significant increase in both the average and the fluctuation over time for MCS compared to VS (this is the case for power in theta, alpha and beta bands, *MSF* and *wSMI$_\theta$*). Yet other measures exhibit dissociation between average and fluctuation. In particular, the state of consciousness is associated with a high average but a low fluctuation of *K*, *PE$_\theta$* and *PE$_\alpha$*, indicating that a stable and lasting increase in complexity and entropy reflects a conscious patient. Conversely, the state of consciousness is asso-

ciated with a low average and high fluctuation of power and *PLI* in the delta band: while fluctuating slow cortical potentials, covering the delta range, are typical in the normal conscious brain (HE AND RAICHLE, 2009), stable and intense delta waves are a sign of unconsciousness in anesthesia and deep sleep (FRANKS, 2008). Finally, the remaining measures were discriminative only for averages (*i.e.*, *SE*) or for fluctuations across trials (*i.e.*, *PLI* in beta and alpha bands). The latter finding suggests that consciousness implies a constantly fluctuating stream of transiently phase-locked brain states.

7.5.3.   COMBINING MEASURES IMPROVES DISCRIMINATION

We next examined whether these EEG measures could be combined to improve discrimination of the different states of consciousness, particularly in the crucial VS-MCS comparison. One goal was to determine whether these markers act in concert, and can thus combine in synergy to improve discrimination between groups or whether these measures are highly redundant. In this latter case, the best measure would provide information comparable to the entire set of measures. To this aim we used a multivariate classification method based on a support vector machine (SVM) (PEDREGOSA ET AL., 2011). The SVM was applied to all VS and MCS recordings. To avoid over-fitting the SVM was repeatedly fitted and evaluated on independent datasets using stratified nested cross-validation. It took as input a measure or set of measures, and output the estimated probability for a given recording to belong to the VS group. Results showed that the best cross-validated single measure reached an AUC of 71% for the VS-MCS comparison. By contrast, using the whole set of measures, AUC was significantly higher than when using the best single measure: VS-MCS: 78% (p < .001). In other words, measures were not entirely redundant, and the SVM provided an efficient way to identify which combination led to a better discrimination of the patients' states of consciousness.

7.5.4.   AUTOMATIC CLASSIFICATION OF PATIENTS' STATE OF CONSCIOUSNESS

A main clinical objective of this work was to develop an automatic system that potentially helps physicians to detect consciousness in non-communicating patients. For this, we evaluated the performance of the SVM classifier to differentiate VS patients from MCS patients, *i.e.* to reliably identify the presence of a clinically detectable state of consciousness. The classifier achieved above-chance levels of accuracy (χ^2(2, N = 143) = 26.7, p = 10^{-7}): 67% (50 out of 75) of VS-diagnosed patients and 76% (52 out of 68) of MCS-diagnosed patients were classified in their respective clinical categories solely from their brain activity (FIGURE 7.5). To test for robustness, we also evaluated whether the same classifier, trained to detect consciousness in VS and MCS patients, generalized to CS patients and healthy subjects. The great majority of these recordings (89%, 34 out of 38) were classified as conscious (MCS rather than VS).

To train our classifier, we relied on clinical labels (VS and MCS) that derive solely from behavioral observations and need not provide a perfect "gold standard" (OWEN ET AL., 2006). A disagreement between the automatic classification and the clinical label may represent an error of the classifier, but it may also indicate the presence of EEG-based information not accessible to the clinician. To investigate whether the information derived from neurophysiological activity may improve diagnosis, we tested whether VS patients classified as MCS from their EEG activity would later show signs of intentional behavior that may have been missed at the time of the recording. Most patients classified as VS on both clinical and EEG-based criteria showed no signs of regaining consciousness in the six weeks following EEG recording (recovery<21 days: 10 (20%); recovery< 42 days: 1(2%); no recovery: 39 (78%)). By contrast, among the clinically VS patients classified as

MCS based on their EEG activity, the proportion of those who later showed signs of consciousness significantly increased (recovery < 21 days: 8 (32%); recovery < 42 days: 3 (12%); no recovery: 12 (48%); unknown: 2 (8%)). The number of subjects who recovered consciousness was significantly higher for VS patients classified as MCS than for those classified as VS ($\chi^2(2, N = 73) = 4.99$, p = 0.025). It should be emphasized that clinical assessment at the time of the recording, based on the full Coma Recovery Scale-Revised (CRS-R) or its sub-scores, neither predicted the VS patients' recovery nor the automatic classification category (see supplementary results). Hence, within a behaviorally indistinguishable group of clinical VS patients, neurophysiological measures provided substantial information about the future improvement of consciousness, suggesting a better functional status at the time of recording.
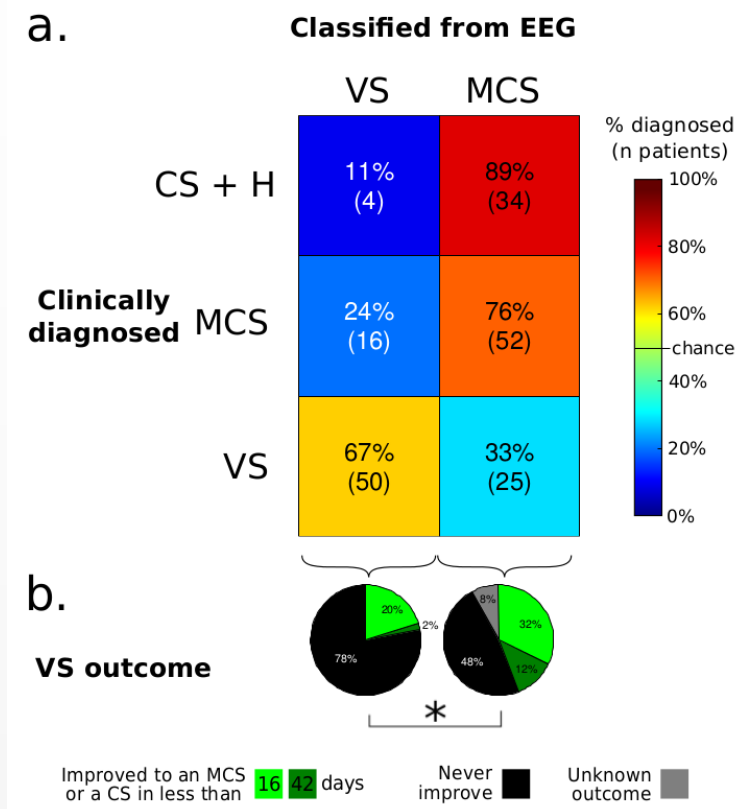
FIGURE 7.5 COMPARISON OF EEG-BASED CLASSIFICATION WITH CLINICAL DIAGNOSIS AND PATIENTS' OUTCOME.

a. Confusion matrix showing, on the y axis, the clinical diagnosis (VS, MCS or CS-Healthy), and on the x axis, the prediction using the automatic classifier based on EEG measures (VS or MCS). The number of recordings and their respective percentages within each clinical state category are reported in each cell. For VS and MCS patients EEG-based classification matches the clinical diagnosis in a majority of cases. Using the same classifier (trained to predict VS or MCS state) the top cells show the predicted condition for CS and Healthy subjects. The majority of these recordings were classified as MCS. Non-matching cells can suggest inappropriate classifications, but may also indicate that EEG measures are detecting information unseen by clinicians.

b. The pie charts show the clinical outcome of the VS patients, as a function of whether EEG measures classified them as VS or in a higher state of consciousness (MCS or CS). The probability of recovery was significantly higher (p = 0.02) for patients classified into a higher state of consciousness than for patients predicted to be truly VS.

7.6. DISCUSSION

We systematically evaluated putative signatures of consciousness in a large dataset of high-density bedside EEG recordings of patients suffering or recovering from disorders of consciousness (DOC). An important feature of our study is that we included all DOC patients within a nearly two-year period, thus ensuring an unbiased sampling and maximizing clinical relevance. By testing a total of 92 candidate measures arising from previous empirical and theoretical research, we showed that EEG contains many useful features that discriminate between VS and CS. Each of these measures can thus index consciousness - either directly, or indirectly through its consequences on arousal, instruction understanding, active maintenance of stimuli and instructions in working memory, task monitoring, etc. Crucially, only a few of these measures were effective in discriminating the minimal contrast between VS and MCS patients. We focus the discussion on this subset of measures, which appear most relevant to the objective identification of conscious processing from the patterns of EEG activity.

Spectral power analysis revealed that alpha and theta power was significantly lower in VS than in MCS patients, whereas delta power showed the opposite pattern. Similar increases in low-frequency oscillations are a classical observation in coma and deep sleep (POSNER ET AL., 2007). Here we demonstrate their relevance to distinguish VS from MCS patients, as recently reported in smaller groups of patients (FELLINGER ET AL., 2011; LEHEMBRE ET AL., 2012; LECHINGER ET AL., 2013).The fronto-parietal topography of these spectral effects is consistent with a crucial role of fronto-parietal networks in a 'global workspace' (GW) mediating a serial stream of conscious states at theta-like frequencies (100-300 ms per state) (ALKIRE ET AL., 2008; VANHAUDENHUYSE ET AL., 2010; DEHAENE AND CHANGEUX, 2011; LAUREYS AND SCHIFF, 2011).This regional hypothesis should be confirmed with cortical source analysis, which was not attempted here given the difficulty of obtaining an accurate source model in patients with massive brain and skull damage (KING ET AL., 2011).

Spectral measures also exhibited greater fluctuations in MCS than in VS patients. This finding agrees with the definition of MCS as a fluctuating state (GIACINO AND KALMAR, 2005) and shows that, contrariwise, a stable state of increased delta and reduced alpha-theta power is a solid sign of unconsciousness. Finally, the structure of the EEG spectrum, as measured by spectral entropy, was increased in MCS and CS as opposed to VS patients. This finding was previously reported to be relevant only in the acute stage and in a much smaller subset of patients (14 VS *versus* 9 MCS) (GOSSERIES ET AL., 2011).

Multiple EEG measures of signal complexity (SE, PE, K) discriminated VS from MCS patients. Indeed, both the average and the inter-trial stability of EEG complexity increased monotonically with the patients' state of consciousness. This result confirms that the complexity of cortical activity indexes consciousness, as explicitly formulated for instance by the dynamic core model of Tononi and colleagues (TONONI, 2004, 2008). According to this model and related ones (SETH ET AL., 2011), a minimal level of complexity in neuronal signals is required to encode a rich and differentiated representation, thus singling it out from the vast repertoire of potential contents of consciousness. Regions specifically implicated in the coding of conscious representations would thus show higher complexity during conscious than during unconscious states, as observed here.

We found that consciousness was indexed not only by a high information complexity, but also by a stability of this complexity, with reduced fluctuations during the 30-minute recording. This result extends to spontaneous EEG the findings of a recent fMRI study showing that neural activation patterns are more reproducible when evoked by a visible than by an invisible stimuli

(SCHURGER ET AL., 2010). We hypothesize that one property of the conscious brain is to achieve both a reproducible perception of identical sensory stimuli and an internal stream of computations of roughly constant complexity even in the absence of sensory stimulation.

One of the most striking differences between patients was an increase in functional connectivity measures around the theta (4-8 Hz) frequency band (wSMI theta) in MCS as compared to VS patients. This result strengthens previous findings relating long-distance synchronization with conscious states in DOC patients in similar frequency bands (SCHIFF ET AL., 2005; LEHEMBRE ET AL., 2012; LEON-CARRION ET AL., 2012). In addition to generalizing this finding to a large dataset, our results clarify the topography of this large-scale increase in communication. We observed a maximal effect over mesio-parietal areas, in close agreement with recent work showing the crucial role of precuneus and posterior cingulate as 'hubs' in a long-distance cortical network that may underlie conscious integration (SCHIFF ET AL., 2005; VOGT AND LAUREYS, 2005). Future research should investigate whether a more detailed description of this functional connectivity network, possibly aided by directional connectivity analyses such as Granger causality (GAILLARD ET AL., 2009; BARRETT ET AL., 2012), may also help to distinguish these clinical groups.

The importance of long-distance cortical communication and signal complexity in consciousness fits with a set of perturbational TMS-EEG studies conducted in DOC patients (ROSANOVA ET AL., 2012), sleep (MASSIMINI ET AL., 2005) and anesthesia (FERRARELLI ET AL., 2010), which revealed that the prolonged propagation of TMS-induced activation to distant sites systematically correlates with consciousness. More recently a quantification of the structure of EEG-evoked responses to the TMS pulse has been presented (CASALI ET AL., 2013). In a small cohort of normal subjects and patients, this measure, coined pertubational complexity index (PCI), was found to discriminate conscious state across a broad range of physiological, pharmacological and pathological conditions. Further research should test whether a similar measure can be obtained without the TMS excitation (SITT ET AL., 2013). It may not be irrelevant that, in the present study, long-distance communication and complexity were measured while patients were stimulated with a series of auditory tones. Our results may partially reflect the brain state evoked by these stimuli, thus paralleling those triggered by a TMS pulse. Recording EEG while patients are stimulated with a challenging set of auditory stimuli, as we did here, presents several advantages, including increased vigilance and the capacity to simultaneously evaluate evoked and spontaneous brain activity patterns. Nevertheless, future research will be needed to disentangle which of our measures would continue to be discriminative when applied to resting-state EEG.

We also found larger fluctuations of functional connectivity in MCS than in VS patients, in particular in PLI (from delta to β) and in wSMI$_\theta$. Recent studies conducted with epileptic patients with implanted electrodes (SEEG) for pre-surgical mapping reported that loss of consciousness during the transition from partial simple to partial complex seizures was marked by a sudden excessive increase in cortico-cortical and thalamo-cortical synchrony (LAMBERT ET AL., 2012). Our results lead to the testable prediction that this excessive synchrony, also observed in propofol anesthesia (SUPP ET AL., 2011), would cause a marked decrease of information complexity, which would in turn mark the loss of consciousness.

EEG studies using active cognitive paradigms to probe conscious states often use ERPs as their main outcome measure (BEKINSCHTEIN ET AL., 2009; SCHNAKERS ET AL., 2009A). Indeed, the auditory regularities violation task used here was designed to dissociate the automatic and unconscious MMN from the P3b complex associated with conscious access. We previously demonstrated that this P3b component, which indexes the detection of the violation of a global regularity, can be useful as a specific marker of consciousness in individual patients, sometimes in advance of a clinical

diagnosis (FAUGERAS ET AL., 2011, 2012). The present results, however, indicate that this traditional ERP averaging approach lacks sensitivity in comparison to other EEG-based measures. ERP components may still contribute importantly to diagnosis, but mostly when analyzed with a multivariate pattern analysis procedure that deals with inter-individual differences (KING ET AL., 2013A), particularly in patients whose ERP topography may be significantly distorted relative to the normal population.

The present results also show that ERP fluctuations across trials provide a sensitive measure of conscious state. Consistent with a previous fMRI study (SCHURGER ET AL., 2010), consciousness was characterized by more stereotyped responses to external stimuli. This result could also reflect the fact that VS patients presented a greater power of spontaneous low-frequency EEG signals, non-phase-locked with incoming stimuli and thus interfering with the reproducibility of evoked signals.

Our conclusions are backed up by a large sample of patients with various etiologies, robust methods controlling for multiple comparisons, and a focus on the minimal contrast between VS and MCS patients. It could be argued that differences in vigilance, rather than consciousness, also distinguish MCS and VS patients. Indeed, the CRS-R sub-score of vigilance, measured just prior to the recording session, appeared slightly larger in MCS than in VS patients. However, most of the identified measures that distinguished VS from MCS patients remained significant when contrasting individuals with matched levels of vigilance. Thus, vigilance per se is unlikely to contribute to the identification of the relevant measures.

A significant gain in discrimination was obtained by combining several EEG measures. This is an important result for both theoretical and clinical reasons. Theoretically, this gain of information suggests that our markers do not simply reflect distinct facets of the same neural process, but tap onto distinct and dissociable features of conscious states. From the medical perspective, our results stress the usefulness of combining a subset of EEG measures (spectral, informational and connectivity based).

While most patients were correctly decoded on the basis of their EEG measures, the number of disagreements between the automated and clinical diagnoses remained too high for individual diagnosis. In particular, 24% of MCS patients, who manifested clear-cut behavioral signs of consciousness on some occasions, were classified as VS. We note, however, that the present study was based on a single half-hour EEG recording. As the minimal conscious state is defined by the presence of fluctuating signs, assessed by repeated clinical evaluation, it seems entirely possible that our examination was performed at a moment when these patients' consciousness lapsed. In the future, multiple sessions or even 24-hour EEG recordings might yield an improved clinical discrimination. While our accuracy in discriminating patients is roughly comparable to that reported by other groups (*e.g.* (SCHNAKERS ET AL., 2008A; FELLINGER ET AL., 2011; GOSSERIES ET AL., 2011; FINGELKURTS ET AL., 2012A; LEHEMBRE ET AL., 2012)), these previous studies used smaller sample sets and were focused on quantifying the power of a single EEG measure in discriminating pre-selected groups of well-differentiated patients (*e.g.* non-overlapping CRS-R scores for MCS and VS groups). The present study, by contrast, tackles the more difficult problem of identifying residual consciousness in a serial cohort of all patients admitted to our clinic. Structural magnetic resonance imaging was also reported to be efficient in discriminating patients (FERNÁNDEZ-ESPEJO ET AL., 2011). Further work will explore if the combination of multimodal (MRI+EEG) information can achieve a better performance.

In the converse direction, 33% of clinically VS patients were classified as MCS by their EEG patterns. Not all of these misclassifications may be errors, however. Rather, in a subset of clinically defined VS patients, our decoder demonstrably discovered information indicating a better functional status, as indicated by a higher rate of clinically detectable recovery in the months following EEG recording. This result fits with previous fMRI findings indicating that the vegetative state is not a homogeneous category, and that some VS patients may actually be minimally or even fully conscious (OWEN ET AL., 2006).

In conclusion, because EEG is a time-resolved, low-cost, widespread, and easily repeatable method, it may prove more efficient than MRI or fMRI in order to identify VS patients with residual consciousness or with a potential for future recovery. Our results point to the possibility that a reduced set of EEG measures, selected for example on the basis of their individual discrimination power, and potentially computed from a few scalp electrodes, could ultimately serve as a reliable bedside tool to probe consciousness in DOC patients.

7.7. SUPPLEMENTARY MATERIALS

7.7.1. MOTIVATIONS FOR EACH MEASURE

In this section we provide a detailed description of the motivations for each measure used in this study. For details of the computations see the supplementary methods.

7.7.1.1. Event related potentials

The auditory paradigm (BEKINSCHTEIN ET AL., 2009) was originally designed to elicit and isolate early and late event-related potentials (ERPs). Recent theories of consciousness indeed argue that early components correspond to unconscious processing stages, whereas late components are associated with conscious access (see review in (DEHAENE ET AL., 2006A; SERGENT AND NACCACHE, 2012)). In addition to early auditory P1 and N1 components, our auditory protocol allows identifying three responses related to the detection and the expectation of an auditory novelty: the contingent negative variation (CNV), the mismatch negativity (MMN) and the P3b component.

The CNV is a slow negative drift generally observed over the frontal electrodes when subjects expect an informative stimulus and terminates when such stimulus is presented (WALTER ET AL., 1964). This component is believed to be generated by a large network and necessitate subjects to be attentive and actively engaged in the task (ROSAHL AND KNIGHT, 1995; NIEDERMEYER, 2003; GÓMEZ ET AL., 2007; CHENNU ET AL., 2013). As these two conditions are generally associated with conscious perception (DEHAENE ET AL., 2006A; DEHAENE AND CHANGEUX, 2011) the CNV could sensitively mark a conscious state. Indeed, in a similar experimental protocol, Faugeras *et al.* has observed a negative drift ranging from the first to the last sound of each trial, proved which distinguished patients in various states of consciousness (FAUGERAS ET AL., 2012).

The MMN is elicited by a change in pitch in the last of the five tones (e.g. xxxxx *versus* xxxxY) (NÄÄTÄNEN ET AL., 1978). This component has been repeatedly reported under non-conscious conditions, although its amplitude can be modulated by subjects' attention (BEKINSCHTEIN ET AL., 2009) and conscious state (in sleep (NASHIDA ET AL., 2000) and in DOC pa-

tients (FISCHER ET AL., 2004, 2010; KOTCHOUBEY ET AL., 2005; NACCACHE ET AL., 2005; WIJNEN ET AL., 2007; BEKINSCHTEIN ET AL., 2009; SCHNAKERS ET AL., 2009A; MORLET AND FISCHER, 2013).

The P300b (P3b) component is observed across a wide variety of tasks and is generally elicited by visible relevant target (*e.g.* (SQUIRES ET AL., 1975B; SERGENT ET AL., 2005; POLICH, 2007)). This component is believed to reflect a large activation of the fronto-parietal cortices, and has thus been repetitively linked to working memory updating processing (POLICH, 2007) and conscious access (DEHAENE AND CHANGEUX, 2011). Specifically in the present experimental protocol, the P300 response to unexpected (rare) sound sequences has only been observed in conscious and attentive subjects (BEKINSCHTEIN ET AL., 2009; FAUGERAS ET AL., 2011, 2012).

7.7.1.2. "Ongoing" activity

The rest of our measures were derived from the EEG activity preceding the onset of the last sound (early time window on FIGURE 7.1). We refer to this time periods as "ongoing activity". It should be noted however that neutral auditory stimuli were presented during these time periods, which are thus different from traditional resting state conditions. However, we reasoned that it may be possible to quantify the "ongoing" EEG activity that dominates over evoked responses by approximately one order of magnitude. Furthermore, one should note that classical resting state conditions are generally uncontrolled stimulation conditions. Finally, the controlled auditory stimulations here limit drowsiness by repeatedly calling the patient's attention, and could thus help to differentiate MCS from VS patients.

"Ongoing" EEG measures were organized according to two dimensions: *i)* whether they capture local dynamics or connectivity; and *ii)* whether their theoretical background lies in a spectral decomposition of the EEG signal, or in information theory.

7.7.1.3. Measures of EEG spectrum

Local dynamics refer to measures computed within a given EEG electrode. At this level, spectral measures are traditionally applied to quantify EEG oscillations or broadband frequency patterns, many of which have been proposed to distinguish conscious states in anesthesia (SUPP ET AL., 2011), sleep (FINELLI ET AL., 2001) and DOC patients (FELLINGER ET AL., 2011; FINGELKURTS ET AL., 2012A). A classical finding is that unconscious subjects, compared to conscious ones, exhibit a reduction in power in the alpha band (8-13 Hz) and an increase in low frequencies such as the delta band (1-4 Hz). In our dataset we estimated power in five frequency bands (delta to low gamma). Frequency analyses were supplemented with spectrum summary measures that summarize the distribution of power over various frequencies using a single value, for instance its median or its spectral entropy (SE, characterizing the complexity of the spectrum). These measures of spectrum summaries have been previously used to characterize the EEG recordings of DOC patients (SCHNAKERS ET AL., 2008A; GOSSERIES ET AL., 2011) and subjects under anesthesia (VAKKURI ET AL., 2004; VELLY ET AL., 2007; LAITIO ET AL., 2008).

7.7.1.4. Measures of complexity

Novel techniques from the fields of dynamical systems and information theory also provide insights into normal and perturbed neural mechanisms (DIMITROV ET AL., 2011). These measures can be used to detect characterize changes in the EEG that may not be unveiled using traditional spectral frequency content methods (STAM, 2005).

We included a representative set of information theory measures of local dynamics. In particular, permutation entropy (*PE*) is an increasingly used method to detect dynamical changes in a time series (CAO ET AL., 2004), which is known for its high resistance to low signal-to-noise ratios compared to other similar methods (BANDT AND POMPE, 2002). PE has been successfully applied to the EEG-based detection of loss of consciousness under anesthesia (JORDAN ET AL., 2008; LI ET AL., 2008). As described in detail below, PE estimates the entropy of a signal transformed into a sequence of discrete "symbols". These symbols are generated from the qualitative (*i.e.* ranking) up and downs of the signal.

We introduce an original method to quantify the complexity of EEG signals based on the application of the Kolmogorov-Chaitin complexity (K). This measure quantifies the algorithmic complexity (see (KOLMOGOROV, 1965; CHAITIN, 1974)) of a single sensor's EEG by measuring his degree of redundancy. Algorithmic complexity of a given string (in this case an EEG sequence) can be described as the length of shortest computer that can generate it. A short program corresponds to a less complex sequence. We estimated K by quantifying the compression size of the EEG using variants of the Lempel-Ziv zip algorithm (LEMPEL AND ZIV, 1976). This measure has been previously applied to detect changes in the cortical activity in anesthetized animals(SHAW ET AL., 1999) and more recently to index conscious state in human subjects from the evoked response to a TMS pulse (CASALI ET AL., 2013).

7.7.1.5.   Measures of information sharing

Connectivity, in the sense of information sharing across distant cortical areas, has been proposed as a key element of several theories of consciousness (BAARS, 1989; REES ET AL., 2002; TONONI, 2008; DEHAENE AND CHANGEUX, 2011). Recent advances in theoretical neuroscience have shown that long-distance communication could be marked (GAILLARD ET AL., 2009; DEHAENE AND CHANGEUX, 2011) or established (FRIES, 2005; SAALMANN ET AL., 2012) by a frequency-specific synchronization across different brain areas (FRIES, 2005). Intracranial recordings and M/EEG comparing neural processing elicited by subliminal and visible images revealed an association between conscious perception and long-range synchrony in the beta and gamma bands (GROSS ET AL., 2004; GAILLARD ET AL., 2009; HIPP ET AL., 2011). Moreover, recent EEG studies suggest that VS patients present lower functional connectivity than MCS and CS patients (FINGELKURTS ET AL., 2012A; LEHEMBRE ET AL., 2012). In the present study, we evaluated synchrony with two traditional spectral methods: phase lag index (PLI) and the imaginary part of coherence (ICOH). The two measures were favored over as they are robust to volume conduction, common source and muscular and eye movements artefacts (NOLTE ET AL., 2004; STAM ET AL., 2007).

However, such spectral methods are poorly sensitive to non-oscillatory functional connectivity. To address this issue, we also computed an original method for quantifying information sharing: weighted symbolic mutual information (wSMI). wSMI can robustly quantify non-oscillatory functional connectivity by transforming the EEG signals into symbolic sequences and estimating the non-trivial association of symbols across sensors. In a previous study, we have successfully applied wSMI to distinguish vegetative from minimally conscious and conscious states patients (KING ET AL., 2013B).

7.7.1.6.   Mean value versus fluctuations across trials

For all measures, we introduced a final distinction between their average value and their fluctuation across time (computed as the standard deviation across trials). First, over the course of an hour, vegetative state patients, and *a fortiori* minimally conscious state patients present strongly

fluctuating vigilance and attention (LAUREYS ET AL., 2004). Measuring the fluctuation of each EEG marker may thus help distinguishing different states of consciousness. Second, fluctuation proved to capture independent information from the BOLD signal in a recent fMRI experiment (GARRETT ET AL., 2010). As a consequence, we studied both the mean (μ) and standard deviation (σ) of each measure across trials.

7.7.2.   DETAILS OF THE COMPUTATION OF EACH MEASURE

In this section we describe the procedures applied to compute all measures.

7.7.2.1.   Event-Related Potentials (ERPs)

Mid-latency auditory potential corresponding to the first sound (P1)

In the present study, the P1 was computed by averaging the voltage of a cluster of 7 EEG electrodes surrounding Fz (electrodes [15, 22, 14, 6, 7, 16, 23] in the EGI 256-electrode net) between 68 ms and 116ms following the onset of the first sound and across all trials.

Contingent Negative Variation (CNV)

Following previous methods (*e.g.* (FAUGERAS ET AL., 2012)), the CNV was computed by averaging the slope of the EEG electrodes' voltage observed between the onset of the 1st sound to the onset of the 5th sound (Linear regression, from 0 to 600 ms). For univariate analyses, the CNV was summarized as the average slope of a cluster of 7 EEG electrodes surrounding Fz (electrodes [15, 22, 14, 6, 7, 16 and 23] in the EGI net).

P3a

Following previous findings (*e.g.* (BEKINSCHTEIN ET AL., 2009; MORLET AND FISCHER, 2013)), the P3a component was computed by averaging the EEG electrodes' voltage between 280 ms to 340 ms following the onset of the 5th sound and across local deviant trials only (xxxxY). For univariate analyses, the P3a was summarized as the average voltage of a cluster of 7 EEG electrodes surrounding Fz (electrodes [15, 22, 14, 6, 7, 16 and 23] in the EGI net)

P3b

Following previous findings (*e.g.* (BEKINSCHTEIN ET AL., 2009; FAUGERAS ET AL., 2012; KING ET AL., 2013A)), the P3b component was computed by averaging the EEG electrodes' voltage between 400 ms to 600 ms following the onset of the 5th sound and across global deviant trials only (rare sequences). For univariate analyses, the P3b was summarized as the average voltage of a cluster of 5 EEG electrodes surrounding Cz (electrodes [9, 186, 132, 81 and 45] in the EGI net).

Mismatch negativity (ΔMMN) and Contrasted P3a (ΔP3a)

The MMN was estimated by contrasting the local deviant trials (LD = xxxxY) *versus* the local standard trials (LS = xxxxx). Each subjects' MMN was thus summarized as the 256-electrode topography of the LD-LS difference in the time window between 140 ms to 192 ms after the onset of the 5th sound. For the univariate analysis, this value was averaged over a subset of electrodes around Fz and Cz (electrodes [15, 22, 14, 6, 7, 16, 23, 9, 186, 132, 81 and 45] in the EGI net)

Similarly, the ΔP3a was estimated using the same contrast than for the MMN but averaging a time window from 280 ms to 340 ms after the onset of the 5th sound. The same electrodes as for the MMN were used for the univariate analysis.

Contrasted P3b (ΔP3b)

The ΔP3b was contrasted between the rare global deviant (GD) trials and the frequent global standard (GS) trials (BEKINSCHTEIN ET AL., 2009). Each subjects' ΔP3b was then summarized as the 256-electrode topography of the GD-GS difference in the time window between 400 ms to 600 ms after the onset of the fifth sound. For the univariate analysis, this difference was averaged over a subset of electrodes around Cz and Pz (electrodes [9, 186, 132, 81, 45, 101, 100, 129, 128, 119 and 110] in the EGI net) Following the Local Global protocol (BEKINSCHTEIN ET AL., 2009), the late P3b component was isolated by contrasting frequent and expected auditory sequences to rare and thus unexpected auditory sequences. For instance, in a given block, subjects were repeatedly presented with xxxxY trials. On rare occasions (20%), an xxxxx sequence was presented. In another block, subjects were frequently presented with xxxxx, and rarely with xxxxY. Contrasting rare and frequent trials can thus be orthogonally tested to the local change in pitch.

Decoding the MMN and P300b

As patients often present significant brain and skull lesions, they may present extremely variable topographies from one subject to another. Following a previous study (KING ET AL., 2013A), we thus implemented multivariate pattern classifiers (MVPA) to optimize the detection of ΔMMN and ΔP300 effects. The MVPA can indeed identify the topographies that best discriminate standard and deviant trials for each subject separately.

Two types of classifiers were trained: (1) local standard *versus* local deviant ("local classification', similar to ΔMMN); (2) global standard *versus* global deviant ('global classification', similar to ΔP300).

A standard ten-fold stratified cross-validation was implemented to avoid over-fitting and circular analysis (KRIEGESKORTE ET AL., 2009; VUL ET AL., 2009B). In each fold, a support vector classifier (SVC) (CHANG AND LIN, 2001) was fitted to the training set and supplemented with a probabilistic output method (PLATT, 1999) (see multivariate pattern analysis section). This continuous classification method was then assessed on its ability to accurately predict the class of the test set.

The amplitude of each electrode at multiple time points was provided to the classifier. To minimize the number of irrelevant features, a time window of interest was used for each classification: Local: [0, 367] ms; Global: [367,736] ms after the onset of the last sound. Each trial was then transformed into a p-dimensional vector x, in which each coordinate corresponds to a single data sample at a given sensor ($p = n_{sensors} \cdot n_{time\ samples}$). The entire dataset can hence be represented as a matrix X in which each row i corresponds to one trial x_i, and each column corresponds to one attribute. All data were normalized $(x - \mu(x_{train}))/\sigma(x_{train})$ across all artefact-free trials in each sample of each sensor. Following a previous study, univariate feature selection was performed with a fixed rate of 10%. The SVC was fitted to find the hyperplane w that best separates standard from deviant trials. To minimize imbalance effects, sample weights were applied in proportion of the trial local and global classes (frequent xxxx & xxxY; rare xxxx & xxxY) so that each category equally affects the fitting of w. Finally, a cumulative probability distribution function was then fitted to the training set using Platt's method (PLATT, 1999). The signed distance of the dot product $w \cdot x$ can thus be used to determine the probability of a given trial to belong to the deviant class. Finally, classification scores, summarized with the area under the curve (AUC), were estimated from the predicted probabilities of the trials from the testing set. All multivariate analyses were performed with the Scikit-learn toolbox (PEDREGOSA ET AL., 2011).

7.7.2.2.   Local dynamics (within electrodes)

Spectral analysis

Power spectral density on each trial was estimated using the Welch method (WELCH, 1967). For each trial, each electrode was divided in 500-ms sections with 400 ms of overlap. Sections were windowed with a Hamming window and zero padded to 4096 samples. The power in each frequency band was calculated as the integral of the power spectral density (PSD) within each frequency bands, and finally log scaled. Frequency-bands of interest were: Delta (δ: 1-4 Hz), Theta (θ: 4-8 Hz), Alpha (α: 8-13 Hz), Beta (β: 13-30 Hz) and Gamma (γ: 30-45 Hz). Higher frequencies were not estimated as they are generally difficult to measure in an artifact-free manner with scalp EEG. Multitaper analyses (MITRA AND BOKIL, 2007) revealed similar phenomena to the Welch method. However, as they do not easily provide a single trial estimates, we opted to only report Welch results.

Estimation of the PSDs can be influenced by several phenomena (*e.g.* electrode impedances, eye movements, etc.) creating inter-individual variance in the absolute EEG power. To bypass this problem, following the method proposed in (VOGT ET AL., 1998), normalized powers were also estimated by dividing the power in each band by the total energy in the trial (thus setting the total power in the five frequency bands to 100%). These estimates are referred to δ_n, θ_n, α_n, β_n, and γ_n respectively.

Spectral summaries

- *Power spectrum centroids (MSF, SEF)*

Spectral summaries were estimated using the following measures: median power frequency (MSF), spectral edge 90 (SEF90) and spectral edge 95 (SEF95) (reviewed in (RAMPIL, 1998)). These measures are defined as the particular frequencies that divide the power spectrum into two parts of equal area (MSF), a lower part equal to 90% of the total area and a higher part equal to 10% (SEF90), or a lower part equal to 95% of the total area and a higher part equal to 5% (SEF95).In all cases, these measures were estimated using the power spectral density for each electrode in each trial.

- *Spectral entropy (SE)*

The entropy of a time series is a measure of signal predictability and is thus a direct estimation of the information it contains (MACKAY, 2003). Entropy can be measured in the time domain but also in the spectral domain. Spectral entropy basically quantifies the amount of organization of the spectral distribution (INOUYE ET AL., 1991). We implemented the spectral entropy (SE) measure using the algorithm described for anesthesia monitors (Viertiö-Oja et al., 2004). The SE index for each electrode in each trial was estimated with the following procedure: *i)* the power spectral density of each trial was normalized (PSD_n) by dividing it by the total energy in that trial; *ii)* SE was calculated, using the Shannon Entropy formula for all frequency bins (f):

$$SE = -\sum_f PSD_n(f)\ \log(PSD_n(f))$$

Signal complexity

- *Permutation entropy*

Permutation entropy (PE), introduced by Bandt & Pompe (BANDT AND POMPE, 2002), is an effective method to compare time series and distinguish different types of behavior (*e.g.* periodic,

chaotic or random). One key feature of the method is its robustness to low signal to noise ratios compared to other similar methods (BANDT AND POMPE, 2002). The basic principle of this method is the transformation of the time signal into a sequence of symbols before estimating entropy. The transformation is made by considering consecutive sub-vectors of the signal of size *n*. These sub-vectors can be made of either consecutive elements or of elements separated by τ samples (where τ is an integer). The τ parameter thus defines a broad frequency-specific window of sensitivity for this measure (see SUPPLEMENTARY FIGURE 7.6 for the spectral sensitivity of the method given the present parameters). Since using τ values larger than 1 induce aliasing effects, the signal was low-pass filtered before PE calculation, in order to maintain the frequency-band specificity of each measure. Cutoff frequencies were set according to the following formula: $f_{LP} = 80\ Hz\ /\ \tau$, appropriate given our sampling rate. Each sub-vector of length   is associated with a unique symbol, based solely on the ordering of its *n* signal amplitudes. Given the parameter *n* there are *n!* possible vectors, corresponding to distinct categories of signal variations. After the symbolic transform, the probability of each symbol is estimated, and PE is computed by applying Shannon's classical formula to the probability distribution of the symbols. In our case we computed PE for every electrode and in every trial with parameters *n* = 3 and τ = [8, 4, 2, and 1], corresponding respectively to PE_θ, PE_α, PE_β, PE_γ respectively. Repeating the analysis with *n* = 4 yielded very similar results. However PE becomes harder to robustly estimate for larger *n* values, because the size of the estimated probability matrix increases rapidly.

- *Kolmogorov Chaitin complexity*

Algorithmic information theory has been introduced by Andreï Kolmogorov and Gregory Chaitin as an area of interaction between computer science and information theory. The concept of algorithmic complexity or Kolmogorov-Chaitin complexity (K) is defined as the shortest description of a string (or in our case a time series). That is to say, K is the size of the smallest algorithm (or computer program) that can produce that particular time series. However, it can be demonstrated by *reductio ad absurdum* that there is no possible algorithm that can measure K (CHAITIN, 1995). To sidestep this issue, we can estimate an upper-bound value of K(x). This can be concretely accomplished by applying a lossless compression of the time series and quantifying the compression size. Capitalizing on the vast signal compression literature, we heuristically used a classical open-source compressors gzip (SALOMON, 2007) to estimate K(x). Is important to normalize the method of representation of the signal before compression in order to avoid non-relevant differences in complexity. To compute K(x)

(1) the time series were transformed into sequences of symbols. Each symbol represents, with identical complexity, the amplitude of the corresponding channel for each time point. The number of symbols was set to 32 and each one corresponds to dividing the amplitude range of that given channel into 32 equivalent bins. Similar results were obtained with binning ranging from 8 to 128 bins.

(2) The time series were compressed using the compressLib library for Matlab, this library implements the Gzip algorithm to compress Matlab variables.

(3) K(x) was calculated as the size of the compressed variable with time series divided by the size of the original variable. Our premise is that, the bigger the size of the compressed string, the more complex the structure of the time series, thus potentially indexing the complexity of the local neural processing captured by that sensor

7.7.2.3.   Information sharing (across electrodes)

All information sharing measures were computed on a spatial Laplacian transformation of the EEG - a computation also known as Current Source Density (CSD) estimate (KAYSER AND TENKE, 2006B).

Phase Lag Index (PLI)

The Phase Lag Index (PLI), initially proposed by Stam, Nolte & Daffertshofer (STAM ET AL., 2007) measures the asymmetry in the distribution of phase differences between two signals. We computed PLI using a series of traditional steps: (1) For each frequency-bin of interest (f, in δ [1-4 Hz], θ [4-8 Hz], α [8-13 Hz], β [13-30 Hz] and γ [30-45 Hz]), each pair of electrodes, and at each trial, the signal X and Y were band-passed filtered at f. (2) Then we applied the Hilbert-transformation to estimate the instantaneous phase $\varphi(\tau)$ and amplitude $\psi(\tau)$ of X and Y at each time point τ. (3) The phase difference (φ_Δ) between the two signals X and Y was then calculated as:

$$\varphi_\Delta(\tau) = \varphi_x(\tau) - \varphi_y(\tau)$$

Finally, the sign of the angle of the difference between $\varphi_x(\tau)$ and $\varphi_y(\tau)$ was calculated, and averaged across time.

$$PLI = \left| \frac{1}{N} \sum_\tau sign\left(\varphi_\Delta(\tau)\right) \right|$$

The mean PLI was calculated for each trial, and then averaged across trials. Note that although PLI is related to Phase Locking Value (PLV (LACHAUX ET AL., 1999)), PLV can more easily conclude that two EEG electrodes are synchronized, because it is sensitive to common sources. By contrast, the PLI is insensitive to perfect, zero-phase synchrony and therefore focuses on connectivity between two electrodes which does not originate from a single common source. Finally, because the PLI is signed across pairs of electrodes, when we needed a summary value of PLI across electrode pairs, we averaged the absolute value of PLI.

weighted Symbolic Mutual Information

In order to quantify the coupling of information flow between electrodes we computed the weighted symbolic mutual information (wSMI, (KING ET AL., 2013B)). This method is based on the PE analysis and is calculated between each pair of electrodes, and for each trial, after the transformation of the time series into sequence of symbols (see methods for permutation entropy). Identically to PE, the symbolic transformation depends on the applied tau parameter (in our case: $\tau = 8$, 4, 2, 1 time sample(s) corresponding to $wSMI_\theta$, $wSMI_\alpha$, $wSMI_\beta$, $wSMI_\gamma$). Then, wSMI was estimated for each pair of transformed EEG signals by estimating the joint probability of each pair of symbols. The joint probability matrix was multiplied by binary weights to reduce spurious correlations between signals. The weights were set to zero for pairs of identical symbols, which could be elicited by a unique common source, and for opposed symbols, which could reflect the two sides of a single electric dipole. wSMI is calculated using the following formula:

where *n* is the size of the vector used for the symbolic transformation, *x* and *y* are all symbols present in signals *X* and *Y* respectively, w*(x,y)* is the weight matrix and *p(x,y)* is the joint probability of co-occurrence of symbol *x* in signal *X* and symbol *y* in signal *Y*. Finally *p(x)* and *p(y)* are the probabilities of those symbols in each signal.

7.7.2.4.   Multivariate Pattern Analyses computation

Multivariate Pattern Analyses (MVPAs) have proven to be an efficient neuroimaging tool to combine multiple sources of evidence within a single test (HAYNES, 2011). In our case we implemented the MVPA to automatically classify the state of consciousness of each patient.

A support vector classification (SVC) method was used to distinguish VS from MCS patients. As described in the multivariate pattern analysis section, the SVC aims at finding the optimal linear combination of features (w) that separates the training samples with distinct classes in the hyperspace of features. As there are more features than samples ($f >> n$), there is an infinity of possible *w*. A penalization parameter is thus used to find a solution which is likely to generalize to another dataset, and hence avoid over-fitting. Here, the penalization parameter C, was chosen by nested cross-validation among the values = [.001 .01 .1 .2 .5 1 2 10] using a grid-search method (PEDREGOSA ET AL., 2011) nested in the cross-validation (see below).

The SVC can provide a continuous probability by fitting the distribution of the samples with regard to *w* (PLATT, 1999). To do so, a sigmoid function is fitted from the distributions of the signed distances separating the train samples and w. This sigmoid fit is then used to monotonically transform the signed distance separating the test samples and w into a meaningful probability (PLATT, 1999).

The data provided to the classifier corresponds to the 92 EEG measures, topographically summarized as the mean and the standard deviation across non-facial electrodes. Similarly to topographical analyses, connectivity measures were first averaged as the median value each electrode shared with all other non-facial electrodes, and subsequently summarized as the mean and standard deviation across these non-facial averages. The data provided to the classifier thus corresponded to a matrix *X* of *n* samples (EEG recordings) by *f* features (*f* = 92 EEG measures * 2 topographical summaries) and a vector *y* of *n* samples corresponding to subjects' states of consciousness (1: VS, 2: MCS).

The Support Vector Classifier (SVC) was repeatedly cross-validated with stratified k-folding (k = 8). Cross validation is a method aiming at testing the performance of a predictive model. It consists in repeatedly fitting this model on a subset of the data (training set) and subsequently testing it on the remaining data (test set). Stratified k-folding consists in arranging the partitioning of the data so that training and test sets keep constant proportion of each category samples. Stratified folding thus aims to minimize fold-specific effects.

Within each fold, we applied two successive preprocessing steps fitted on the train samples and subsequently applied to the test samples. 1) Normalization of each feature (remove mean, divide by standard deviation). 2) Feature selection (best single feature or best 20%) based on F-tests.

The classifier is fitted on the train set and subsequently assigns, to each test sample, a continuous probability of belonging to each class (VS, MCS). To minimize folding effects, the predicted probabilities of each sample were averaged across 250 repetitions of the SVC, each using pseudo-randomly partitioned stratified folding.

All MVPAs analyses were performed with the Scikit-learn package (PEDREGOSA ET AL., 2011).

7.7.3. SUPPLEMENTARY RESULTS

7.7.3.1. Automatic classification and recovery: comparison of EEG versus the CRS-R scale

To assess whether the recovery of the patients from the VS state could be predicted from the Coma Recovery Scale Revised (CRS-R) scores at the moment of clinical evaluation of consciousness, we compared the CRS-R between the clinical VS patients that did recover and the VS patients that did not recover. None of the CRS-R subscores or the full sum distinguished between the two groups (Mann-U Whitney, $p > 0.08$ for CRS1, $p > 0.24$ for CRS2, $p > 0.28$ for CRS3, $p > 0.60$ for CRS4, 1 for CRS5, $p > 0.35$ for CRS6 and $p > 0.55$ for sum of CRS-R subscores).

The analysis was then repeated but specifically compared clinically VS patients' CRS-R scores depending on whether they were classified by the SVC as "VS" or as "MCS". None of the CRS-R subscores could differentiate between these two groups. (Mann-U Whitney, $p > 0.07$ for CRS1, $p > 0.07$ for CRS2, $p > 0.26$ for CRS3, $p > 0.87$ for CRS4, 1 for CRS5[23], $p > 0.08$ for CRS6 and $p > 0.14$ for sum of CRS-R subscores). This shows that, none of the clinical descriptions assessed on the patients at the moment of the recording could predict the distinction done by the EEG-based classifier.

---

[23] Since all VS patients have a score of zero in Subscore 5 of the CRS-R scale a comparison cannot be computed.

7.7.4. SUPPLEMENTARY FIGURES
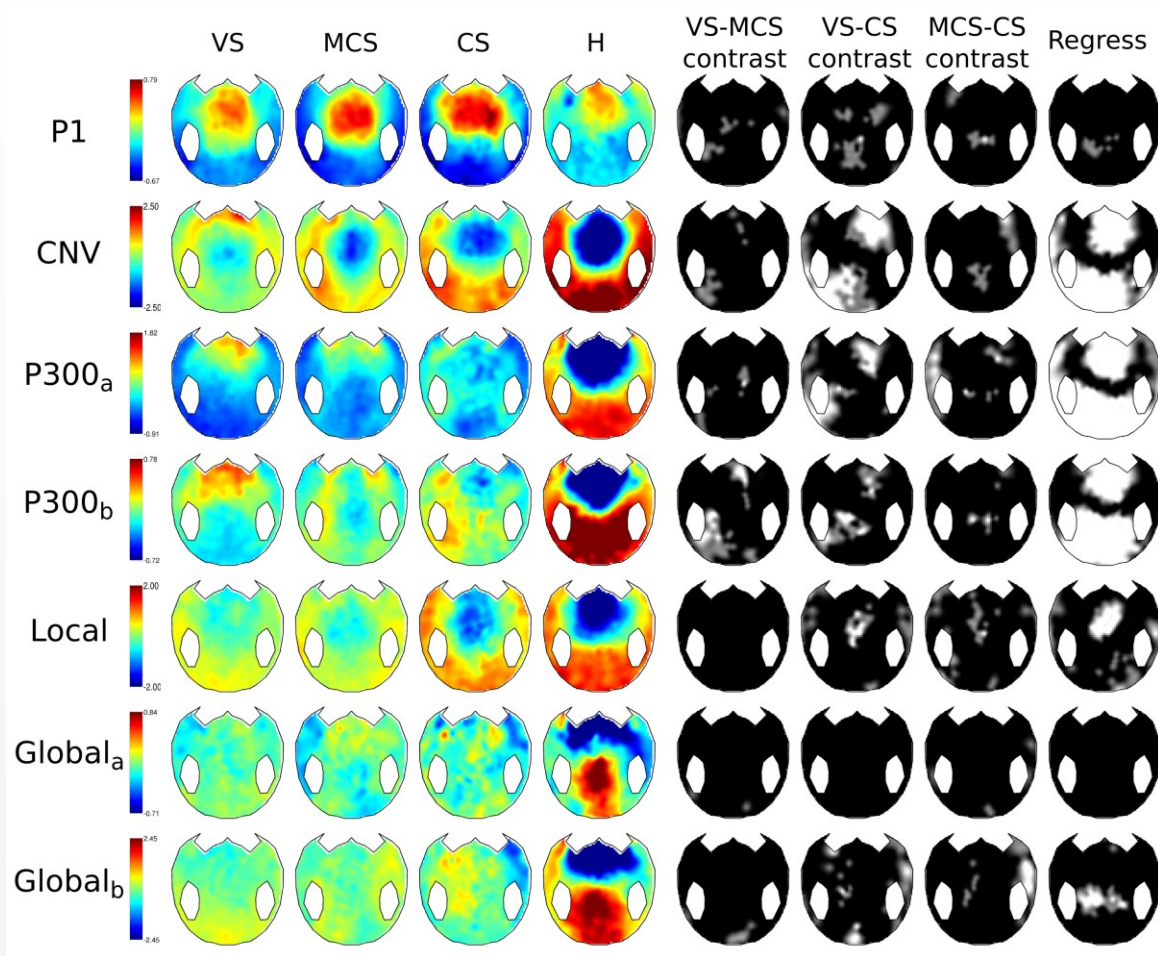
FIGURE 7.6 SCALP TOPOGRAPHY OF ALL COMPUTED EEG EVENT RELATED POTENTIALS (ERPS) MEASURES

The topographical 2D projection (top = front) of each measure is plotted for each state of consciousness (columns 1 = VS, 2 = MCS, 3 = CS, 4 = Healthy control = CS). The fifth to seventh column indicates whether significant differences were observed across these states (p<.05, light gray black and p<0.01, uncorrected). The eight column shows the statistics of a robust regression analysis of the measure across the four states of consciousness (VS<MCS<CS<Healthy controls. light gray indicates p<0.05, black p<0.01 uncorrected).
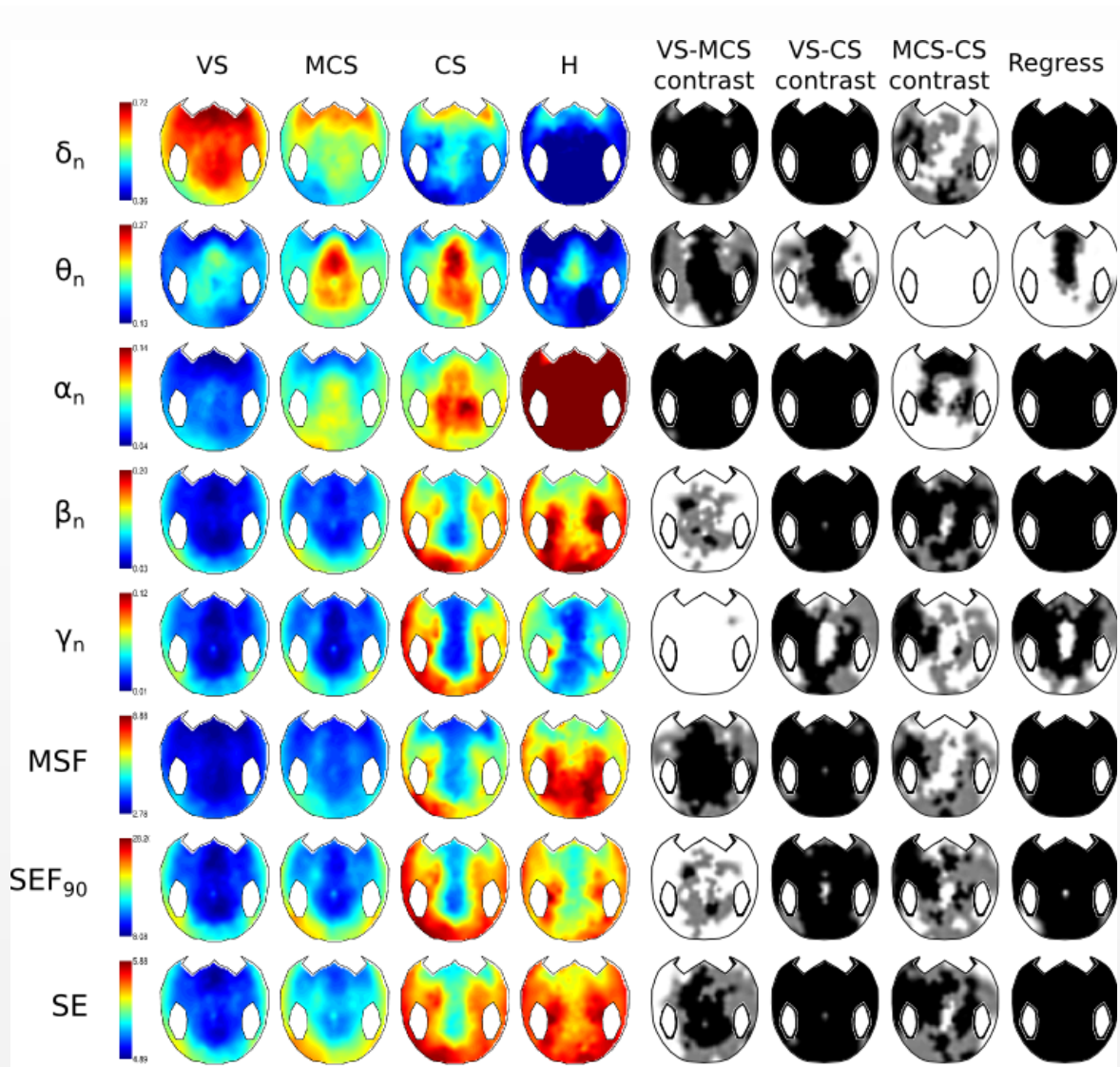
FIGURE 7.7 SCALP TOPOGRAPHY OF ALL COMPUTED EEG SPECTRAL MEASURES

The topographical 2D projection of each spectral measure is plotted for each state of consciousness following the same nomenclature as in FIGURE 7.6.
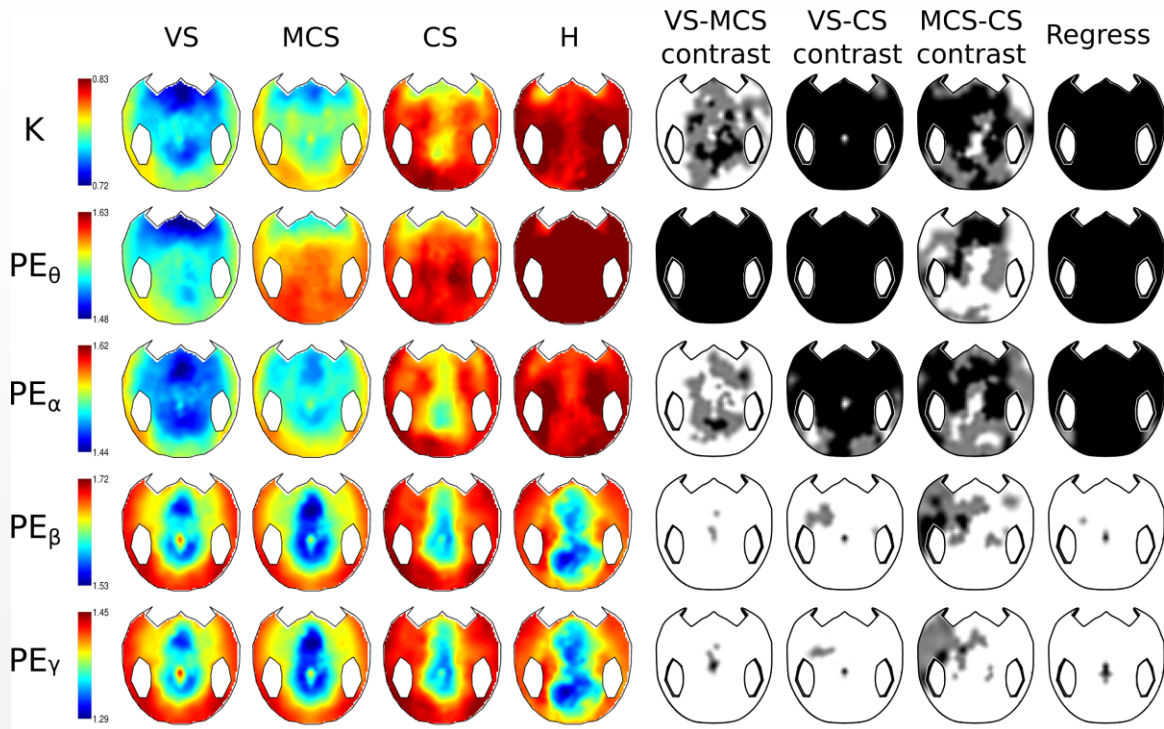
FIGURE 7.8 SCALP TOPOGRAPHY OF ALL COMPUTED EEG COMPLEXITY MEASURES

The topographical 2D projection of each complexity measure is plotted for each state of consciousness following the same nomenclature as in FIGURE 7.6.
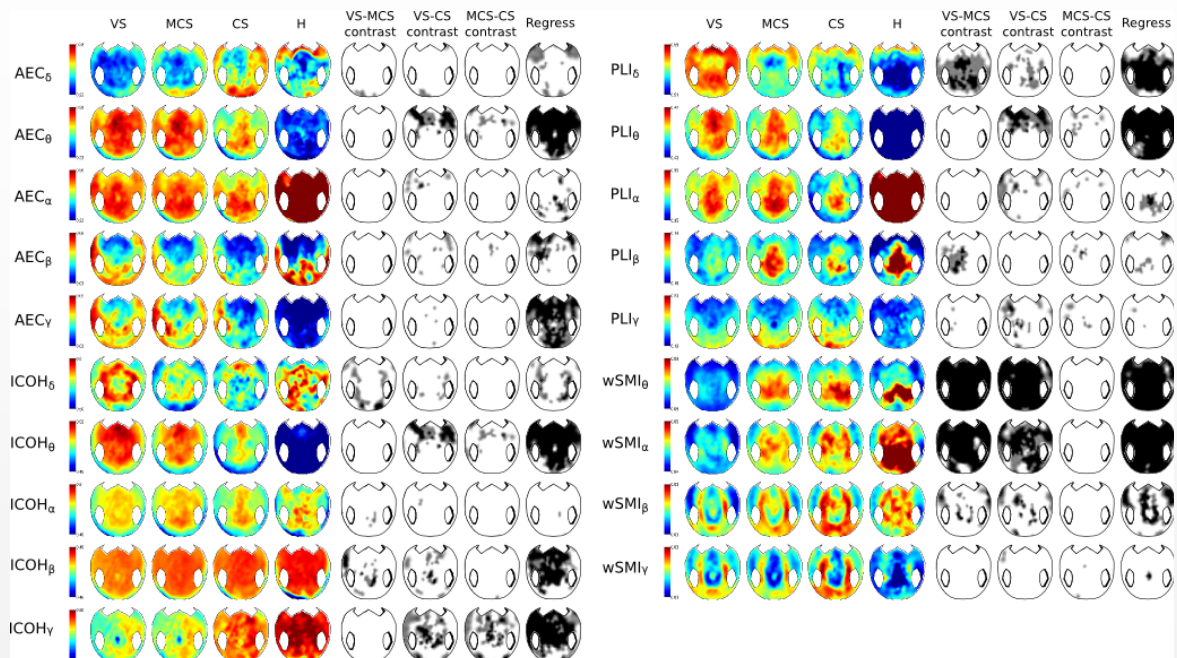
FIGURE 7.9 SCALP TOPOGRAPHY OF ALL COMPUTED EEG CONNECTIVITY MEASURES

The topographical 2D projection of each summary of the connectivity measures is plotted for each state of consciousness following the same nomenclature as in FIGURE 7.6.
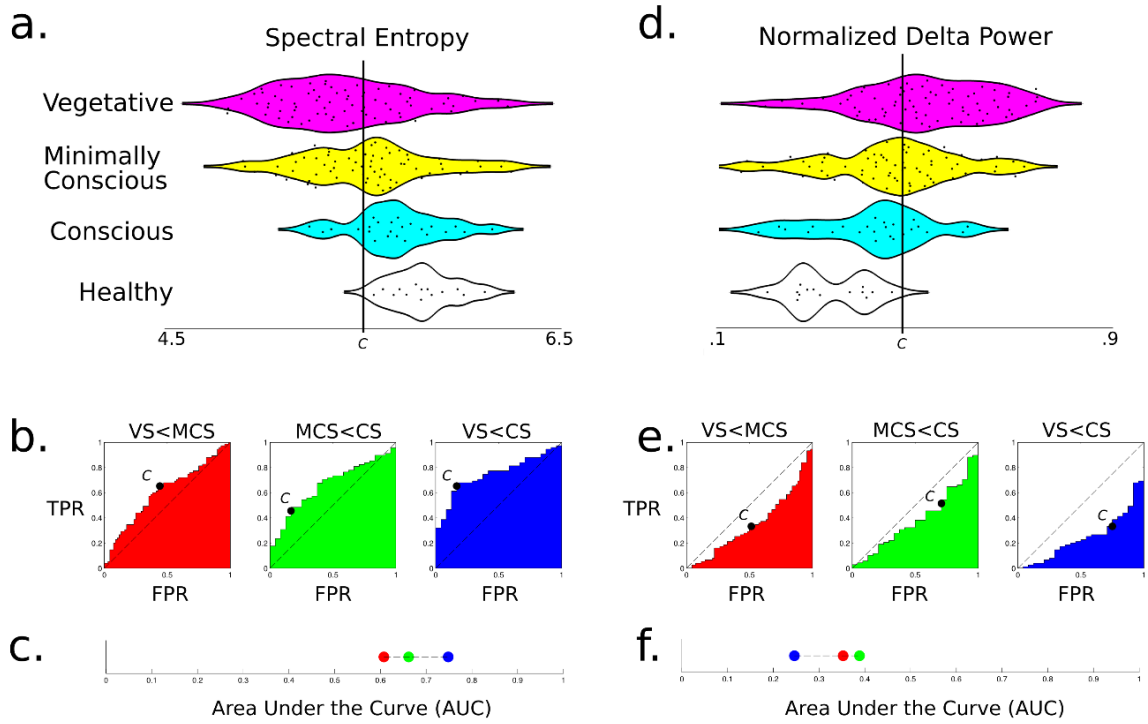
FIGURE 7.10 EXAMPLES OF RECEIVER OPERATING CHARACTERISTIC (ROC) CALCULATION.

ROC curves are calculated from a comparison of the distributions of a spectral entropy (SE) (left) and normalized delta power ($|\delta_n|$) (right) for all clinical groups. a) Histograms summarizing the spectral entropy (SE) of each state of consciousness. The black dots depict single EEG recordings. b) True positive rate (FPR) and True positive rates (TPR). c) Empirical areas under the curve (AUC) observed in b) are summarized, following FIGURE 7.2's nomenclature. A similar analysis is plotted for normalized delta power in d-f. Because in this case, the measure is anti-correlate with consciousness, AUCs are below 50%.
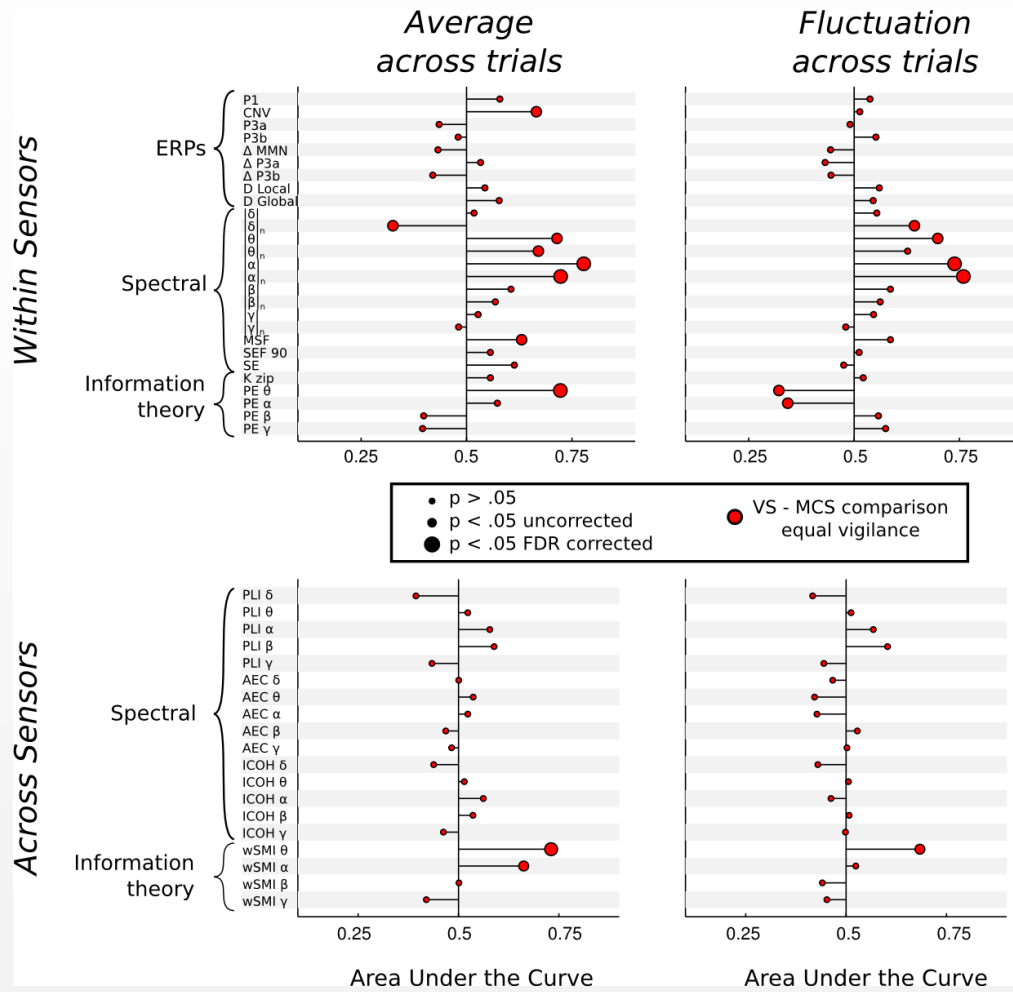
FIGURE 7.11 UNIVARIATE EQUATED VIGILANCE

This figure is identical to FIGURE 7.3, where each line provides a summary report of one measure, but focuses on the comparison between VS and MCS patients who presented similar arousal (VS: 52 patients, MCS: 32 patients).

7.7.5. SUPPLEMENTARY TABLES

Table 1

Statistics for all comparisons. Areas under the curve (AUC) and Mann-Whitney, FDR corrected, p values for all comparisons.

Table 2

Median value and standard error for each measure in each clinical group (VS, MCS and CS).

Table 3

Statistics for all comparisons. Areas under the curve (AUC) and Mann-Whitney, FDR corrected, p values for the VS-MCS patients comparison with equated arousal.

Table 4

Median value and standard error for each measure for VS and MCS patients with equated arousal.

Table 5

Detailed clinical description of the patients

Table S1

Measure	Average across trials									Fluctuations across trials								
	VS (n=75)-MCS (n=68)			MCS(n=68)-CS (n=24)			VS(n=75)-CS (n=24)			VS (n=75)-MCS (n=68)			MCS(n=68)-CS (n=24)			VS(n=75)-CS (n=24)		
	AUC	U	p_{FDR}	AUC	U	p_{FDR}	AUC	U	p_{FDR}	AUC	U	p_{FDR}	AUC	U	p_{FDR}	AUC	U	p_{FDR}
P1	55,3%	2818	4,2E-01	53,4%	871	7,5E-01	59,5%	1071	2,9E-01	52,1%	2659	7,7E-01	25,6%	417	3,4E-03	29,3%	528	1,5E-02
CNV	57,5%	2934	2,4E-01	55,2%	901	5,9E-01	66,1%	1189	5,9E-02	46,7%	2383	6,4E-01	24,0%	392	1,6E-03	21,6%	388	4,5E-04
P3a	44,6%	2275	4,1E-01	41,4%	675	3,5E-01	36,3%	653	1,1E-01	45,7%	2333	5,3E-01	25,2%	412	3,0E-03	22,8%	411	8,0E-04
P3b	47,3%	2413	7,1E-01	56,2%	918	5,2E-01	54,1%	973	6,8E-01	50,1%	2557	9,8E-01	31,0%	506	2,8E-02	32,7%	589	4,6E-02
Δ MMN	49,0%	2499	9,0E-01	66,4%	1084	5,7E-02	70,4%	1267	1,6E-02	42,1%	2148	2,1E-01	58,6%	957	3,5E-01	48,7%	877	9,1E-01
Δ P3a	55,8%	2845	3,7E-01	47,6%	777	8,3E-01	53,1%	955	7,8E-01	44,4%	2262	3,9E-01	60,1%	981	2,7E-01	56,2%	1012	5,2E-01
Δ P3b	45,9%	2340	5,4E-01	61,2%	999	2,1E-01	58,6%	1055	3,5E-01	46,3%	2363	5,9E-01	51,4%	839	9,0E-01	46,9%	845	7,7E-01
Decod Local	54,1%	2761	5,4E-01	65,9%	1076	6,3E-02	70,1%	1261	1,8E-02	56,4%	2875	3,3E-01	66,7%	1089	5,2E-02	72,4%	1304	7,6E-03
Decod Global	62,0%	3161	4,8E-02	70,8%	1156	1,5E-02	81,2%	1461	1,9E-04	61,2%	3122	6,3E-02	77,8%	1269	7,5E-04	85,2%	1534	6,4E-05
δ	45,6%	2327	5,2E-01	28,7%	468	1,3E-02	26,6%	479	5,0E-03	46,9%	2391	6,5E-01	32,5%	531	4,6E-02	30,4%	548	2,2E-02
δN	31,4%	1599	1,3E-03	34,9%	569	8,0E-02	19,3%	347	1,8E-04	61,8%	3150	5,3E-02	49,7%	811	9,8E-01	59,9%	1078	2,7E-01
θ	65,1%	3321	1,2E-02	33,9%	554	6,2E-02	49,2%	885	9,4E-01	63,5%	3237	2,6E-02	36,3%	592	1,2E-01	50,3%	905	9,8E-01
θN	63,7%	3248	2,3E-02	54,1%	883	6,8E-01	68,7%	1236	2,8E-02	60,3%	3077	9,0E-02	47,7%	778	8,3E-01	58,7%	1056	3,5E-01
α	73,5%	3748	8,9E-05	40,2%	656	2,8E-01	62,6%	1127	1,5E-01	71,7%	3655	2,0E-04	41,4%	676	3,5E-01	63,4%	1142	1,2E-01
αN	72,0%	3673	2,0E-04	65,6%	1071	7,0E-02	84,8%	1527	4,3E-05	70,9%	3616	3,0E-04	57,7%	941	4,1E-01	79,7%	1434	3,0E-04
β	63,9%	3258	2,1E-02	52,5%	856	8,2E-01	66,1%	1190	5,8E-02	62,0%	3163	4,8E-02	47,4%	773	8,1E-01	60,4%	1087	2,5E-01
βN	61,3%	3124	6,3E-02	72,1%	1176	1,0E-02	77,2%	1390	8,1E-04	60,0%	3061	1,0E-01	68,7%	1121	3,1E-02	75,1%	1351	2,2E-03
γ	58,1%	2961	2,0E-01	52,1%	851	8,4E-01	61,4%	1105	2,0E-01	59,5%	3036	1,2E-01	47,1%	769	7,9E-01	58,5%	1053	3,5E-01
γN	55,3%	2819	4,2E-01	66,7%	1089	5,2E-02	70,2%	1263	1,7E-02	55,8%	2846	3,7E-01	62,8%	1025	1,5E-01	67,3%	1212	4,5E-02
MSF	66,5%	3392	5,4E-03	66,7%	1088	5,2E-02	78,4%	1411	4,5E-04	62,2%	3174	4,6E-02	63,2%	1031	1,4E-01	71,3%	1284	1,2E-02
SEF90	60,5%	3084	8,6E-02	71,1%	1161	1,4E-02	75,9%	1366	1,5E-03	55,4%	2826	4,1E-01	62,8%	1025	1,5E-01	67,8%	1221	3,8E-02
SE	64,7%	3299	1,5E-02	71,2%	1162	1,4E-02	79,2%	1426	3,1E-04	48,5%	2473	8,4E-01	51,5%	841	8,9E-01	48,8%	879	9,1E-01

K zip	62,3%	3175	4,6E-02	73,0%	1192	6,6E-03	81,9%	1475	1,3E-04	45,9%	2340	5,4E-01	36,8%	600	1,3E-01	32,8%	591	4,5E-02
PE θ	72,0%	3672	1,8E-04	65,4%	1068	7,4E-02	82,8%	1490	8,2E-05	31,3%	1594	1,2E-03	37,1%	605	1,4E-01	20,6%	370	3,0E-04
PE α	60,9%	3104	7,4E-02	69,8%	1139	2,1E-02	74,6%	1343	2,8E-03	35,3%	1801	1,5E-02	35,4%	578	9,3E-02	23,6%	425	1,2E-03
PE β	46,8%	2386	6,4E-01	63,5%	1037	1,2E-01	60,0%	1080	2,7E-01	53,5%	2728	6,1E-01	34,9%	570	8,1E-02	37,9%	683	1,7E-01
PE γ	46,5%	2374	6,1E-01	62,1%	1014	1,7E-01	57,9%	1042	3,9E-01	55,4%	2826	4,1E-01	35,1%	573	8,5E-02	40,9%	736	3,2E-01
PLI δ	38,0%	1936	4,8E-02	48,2%	787	8,7E-01	37,3%	671	1,4E-01	38,1%	1943	5,0E-02	47,1%	769	7,9E-01	34,9%	629	7,7E-02
PLI θ	49,4%	2519	9,4E-01	42,2%	689	4,1E-01	39,0%	702	2,2E-01	49,3%	2514	9,3E-01	42,3%	690	4,1E-01	38,5%	693	1,9E-01
PLI α	50,5%	2578	9,4E-01	41,1%	670	3,4E-01	40,1%	721	2,7E-01	50,8%	2592	9,2E-01	40,4%	659	2,9E-01	40,4%	728	2,9E-01
PLI β	58,5%	2986	1,7E-01	41,1%	670	3,4E-01	50,5%	909	9,6E-01	59,7%	3044	1,2E-01	40,2%	656	2,8E-01	50,6%	910	9,6E-01
PLI γ	54,3%	2770	5,2E-01	57,0%	930	4,6E-01	61,7%	1111	1,8E-01	55,2%	2817	4,2E-01	55,8%	910	5,5E-01	62,2%	1120	1,6E-01
AEC δ	53,8%	2742	5,8E-01	54,5%	889	6,5E-01	58,2%	1048	3,7E-01	37,8%	1928	4,5E-02	41,3%	674	3,5E-01	30,4%	548	2,1E-02
AEC θ	48,1%	2455	8,1E-01	41,4%	675	3,5E-01	39,8%	717	2,6E-01	45,9%	2341	5,4E-01	57,1%	932	4,5E-01	51,9%	935	8,6E-01
AEC α	47,5%	2423	7,3E-01	47,7%	778	8,3E-01	44,4%	799	5,5E-01	38,5%	1962	5,7E-02	41,2%	672	3,4E-01	32,6%	586	4,4E-02
AEC β	44,9%	2290	4,4E-01	43,8%	715	5,2E-01	39,6%	712	2,5E-01	49,2%	2508	9,2E-01	40,1%	654	2,8E-01	39,9%	719	2,7E-01
AEC γ	48,2%	2459	8,1E-01	41,0%	669	3,3E-01	39,2%	705	2,2E-01	48,5%	2472	8,4E-01	31,7%	518	3,5E-02	30,7%	553	2,3E-02
ICOH δ	42,6%	2175	2,5E-01	49,3%	805	9,5E-01	42,0%	756	3,8E-01	37,0%	1885	3,2E-02	49,4%	807	9,6E-01	38,2%	688	1,8E-01
ICOH θ	45,7%	2331	5,2E-01	37,1%	605	1,4E-01	34,0%	612	5,9E-02	46,1%	2350	5,6E-01	43,7%	713	5,2E-01	37,9%	683	1,7E-01
ICOH α	53,0%	2704	6,7E-01	49,5%	808	9,6E-01	51,1%	920	9,2E-01	40,1%	2046	1,1E-01	44,7%	730	5,9E-01	34,9%	628	7,7E-02
ICOH β	59,1%	3014	1,5E-01	55,1%	900	5,9E-01	63,3%	1140	1,2E-01	45,0%	2297	4,5E-01	45,7%	746	6,6E-01	39,4%	709	2,4E-01
ICOH γ	51,9%	2648	8,0E-01	67,2%	1097	4,7E-02	68,2%	1228	3,3E-02	47,4%	2415	7,1E-01	36,1%	589	1,1E-01	33,1%	595	4,8E-02
wSMI θ	73,6%	3752	1,1E-04	55,3%	903	5,8E-01	77,7%	1398	6,7E-04	71,1%	3625	3,0E-04	51,8%	846	8,7E-01	71,5%	1287	1,1E-02
wSMI α	70,4%	3589	4,4E-04	51,7%	844	8,7E-01	71,6%	1288	1,1E-02	58,1%	2961	2,0E-01	43,8%	715	5,2E-01	54,5%	981	6,4E-01
wSMI β	57,3%	2922	2,6E-01	52,0%	848	8,5E-01	61,6%	1108	1,9E-01	52,2%	2660	7,7E-01	46,3%	756	7,2E-01	50,3%	905	9,7E-01
wSMI γ	47,8%	2436	7,7E-01	56,7%	925	4,9E-01	55,1%	991	5,9E-01	51,6%	2632	8,3E-01	43,7%	713	5,2E-01	45,9%	826	6,8E-01

Table S2

Measure	Average across trials						Fluctuation across trials					
	VS(n=75)		MCS(n=68)		CS(n=24)		VS(n=75)		MCS(n=68)		CS(n=24)	
	MEAN	S.E.	MEAN	S.E.	MEAN	S.E.	MEAN	S.E.	MEAN	S.E.	MEAN	S.E.
P1	0,419	0,09246	0,536	0,09739	0,69	0,1338	9,556	0,38417	10,881	1,01108	7,339	0,46702
CNV	0,299	0,31808	0,963	0,42501	1,99	0,54373	26,685	1,22161	28,027	2,09814	16,766	1,26915
P3a	0,579	0,17689	0,437	0,17289	-0,216	0,28424	14,797	0,62912	15,646	1,33271	10,117	0,71622
P3b	-0,157	0,09152	-0,128	0,11826	-0,056	0,11121	12,01	0,49845	14,009	2,06977	9,56	0,64193
Δ MMN	0,445	0,15208	0,196	0,24457	1,149	0,19252	-0,17	0,1384	0,16	0,63683	0,02	0,20015
Δ P3a	-0,071	0,10937	0,084	0,14172	-0,04	0,25167	-0,072	0,10582	-0,156	0,35066	0,28	0,3271
Δ P3b	0,024	0,1198	-0,272	0,16346	0,206	0,17543	0,005	0,08828	0,522	0,98308	0,146	0,34234
Decod Local	0,557	0,00661	0,569	0,00942	0,607	0,01432	0,077	0,004	0,085	0,00486	0,11	0,00862
Decod Global	0,499	0,00526	0,524	0,00824	0,569	0,01399	0,045	0,00294	0,058	0,00427	0,09	0,00766
δ	6,672	0,10071	6,679	0,08967	6,033	0,16475	6,906	0,0963	6,968	0,09916	6,345	0,17603
δN	0,623	0,01703	0,537	0,01615	0,463	0,02516	0,192	0,00302	0,203	0,00228	0,201	0,00492
θ	4,967	0,09377	5,387	0,08101	4,998	0,14857	4,903	0,08815	5,309	0,10224	4,913	0,14173
θN	0,18	0,00838	0,218	0,0097	0,227	0,01359	0,119	0,00366	0,13	0,00371	0,13	0,00364
α	3,795	0,07803	4,362	0,08569	4,142	0,13067	3,668	0,07994	4,217	0,11457	3,941	0,12309
αN	0,064	0,00367	0,088	0,00422	0,111	0,00928	0,053	0,00193	0,066	0,00226	0,073	0,00387
β	3,831	0,10668	4,316	0,12615	4,22	0,13411	3,689	0,12328	4,206	0,16256	3,944	0,15705
βN	0,077	0,00864	0,088	0,00795	0,12	0,01002	0,055	0,00358	0,063	0,00318	0,079	0,00414
γ	3,192	0,14617	3,693	0,20886	3,558	0,20893	3,258	0,17426	3,913	0,24627	3,568	0,24841
γN	0,049	0,00681	0,058	0,00888	0,067	0,00814	0,042	0,004	0,049	0,00508	0,057	0,0058
MSF	4,251	0,36033	5,1	0,39385	5,57	0,37563	2,675	0,22798	3,148	0,28194	3,359	0,28688
SEF90	13,74	0,96614	15,738	1,01946	19,318	1,17769	6,676	0,34582	7,096	0,32069	8,316	0,4127
SE	5,141	0,04568	5,296	0,04077	5,496	0,04993	0,403	0,0096	0,393	0,00838	0,396	0,01575
K zip	0,753	0,0049	0,771	0,0047	0,798	0,00469	0,069	0,00122	0,067	0,00149	0,063	0,00317
PE θ	1,529	0,00767	1,575	0,00651	1,606	0,00963	0,122	0,00354	0,103	0,00292	0,091	0,00416

PE α	1,495	0,00997	1,522	0,00803	1,559	0,0092	0,095	0,00239	0,086	0,00189	0,079	0,0027
PE β	1,619	0,0105	1,61	0,01116	1,654	0,01188	0,077	0,0031	0,08	0,00318	0,067	0,00367
PE γ	1,368	0,00909	1,359	0,00994	1,391	0,01085	0,069	0,00208	0,073	0,00224	0,063	0,00276
PLI δ	0,56	0,00506	0,543	0,00508	0,54	0,00962	0,326	0,001	0,323	0,00111	0,321	0,00196
PLI θ	0,411	0,00166	0,41	0,00199	0,405	0,00218	0,279	0,00085	0,279	0,00105	0,276	0,00118
PLI α	0,357	0,00118	0,356	0,00094	0,355	0,00189	0,251	0,00065	0,25	0,00053	0,25	0,00102
PLI β	0,189	0,00146	0,189	0,00082	0,187	0,0009	0,141	0,0011	0,141	0,00058	0,139	0,00066
PLI γ	0,199	0,00095	0,199	0,0008	0,199	0,00075	0,147	0,00078	0,148	0,00095	0,147	0,0005
AEC δ	0,243	0,0074	0,254	0,00873	0,261	0,01316	0,467	0,00123	0,462	0,00152	0,459	0,00257
AEC θ	0,367	0,00279	0,369	0,00442	0,36	0,00579	0,382	0,00067	0,382	0,0008	0,383	0,0014
AEC α	0,257	0,00301	0,258	0,0045	0,255	0,00508	0,371	0,00062	0,37	0,00123	0,369	0,00225
AEC β	0,058	0,00523	0,055	0,00638	0,048	0,00652	0,244	0,00186	0,245	0,00363	0,243	0,00613
AEC γ	0,056	0,00475	0,057	0,00651	0,052	0,00785	0,255	0,00169	0,257	0,00359	0,253	0,00593
ICOH δ	0,506	0,00127	0,5	0,00262	0,501	0,00306	0,175	0,00105	0,172	0,00174	0,172	0,00288
ICOH θ	0,507	0,00159	0,503	0,00267	0,501	0,00287	0,17	0,00044	0,17	0,00133	0,17	0,00253
ICOH α	0,5	0,00121	0,499	0,0024	0,5	0,00243	0,149	0,00052	0,149	0,00142	0,149	0,00274
ICOH β	0,478	0,00163	0,479	0,00247	0,481	0,00267	0,084	0,00089	0,085	0,00204	0,084	0,00379
ICOH γ	0,487	0,00146	0,486	0,00252	0,49	0,00299	0,088	0,00079	0,09	0,00208	0,089	0,00375
wSMI θ	0,088	0,00045	0,091	0,00061	0,093	0,00134	0,052	0,00056	0,057	0,001	0,059	0,00214
wSMI α	0,045	0,00026	0,046	0,00049	0,046	0,0008	0,037	0,00068	0,039	0,00121	0,039	0,00183
wSMI β	0,028	0,00035	0,029	0,00076	0,029	0,00097	0,028	0,00073	0,03	0,00177	0,029	0,00212
wSMI γ	0,027	0,00029	0,028	0,00082	0,028	0,00068	0,021	0,00049	0,023	0,00167	0,022	0,00164

Table S3

Measure	Average across trials	Fluctuations across trials
	VS (n=52)-MCS (n=32)	VS (n=52)-MCS (n=32)

	AUC	U	p_{FDR}	AUC	U	p_{FDR}
P1	57,9%	964	6,7E-01	53,8%	895	8,4E-01
CNV	66,6%	1108	7,9E-02	51,4%	855	9,4E-01
P3a	43,5%	724	6,7E-01	49,0%	816	9,5E-01
P3b	48,0%	799	9,1E-01	55,2%	918	7,1E-01
Δ MMN	43,3%	720	6,7E-01	44,4%	739	6,8E-01
Δ P3a	53,4%	888	8,4E-01	43,1%	718	6,8E-01
Δ P3b	42,0%	699	7,1E-01	44,5%	741	6,8E-01
Decod Local	54,4%	905	7,6E-01	56,0%	932	6,9E-01
Decod Global	57,8%	961	6,4E-01	54,6%	908	7,6E-01
δ	51,1%	851	9,4E-01	54,9%	913	7,4E-01
δN	32,6%	542	7,0E-02	64,3%	1070	1,7E-01
θ	69,8%	1161	3,3E-02	67,4%	1121	6,6E-02
θN	67,1%	1116	6,9E-02	62,7%	1044	2,6E-01
α	77,3%	1287	2,6E-03	72,1%	1200	1,1E-02
αN	72,4%	1204	1,4E-02	76,0%	1264	3,2E-03
β	61,1%	1017	4,1E-01	58,5%	974	6,6E-01
βN	56,9%	946	7,0E-01	56,2%	935	6,9E-01
γ	53,1%	884	8,5E-01	54,6%	908	7,5E-01
γN	48,1%	801	9,1E-01	48,0%	799	9,0E-01
MSF	63,1%	1050	2,4E-01	58,7%	976	6,6E-01
SEF90	55,6%	926	7,0E-01	51,2%	852	9,4E-01
SE	61,4%	1021	4,0E-01	47,5%	791	8,9E-01
K zip	55,6%	926	6,9E-01	52,2%	868	9,0E-01
PE θ	72,3%	1203	1,2E-02	32,2%	535	6,5E-02
PE α	57,3%	954	6,7E-01	34,3%	570	9,8E-02
PE β	39,8%	663	4,6E-01	55,8%	928	7,0E-01

PE γ	39,6%	659	4,7E-01	57,5%	957	6,6E-01
PLI δ	39,4%	656	4,6E-01	41,7%	694	6,7E-01
PLI θ	52,3%	871	9,0E-01	51,3%	853	9,4E-01
PLI α	57,8%	962	6,7E-01	56,8%	945	6,7E-01
PLI β	58,9%	980	6,4E-01	60,3%	1004	4,6E-01
PLI γ	43,4%	722	6,7E-01	44,5%	740	6,8E-01
AEC δ	50,1%	833	1,0E+00	46,7%	777	8,3E-01
AEC θ	53,7%	893	8,2E-01	42,2%	702	6,5E-01
AEC α	52,3%	871	8,9E-01	42,8%	712	6,7E-01
AEC β	46,9%	780	8,3E-01	52,8%	879	8,7E-01
AEC γ	48,3%	804	9,2E-01	50,2%	836	1,0E+00
ICOH δ	43,9%	730	6,8E-01	43,0%	715	6,9E-01
ICOH θ	51,5%	857	9,3E-01	50,6%	842	9,7E-01
ICOH α	56,2%	935	7,1E-01	46,3%	770	8,2E-01
ICOH β	53,6%	892	8,1E-01	50,8%	845	9,6E-01
ICOH γ	46,3%	770	8,3E-01	49,9%	830	1,0E+00
wSMI θ	73,1%	1216	1,3E-02	68,4%	1138	5,6E-02
wSMI α	66,3%	1103	8,4E-02	52,5%	873	9,1E-01
wSMI β	50,1%	834	1,0E+00	44,1%	734	6,9E-01
wSMI γ	42,0%	699	6,8E-01	45,3%	753	7,4E-01

Table S4

Measure	Average across trials				Fluctuation across trials			
	VS(n=52)		MCS(n=32)		VS(n=52)		MCS(n=32)	
	MEAN	**S.E.**	**MEAN**	**S.E.**	**MEAN**	**S.E.**	**MEAN**	**S.E.**
P1	0,402	0,09727	0,592	0,16385	9,595	0,45128	12,384	2,07281

CNV	0,181	0,4016	1,668	0,55732	27,064	1,5452	31,719	3,86449
P3a	0,574	0,2133	0,329	0,21267	14,853	0,77643	17,656	2,63366
P3b	-0,158	0,11411	-0,031	0,20091	12,094	0,6208	16,885	4,30376
Δ MMN	0,301	0,15607	-0,231	0,39463	-0,323	0,17958	0,631	1,33751
Δ P3a	-0,087	0,1315	0,125	0,15129	-0,081	0,12849	-0,046	0,7212
Δ P3b	0,165	0,13937	-0,324	0,26527	0,037	0,1143	1,308	2,09126
Decode Local	0,551	0,0068	0,557	0,00975	0,073	0,00439	0,081	0,00601
Decode Global	0,503	0,00592	0,515	0,00882	0,046	0,00377	0,05	0,00494
δ	6,637	0,1223	6,84	0,14008	6,861	0,1178	7,195	0,16912
δN	0,628	0,02061	0,557	0,02239	0,192	0,00367	0,205	0,00326
θ	4,908	0,11298	5,492	0,13959	4,86	0,10762	5,478	0,19165
θN	0,174	0,00982	0,22	0,01262	0,117	0,00467	0,133	0,00501
α	3,783	0,08672	4,468	0,14955	3,675	0,09297	4,368	0,22198
αN	0,063	0,00377	0,091	0,00612	0,053	0,00212	0,071	0,0033
β	3,825	0,12671	4,262	0,21185	3,675	0,1502	4,15	0,29643
βN	0,078	0,01115	0,074	0,00754	0,056	0,00438	0,059	0,00419
γ	3,168	0,17523	3,557	0,37959	3,211	0,2108	3,754	0,46289
γN	0,05	0,00863	0,048	0,01313	0,042	0,00481	0,042	0,00847
MSF	4,309	0,48341	4,64	0,5418	2,686	0,27291	2,866	0,4653
SEF90	13,699	1,15843	14,256	1,38304	6,645	0,42615	6,612	0,47465
SE	5,133	0,05516	5,235	0,05383	0,406	0,01203	0,392	0,01021
K zip	0,752	0,00584	0,759	0,00617	0,068	0,00148	0,07	0,00214
PE θ	1,526	0,00908	1,572	0,00925	0,124	0,00447	0,107	0,00436
PE α	1,496	0,0119	1,511	0,01073	0,096	0,00301	0,087	0,00244
PE β	1,619	0,01278	1,588	0,01689	0,078	0,00353	0,083	0,00431
PE γ	1,368	0,01099	1,341	0,01527	0,07	0,00235	0,074	0,00298
PLI δ	0,562	0,00623	0,549	0,00821	0,326	0,00121	0,324	0,00165

PLI θ	0,41	0,00196	0,412	0,00268	0,279	0,00101	0,279	0,00138
PLI α	0,357	0,00156	0,358	0,00134	0,251	0,00086	0,252	0,00074
PLI β	0,19	0,00198	0,19	0,001	0,141	0,00151	0,141	0,00072
PLI γ	0,199	0,00136	0,198	0,00157	0,148	0,00112	0,148	0,00197
AEC δ	0,246	0,00921	0,258	0,01668	0,467	0,00153	0,466	0,00233
AEC θ	0,367	0,00336	0,377	0,00803	0,382	0,00086	0,382	0,00143
AEC α	0,258	0,0041	0,267	0,00899	0,371	0,00079	0,373	0,00248
AEC β	0,061	0,00721	0,066	0,01305	0,244	0,00248	0,252	0,0075
AEC γ	0,059	0,00668	0,066	0,01338	0,255	0,00222	0,263	0,00743
ICOH δ	0,505	0,00158	0,497	0,00536	0,175	0,00136	0,176	0,0033
ICOH θ	0,506	0,00198	0,503	0,00506	0,169	0,00054	0,173	0,00266
ICOH α	0,499	0,00164	0,496	0,00493	0,149	0,0007	0,152	0,00292
ICOH β	0,477	0,00226	0,474	0,00505	0,084	0,0012	0,089	0,00422
ICOH γ	0,487	0,00201	0,481	0,00516	0,088	0,00106	0,093	0,00434
wSMI θ	0,088	0,00054	0,091	0,00094	0,052	0,00067	0,057	0,00186
wSMI α	0,045	0,00035	0,047	0,00099	0,037	0,00089	0,04	0,00244
wSMI β	0,028	0,00049	0,03	0,00161	0,029	0,00101	0,032	0,00372
wSMI γ	0,027	0,0004	0,029	0,00172	0,021	0,00067	0,025	0,00347

Table S5

| Name | age | sex | state | delay | CRS | | | | | | | Etiology |
					1	2	3	4	5	6	All	
1	67	M	VS	66	2	1	1	1	0	2	7	anoxia
2	49	M	MCS	31	2	3	2	2	0	1	10	anoxia
			CS	48	4	5	6	3	2	2	22	anoxia
3	62	M	CS	47	4	5	6	3	2	2	21	stroke
4	62	M	VS	19	1	1	2	1	0	2	7	stroke
			MCS	27	3	0	2	1	0	2	8	stroke
				41	3	0	2	1	0	2	8	stroke
				55	2	0	3	1	0	1	7	stroke
				70	3	0	4	1	0	2	10	stroke
5	33	F	MCS	10	1	3	2	2	0	2	10	stroke
				40	2	3	2	3	1	1	12	stroke
6	71	M	VS	17	1	0	1	1	0	1	4	anoxia
				22	1	0	1	1	0	1	4	anoxia
7	61	M	MCS	6	3	0	2	2	1	1	9	anoxia
			CS	20	4	5	6	3	2	3	23	anoxia
8	35	F	CS	137	4	5	6	3	2	2	22	anoxia
9	47	F	VS	54	1	0	1	0	0	1	3	anoxia
10	22	M	VS	16	1	0	1	1	0	2	5	anoxia
			MCS	29	3	1	2	1	0	2	9	anoxia
			CS	38	4	5	6	3	2	2	22	anoxia
11	42	F	MCS	46	3	0	1	1	0	1	6	stroke
12	73	F	VS	62	1	1	2	2	0	1	7	stroke
13	21	M	MCS	22	1	3	1	1	0	2	8	tbi
14	34	M	MCS	19	2	2	4	1	0	1	10	tbi
				26	2	3	4	1	0	2	12	tbi
15	73	M	VS	9	0	0	2	1	0	1	4	anoxia
16	48	M	VS	200	1	0	2	1	0	1	5	stroke
17	45	M	MCS	31	3	3	5	2	1	2	16	stroke
18	46	M	VS	155	1	0	1	1	0	2	5	anoxia
19	24	M	MCS	1258	1	3	2	2	0	2	10	tbi
20	62	M	VS	30	0	0	0	0	0	1	1	other
21	53	F	MCS	47	3	4	5	3	1	2	18	stroke
22	21	F	MCS	21	3	1	2	1	0	1	8	tbi
				24	2	1	3	1	0	1	8	tbi
23	29	M	VS	33	2	1	2	1	0	1	7	tbi
			MCS	40	1	2	2	1	0	1	7	tbi
24	63	M	VS	25	1	0	2	1	0	2	6	other
25	59	M	MCS	9	3	3	2	1	0	1	10	anoxia
26	56	M	MCS	134	1	3	0	1	0	1	6	other

27	44	M	VS	204	1	0	1	1	0	1	4	anoxia
28	62	M	MCS	23	0	3	2	1	0	1	7	stroke
29	64	M	MCS	48	3	5	1	1	1	1	12	stroke
			CS	97	4	5	1	1	2	2	15	stroke
30	42	M	MCS	28	1	3	2	1	0	2	9	tbi
31	21	M	CS	14	4	5	6	2	2	2	21	anoxia
32	19	M	VS	22	1	1	1	0	0	1	4	tbi
				25	1	1	1	1	0	2	6	tbi
33	37	F	VS	194	1	0	2	0	0	1	4	stroke
				195	1	0	2	0	0	1	4	stroke
			MCS	866	1	3	2	1	0	1	8	stroke
				867	1	3	1	1	0	2	8	stroke
34	74	F	VS	610	1	1	1	1	0	1	5	anoxia
35	31	M	VS	7	1	0	0	1	0	1	3	anoxia
36	57	M	CS	30	4	5	6	2	2	2	21	anoxia
37	29	F	VS	26	0	0	1	1	0	2	4	anoxia
			MCS	38	3	3	5	2	0	2	15	anoxia
38	80	M	VS	20	1	1	2	1	0	1	6	other
39	41	F	VS	7	0	0	2	1	0	1	4	anoxia
40	39	M	MCS	26	3	3	1	1	0	2	10	stroke
41	69	M	MCS	25	3	1	2	1	1	1	9	stroke
42	43	M	VS	26	2	1	1	1	0	1	6	other
43	29	F	VS	85	1	0	1	1	0	1	4	stroke
44	44	M	VS	42	1	0	1	1	0	2	5	stroke
45	40	M	VS	41	1	1	2	1	0	1	6	tbi
				51	1	1	2	1	0	1	6	tbi
				62	1	1	2	1	0	1	6	tbi
				72	1	1	2	1	0	1	6	tbi
46	62	M	VS	10	2	1	1	2	0	1	7	anoxia
47	59	M	VS	30	1	0	0	1	0	1	3	tbi
48	23	M	VS	43	2	0	0	0	0	2	4	other
				56	1	0	0	0	0	2	3	other
			MCS	87	2	3	0	1	0	2	8	other
				183	4	5	3	2	1	2	17	other
49	16	F	CS	697	4	5	6	3	2	3	23	anoxia
50	51	F	MCS	14	1	3	2	1	0	1	7	other
51	65	F	VS	20	1	0	1	1	0	1	4	anoxia
52	21	F	MCS	21	3	4	5	2	1	3	18	other
53	27	M	VS	194	1	0	1	2	0	1	5	anoxia
54	61	M	MCS	36	3	3	5	1	1	2	15	stroke
55	64	F	VS	23	1	1	2	1	0	2	7	other
56	16	M	MCS	30	3	3	4	1	0	1	12	tbi

57	67	M	VS	25	1	1	1	1	0	1	5	stroke
58	45	M	VS	19	2	1	1	1	0	2	7	anoxia
59	65	F	VS	31	1	1	0	1	0	1	4	anoxia
60	37	F	VS	62	1	1	1	1	0	1	5	stroke
61	24	M	VS	30	1	0	1	1	0	1	4	tbi
			VS	38	1	0	1	1	0	1	4	tbi
			VS	45	1	0	1	1	0	1	4	stroke
			MCS	62	3	3	1	1	0	1	9	tbi
62	48	M	CS	11	4	5	0	2	2	3	16	tbi
63	38	F	MCS	17	3	3	5	2	1	1	15	anoxia
64	76	F	VS	46	2	1	2	2	0	1	8	anoxia
			MCS	53	3	3	1	1	0	2	10	anoxia
65	48	F	VS	14	0	0	1	1	0	1	3	anoxia
66	44	M	CS	4383	4	5	3	1	2	3	18	tbi
67	20	M	MCS	25	3	3	2	1	0	2	11	tbi
68	31	M	VS	8	0	0	2	0	0	1	3	anoxia
69	60	M	MCS	24	3	1	1	2	0	2	9	stroke
70	41	M	VS	350	1	0	1	2	0	1	5	stroke
71	22	M	VS	27	2	1	2	1	0	1	7	tbi
			MCS	33	2	3	2	1	0	1	9	tbi
				39	3	4	2	1	0	2	12	tbi
			CS	49	4	5	3	1	2	2	17	tbi
72	30	M	CS	2190	3	3	1	2	2	2	13	other
73	28	M	MCS	151	3	2	2	2	0	2	11	anoxia
74	58	M	VS	41	1	0	1	1	0	1	4	sttroke
75	62	F	CS	517	4	5	5	2	2	3	21	stroke
76	51	M	VS	11	0	0	1	1	0	1	3	tbi
			VS	15	1	1	1	1	0	1	5	tbi
			MCS	22	3	0	1	1	0	1	6	tbi
			VS	29	2	1	1	1	0	1	6	tbi
77	78	F	MCS	27	1	1	3	1	0	1	7	other
78	45	M	CS	883	4	5	6	2	2	1	20	stroke
79	75	F	MCS	657	1	3	1	1	0	2	8	tbi
80	38	F	VS	30	1	1	2	1	0	2	7	stroke
81	43	F	VS	2554	1	0	1	1	0	2	5	tbi
82	41	M	MCS	2611	4	5	1	3	1	3	17	tbi
83	55	M	MCS	7	2	3	1	1	0	1	8	stroke
			MCS	23	2	3	1	1	0	1	8	stroke
84	47	M	VS	11	0	0	1	1	0	1	3	anoxia
85	44	M	CS	83	4	5	2	2	2	1	16	stroke
86	69	M	MCS	9	3	3	4	2	0	1	13	anoxia
87	26	F	VS	469	0	0	1	1	0	1	3	other

88	52	M	CS	2537	4	5	6	3	2	3	23	stroke
89	67	M	MCS	11	2	3	2	0	0	1	8	stroke
90	63	M	MCS	35	3	0	1	1	0	1	6	stroke
				41	3	3	1	1	0	2	10	stroke
			CS	57	4	5	6	3	2	2	22	stroke
91	70	F	VS	17	1	1	2	1	0	1	6	stroke
92	62	F	VS	25	0	0	0	0	0	1	1	other
93	76	M	MCS	110	2	1	2	3	1	2	11	other
94	28	M	VS	1486	1	0	1	1	0	2	5	tbi
95	52	M	MCS	25	2	2	3	1	1	2	11	tbi
96	39	M	VS	37	1	1	1	1	0	2	6	stroke
				42	1	0	1	1	0	1	4	stroke
97	64	M	VS	57	0	0	1	1	0	1	3	stroke
98	52	F	MCS	34	4	5	5	2	1	2	19	other
99	18	M	VS	10	0	0	1	0	0	1	2	anoxia
				11	0	0	1	0	0	1	2	anoxia
100	36	M	MCS	24	1	1	0	1	1	2	6	stroke_brainstem
101	56	M	MCS	10	3	3	5	2	1	1	15	anoxia
102	59	F	VS	21	1	1	2	1	0	1	6	stroke_cortical
				28	0	1	2	1	0	1	5	stroke_cortical
			MCS	34	1	3	2	1	0	2	9	stroke_cortical
103	23	M	VS	20	1	0	0	0	0	2	3	other
104	80	M	VS	62	1	1	2	1	0	2	7	tbi
105	83	M	CS	11	4	5	0	2	2	3	16	other
				46	3	5	0	2	1	3	14	other
				53	4	5	0	2	2	3	16	other
				62	4	5	0	2	2	3	16	other
				117	4	5	0	2	2	3	16	other
106	45	M	MCS	20	0	0	4	1	0	1	6	tbi
107	45	M	VS	27	2	1	2	1	0	2	8	stroke
			MCS	36	3	3	4	2	1	2	15	stroke
				44	3	4	4	2	1	1	15	stroke
				50	3	4	4	2	1	1	15	stroke
			CS	58	4	5	6	2	2	3	22	stroke
				93	4	5	6	2	2	2	21	stroke
108	79	F	VS	30	1	0	1	1	0	1	4	other
				66	2	0	2	1	0	2	6	other
				29	1	1	1	1	0	2	6	other
109	59	F	MCS	60	2	0	3	3	1	0	9	other
110	28	M	MCS	17	1	3	0	1	0	1	6	tbi

				33	2	3	5	2	1	2	15	tbi
111	54	M	MCS	21	2	3	2	1	0	2	10	stroke
112	46	M	VS	89	1	0	1	1	0	2	5	stroke
113	61	M	VS	25	0	0	0	1	0	2	3	stroke

7.8. ACKNOWLEDGMENTS

CHAPTER 8. A MODEL OF SUBJECTIVE REPORT AND OBJECTIVE DISCRIMINATION AS CATEGORICAL DECISIONS IN A VAST REPRESENTATIONAL SPACE

8.1. INTRODUCTION OF THE ARTICLE

I conclude this series of neuroimaging studies by going back to theoretical considerations.

So far, the approach undertaken in the present thesis has been to compare the brain activity observed in different states of consciousness. As explained in the CHAPTER 1. , the obtained results therefore heavily depend on the adopted definition of consciousness.

Patients' *state* of consciousness is defined according to their abilities to interact with their environment, as formally delineated by the revised version of the Coma Recovery Scale (GIACINO ET AL., 2004; SCHNAKERS ET AL., 2008B). Similarly, the subjects' *content* of consciousness is experimentally assessed *via* subjective reports and confidence ratings. In other words, the state and the content of consciousness are defined on a (set of) behaviour(s).

An obvious question thus follows: on what bases, and with which justification, could *these* behaviours be considered adequate to index subjective content?

This issue is perhaps most obvious in the case of blindsight phenomena, in which subjects discriminate stimuli that they claim not seeing (WEISKRANTZ, 1986; STOERIG AND COWEY, 2009). In this case the two types of behaviours (discrimination response and visibility reports) do not appear essentially different to the experimenter – *i.e.* in both cases they are recorded through a simple button press.

In the course of this PhD, I discover that a minimalist framework, based on Bayesian inference, could explain the dissociation between different types of behavioural measures (discrimination, visibility reports, *etc.*). While this approach is simplistic and undoubtedly oversimplifies the ins and outs of consciousness, it appeared to account for several empirical findings that have grounded the scientific study of consciousness.

8.2. ABSTRACT

Subliminal perception studies have shown that one can objectively discriminate a stimulus without subjectively perceiving it. We show how a minimalist framework based on Signal Detection Theory and Bayesian inference can account for this dissociation, by describing subjective and objective tasks with similar decision-theoretic mechanisms. Each of these tasks relies on distinct response classes, and therefore distinct priors and decision boundaries. As a result, they may reach different conclusions. By formalizing, within the same framework, forced-choice discrimination responses, subjective visibility reports and confidence ratings, we show that this decision model suffices to account for several classical characteristics of conscious and unconscious perception. Furthermore, the model provides a set of original predictions on the non-linear profiles of discrimination performance obtained at various levels of visibility. We successfully test this prediction in a novel experiment: when varying continuously the degree of perceptual ambiguity between two visual symbols presented at perceptual threshold, identification performance varies quasi-linearly when the stimulus is unseen and in an "all-or-none" manner when it is seen. The present model highlights how conscious and non-conscious decisions may correspond to distinct categorizations of the same stimulus encoded by a high-dimensional neuronal population vector.

8.3. INTRODUCTION

Since Helmholtz (1867/1910)'s proposal of perception as unconscious inference, several computational models have been put forward to describe the mechanisms of this process (KERSTEN ET AL., 2004; KNILL AND RICHARDS, 2008). The hypothesis that perception corresponds to an inferential decision on sensory data has received support from neurophysiological recordings during perceptual tasks (POUGET ET AL., 2002; FRISTON, 2010). For instance, intracranial (GOLD AND SHADLEN, 2000) and scalp recordings (DE LANGE ET AL., 2011; WYART ET AL., 2012) have revealed a neural response seemingly reflecting the accumulation of sensory evidence following the presentation of a stimulus and which may predict how subjects perceive the stimulus (SHADLEN ET AL., 2008).

Nevertheless, superficially at least, conscious perception does not always seem to obey the logic of optimal perceptual inference. For instance, one can objectively discriminate a stimulus at above-chance level while subjectively claiming not to have seen it (DEHAENE ET AL., 2006B; DEHAENE AND CHANGEUX, 2011). This paradoxical dissociation, referred to as "subliminal perception", has nourished a vast body of philosophical and scientific proposals on the nature of conscious and unconscious perception. For instance, Tononi and Edelman (TONONI AND EDELMAN, 1998) have argued that conscious processes are quantitatively more complex, integrated and differentiated, than unconscious processes. Lau (LAU, 2008) and Rosenthal (ROSENTHAL, 1997) claim that conscious perception is qualitatively different from unconscious perception as it relies on higher-order metacognitive representations. Recent empirical studies challenge these accounts, however. First, subliminal stimuli can recruit complex semantic and integrative processes (GREENWALD ET AL., 1996; DEHAENE ET AL., 1998B; KOUIDER AND DEHAENE, 2007). Second, even second-order metacognitive inferences can apparently be performed above chance on unseen stimuli (KANAI ET AL., 2010; CHARLES ET AL., 2013).

Here, building upon earlier proposals (LAU, 2008; SHADLEN ET AL., 2008), we explore a simple theoretical idea: objective and subjective tasks rely on the same inference principles, but they differ in the nature and the size of the decision space. Our proposal stems from Signal Detection Theory (SDT) and outlines how a minimal extension of the classic unidimensional depiction of SDT to multiple dimensions provides geometrical intuitions on several empirical findings in conscious and unconscious perception.

Specifically, we identified six major categories of empirical findings that should be accounted for:

- EF1. Stimuli which are subjectively reported as "unseen" can nevertheless be objectively discriminated above chance in a two-alternative forced-choice task (WEISKRANTZ, 1986; MARSHALL AND HALLIGAN, 1993; DRIVER ET AL., 2001; DEHAENE ET AL., 2006B; KOUIDER AND DEHAENE, 2007; STOERIG AND COWEY, 2009).
- EF2. Discrimination performance is typically better on seen than on unseen trials, even when sensory stimuli are physically identical (LAU AND PASSINGHAM, 2006; DEL CUL ET AL., 2007; NEUROSCIENCE ET AL., 2012).
- EF3. Experimental protocols can be designed in which objective discrimination performance is identical, while subjective visibility differs (LAU AND PASSINGHAM, 2006; LAU, 2008; RAHNEV ET AL., 2011).
- EF4. Subjective reports vary non-linearly as a function of sensory strength. For instance, brief or faint visual stimuli are generally reported as "completely unseen", but once their duration or contrast reaches a threshold level, subjects tend to report items as "clearly seen" (SERGENT AND DEHAENE, 2004; SERGENT ET AL., 2005; DEL CUL ET AL., 2007; MELLONI ET AL., 2011; NEUROSCIENCE ET AL., 2012).

- EF5. Prior knowledge increases the subjective visibility of physically identical stimuli (SIMONS AND CHABRIS, 1999; CUL ET AL., 2006; MELLONI ET AL., 2011; PITTS ET AL., 2012).

- EF6. Attention generally increases subjective visibility, but has also been found to decrease it (DEHAENE ET AL., 2006B; RAHNEV ET AL., 2011).

8.3.1. GENERAL ASSUMPTIONS OF THE MODEL

Our first assumption is that incoming stimuli are encoded as continuous vectors in a vast representational space. In the visual domain, for instance, a hierarchy of specialized visual processors decompose any visual scene into a broad variety of features that range from low-level (line orientation, contrast, colour etc) to higher-level attributes (face/non-face, etc). Each of these features may be encoded by the firing rate of a group of neurons. Mathematically, each stimulus is therefore encoded by a set of coordinates, one for each feature dimension (FIGURE 8.1.1).

Second, stimulus strength is assumed to be directly reflected in the length (i.e. the norm) of the input vector. This assumption corresponds to the observation that the depth of sensory encoding varies with the quality of the incoming stimulus: a briefly flashed and masked stimulus only evokes modest activity in higher visual cortices (SERGENT ET AL., 2005; DEL CUL ET AL., 2007), and thus, its internal vector has a small projection, particularly on high-level dimensions. Conversely, an unmasked high-contrasted image results in a long internal vector (FIGURE 8.1).

Our third assumption is that each behavioural task imposes, in a top-down manner, a categorical structure of classes to this continuous vector space (e.g. "click left for faces, and right for non-faces"). Performing the task consists in identifying, on every trial, the class in which the input vector falls. Formally, this is a statistical inference: given a sensory input and prior knowledge, subjects attempt to compute the posterior probability of each of the classes in order to select the maximum a posteriori (MAP) choice, which is the response most likely to be correct. Each task imposes distinct, possibly overlapping response classes, and may therefore lead to different answers.

Our fourth assumption is that the content of conscious perception, which can be reported verbally, is the outcome of such an inferential decision process, but with the specific characteristic of having a very rich set of classes. While simple binary decisions may be performed non-consciously (e.g. press right or press left (DEHAENE ET AL., 1998B)), the inference system that underlies conscious perception must remain constantly open to myriads of possible contents, including unexpected ones (e.g. a fire alarm). We propose that what the subject experiences as a conscious percept is the class with the highest posterior probability, amongst all possible classes. As we shall see, "negative" classes, such as "I didn't see anything", must be considered too.

8.3.2. GEOMETRICAL APPROXIMATION IN TWO DIMENSIONS

The vast number of input features, classes and tasks makes the present proposal difficult to apprehend in its full generality. However, most of its properties can be approximately captured by projecting the large vector space onto a plane defined by the two main axes of interest (FIGURE 8.1.2-3). These axes are chosen to be two features or feature bundles that are most relevant to the task under consideration (e.g. the mean vectors of neuronal activity evoked by face and by non-face stimuli, if the task is face/non-face discrimination). Each circle represents the top of the distribution of a particular class of stimuli (i.e. likelihood function, given sensory and internal noise). Lines delimit the regions of space where response decisions change. Although one should not forget that this is just a considerable simplification of the underlying multidimensional space and stimuli distribution, this 2D representation brings the present model closer to the classic two-class problem of Signal Detection Theory. Indeed, although Signal Detection

Theory is not limited to a single dimension, it is often depicted as a binary problem with two Gaussian distributions plotted along a single axis. We argue that this classic diagram fails to capture the interaction between multiple features, classes and tasks, whereas a 2D depiction fulfils these requirements (see (GREEN AND SWETS, 1966; KLEIN, 1985; KO AND LAU, 2012) for similar proposals using 2D representations to dissociate tasks such as discrimination and detection).

8.3.3.   MATHEMATICAL FORMULATION

Bayesian theory describes the optimal way of selecting the most likely model of the environment, referred to as "hypothesis" (H, here the response class), in the presence of sensory evidence (E), here the input vector. Each class is characterized by a likelihood function P(E|H) and a prior probability P(H). P(E|H) indicates the probability that the evidence E was generated by the class H, and therefore captures how sensory samples from a given class are distributed within the vector space. The prior probability P(H) defines the probability of H to occur independently of any evidence. Bayes' theorem stipulates that the posterior probability of H is a function of its prior probability and of its likelihood: P(H|E) = P(E|H) * P(H) / P(E). Finally, decisions result from the selection of the class that has the maximum posterior probability (MAP). This MAP criterion results in the segregation of representational space into distinct regions separated by sharp decision boundaries (importantly, these boundaries play no functional role in the model, but are just a consequence of the MAP criterion).

In the following simulations, we use a series of computational simplifications. First, we neglect the cost function associated with each decision – sometimes referred to as "loss" or "utility" function. In the presence of costs, the optimal decision is the ones which minimizes the expected loss and may differ from the MAP. Mathematically, however, priors and costs play a similar role and were thus merged in the present paper for simplicity. Second, the present model assumes that priors are fixed in a given context, rather than continuously updated after each decision. Assuming modifiable priors would lead to important new predictions, but would also increase the number of ad-hoc parameters in the models (e.g. learning rate, estimated world volatility, creation or deletion of classes etc.). Third, we assume Gaussian distributions in order to facilitate the computations. Fourth, importantly, we assume that subjects have an accurate estimate of stimulus distributions – although following Lau (LAU, 2008; KO AND LAU, 2012), we will discuss the important consequences that ensue when subjects' priors and likelihood functions are inappropriately calibrated. Fifth, we assume that, on a given trial, the same input vector enters into different tasks, thus neglecting the possibility that the internal evidence evoked by a fixed stimulus may vary with the task, due for instance to decay (GREENWALD ET AL., 1996; DUPOUX ET AL., 2008), noise level (DEL CUL ET AL., 2007), attention (SERGENT ET AL., 2013) or other top-down changes. Finally, we treat stimulus evidence on a given trial as a single discrete point in the n-dimensional space. In the discussion, we briefly examine the additional properties that arise if these simplifying assumptions are relaxed.

8.3.4.   THE FUNDAMENTAL THREE-CLASS PROBLEM

Given these assumptions, binary decision experiments can be simplified to a stereotypical three-class problem: either nothing is presented (absent trial, denoted A), or one of two stimuli B or C is displayed (FIGURE 8.1.2). Absent trials are assumed to correspond to a null vector whose likelihood function peaks at the origin of vector space. B and C trials are represented by two base vectors which are chosen as the axes of the 2D representation.

In this typical setup, three different tasks can be performed:

i)   Identification consists in determining which hypothesis has the highest posterior probability (A, B, or C?) – thus crucially including the "absent" category.

      ii)   Forced-choice discrimination consists in restricting the responses to a subset of classes (e.g. B or C, excluding the A category).

      iii)   Visibility judgment consists in reporting whether the stimulus is seen or unseen. We assume that this instruction is interpreted as a decision whether the stimulus is most likely to be absent or present (i.e. A or not A?).

      Formally, these are all first-order tasks, because they all ask a simple question: which class (or set of classes) could have led to the observed input vector? For each of them, a second-order "confidence" judgment can also be performed by setting additional response categories, corresponding to whether the first-order decision has a high or a low probability of being correct. As shown graphically in FIGURE 8.1.2, there is a distinct confidence judgment associated with each primary task. At expense with Persaud et al. (PERSAUD ET AL., 2007) and Lau et al. (LAU, 2008), we note that second-order tasks need not coincide with visibility judgment. Also note that, for both first- and second-order decisions, the decision boundaries can be derived directly from the definition of the task, the priors, and the likelihood functions for each class, and therefore do not constitute additional assumptions of the model.
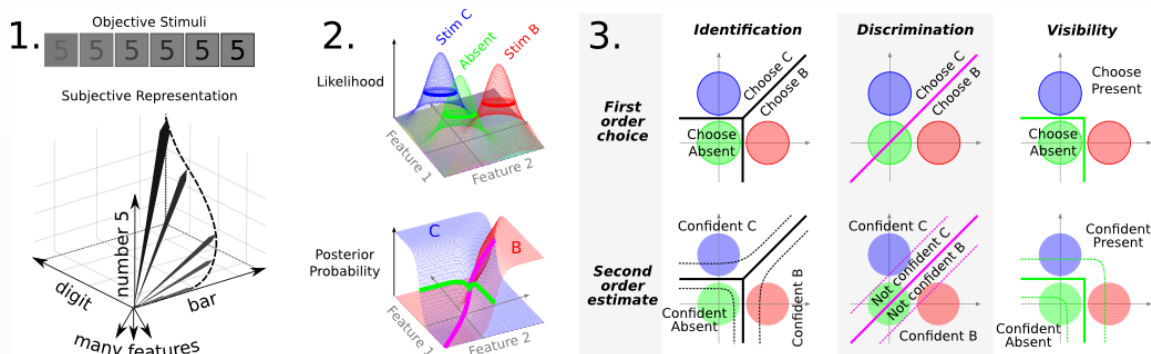
FIGURE 8.1 A MULTIDIMENSIONAL DECISION-THEORY FRAMEWORK FOR OBJECTIVE DISCRIMINATION AND SUBJECTIVE REPORTS.

1. Stimulus information is represented in a vast vector space, in which each dimension encodes the evidence about a particular feature. Each sensory stimulus thus corresponds to an input vector whose length and direction changes depending on the quality of the stimulus.

2. When considering binary decisions (e.g. perceiving stimulus B or stimulus C), the huge dimensionality of the representational space can be approximated by a 2D feature space. In this space, assuming that the true stimulus distributions are known, the likelihood (top), the prior and the posterior probability (bottom) of belonging to a given class (absent trial [A], stimulus B, or stimulus C) can be computed for each input vector (here the posterior probability of the Absent class has been removed for readability.)

*3. Posteriors can be used to perform different tasks. In each case, the regions of the problem space corresponding to a fixed decision are delineated by a boundary. **Identification** consists in finding the maximum a posteriori (MAP) across all classes (A, B, or C; black). **Discrimination** consists in determining the MAP amongst a restricted set of classes (B or C; purple). **Visibility judgment** consists in determining whether the absent class is the most likely amongst all classes (A or not-A; green). Each of these first-order decisions can be supplemented by a second-order confidence judgment task, which is modeled as the estimation of the likelihood of a correct response in the primary task. Samples far away from the decision border are associated with higher posterior probabilities and can thus be classified as more "confident" than samples close to the border. This geometrical representation makes it clear that each confidence judgment is always attached to a specific task, and is thus not necessarily identical to visibility judgment.*

8.4. EMPIRICAL CONSEQUENCES OF THE DECISION FRAMEWORK

We shall now see how this framework accounts for the six fundamental empirical properties listed above.

8.4.1.   ABOVE-CHANCE DISCRIMINATION OF STIMULI REPORTED AS "UNSEEN"

Empirical finding 1 is that perceptual decisions can be performed at above-chance level even when subjects report not seeing any stimulus (MARSHALL AND HALLIGAN, 1993; COWEY AND STOERIG, 1995; DRIVER ET AL., 2001; PERSAUD ET AL., 2007; TAMIETTO ET AL., 2007). For example, blindsight patients can perform simple discriminations on visual stimuli they report not seeing (STOERIG AND COWEY, 2009). This paradoxical ability also exists in healthy subjects whose discrimination performance has been repeatedly shown to be dissociated from subjective reports (see review in (KOUIDER AND DEHAENE, 2007; OVERGAARD AND SANDBERG, 2012)).
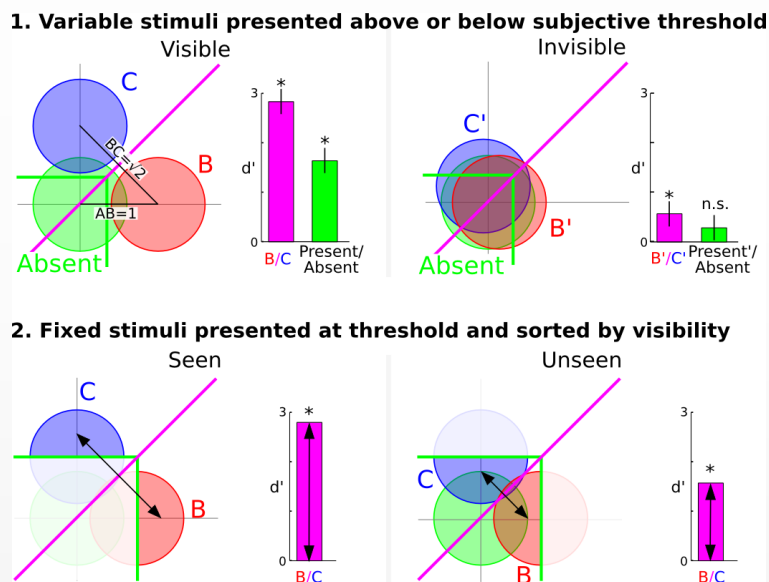
FIGURE 8.2 AN ACCOUNT OF UNCONSCIOUS AND CONSCIOUS DISCRIMINATION PERFORMANCE IN TWO TYPES OF EXPERIMENTAL DESIGNS.

Top. In the stimulus degradation design, stimuli are made invisible by reducing the evidence (e.g. lowered contrast, masking, inattention, etc). This manipulation makes the stimuli more similar to the Absent category (right). As the BC distance can be longer than the AB and AC distances, discrimination performance (purple) can remain significant while detection sensitivity (green) is not detectably better than chance.

Bottom. In the fixed-stimulus design, near-threshold stimuli are sorted as a function of whether they are reported as seen or unseen. Unseen stimuli can be discriminated at above-chance levels, but discrimination performance improves drastically on seen trials.

For simplicity, we only consider here the case in which two stimuli (B and C) become undetectable when they are visually degraded (B' and C'). We assume that the degraded stimuli are generated from the same class as B and C, yet with lower evidence (i.e. shorter vector length). As shown in FIGURE 8.2.1, it is quite possible for degraded stimuli B' and C' to fall in the region reported as "unseen" during visibility judgment (i.e. the most likely class is Absent), and yet to yield above-chance performance in a forced-

choice task when discrimination is restricted to classes B and C. This finding could be trivial if the visibility judgment was systematically biased towards the "unseen" response (and indeed such response bias has often been proposed as an interpretation of subliminal perception experiments (HOLENDER, 1986)). However, our simulations assume a Bayes-optimal inference process. Thus, we show that there are conditions under which the Absent or "unseen" response is the most probable one, and yet B versus C can still be discriminated.

The geometry of the 2D model reveals why discrimination performance (i.e. d' of B/C discrimination) can be higher than detection sensitivity (i.e. d' of A/not-A judgment): the distance separating the B and C vectors is larger than the distance separating them from the Absent class. In the two-dimensional case, discrimination performance is √2 higher than detection performance (FIGURE 8.2.1). Consequently, given adequate statistical power, discrimination may be significantly above chance when detection sensitivity is not.

The above account can also be extended to second-order judgments such as confidence rating and post-decision wagering on the first-order forced-choice B/C discrimination task. Because such second-order judgments rely on similar decisional principles as the first-order tasks (FIGURE 8.1.2), confidence in discrimination can be above-chance on "unseen" trials, and confidence in visibility can be lower than confidence in discrimination. This conclusion fits with two recent experiments in which subjects performed above-chance in their confidence judgments, even on trials reported as unseen (KANAI ET AL., 2010; CHARLES ET AL., 2013).

8.4.2. DISCRIMINATION PERFORMANCE GENERALLY IMPROVES WITH SUBJECTIVE VISIBILITY

Empirical finding 2 is that, although objective discrimination can be above chance with subjectively invisible stimuli, such unconscious performance is generally mediocre. In many studies, objective discrimination performance improves dramatically when the stimuli are subjectively reported as "seen" compared to "unseen", even when sensory stimulation is identical (SERGENT AND DEHAENE, 2004; DEL CUL ET AL., 2007; NEUROSCIENCE ET AL., 2012).

How does the model account for these findings? In experiments that compare high-contrast visible stimuli with degraded invisible stimuli, the improvement in discrimination performance with subjective visibility is trivial (FIGURE 8.2.1): stimulus degradation diminishes the evidence for B and C, and thus worsens both visibility judgment and B/C discrimination. The two tasks are thus necessarily correlated (LAU AND PASSINGHAM, 2006; LAU, 2008). Less trivially, however, the model predicts the same effect for fixed stimuli presented at perceptual threshold. Even when the stimuli are physically identical, internal variability can explain why ~50% of them are reported as "unseen" (those which are most similar to the absent class). As a consequence of this variability, sensory inputs reported as "unseen" are associated with a shorter input vector and are therefore closer to the B/C discrimination border than samples reported as "seen" (FIGURE 8.2.2). The simple hypothesis of a noisy input vector, together with non-orthogonal discrimination and detection tasks, suffices to explain why unseen trials generally exhibit a lower discrimination performance than seen trials.

8.4.3. DISCRIMINATION PERFORMANCE CAN BE EQUATED ON "SEEN" AND "UNSEEN" TRIALS

Empirical finding 3 is that it is possible to find experimental conditions in which discrimination performance is equated while visibility varies. For instance, blindsight patients do not always show different discrimination performance in their blind and healthy visual fields (WEISKRANTZ, 1986; COWEY, 2010; KO

AND LAU, 2012). In healthy subjects, using metacontrast masking and inattention, stimuli have been created that differ in visibility, but are equated for objective discrimination performance (LAU AND PASSINGHAM, 2006; RAHNEV ET AL., 2011, 2012A).
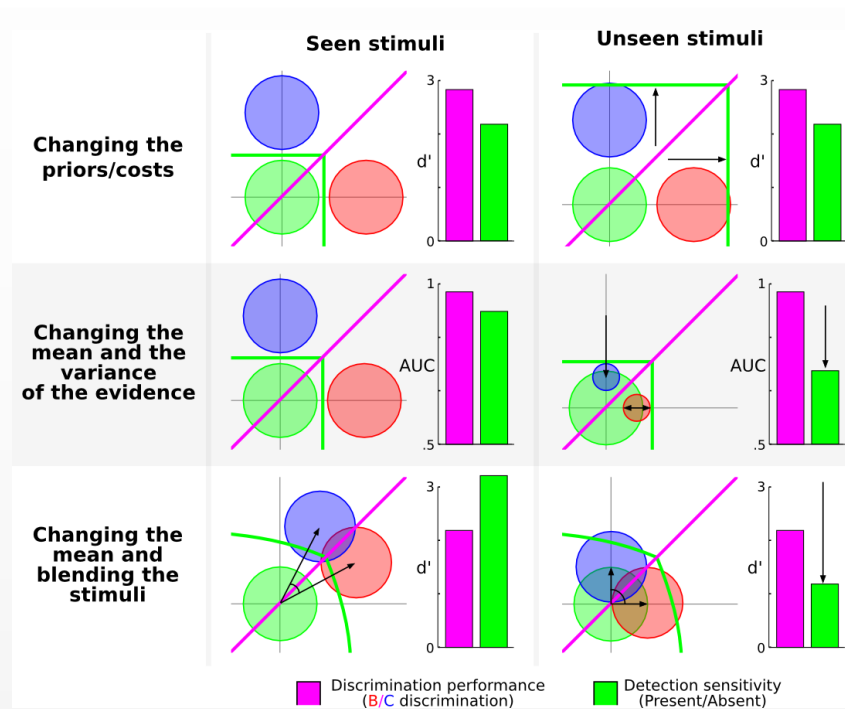
FIGURE 8.3 THREE WAYS IN WHICH STIMULUS VISIBILITY CAN BE MANIPULATED INDEPENDENTLY OF STIMULUS DISCRIMINABILITY.

Top. Changing the prior of the Absent class affects the placement of the criterion for subjective visibility reports and can thus lead to a systematic report of invisibility, without affecting objective discrimination performance (purple) or detection sensitivity (green).

Middle. Simultaneously changing the length and the variance of the input vectors jointly affects detection sensitivity and subjective visibility reports while preserving objective discrimination performance. (The Area Under the Curve (AUC) is an equivalent of d' for continuous measures.)

Bottom. Simultaneously changing the length (e.g. contrast) and the angle (e.g. ambiguity) of the input vectors can lead to a similar pattern of results.

In the model, three major circumstances (and mixtures of them) may lead to identical discrimination performance for seen and unseen stimuli.

- First, for fixed stimuli B and C, an increase in the prior probability (or cost) of the Absent class may lead to an increase in "unseen" responses while leaving B/C discrimination unaffected (FIGURE 8.3.1). This account formalizes the hypothesis that blindsight patients have an inappropriate "criterion" for visibility judgment (e.g. (LAU, 2008; COWEY, 2010; KO AND LAU, 2012)). Note however that the concept of criterion can be misleading because it incorrectly suggests a single scalar value. In the present framework, the "criterion" emerges as a set of decisional boundaries that delimit the categorical regions in the representational space, and that are specific to the selected task. A change in the task or in the priors may thus impose a different division of space, and hence a shift in decision boundaries.

- Second, consider experiments in which, within each class, the experimenter presents two visible targets B and C, and two invisible targets B' and C'. If both the length and the variance of the input vectors B' and C' are reduced compared to B and C, their visibility can drop without affecting discrimination performance (FIGURE 8.3.2). This case could correspond to a simultaneous manipulation of stimulus

strength (length of input vector) and of attention (variance of the input vector) as proposed by Rahnev and collaborators (RAHNEV ET AL., 2011).

- Third, if both the amplitude and the angle of the input vectors B' and C' are decreased compared to B and C, then B/C discrimination performance could be manipulated independently of visibility (FIGURE 8.3.3). This case could correspond to a simultaneous change in contrast and in stimulus ambiguity, for instance using morphing or blending to reduce the difference between B and C stimuli.

The present account provides no less than three mechanisms by which blindsight, meta-contrast and inattention could produce their effects. Each mechanism could be explicitly tested by experimentally manipulating the contrast, the variance and/or the blending of sensory stimuli as well as the prior probability associated with each class.

8.4.4. SUBJECTIVE REPORTS ARE OFTEN NON-LINEARLY RELATED TO SENSORY STRENGTH

Empirical finding 4 is that a non-linear curve often relates the strength of sensory stimulation and visibility ratings (SERGENT AND DEHAENE, 2004; DEL CUL ET AL., 2007; MELLONI ET AL., 2011). For example, when the stimulus onset asynchrony (SOA) separating a briefly flashed digit and its subsequent mask is varied linearly, a sharp transition in visibility occurs around an SOA of 50 ms: below this duration, subject tend to report the stimulus as completely unseen, whereas above it, stimuli are reported as clearly visible (SERGENT AND DEHAENE, 2004; DEL CUL ET AL., 2007). However, this all-or-none visibility pattern does not characterize all types of subjective reports (SERGENT AND DEHAENE, 2004; SANDBERG ET AL., 2011; OVERGAARD AND SANDBERG, 2012; WINDEY ET AL., 2013). For example, Sergent and Dehaene (SERGENT AND DEHAENE, 2004) showed that the attentional blink leads to a much sharper non-linear pattern than backward masking.

We consider two classes B and C, within which the stimuli can vary parametrically in strength from trial to trial (FIGURE 8.4.1). This parametric variation is assumed to have a linear effect on the amount of sensory evidence in favour of the corresponding stimulus (*i.e.* the length of the input vector). In such cases, the model predicts that visibility responses are non-linearly related to stimulus evidence, as the MAP criterion imposes a decision boundary that sharply delineates the regions of space respectively responded with the "seen" and "unseen" labels. Interestingly, although the fraction of "seen" responses is always a sigmoid, its slope may vary from a step-wise "all-or-none" pattern to a shallow and near-linear function. The parameter driving this change in sigmoid slope is the variance in representational space. With higher variance, visibility becomes more linearly related to sensory evidence (FIGURE 8.4.1 right). This is because when variance increases, a greater number of Absent samples fall outside of the region responded classified as Absent, and, analogously, a greater number of present trials (B or C) fall outside their respective regions – ultimately leading to a flat relationship between stimulus evidence and discrimination performance. This change is also accompanied by an increased proportion of unseen responses. Contrarily, the sigmoid becomes sharper and the number of seen responses increases when the variance of the stimulus diminishes (FIGURE 8.4.1 left).

The present model thus shows how both near-linear and non-linear visibility patterns can be produced by a single type of decision. The model also predicts that unseen trials should tend to be characterized by linear patterns, and seen trials with all-or-none patterns – an empirically verified phenomenon (SERGENT AND DEHAENE, 2004; DEL CUL ET AL., 2007; DE GARDELLE ET AL., 2011; DE LANGE ET AL., 2011; MELLONI ET AL., 2011). Because there is no unequivocal way of determining the internal variance of sensory inputs in existing experiments, the present account remains speculative. Nevertheless, stimulus variance could be explicitly manipulated in future experiments.

8.4.5. PRIOR KNOWLEDGE CAN LOWER THE VISIBILITY THRESHOLD
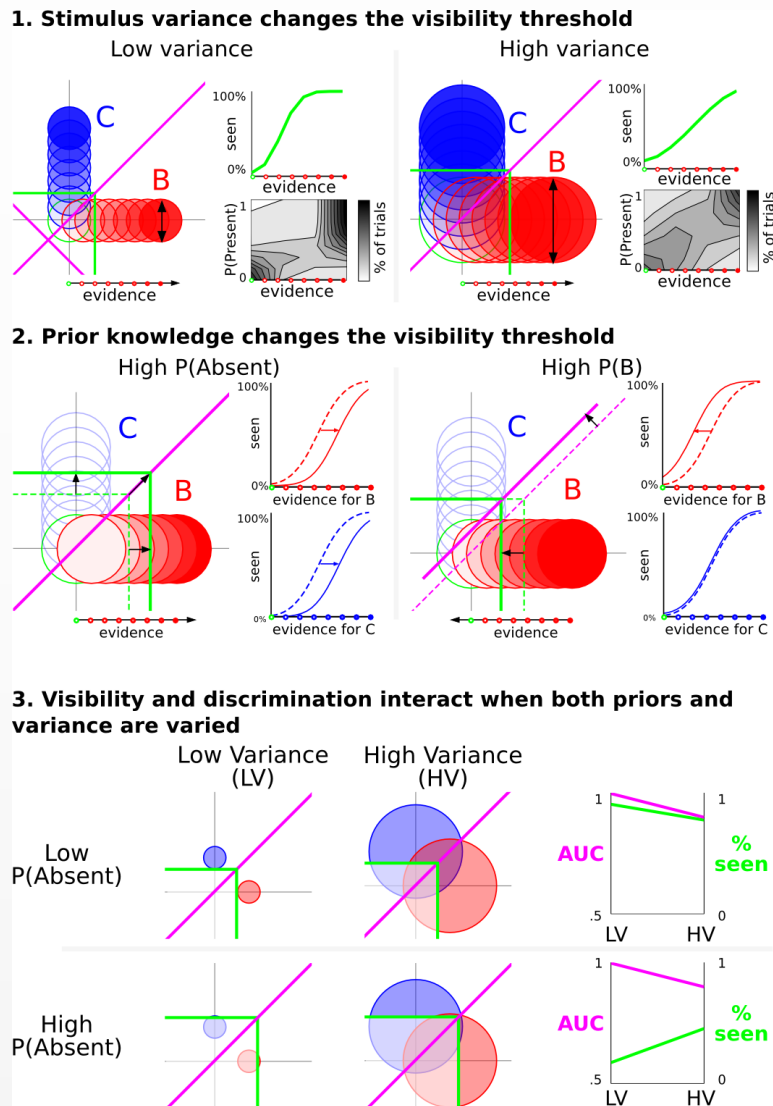
FIGURE 8.4 *INPUT VARIANCE AND PRIOR KNOWLEDGE CAN AFFECT THE NON-LINEARITY AND THE THRESHOLD OF SUBJECTIVE VISIBILITY REPORTS.*

Top. Parametrically varying stimulus strength directly changes the amplitude of the input vector and leads to a non-linear pattern of subjective visibility reports. The slope and the intercept of the resulting sigmoid depend on stimulus variance: low variance leads to an all-or-none relationship between the evidence and the visibility reports (left), whereas high variance leads to a more linear relationship as well as an increase in the visibility threshold (right).

Middle. Prior knowledge can also affect the visibility threshold. Increasing the prior probability of the Absent class increases the visibility threshold for all stimuli, thus lowering subjective visibility reports. When only the prior probability of B is increased (capturing "hysteresis" experiments where subjects come to expect the next stimulus), then the visibility threshold is lowered for B alone, while the visibility threshold for C barely changes.

Bottom. If the probability of the Absent class is relatively low (or similarly if the evidence is relatively high), increasing the variance reduces both visibility ratings and discrimination performance. However, when P(Absent) is high (or similarly, if the evidence is low), increasing the variance can diminish discrimination performance while increasing visibility ratings. This diagram captures the paradoxical finding that increased attention can lead to reduced visibility (RAHNEV ET AL., 2011).

Empirical finding 5 is that the threshold of subjective visibility is affected by prior knowledge (MOONEY, 1957; RODRIGUEZ ET AL., 1999; SIMONS AND CHABRIS, 1999; TALLON-BAUDRY AND BERTRAND, 1999; CUL ET AL., 2006; MELLONI ET AL., 2011). Prior exposure to a given word increases its objective identification and subjective visibility when the same word is later presented under stronger masking (CUL ET AL., 2006). Similarly, Melloni *et al.* (MELLONI ET AL., 2011) recently used a hysteresis experiment in which letters were embedded in white noise. Across a series of trials, the identity of the letter was fixed while its signal-to-noise gradually increased, then gradually decreased. Subjects reported seeing the letter better in the descending than in the ascending condition (*i.e.* once they knew the identity of the letter), even for identical physical stimulation.

In the present model, these effects arise from changes in the priors for classes B and C. At the beginning of the ascending condition, stimulus evidence is low, and the B and C classes are equally likely. Once the stimulus has been identified, at the beginning of the descending condition, its prior probability P(B) is increased, and consequently P(A) and P(C) are decreased. Because the decision boundary for the "seen" response is partly determined by P(B), the "seen" response is more likely in the descending sequence than in the ascending one (FIGURE 8.4.2).

Although this account captures the influence of prior knowledge on visibility reports (CUL ET AL., 2006), it oversimplifies the hysteresis experiment (MELLONI ET AL., 2011). Indeed, subjects are also likely to learn the structure of the ascending and of the descending sequences, and expect a higher frequency of absent trials towards the beginning of the ascending sequence and towards the end of the descending sequence. This expectation, if present, would again increase the prior probability of the "unseen" response, thus leading to increased reports of invisibility for these stimuli compared to physically identical stimuli presented in a random sequence. The model further predicts that B/C discrimination should remain identical in ascending and descending sequences. During the descending sequence, subjects should exhibit a bias towards B reports, due to the increased prior for B, but no change in *d'*. These predictions offer a way to test the validity of the present model.

8.4.6.   ATTENTION CAN EITHER INCREASE OR DECREASE VISIBILITY

Empirical finding 6 is that attention and visibility can be paradoxically decorrelated. In many studies, attention increases detection sensitivity and subjective visibility (*e.g.* (KIM AND BLAKE, 2005; RAHNEV ET AL., 2011; SERGENT ET AL., 2013)). However, inattention can also lead to increased subjective visibility (RAHNEV ET AL., 2011). In Rahnev *et al.*'s study (RAHNEV ET AL., 2011), subjects performed a basic detection task on a target whose location was validly cued on 70% of trials. Crucially, the contrast of the unattended target was adjusted to yield the same level of objective performance as the attended target. Remarkably, subjects reported that unattended trials were more visible than attended ones.

If we assume that attention affects the variance of the input vector, the present model predicts that attention can lead to opposite visibility effects depending on the proportion of trials reported as seen or unseen (FIGURE 8.4.3). If P(Absent) is low, so that most trials are reported as seen, then increasing the variance diminishes both discrimination performance and visibility, because it increases the proportion of input vectors that fall close to the Absent class. This captures the classical effect that inattention increases noise and thus reduces both objective performance and subjective visibility. Importantly, however, if P(Absent) is high, so that most trials are reported as unseen, then increasing the stimulus variance still diminishes discrimination performance, but may paradoxically *increase* visibility ratings. This is because with higher variance, a greater number of samples fall outside of the region responded as "unseen" and thus become subjectively visible (see FIGURE 8.4.3).

The model therefore predicts that attention can induce opposite effects on visibility and discrimination performance even when the mean evidence is unchanged. Contrarily to Rahnev *et al.* (RAHNEV ET AL., 2011), who argue that attention induces a conservative visibility bias by changing the inter-trial variance of the stimulus, we predict that visibility ratings are influenced by an interaction between the variance and the initial visibility threshold (determined by prior knowledge or stimulus evidence). Once again, this prediction could be tested in an experiment explicitly manipulating stimulus variance, contrast and priors.

8.5. EXPERIMENTAL TEST OF THE MODEL

Most the above arguments account for empirical observations only in retrospect. We thus opted to confront the present model to a novel experimental setup. The model critically predicts that linear and non-linear profiles of behavioural responses arise from the *same decision mechanism*. In particular, it predicts that the discrimination profile of *physically identical* stimuli will increasingly become non-linear as visibility increases (FIGURE 8.2.2 and FIGURE 8.4.1).

We tested this prediction by linearly varying a parameter λ to create a continuum between two perceptual classes B and C. For λ=0, the stimulus is B, for λ=1, the stimulus is C, but we can create an arbitrary series of intermediate stimuli S(λ)= λA+ (1- λ)B. Whereas de Gardelle *et al.* (DE GARDELLE ET AL., 2011) used a linear morph between two faces, here we varied the contrast of a single line to create a continuum between two different digits (*e.g.* 55599999). Geometrically, such a continuum can be represented as a line joining the prototypical vectors of each class (FIGURE 8.5). We presented the stimuli at perceptual threshold, such that for a fixed stimulus, there was a large number of both "seen" and "unseen" subjective reports.

The model predicts that the steepness of discrimination performance should increase as subjective visibility increases. Stimuli rated as "unseen" should be categorized better than chance (FIGURE 8.2.1), but with a shallow slope because such stimuli are necessarily close to the "absent" class. Conversely, highly visible stimuli should yield a steeper sigmoidal function (FIGURE 8.4.1). Thus, we expected significantly better identification performance on "seen" compared to "unseen" trials (FIGURE 8.1.2), and an increasingly "all-or-none" response pattern as a function of stimulus ambiguity λ (FIGURE 8.5).

8.5.1. METHOD

Nineteen healthy volunteers, with normal or corrected-to-normal vision, participated after giving informed consent (29% males, Age: 25 ± 5 years old, 88% right handed). Each trial began with the presentation of an ambiguous digit (target) presented for 83 ms and subsequently masked by pseudo-random black surrounding letters displayed for 67 ms. Subjects were asked to identify in less than 2 s which of four digits was presented (5, 6, 8 or 9), using their left and right index and middle fingers. Visual feedback was given for non-ambiguous trials (morphs at 0% or 100%): misidentifications were followed by a 100 ms red fixation cross, whereas correct identifications were followed by 100 ms green fixation cross. Subjects subsequently reported subjective visibility using a 10-point vertical rating scale (bottom: not seen, top: clearly visible). Subjects used the two middle fingers to change the location of the randomly-placed visibility cursor, and pressed the space bar with their thumb to validate the visibility rating. The inter-trial interval was fixed at 300 ms. Subjects performed a total of 1000 trials divided into 25 blocks, at the end of which their median reaction times and their accuracy were displayed. The experiment lasted approximately one hour.

Prior to the main experiment, subject performed a staircase procedure similar to the main task (100 trials with unambiguous targets, no visibility ratings, and no time limit). The contrast was lowered to reach an accuracy of ~70% (KAERNBACH, 1991). Target contrast then remained fixed throughout the main experiment. The staircase procedure was repeated up to five times in case of an unstable perceptual threshold. Two subjects who failed to converge to a stable threshold were excluded.

All stimuli were generated on a computer using INKSCAPE, MATLAB 2009b and the Psychophysics Toolbox and were displayed on a 17" computer CRT screen (1600 x 900 refreshed at 60 Hz). The screen background colour was 50% gray throughout the whole experiment and a black fixation-cross was constantly presented in the middle of the screen. Targets were morphs between two digits (5-6, 5-9, 6-8, 9-8) each made of 5 to 7 black bars (FIGURE 8.5). In each pair, a single bar varied between gray (background colour) to maximal contrast in eight linear steps (parameter λ varying from 0 to 1 in steps of 0.143). Masks were composed of four pseudo-random capital letters constructed from the same basic visual features as the digits and were located at the top (E, O, U, Z), at the bottom (A, F, P Z), to the left (A, H, O, U) and to the right (E, F, P H) of the target digit. Symbols subtended 0.45° x 0.85° and were presented to the left or to the right side of the fixation (2.12°). Masks were centred on the previously presented target (1.23° x 2.27°). Targets, masks and their respective location were randomly selected at each trial. On 15% of trials, the target was absent and replaced by a gray background.

8.5.2. RESULTS
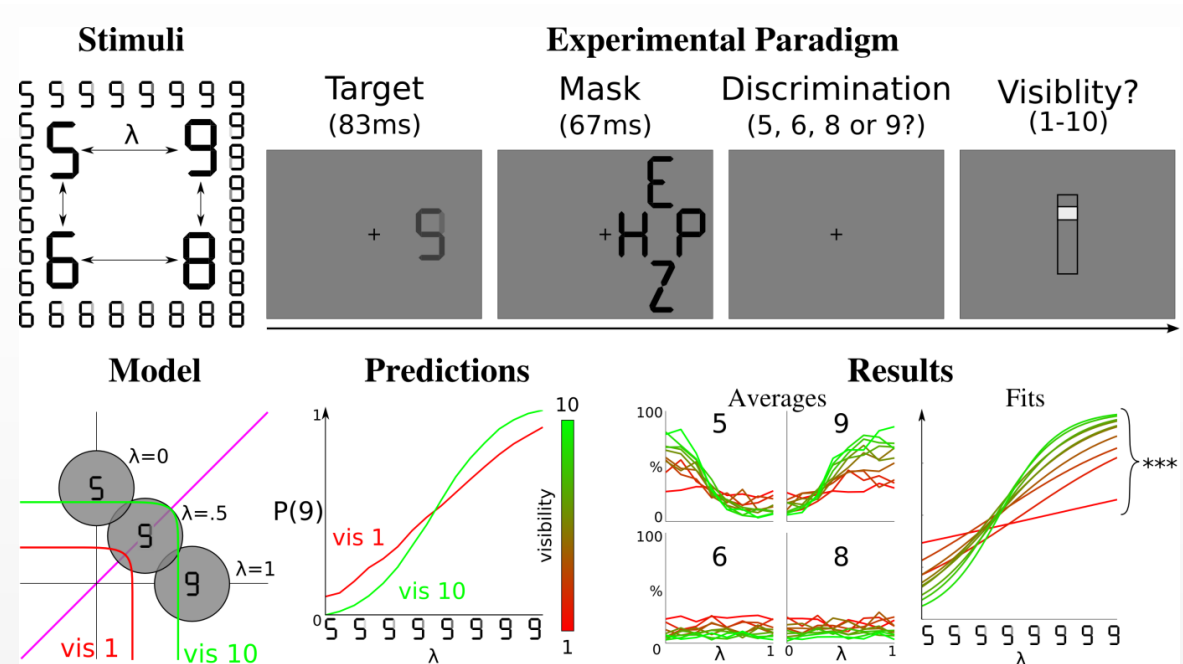
FIGURE 8.5 EMPIRICAL TEST OF THE PREDICTED VARIATION IN NON-LINEAR CATEGORIZATION AS A FUNCTION OF VISIBILITY.

To test whether linear and non-linear subjective reports could be accounted by a single type of decision, we parametrically varied the evidence (λ) favouring four different stimuli (5, 6, 8, 9) by creating morphs between pairs of these digits. For each morph, on each trial, subjects performed a forced-choice identification task and provided a subjective visibility report. The present framework predicts that the steepness of the sigmoid characterizing discrimination performance as a function of λ should increase with subjective visibility. The results (n=17) confirm that i) stimuli could be identified above chance even at the lowest visibility ratings ii) discrimination performance correlated with visibility ratings, and iii) increasingly steeper sigmoids indicated that identification performance was more categorical for clearly visible stimuli than for unseen stimuli.

Unambiguous targets were accurately identified on 67.7% of trials (SD = 14.1%, t(16) = 5.00, p < .001) confirming that the staircase procedure was efficient (targeted accuracy: 70%). Subjects used the visibility scale appropriately, as indicated by their more frequent use of the 0% visibility response on target-absent trials than on target-present trials (36.7% *vs.* 16.9% of trials, t(16) = 4.867, p = < .001). Subjects used the entire visibility scale on target-present trials, from 0% visibility (16.9% of trials) up to 100% visibility (18.7% of trials).

We sorted trials as a function of reported visibility (10 levels), and within each level, examined how identification responses varied as a function of bar contrast (parameter λ). We only focused on the two adequate responses to a given morph (*e.g.* responses 5 or 9 for the 5-9 morph), and computed the fraction of these responses that corresponded to reporting the presence of a bar. We used R software to fit a binomial distribution as a function of bar intensity, separately for each subject and each visibility level. As seen in FIGURE 8.5, subjects' choices varied significantly as a function of bar contrast at all visibility ratings (all p < .001). Thus, subjects discriminated digits at above-chance level even on trials when they reported no subjective perception. Furthermore, as predicted, the slope of the sigmoid function increased significantly with visibility ratings (r² (15) = .79, p = .004). Thus, discrimination performance improved with subjective visibility ratings. Trials rated as invisible had such a shallow slope that the response proportion were nearly linearly related to the intensity of the bar, while trials rated as highly visible resulted in a nearly stepwise, "all-or-none" response function.

8.5.3. DISCUSSION OF THE EXPERIMENT

Although subjects were presented with identical stimuli, subjective reports varied considerably from trial to trial, from total invisibility to maximal visibility. Furthermore, three predictions were verified: (1) identification scores were always higher than chance level; (2) they increased with visibility; (3) when varying the degree of ambiguity λ, objective identification became increasingly non-linear as subjective visibility increased. These results confirm that, for physically identical stimuli, visibility is associated with a greater degree of "all-or-none" perception, a finding that the framework can explain without any additional assumption (*i.e.* no need to postulate a qualitative difference between conscious and unconscious processing).

Our results extend a previous study by de Gardelle *et al.* (DE GARDELLE ET AL., 2011), which examined the amount of masked repetition priming elicited by a morphed face when the prime was unmasked (SOA = 300 ms) or heavily masked stimuli (SOA = 43 ms). As in the present experiment, they observed linearly increasing priming for invisible morphs, and categorical priming for visible morphs. Although the authors proposed that this dissociation reflected two distinct processes (unconscious analogue versus conscious discrete), the present model suggests that this interpretation is unnecessary: even within a single decision process, response patterns may vary in their degree of non-linearity depending on the mean and variance of the stimulus evidence.

The model further predicts that, when conscious perception occurs, subjects perceive the stimuli strictly categorically (digit 5 or 9, but no intermediate percept). According to Harnad's definition (HARNAD, 2003), categorical perception is defined by "within-category compression and between-category separation". Such a definition, implying an increased discriminability of items presented close the decision threshold, can only be tested using an experimental method in which two stimuli are compared. In another paper (KING ET AL., IN PREPARATION), we present additional evidence that the conscious experience of our morphs follows Harnad's definition of categorical perception (HARNAD, 2003). First, discriminability is indeed enhanced for pairs of digits presented near the perceptual boundary. Second, when presented with two identical ambiguous morphs, subjects frequently judge that the stimuli differ, as predicted if each has a ~50% chance of falling in either of two discrete perceptual categories. Third, when the present identifi-

cation task is replicated using a continuous response scale, subjects respond bimodally and barely use the intermediate levels to report perceiving a mixture of two digits. Thus, at least for this type of stimuli, and as postulated in our theoretical premises, what we consciously perceive seems to result from a categorical decision among a limited number of classes (see also (MORENO-BOTE ET AL., 2011; GERSHMAN ET AL., 2012)).

8.6. GENERAL DISCUSSION

We have shown how a simple geometrical framework for subjective report and objective discrimination tasks, based on Signal Detection and Bayesian Theories, can account for six fundamental findings in behavioural studies of conscious and unconscious perception. The present model subsumes a series of frameworks describing both conscious and unconscious perception as statistical inferences (KERSTEN AND YUILLE, 2003; KERSTEN ET AL., 2004; KNILL AND POUGET, 2004; DOYA, 2007; KNILL AND RICHARDS, 2008; LAU, 2008; SHADLEN ET AL., 2008). The core of our hypothesis is that, during perception, the brain is faced with a massive classification problem. Each task, including conscious identification and subjective report, imposes, in a top-down manner, a set of classes along which the stimuli can be classified. Contrarily to most laboratory tasks, open-ended subjective reports are typically based on numerous features and classes. A picture naming task, for instance, typically involves tens of thousands of classes. Like others before us (GREEN AND SWETS, 1966; KLEIN, 1985; KO AND LAU, 2012), we thus insist on the necessity to conceptualize decisions within a multidimensional framework. This conceptualization leads to several important methodological and theoretical consequences.

Firstly, the present model goes against the idea that subjective reports of "not seeing" are necessarily unreliable because they can be affected by conservative response biases (ERIKSEN, 1960; GREEN AND SWETS, 1966; MERIKLE, 1982; HOLENDER, 1986), and that objective measures such as detection sensitivity (d') should be favoured (see review in (KOUIDER AND DEHAENE, 2007)). On the contrary, we show that subjective reports cannot be reduced to objective measures (ERIKSEN, 1960; MERIKLE, 1982; HOLENDER, 1986) nor to second-order measures such as confidence rating and post-decision wagering (LAU AND PASSINGHAM, 2006; PERSAUD ET AL., 2007; LAU, 2008; RAHNEV ET AL., 2011). In particular, the present model predicts that visibility and confidence should be partially correlated (FIGURE 8.2) but experimentally dissociable. This prediction is well supported by recent empirical findings showing that second-order judgments can be performed above chance on unseen stimuli (KANAI ET AL., 2010; SANDBERG ET AL., 2011; OVERGAARD AND SANDBERG, 2012; CHARLES ET AL., 2013). In the present model, subjective visibility reports reflect a legitimate decision process whose details can and should be accounted for. As recently demonstrated (CUL ET AL., 2006; SCHWIEDRZIK ET AL., 2009; MELLONI ET AL., 2011), a shift in visibility criterion reflects the underlying prior probabilities and cost functions of the subjects' internal model of the world, and, consequently, should not be disregarded as an experimental confound. What we call a "subjective" report may simply be the brain's best attempt at solving a difficult perceptual decision problem with myriad of potential classes, each with different costs and prior probabilities that depend on the subject's prior experience.

Secondly, the model shows, in a principled manner, how experimental conditions can be designed to equate discrimination performance between seen and unseen trials (FIGURE 8.3). In a series of behavioural experiments, Lau and collaborators have equated objective discrimination performance between seen and unseen responses, in an attempt to isolate conscious processing independently of other pre- or post-perceptual increases in information processing (LAU AND PASSINGHAM, 2006; LAU, 2008; RAHNEV ET AL., 2011). The present geometrical analysis suggests that Lau's experiments have adopted only a subset of the possible solutions: masking the stimuli at different levels (LAU AND PASSINGHAM, 2006) or changing the

amount of attention they receive (RAHNEV ET AL., 2011) may both change the signal-to-noise ratio of the incoming evidence. However, under such conditions, discrimination performance is equated at the expense of introducing physical differences between the visible and invisible stimuli. It is therefore unclear whether contrasting the two reflects an effect of visibility or of the stimulus' physical properties. Consequently, it may be preferable to use physically identical stimuli and alter subjective visibility by changing the priors (FIGURE 8.3, top) – a solution indeed adopted in several recent studies (CUL ET AL., 2006; SCHWIEDRZIK ET AL., 2009; MELLONI ET AL., 2011).

Finally, the empirical finding of a non-linear sigmoidal relationship between subjective visibility reports and the physical properties of a stimulus (VORBERG ET AL., 2003; DEHAENE ET AL., 2006B; DECO ET AL., 2007; KOUIDER AND DEHAENE, 2007; QUIROGA ET AL., 2008; DE GARDELLE ET AL., 2011; DE LANGE ET AL., 2011) has led to the notion that conscious perception is an all-or-none phenomenon (SERGENT AND DEHAENE, 2004; DEL CUL ET AL., 2007; MELLONI ET AL., 2011). The present model readily reproduces this non-linear pattern (FIGURE 8.4.1), but it also predicts exceptions in cases of high stimulus variance or low signal-to-noise ratio. These predictions remain untested, but may offer potential explanations to studies revealing a linear relationship between stimulus evidence and subjective reports (SERGENT AND DEHAENE, 2004; SANDBERG ET AL., 2011; OVERGAARD AND SANDBERG, 2012; WINDEY ET AL., 2013). In the future, directly manipulating the mean and the variance of stimulus evidence could clarify the role of each of these factors in linear and non-linear response patterns to sensory manipulations.

According to the present model, the reason why unconscious responses tend to be linearly related to stimulus evidence is simple: when perceptual evidence is low enough to be categorized as "unseen", the evidence necessarily lies close to the origin of the multidimensional space and therefore leads to shallow (though above-chance) forced-choice curves. We tested this idea in an original experiment, and the results confirmed that fixed stimuli presented at threshold lead to quasi-linear discrimination when reported as unseen, but to a sharp sigmoid discrimination curve when reported as seen. Contrarily to previous proposals (DEL CUL ET AL., 2007; DE GARDELLE ET AL., 2011; CHARLES ET AL., 2013) the present model accounts for these findings without having to postulate that distinct processes operate below and above the threshold for conscious perception.

8.6.1. LIMITS OF THE MODEL AND POSSIBLE EXTENSIONS

For simplicity we postulated that the very same representational vector is used for different tasks. The idea is that the same input vector is "resampled" several times with different response classes (*e.g.* a discrimination task followed by a visibility task on the same trial). This resampling assumption is supported by a recent experiment (VUL ET AL., 2009A) in which, within a rapid stream of letters, subjects were asked to identify the one that was circled by a visual cue. On each trial, subjects provided as many as four mutually exclusive guesses about the target letter. The results showed that all guesses were sampled from an identical distribution centred on the position and/or the time of the cue. This experiment suggests that the posterior probability of each letter was computed once and for all, and that successive guesses corresponded to the maximum a-posteriori (MAP) after excluding the previous answers, exactly as expected from the present model.

Nevertheless, in other contexts, the hypothesis that the input vector remains unchanged and identically available for a series of successive judgments may turn out to be simplistic. Temporal decay may affect the quality of decisions made after a delay (SPERLING, 1960), particularly for unconscious stimuli (GREENWALD ET AL., 1996; DUPOUX ET AL., 2008). A recent study suggests that an attentional cue presented *after* a sensory stimulus can retroactively improve its visibility (SERGENT ET AL., 2013). The task set imposed by a first task may also change the quality of the evidence available for a second task (JAZAYERI AND MOVSHON, 2007). Similarly, the order in which two questions are presented may influence the subject's

answers (GILOVICH ET AL., 2002). Busemeyer *et al.* (BUSEMEYER ET AL., 2011) have proposed to account for the latter phenomenon with a computational principle inspired from quantum mechanics, according to which each successive judgment alters the input vector by projecting it onto a subspace defined by the task. As projections are not commutative, the order of successive questions can change the successive decisions. It remains to be seen whether such non-commutativity is a fundamental principle that should be added to the present model.

Another limit of the present model lies in its assumption, shared with SDT that decisions are based on a single input vector. A natural extension of the model would represent a sensory input as a series of samples, *i.e.* a trajectory in multidimensional space. Indeed, SDT has been superseded by sequential sampling models (RATCLIFF AND ROUDER, 1998; GOLD AND SHADLEN, 2001; LEITE AND RATCLIFF, 2010), according to which each decision is based on an accumulation of noisy samples arising from the stimulus. Whichever accumulator first reaches a fixed threshold is selected as the winner of the perceptual decision. Models of this kind are supported by a large set of empirical findings, (RATCLIFF ET AL., 1999; KNILL AND RICHARDS, 2008; SHADLEN ET AL., 2008; DEHAENE, 2009; LIU AND PLESKAC, 2011) and account, not only for response proportions, but also for response times and their distributions (RATCLIFF ET AL., 1999; RATCLIFF AND MCKOON, 2008; LEITE AND RATCLIFF, 2010). Extending the present model in this direction, as attempted by Del Cul *et al.* (DEL CUL ET AL., 2007), would lead to precise predictions about subjects' reaction times in objective and subjective tasks.

In the tradition of "ideal observer" analyses, we also assumed that the decision system is fully informed of the stimulus distributions and uses optimal priors and likelihood functions to compute the posterior probability of each response class. This is undoubtedly an idealization. A dynamic model in which the likelihood functions, priors and costs would be learned by updating them after each trial, and may therefore be ill-estimated, may go a long way towards explaining a variety of human deviations from optimality. For instance, using a model similar to the present one, Ko and Lau (KO AND LAU, 2012) proposed an account of blindsight as an inadequate revision of priors following the radical decrease in visual input strength caused by a lesion to area V1 (similar to FIGURE 8.3, top). Confidence judgments and visibility ratings would be particularly affected by inadequate priors and likelihoods, because the present model assumes that these tasks require a quantitative estimation of the posterior probabilities (FIGURE 8.1). In agreement with this idea, Rahnev, Lau and collaborators (RAHNEV ET AL., 2011, 2012A) performed a series of experiments in which human observers deviated radically from optimality in their confidence judgments. Their findings could be explained by assuming that subjects used a single estimate of input variance for distinct experimental conditions (*e.g.* for attended versus unattended trials). This interpretation is compatible with the present model, and with the general idea that there are sharp limits to the number of decision criteria that subjects may deploy on a given trial (GOREA AND SAGI, 2000, 2010).

8.6.2. NEURAL MECHANISMS

The present model was framed at an abstract mathematical level of description. While this approach provides useful geometrical intuitions and a simple testable framework, an important future endeavour will be to flesh it out at the neural level. The vast representational space may correspond to the function of posterior unimodal and multimodal sensory areas, where many neurons render explicit dimensions of the stimuli that are only encoded implicitly and in a distributed form in the sensory periphery. Their role may be to augment the dimensionality of sensory inputs and therefore facilitate decision making by turning decisions into linearly separable problems (DICARLO ET AL., 2012). The categorical decision system, in turn, could be subserved by areas of the dorsolateral and inferior prefrontal cortices as well as anterior temporal and superior parietal cortices. These areas have been proposed to form a "global workspace" where conscious information is maintained and broadcasted to additional processes (DEHAENE AND CHANGEUX, 2011). They receive the necessary convergence of multimodal inputs and are known to con-

tribute to both decision making and to all-or-non conscious perception (FREEDMAN ET AL., 2002; WOOD AND GRAFMAN, 2003; DEHAENE AND CHANGEUX, 2011). Explicit simulations of such recurrent networks with winner-take-all dynamics show how they tend to quickly converge to a discrete stable attractor (DEHAENE ET AL., 2003) which approximates the maximum-likelihood estimate (DENEVE ET AL., 1999; WANG, 2008). The dynamics of such networks may therefore account for the categorization which the present model considers as inherent to conscious perception.

8.7. ACKNOWLEDGEMENTS

CHAPTER 9. GENERAL DISCUSSION

9.1. SUMMARY

9.1.1.   AIM OF THE THESIS

Over the last five decades, subjectivity has become progressively objectified. The computational mechanisms and neural bases responsible for conscious perception have now started to be empirically and systematically dissected in the laboratory and in clinics. Two main experimental methods have been developed for that purpose, each referring to transitive (*e.g.* conscious of something) and non-transitive (*i.e.* she is conscious) meanings of consciousness:

- A first set of experimental methods have been used to compare subjects' behaviour and brain activity in response to conscious and unconscious stimuli in healthy subjects (*e.g.* backward masking, attentional blink *etc.*) as well as in patients (*e.g.* blindsight, neglect *etc.*)
- A second set of experiments have been used to compare subjects' brains and behaviours under normal wakefulness and under physiological (*e.g.* wake *versus* sleep), pharmacological (*e.g.* anaesthesia) and pathological loss of consciousness (*e.g.* epilepsy).

The present thesis focused on vegetative and minimally conscious state patients, who offer an exceptional situation in which arousal and consciousness can apparently be dissociated. Arguably, this dissociation provides an even more subtle contrast that the physiological and pharmacological losses of consciousness, and thus explores the neural theories of consciousness in a novel situation. In particular, two questions motivated the present research:

- Can the vegetative and minimally conscious state patients improve our scientific understanding of conscious and unconscious processes?
- And, in return, can science improve the diagnoses, and therefore the clinical care, of these patients?

9.1.2.   MAIN RESULTS

The precise results obtained in each study have already been summarized in each chapter. However, the discussion section can be taken as an occasion to regroup them along two transversal axes:

- In a first series of studies, I have investigated the extent to which the putative neural signatures of consciousness, as predicted by several neuronal theories of consciousness, efficiently discriminated the brain activity of vegetative and minimally conscious state patients. In this regard, I have presented in CHAPTER 3. and CHAPTER 7. (also see FIGURE 1.24 from COMMENT 1) a series of experimental findings supporting the idea that conscious processes are best indexed by late (as opposed to early) evoked related potentials (DEHAENE ET AL., 1998A, 2006B; DEHAENE AND NACCACHE, 2001; SUPÈR ET AL., 2001; LAMME, 2006B, 2010; DEHAENE AND CHANGEUX, 2011; SERGENT AND NACCACHE, 2012). Indeed, a change of tone within a series of five sounds elicited similar early brain activity in vegetative and minimally conscious state patients. In contrast, the rare and unex-

pected occurrence of five sound sequences elicited a late change of brain activity *only* in the group of patients who demonstrated residual signs of conscious behaviour. Moreover, I have presented in CHAPTER 6. evidence suggesting that the amount of information shared across different brain regions was largely impaired in vegetative state patients as compared to conscious and minimally conscious state patients. Finally, and as detailed in CHAPTER 6. and CHAPTER 7. , this change was accompanied by an overall increase of low frequency rhythms and of the complexity of the electrophysiological activity, as explicitly predicted by several theories of consciousness (TONONI AND EDELMAN, 1998; TONONI ET AL., 1998; TONONI, 2004, 2008; SETH ET AL., 2006, 2008, 2011; SETH, 2007).

- These clinically-oriented studies have been accompanied by a series of original methods, empirical evidence and theoretical concepts aimed at refining the current models of conscious processing. In CHAPTER 3. , I have shown how multivariate pattern analyses could be used to maximize the extraction of information from the brain activity evoked by unexpected auditory stimuli. This technical achievement led to the formalization of a novel analysis that characterizes the dynamical structure of neural responses to sensory stimulations. Indeed, in CHAPTER 4. and CHAPTER 5. , I have shown that temporal generalization method can reveal qualitatively different neural dynamics and thus offer a powerful research tool. Multivariate approaches can also be useful for theories of consciousness. In CHAPTER 8. , I have sketched a simple multidimensional model, based on signal detection theory and Bayesian inferences that captures several important findings from previous studies on consciousness. Together, these methodological and theoretical proposals open novel avenues to the study of conscious and unconscious processes.

However, this work is still in progress, and several bridges should still be established to completely link these studies. In particular, the framework proposed in CHAPTER 8. remains simplistic and, perhaps most importantly, disconnected from the brain. Future developments and research will thus be necessary to pursue and precise this approach and ultimately test whether unresponsive patients present a specific impairment of their perceptual decision making system.

9.2. IMPLICATIONS FOR THE THEORIES OF CONSCIOUSNESS

The empirical results obtained over the course of the present thesis can be used to refine current neural theories of consciousness. The relationships between conscious perception, information sharing and information maintenance will be discussed.

9.2.1.   IS CONSCIOUSNESS IDENTICAL TO INFORMATION SHARING?

As detailed in the literature review, a number of theories establish a strong link between consciousness and information sharing (TONONI, 2004; DEHAENE ET AL., 2006B; LAMME, 2010; DEHAENE AND CHANGEUX, 2011) and some even go as far as to equate the two (TONONI, 2004, 2008). This concept, already proposed by Dennett in his "fame in the brain" metaphor (DENNETT, 1992), postulates that a particular neural event would lead to conscious perception if, and only if, it significantly impacted on the rest of the brain activity. Similarly, Baars has argued that information is consciously accessible if, and only if, it is "globally broadcasted" (BAARS, 1989). More recently, Tononi has formalized the quantification of information sharing in a mathematical equation (TONONI, 2004, 2008) and claims that the extent to which information is "integrated" across the multiple elements of a system directly reflects its level of consciousness. Similar methods are based on different information theory principles such as complexity and causal density (SETH, 2007).

In the present set of studies, I have shown that the amount of mutual information shared across brain regions appeared to be proportional to the state of consciousness of poorly and non-communicating patients. Furthermore, entropy measures of the EEG signal, applied to both the time and frequency domains, revealed that the complexity of patients' brain activity correlated with their state of consciousness. Together, these results fit with the above theoretical proposals: the state of consciousness appears to be indexed by the amount of information shared within the brain.

However, the present evidence remains superficial. First, the above empirical findings are solely based on EEG signals. Our ability to measure information sharing across neuronal assemblies, and in particular, our ability to quantify the directed flow of information across them is therefore extremely limited. As discussed below, the brain areas that contribute to this finding and the precise dynamics of their underlying neuronal activity remain unknown.

Beyond these empirical limitations lies a potentially more profound epistemological issue. Indeed, equating consciousness to information sharing implies that consciousness is a homogeneous and continuous property. However, the working definitions proposed at the beginning of the present thesis are based on specific and generally *qualitative* behaviours. For example, the state of consciousness is determined according to subjects' qualitative response to sensory stimulations. Measuring the state of consciousness is thus a way to summarize the preservation of a number of *distinct* behavioural abilities, and not the amount of a homogeneous quality. It is thus currently unclear how the state of consciousness could be measured with a continuous measurement. However, this may not be a helpless situation. Indeed, in masking protocols, Sergent and collaborators have for instance demonstrated that subjects could use continuous visibility reports (SERGENT AND DEHAENE, 2004; SERGENT ET AL., 2005). Interestingly, in attentional blink experiments, subjects demonstrated bimodal responses: they tended to either report the stimulus as completely seen, or, conversely, as completely unseen. It would thus be particularly interesting to propose an analogous continuous metric of subjects' state of consciousness, and test it to legitimate or, conversely, invalidate the premise of a categorical distinction between conscious and unconscious states.

9.2.2. IS CONSCIOUSNESS IDENTICAL TO INFORMATION MAINTENANCE?

Information maintenance is also at the core of several of the models of consciousness. This is particularly the case for the global neuronal workspace theory in which the neurons of the "global workspace" send top down signals in the selected areas, in order to sustain the relevant neuronal activity (DEHAENE ET AL., 1998A, 2006B; DEHAENE AND CHANGEUX, 2011).

The results found in the present thesis fit with this idea by revealing several links between conscious perception and information maintenance:

- While a change of sounds elicited both early and late event-related potentials in minimally conscious and conscious patients, only the early EEG components were preserved in vegetative state patients. As discussed in CHAPTER 3. and CHAPTER 7. , this result thus suggests that vegetative state patients are specifically impaired in their ability to produce sustained brain responses.
- The Local Global protocol establishes two types of auditory regularities, one of which is based on the learning of a regular sequence of sounds across trials. Consequently, subjects are required to sustain the specific sequence (*i.e.* the "rule") in working memory from trial to trial. On average, vegetative state patients did not present any specific brain responses to the violation of this rule. This result therefore suggests that these patients were not able to form and/or maintain the auditory sequence in working memory.
- Time generalization analyses applied to MEG recordings of healthy subjects demonstrated that the violation of such global rule (arguably associated with consciousness) induced a sustained

brain activity, whereas the local rule (considered to be partially independent of consciousness) induced a series of transient activations. Unfortunately, the signal to noise ratio in patients' EEG was too low apply a time generalization across time analysis. As a consequence, it remains difficult to determine whether the sustained brain activity observed in healthy subjects is similar in patients.

- The above results are all linked to the P3 component. It may be further noted that the contingent negative variation (CNV), known to mark subjects' attention towards an incoming stimulus (WALTER ET AL., 1964; FAUGERAS ET AL., 2012), was largely diminished, if not completely absent, in vegetative state patients. This result, which confirms a recent finding (FAUGERAS ET AL., 2012), may reflect patients' inability to sustain their attention to the auditory stimuli, and thus provides further evidence for the link between sustained neural activity and conscious perception.

Finally, it is interesting to note that the temporal generalization method detailed in CHAPTER 4. and CHAPTER 5. would potentially provide a powerful tool to precisely investigate the link between sustained neural activity and conscious processing. In particular, the models of Lamme (SUPÈR ET AL., 2001; LAMME, 2006B, 2010) and of Dehaene *et al.* (DEHAENE ET AL., 1998A, 2006B; DEHAENE AND CHANGEUX, 2011)postulate the existence of two very distinct types of neural responses. The so-called fast feedforward sweep is believed to transiently recruit a series of different brain regions in response to both visible and invisible stimuli, and should thus lead to a "diagonal pattern" of generalization across time (see CHAPTER 4. and CHAPTER 5.). By contrast, the feedback mechanisms, believed to integrate and maintain neural information, should generate sustained brain activity patterns, and thus led to a "square pattern" of generalization across time.

In an ongoing collaboration with Lucie Charles, I have tested these two predictions. I applied the temporal generalization method to MEG recordings of subjects who participated in a classic backward masking experiment (DEL CUL ET AL., 2007; CHARLES ET AL., 2013, N.D.). The time separating the stimulus and its subsequent mask was varied between 16 ms and 83 ms (present trials). For each subject, the temporal generalization analysis compared the activation elicited by each stimulus to the mask only condition. The results, summarized in FIGURE 9.1 reveal that:

- the stimuli masked after 16 ms, and thus generally reported as unseen, evoked a diagonal generalization matrix.
- the stimuli masked after 83 ms, and thus generally reported as seen, evoked both a strong diagonal and a square pattern of generalization across time.

In other words, both visible and invisible conditions were accompanied by a series of distinct brain activations, as predicted by the feedforward sweep. By contrast, only the visible trials were accompanied by a sustained neural activity, rising from 250 ms to 800 ms after the presentation of the stimulus. If confirmed, this result would particularly well fit with Lamme's and Dehaene and colleagues' theories of conscious processing and thus reinforce the idea that conscious perception is strongly associated with sustained neural activity.
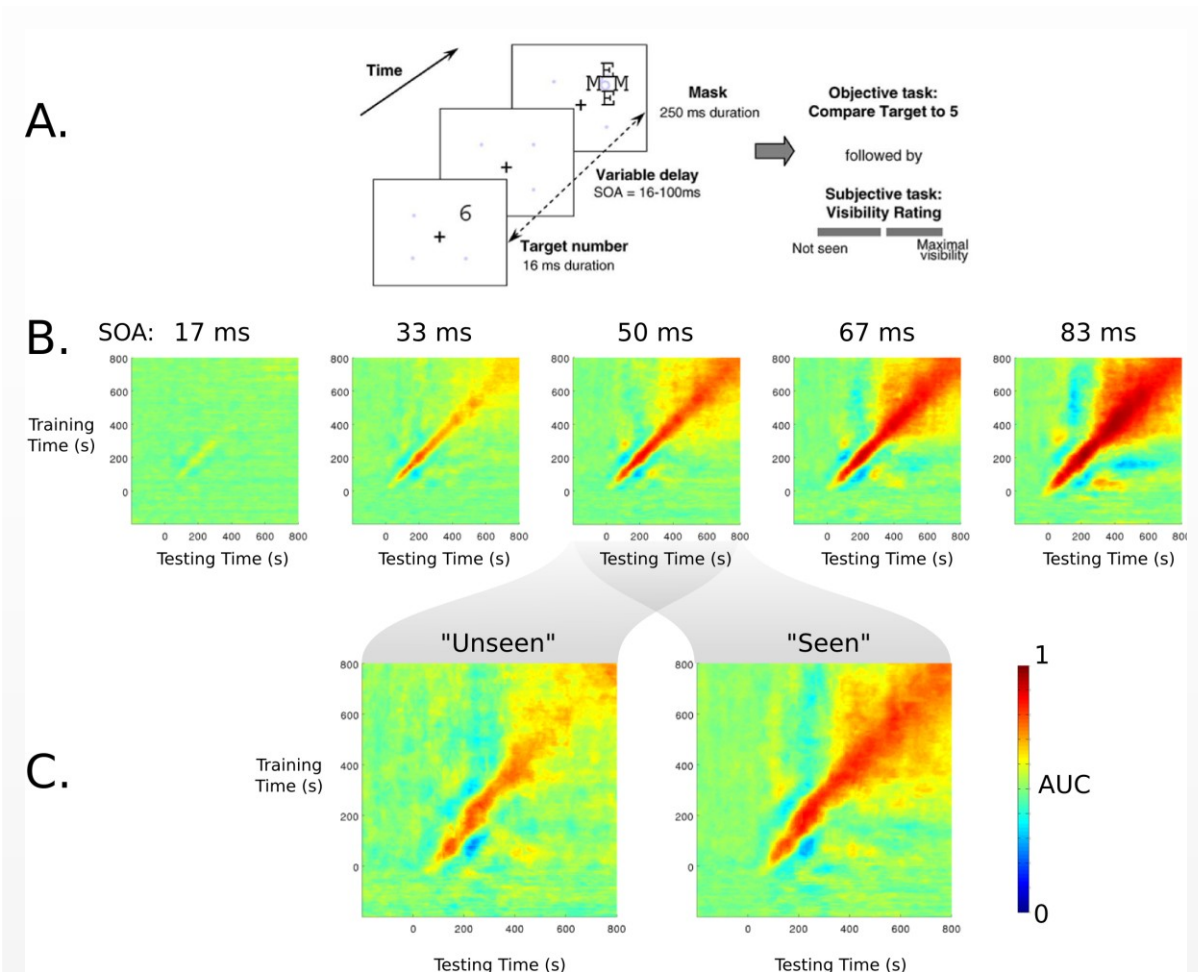
FIGURE 9.1 TEMPORAL GENERALIZATION METHOD APPLIED TO BACKWARD MASKING PROTOCOL (KING, CHARLES, DEHAENE, IN PREP)

(A) *Subjects had to determine whether a masked digit was higher or lower than 5 and subsequently indicated the visibility of the stimulus on a 10 point scale (DEL CUL ET AL., 2007; CHARLES ET AL., 2013, N.D.). The visibility of the stimulus was experimentally manipulated by varying the stimulus onset asynchrony (SOA) between the digit and the mask.*

(B) *Applying the temporal generalization analysis decode the presence of the stimulus from subjects' MEG recordings revealed quantitative and qualitative changes with the increase of SOA duration. Brief SOAs tended to elicit a weak diagonal generalization matrix suggestive of a sequential activation of different brain regions. By contrast, longer SOAs tended to elicit a combination of a strong diagonal generalization pattern, a reactivation of the early ERFs around 300 ms and a sustained brain response between, 400 and 800 ms after stimulus onset.*

(C) *Only stimuli reported as seen evoked a sustained brain response between 400 and 800 ms.*

9.2.3.   WHICH AREA(S) CRITICALLY SUPPORT(S) CONSCIOUS PERCEPTION?

As detailed in the literature review, the various theories of consciousness propose different neural mechanisms to explain conscious and unconscious processes. Several authors have for instance argued that neural information is bound into a single conscious perception by a synchronizing mechanisms either distributed over the cortex (*e.g.* (CRICK AND KOCH, 1990A; SINGER AND GRAY, 1995B; FRIES, 2005; TALLON-BAUDRY, 2009)) or coordinated by the thalamus (*e.g.* (RIBARY ET AL., 1991; LLINÁS ET AL., 1998)). By contrast, others have proposed that information sharing is implemented via horizontal and top-down cortico-

cortical connections (SPORNS ET AL., 1989; LAMME AND ROELFSEMA, 2000; DEHAENE ET AL., 2003; ZYLBERBERG ET AL., 2010).

In the present set of studies, and with the exception of the intracranial recordings (CHAPTER 3.), the precise anatomical location of the brain activity we recorded is difficult to establish. Furthermore, since EEG and MEG are most likely unable to capture thalamic activity (HÄMÄLÄINEN ET AL., 1993), the present findings cannot support, nor completely rule out, the involvement of the thalamus in conscious processing. The present results therefore remain limited in their ability to provide a precise anatomical understanding of conscious and unconscious processes.

Nevertheless, two relatively unexpected results are worth underlining in this regard:

- A minimal difference in the state of consciousness (vegetative *versus* minimally conscious) is not accompanied by a focal topographical change, nor by a unique change in brain activity. Rather, the results demonstrate a myriad of changes observable all over the scalp, and in many different dimensions (CHAPTER 3. , CHAPTER 6. and CHAPTER 7.).
- The topography of the EEG markers that correlated with patients' states of consciousness did not suggest a particular role of anterior brain regions. Indeed, and with the exception of the contingent negative variation (CNV) and the delta power (< 4 Hz), most markers did not present a frontal topography but rather revealed a centro-posterior topography. This particularly the case of wSMI, the P3b and spectral markers.

Therefore, this set of results does not particularly favour a preponderant role of the prefrontal cortex in conscious perception. Rather, it insists on i) the distributed nature of the neural mechanisms involved in conscious processing and ii) the importance of posterior regions, and most likely, of its underlying regions. Indeed, as detailed in the LITERATURE REVIEW, the precuneus is particularly affected in vegetative state patients (LAUREYS ET AL., 2004) and is one of the main hubs of the default mode network (BUCKNER ET AL., 2008; NORTHOFF, 2012). Together, these empirical findings should thus suggest that this area plays a critical role in the maintenance of a conscious state. Furthermore, the dissociation between frontal and parietal activity and their respective link to conscious perception remains insufficiently described by the current neuronal models of consciousness. In particular, it is unclear whether these two regions play a similar role in the selection, maintenance and broadcasting of information in and across the cortex, or, conversely, whether they are specialize in one of these functions. A major goal for future research will thus consists in clarifying the specific functions of the frontal and parietal cortices in both stimulated and "resting-state" conditions.

9.3. GENERAL LIMITS

Each of the present studies is subject to a number of limits and potential criticisms that have been covered in the discussion part of each chapter. However, two limitations that apply to the general approach undertaken in the present thesis are worth highlighted here.

9.3.1. DISENTANGLING CAUSATION AND CORRELATION

One of the aims of the present thesis was to identify the neural signatures of consciousness in non- or poorly communicating patients. As detailed in the literature review, the quest for the "neural signatures of consciousness" implies two general goals: finding a marker that necessarily marks the pres-

ence of conscious processes (marker => consciousness), and finding a marker that is systematically present when the subject is conscious (consciousness => marker).

This equivalence (consciousness <=> marker) designates a goal rather than an empirical finding. Indeed, as in all neuroimaging studies, the approach undertaken in the current thesis is purely correlational and cannot establish causal relationships links between electrophysiological markers and subjects' behaviour:

- **Consciousness => marker**: The premise in this case is that conscious perception will systematically recruit particular neurons, networks or types of brain activity. This is, for example, what is postulated by the global neuronal workspace theory, which predicts that conscious perception necessarily induces a late P3b, the neural marker of the ignition of the global workspace. However, some markers may be sensitive to the preservation of conscious processes while not necessarily being specific to it. For instance, the large slow waves observed in vegetative and minimally conscious state patients (CHAPTER 7.), as well as in other types of loss of consciousness (see LITERATURE Review), are generally interpreted as the correlate of a general disruption of neural processing. Inversely, consciousness would therefore imply low amplitude slow waves. Yet, it is quite probable that the absence of large amplitude slow waves is not sufficient to be conscious. Slow waves would thus be sensitive, but not specific, to consciousness.

- **Marker => consciousness**: The premise in this case is that the presence of the marker necessarily implies that the person is conscious. For example, if the subject says that he/she has perceived a stimulus (behavioural marker), it is traditionally assumed that he/she is conscious. Yet, the absence of subjective report does not necessarily reflect lack of conscious perception. The same logic could thus apply to brain activity: some neurophysiological markers may index a cognitive function that depends on conscious perception, such as episodic memory formation. In a hypothetical case like this, detecting a brain signature of episodic memory formation would imply that the person is conscious. Yet, the absence of this marker would not necessarily imply an unconscious state. The marker is thus specific, but not sensitive, to consciousness. To the extreme, this case is particularly well illustrated by Owen's imagining tennis experiment (OWEN ET AL., 2005). Indeed, in this scenario, detecting a sustained tennis-related activity is extremely suggestive of a conscious state, even though it is clear that the absence of such activity would never suggest and unconscious state (NACCACHE, 2006).

To compensate for these issues, I have reported the extent to which each marker is sensitive and specific to vegetative state patients. These analyses, generally summarized with the area under the curve (AUC) however remain correlational. The results presented throughout the present thesis should thus be taken and interpreted as a body of evidence that globally fir and favour specific theories of consciousness.

9.3.2.   THE ABSENCE OF EVIDENCE AND EVIDENCE OF ABSENCE

A second challenge faced in the study of non-communicating patients, relates to the clinical definition of consciousness. Although one of the aims of the present research is to complement the purely behavioural diagnoses of patients' state of consciousness, consciousness is defined in the clinics with a set of behavioural abilities. It for example consists in testing whether the patient fixate a stimulus, track its movements *etc*. In other words, the present neuroimaging results are still heavily dependent on patients' behaviour. In such conditions, is it possible to outperform clinical diagnoses with neuroimaging techniques?

First, it should be noted that the present research is based on a relatively large cohort of patients. If it is assumed that the majority of the diagnoses are correct, in the sense that they accurately reflect pa-

tients' ability to consciously perceive their environment, then the brain activity that indexes consciousness states could still be accurately distinguished. In fact, the number of "misdiagnoses" would only lower the signal-to-noise ratio of the correlation between brain and behaviour.

Second, the markers of consciousness identified throughout the present thesis may be tested on their ability to accurately predict the *evolution* of patients' consciousness states. For example, imagine that the presence of a P3b is found in some vegetative state patients. A rapid conclusion may be that this marker is not a good signature of consciousness. Now, if these patients demonstrate behavioural signs of consciousness shortly after, one may prudently conclude that these vegetative patients were in fact initially misdiagnosed (in the sense that their introspection abilities were preserved), and that the electrophysiological marker then outperformed the clinical diagnosis. This scenario is not purely hypothetical. Indeed, Faugeras and collaborators (FAUGERAS ET AL., 2012) identified two vegetative state patients who presented a P3b during the Local Global protocol. Interestingly, these two patients presented signs of shortly after.

Still, it may be argued that the possibility that all patients, including the ones in a vegetative state, are conscious (in the sense that they have introspection abilities). This hypothesis cannot be completely rejected: an absence of conscious behaviour does not necessarily imply an absence of consciousness. Note, however, that the very same argument could be applied to any other situations, including coma, and even brain death. The only, modest, alternative to this epistemic issue is thus to trust the convergent body of evidence, drawn from different experiments, and constantly refining the theoretical frameworks that provide precise predictions about the neural machinery responsible for our ability to introspect.

Overall, these two general limits stress the notion that, at present, neuroimaging methods will most likely not replace clinical examinations. Rather, they constitute complementary tools to the traditional diagnosis realized in the clinics.

9.4. GENERAL PERSPECTIVES

The research presented in the current thesis calls for a number of follow-up clinical and fundamental studies. I will here briefly outline three general avenues that I find particularly interesting.

9.4.1. TESTING THE MARKERS OF CONSCIOUSNESS IN OTHER TYPES OF LOSS OF CONSCIOUSNESS

First, the repertoire of EEG markers identified throughout the thesis should be directly tested and compared to other types of patients. As detailed in the literature review, several studies have already demonstrated that some rare patients diagnosed in a vegetative state could surprisingly present covert command-following abilities (OWEN ET AL., 2006; CRUSE ET AL., 2011). These seemingly intentional behaviours could be evidenced by quantifying the specific activity elicited in motor areas in response to different types of instructions (FIGURE 1.2). A critical test for our methodological proposal would thus consist in assessing whether these misdiagnosed patients systematically present patterns of EEG activity suggestive of a conscious state. Specifically, we predict that these misdiagnosed patients would present lowered low-frequency oscillations, preserved alpha rhythms, a relatively high level of complexity, high functional connectivity values and preserved late event-related potentials in response to the global deviant stimuli. Furthermore, comparing these misdiagnosed patients to the "classic" vegetative state patients would offer an even more minimal contrast than the one adopted in the present thesis (*i.e.* vegetative *versus* minimally

conscious). Contrasting two behaviourally indistinguishable groups of patients would provide a challenging yet critical test for the neural theories of consciousness.

Second, the EEG markers tested in the present set of studies should be systematically investigated with different recordings apparatus and in sleeping, anesthetized and epileptic subjects. Indeed, as discussed throughout the chapters, one of the limitations of the present research is directly related to the EEG method. Indeed, volume conduction, movement artefacts as well as source reconstruction difficulties all limit our ability to precisely local the neuronal generator of scalp activity. Intracranial recordings of awake and sleeping subjects could thus be used to confirm that consciousness is indeed directly associated with an increasing of information sharing across distant brain regions. In an on-going research with Pierre Bourdillon, we precisely tested this prediction. Using intracranial recordings of awake and sleeping patients suffering from intractable epilepsy, we show that wSMI is maximal in wakefulness, and progressively diminishes in paradoxical and deep sleep respectively (FIGURE 9.2). Moreover, similar distance analyses to the one employed in CHAPTER 6. suggest that REM and deep sleep are only different in the amount of information shared across *distant* but not *adjacent* brain areas. These promising results thus *i)* replicate our findings in a physiological rather than pathological loss-of-consciousness, but they also *ii)* unambiguously overcome the issues related to scalp-recordings.
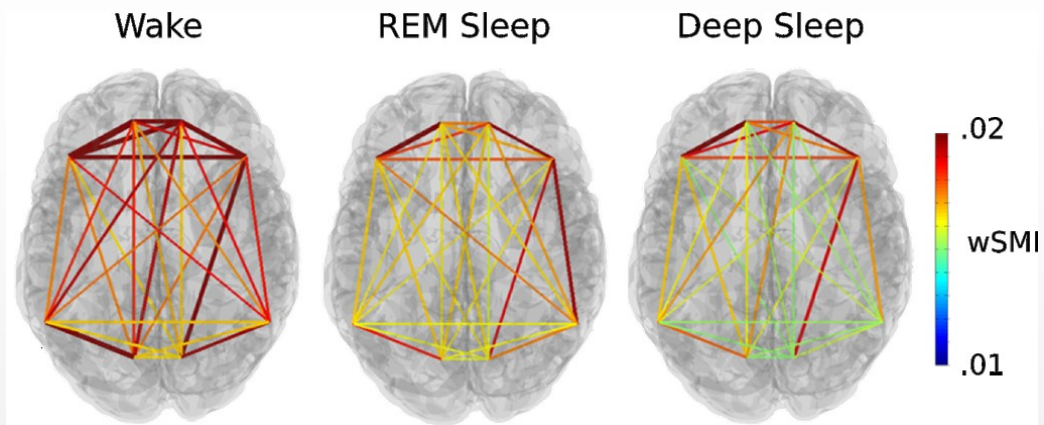
FIGURE 9.2 wSMI ANALYSIS OF INTRACRANIAL RECORDINGS DURING VARIOUS SLEEP STAGES.

(BOURDILLON ET AL., IN PREP.)

Furthermore, as these intracranial recordings were acquired from epileptic subjects for clinical purposes, the very same protocol and analyses could be implemented when patients lose consciousness because of a seizure. Following recent studies (GUYE ET AL., 2006; ARTHUIS ET AL., 2009; BARTOLOMEI AND NACCACHE, 2011; LAMBERT ET AL., 2012), one could indeed test whether wSMI also indexes seizure-induced loss of consciousness by comparing simple and complex partial seizures. Once again, we predict that wSMI should dramatically drop during the seizure, and particularly when it is accompanied by a loss of consciousness. Overall, the methods introduced in the present thesis could thus be tested in a variety of clinical situations and with different recording devices to confirm and clarify our findings.

9.4.2. SINGLE TRIAL ANALYSES

A second line of research relates to the decoding of electro and magnetoencephalographic responses to sensory stimulations. In the present thesis, I have shown how multivariate pattern analyses could be particularly useful when faced to large inter-individual variability, low signal-to-noise ratio, or to the necessity to make single trial predictions. Applying decoding techniques on poorly or unresponsive

subjects offer the possibility of characterizing the state of consciousness at the single trial level. Such opportunity would present several advantages.

First around 1 in 500 anesthetized patients recovers consciousness during surgical interventions (SEBEL ET AL., 2004; AVIDAN ET AL., 2011); a proportion which clearly exhibits the need for efficient real-time monitoring of consciousness level. Although such methods already exist, they are generally empirically rather than theoretically driven. For instance, the BIS index is one of the most common EEG measures used to monitor the level of consciousness of anesthetized patients. The way this measure is derived remains unknown because it uses a proprietary algorithm, empirically constructed from a large database of EEG recordings (n~ 1000). A complementary, theory-driven method, such as the one deployed in this thesis, is therefore needed.

Second, the existing monitoring tools solely focus on consciousness *states*, and are thus generally based on EEG recordings acquired independently of sensory stimulation. Yet, and as detailed in the literature review, many if not most theories of consciousness are derived from experimental methods used to minimally distinguish conscious and unconscious *contents* (*i.e. via* backward masking, attentional blinks *etc.*). As a consequence, being able to decode stimulus processing at the single trial level could provide a way to monitor the content rather than the state of consciousness in sleeping and anesthetized patients.

Third, decoding single-trial information can be particularly useful to the study of the transition periods between normal wakefulness and loss of consciousness. Unlike vegetative and minimally conscious state patients, the precise time at which sleeping and anesthetized subjects lose consciousness is relatively precise, and can thus be well identified (*e.g.* by asking subjects to press a button every time they hear a sound). With single-trial analyses, one could thus identify whether the disappearance of the late P3b is sudden and all-or-none, or, on the contrary, whether this EEG component gradually decreases over time. Similarly, this approach could help determine whether the EEG markers of consciousness all reflect different facets of a single coherent neural mechanism, or, conversely, whether these markers could be dissociated along the progressive loss of consciousness.

Finally, single trial analyses are particularly important for patients suffering from disorders of consciousness. As detailed in the introduction, patients' arousal fluctuates. Moreover, recent evidence suggests that their wake-sleep cycles may be partially impaired (LANDSNESS ET AL., 2011; COLOGAN ET AL., 2013; CRUSE ET AL., 2013B). Beyond providing a discrete and unique diagnosis, it would therefore be crucial to identify the precise moments at which these patients are most likely to consciously perceive their surrounding environment. Not only could these time periods constitute critical windows of communication, but it would extend the present "correlational" approach to a more causal investigation. In particular, one could design a "closed-loop" experiment in which patients' brain activity is monitored in real time. Pleasant stimuli could then be presented when patients' EEG activity suggests a conscious state (*e.g.* when wSMI is high, delta power is low *etc.*) in order to help and motivate them to remain conscious. Crucially, such a study might transform current diagnostic tools into a therapeutic approach.

9.4.3. TOWARD A DESCRIPTION OF CONSCIOUS PERCEPTION AS A PERCEPTUAL INFERENCE

The methodological tools developed throughout thesis have been accompanied by theoretical considerations. In particular, in CHAPTER 8. , I have argued that conscious perception could be formally described as a perceptual inference. This proposal is not unique in the community (*e.g.* (KNILL AND POUGET, 2004; GOLD AND SHADLEN, 2007; LAU, 2008)), but the existence of unconscious inferences raises a number of questions. If both conscious and unconscious perceptions are inferences, why do they feel so different? What makes some inferences conscious? I have shown how extending the classic unidimen-

sional depiction of Signal Detection Theory to a two dimensional problem can provide a formal yet intuitive explanation of conscious and unconscious inferences. This framework allows the experimental tasks used in consciousness research to be described as multi-feature (*sensory information is coming from multiple channels*) and multi-class (*more than two hypotheses can be considered at once*) problems. This view can account for a number of paradoxical findings observed over the past decades in consciousness research (*e.g.* blindsight, significant discrimination under subjective reports of invisibility *etc.*). The main strength of this proposal probably lies in its simplicity. If valid, the generic principles of signal detection theory (SDT) and Bayesian theory could be adopted and applied to the specific case of conscious and unconscious perception. In particular, the elementary components of this inference (*i.e.* the number of hypotheses considered, the mean and variance of their respective likelihood functions, priors and costs *etc.*) could be directly manipulated by the experimenter.

I have already empirically tested one of the behavioural predictions of this model – the link between visibility reports and the non-linear relationship between stimulus intensity and discrimination performance (CHAPTER 8.). An obvious avenue of research would thus consist in translating this behavioural experiment to a neuroimaging study. Such approach could provide two general advantages:

- First, most experiments contrast visibility conditions independently of the actual content that was reported as "seen". For example, in del Cul's experiment (DEL CUL ET AL., 2007), subjects were asked to discriminate a variably masked digit and report its visibility. The EEG signals were then compared across SOA and visibility, independently of the actual nature of the target (*i.e.* whether the digit was higher or lower than 5). It is thus unclear whether the brain response that correlates with visibility reports actually reflects content-specific information or whether it reflects a non-specific response related to attention, arousal, recruitment of mnemonic processes *etc.* This limitation could be significantly improved thanks to multivariate pattern analyses. By decoding the brain responses to subliminal and supraliminal stimuli, we could determine whether these representations share a similar format, are re-activated and/or sustained across time.

- Second, consciousness studies have generally focused on a single component of the SDT / Bayesian computation and did not systematically compare the impact of each of these factor on brain activity (although see (MELLONI ET AL., 2011)). Varying priors, stimulus evidence, task relevance *etc.* could recruit different brain regions, different cortical layers, and generate different dynamics of neural responses. An obvious avenue of research would thus consists in testing these different manipulations within the very same study, and thus isolate the neural mechanisms responsible for conscious inferences.

This area of research remains largely unexplored. Interestingly, the decoding techniques developed in CHAPTER 3. and CHAPTER 4. provide could help clarifying a number of questions: does task relevance only vary the intensity and the sharpness of the neural activity (*e.g.* (REYNOLDS ET AL., 1999; WYART ET AL., 2011; ZHANG ET AL., 2011)) or can it also delay or speed up the bottom-up and top-down signals (*e.g.* (WELFORD, 1952; MARTI ET AL., 2012))? Do prior expectations bias the decoded representations at all, or only at some specific stages of the hierarchical processing (*e.g.* (SUMMERFIELD AND KOECHLIN, 2008; KOK ET AL., 2012))? Are expectation-related signals triggered before or after the presentation of the stimulus? The perceptual decision framework combined with the decoding methods developed in the present thesis open up the possibility of clarifying and refining the way our brain actively interpret its surrounding environment. Ultimately, tightly connecting the perceptual inference and loss-of-consciousness literatures could substantially help diagnose unresponsive patients' state of consciousness.

CONCLUSION

We have gone a long way since the philosophical considerations on the dualistic or monistic nature of our mental life. Throughout the thesis, I have tried to show how the often loosely-defined concept of consciousness could, in fact, be formally and systematically tackled in the laboratory. In particular, the dissociation between cognitive processes and subjective experience has helped us to isolate the neural mechanisms that allow one to consciously perceive – *to actively and accurately interpret* – his or her surrounding environment.

In the present thesis, I primarily focused on determining whether these neural systems could help differentiating the state of consciousness of awake but non-communicating patients. Following the convergent predictions of several leading computational and neuronal models of conscious processing (TONONI AND EDELMAN, 1998; DEHAENE AND NACCACHE, 2001; DEHAENE ET AL., 2003; LAMME, 2003, 2006B, 2010; TONONI, 2004, 2008; DEL CUL ET AL., 2006; DEHAENE AND CHANGEUX, 2011), I have shown that vegetative state patients can be distinguished from minimally conscious and conscious patients through a series of different brain activity measures. These various electrophysiological markers suggest that conscious perception relies on a distributed neural network that supports the selection, the maintenance and the sharing of information across cortical modules.

While the ins and outs of consciousness remain to be fully explained, I hope that the modest contribution of the present thesis to our scientific understanding of subjective experience will prove useful to the diagnosis, the monitoring and the care of non-communicating patients.

REFERENCES

ADRIAN ED, MATTHEWS BHC (1934) The Berger rhythm: potential changes from the occipital lobes in man. Brain 57:355–385.

ALBERS AM, KOK P, TONI I, DIJKERMAN HC, DE LANGE FP, LANGE FP DE (2013) Shared representations for working memory and mental imagery in early visual cortex. Current Biology 23:1427–1431.

ALKIRE M (2009) General Anesthesia and Consciousness. In: The neurology of consciousness: cognitive neuroscience and neuropathology, pp 118–134.

ALKIRE MT, HAIER RJ, BARKER SJ, SHAH NK, WU JC, KAO YJ (1995) Cerebral metabolism during propofol anesthesia in humans studied with positron emission tomography. Anesthesiology 82:393–403; discussion 27A.

ALKIRE MT, HAIER RJ, SHAH NK, ANDERSON CT (1997) Positron emission tomography study of regional cerebral metabolism in humans during isoflurane anesthesia. Anesthesiology 86:549–557.

ALKIRE MT, HUDETZ AG, TONONI G (2008) Consciousness and Anesthesia. 322:876–880.

ALKIRE MT, MILLER J (2006) General anesthesia and the neural correlates of consciousness. The Boundaries of Consciousness: Neurobiology and Neuropathology:229.

ALLEN J, KRAUS N, BRADLOW A (2000) Neural representation of consciously imperceptible speech sound differences. Perception & psychophysics 62:1383–1393.

AMMERMANN H, KASSUBEK J, LOTZE M, GUT E, KAPS M, SCHMIDT J, RODDEN F A, GRODD W (2007) MRI brain lesion patterns in patients in anoxia-induced vegetative state. Journal of the neurological sciences 260:65–70.

AMOR F, BAILLET S, NAVARRO V, ADAM C, MARTINERIE J, QUYEN ML VAN (2009) Cortical local and long-range synchronization interplay in human absence seizure initiation. NeuroImage 45:950–962.

AMZICA F, STERIADE M (1998) Electrophysiological correlates of sleep delta waves. Electroencephalography and clinical neurophysiology 107:69–83.

ANDERSON RE, JAKOBSSON JG (2004) Entropy of EEG during anaesthetic induction: a comparative study with propofol or nitrous oxide as sole agent . British Journal of Anaesthesia 92:167–170.

ANDREWS K, MURPHY L, MUNDAY R, LITTLEWOOD C (1996) Misdiagnosis of the vegetative state: retrospective study in a rehabilitation unit. BMJ (Clinical research ed) 313:13–16.

ANDRONACHE A, ROSAZZA C, SATTIN D, LEONARDI M, D'INCERTI L, MINATI L (2013) Impact of functional MRI data preprocessing pipeline on default-mode network detectability in patients with disorders of consciousness. Frontiers in neuroinformatics 7:16.

ANSELL BJ, KEENAN JE (1989) The Western Neuro Sensory Stimulation Profile: a tool for assessing slow-to-recover head-injured patients. Archives of physical medicine and rehabilitation 70:104–108.

ARTHUIS M, VALTON L, RÉGIS J, CHAUVEL P, WENDLING F, NACCACHE L, BERNARD C, BARTOLOMEI F (2009) Impaired consciousness during temporal lobe seizures is related to increased long-distance cortical-subcortical synchronization. Brain 132:2091–2101.

ARU J, AXMACHER N, DO LAM AT A, FELL J, ELGER CE, SINGER W, MELLONI L (2012a) Local category-specific gamma band responses in the visual cortex do not reflect conscious perception. The Journal of Neuroscience 32:14909–14914.

ARU J, BACHMANN T (2009a) Boosting up gamma-band oscillations leaves target-stimulus in masking out of awareness: Explaining an apparent paradox. Neuroscience letters 450:351–355.

ARU J, BACHMANN T (2009b) Occipital EEG correlates of conscious awareness when subjective target shine-through and effective visual masking are compared: bifocal early increase in gamma power and speed-up of P1. Brain research 1271:60–73.

ARU J, SINGER W, BACHMANN T, MELLONI L (2012b) Distilling the neural correlates of consciousness. Neuroscience & Biobehavioral Reviews 36:737–746.

ATIENZA M, CANTERO JL, ESCERA C (2001) Auditory information processing during human sleep as revealed by event-related brain potentials. Clinical Neurophysiology 112:2031–2045.

ATIENZA M, CANTERO JL, GÓMEZ CM, CANTERO L (1997) The mismatch negativity component reveals the sensory memory during REM sleep in humans. Neuroscience letters 237:21–24.

AVIDAN MS, JACOBSOHN E, GLICK D, BURNSIDE BA, ZHANG L, VILLAFRANCA A, KARL L, KAMAL S, TORRES B, O'CONNOR M, EVERS AS, GRADWOHL S, LIN N, PALANCA BJ, MASHOUR GA (2011) Prevention of intraoperative awareness in a high-risk surgical population. The New England Journal of Medicine 365:591–600.

BAARS BJ (1989) A Cognitive Theory of Consciousness (Cambridge MUP, ed).

BABILONI C, SARÀ M, VECCHIO F, PISTOIA F, SEBASTIANO F, ONORATI P, ALBERTINI G, PASQUALETTI P, CIBELLI G, BUFFO P, ROSSINI PM (2009) Cortical sources of resting-state alpha rhythms are abnormal in persistent vegetative state patients. Clinical neurophysiology 120:719–729.

BADDELEY AD, HITCH G (1975) Working Memory. The psychology of learning and motivation 8:47–89.

BAGSHAW AP, CAVANNA AE (2011) Brain mechanisms of altered consciousness in focal seizures. Behavioural neurology 24:35–41.

BALCONI M, ARANGIO R, GUARNERIO C (2013) Disorders of Consciousness and N400 ERP Measures in Response to a Semantic Task. The Journal of neuropsychiatry and clinical neurosciences 25:237–243.

BANDT C, POMPE B (2002) Permutation entropy: a natural complexity measure for time series. Physical review letters 88:174102.

BARCELÓ F, SUWAZONO S, KNIGHT RT (2000) Prefrontal modulation of visual processing in humans. Nature neuroscience 3:399–403.

BARDIN JC, FINS JJ, KATZ DI, HERSH J, HEIER L A, TABELOW K, DYKE JP, BALLON DJ, SCHIFF ND, VOSS HU (2011) Dissociations between behavioural and functional magnetic resonance imaging-based evaluations of cognitive function after brain injury. Brain 134:769–782.

BARRETT AB, MURPHY M, BRUNO M-A, NOIRHOMME Q, BOLY M, LAUREYS S, SETH AK (2012) Granger causality analysis of steady-state electroencephalographic signals during propofol-induced anaesthesia. PLoS ONE 7:e29072.

BARTOLOMEI F, NACCACHE L (2011) The global workspace (GW) theory of consciousness and epilepsy. Behavioural neurology 24:67–74.

BASTUJI H, GARCÍA-LARREA L, FRANC C, MAUGUIÈRE F (1995) Brain processing of stimulus deviance during slow-wave and paradoxical sleep: a study of human auditory evoked responses using the oddball paradigm. Journal of clinical neurophysiology 12:155–167.

BATTERINK L, KARNS CM, NEVILLE H (2012) Dissociable mechanisms supporting awareness: the P300 and gamma in a linguistic attentional blink task. Cerebral cortex 22:2733–2744.

BATTERINK L, NEVILLE HJ (2013) The human brain processes syntax in the absence of conscious awareness. The Journal of Neuroscience 33:8528–8533.

BAYNE T (2011) The presence of consciousness in absence seizures. Behavioural neurology 24:47–53.

BECK DM, REES G, FRITH CD, LAVIE N (2001) Neural correlates of change. :645–650.

BEKINSCHTEIN T A., DEHAENE S, ROHAUT B, TADEL F, COHEN L, NACCACHE L (2009) Neural signature of the conscious processing of auditory regularities. Proceedings of the National Academy of Sciences of the United States of America 106:1672–1677.

BERGER H (1929) Über das Elektrenkephalogramm des Menschen. Archiv für Psychiatrie und Nervenkrankheiten 87:527–570.

BERNAT E, BUNCE S, SHEVRIN H (2001a) Event-related brain potentials differentiate positive and negative mood adjectives during both supraliminal and subliminal visual processing. International Journal of Psychophysiology 42:11–34.

BERNAT E, SHEVRIN H, SNODGRASS M (2001b) Subliminal visual oddball stimuli evoke a P300 component. Clinical neurophysiology 112:159–171.

BEUTHIEN-BAUMANN B, HANDRICK W, SCHMIDT T, BURCHERT W, OEHME L, KROPP J, SCHACKERT G, PINKERT J, FRANKE W-G (2003) Persistent vegetative state: evaluation of brain metabolism and brain perfusion with PET and SPECT. Nuclear medicine communications 24:643–649.

BINDER JR, FROST JA, HAMMEKE TA, BELLGOWAN PS, RAO SM, COX RW (1999) Conceptual processing during the conscious resting state. A functional MRI study. Journal of cognitive neuroscience 11:80–95.

BISCHOFF-GRETHE A, PROPER SM, MAO H, DANIELS KA, BERNS GS, TECH G, BIOMEDICAL E (2000) Conscious and Unconscious Processing of Nonverbal Predictability in Wernicke ' s Area. 20:1975–1981.

BLANKENBURG F, TASKIN B, RUBEN J, MOOSMANN M, RITTER P, CURIO G (2003) Sensory Processing Impediment. 299:12200.

BLUME WT, LEMIEUX JF (1988) Morphology of spikes in spike-and-wave complexes. Electroencephalography and clinical neurophysiology 69:508–515.

BLUMENFELD H (2005) Consciousness and epilepsy: why are patients with absence seizures absent? Progress in brain research 150:271–286.

BLUMENFELD H, McNALLY K A, VANDERHILL SD, PAIGE a L, CHUNG R, DAVIS K, NORDEN AD, STOKKING R, STUDHOLME C, NOVOTNY EJ, ZUBAL IG, SPENCER SS (2004) Positive and negative network correlations in temporal lobe epilepsy. Cerebral cortex 14:892–902.

BLUMENFELD H, VARGHESE GI, PURCARO MJ, MOTELOW JE, ENEV M, McNALLY KA, LEVIN a R, HIRSCH LJ, TIKOFSKY R, ZUBAL IG, PAIGE AL, SPENCER SS (2009) Cortical and subcortical networks in human secondarily generalized tonic-clonic seizures. Brain 132:999–1012.

BODEN M (2006) Mind as Machine: A History of Cognitive Science. Oxford University Press, Inc.

BOEHLER CN, SCHOENFELD MA, HEINZE H-J, HOPF J-M (2008) Rapid recurrent processing gates awareness in primary visual cortex. Proceedings of the National Academy of Sciences of the United States of America 105:8742–8747.

BOLLIMUNTA A, CHEN Y, SCHROEDER CE, DING M (2008) Neuronal mechanisms of cortical alpha oscillations in awake-behaving macaques. The Journal of Neuroscience 28:9976–9988.

BOLY M, BALTEAU E, SCHNAKERS C, DEGUELDRE C, MOONEN G, LUXEN a, PHILLIPS C, PEIGNEUX P, MAQUET P, LAUREYS S (2007) Baseline brain activity fluctuations predict somatosensory perception in humans. Proceedings of the National Academy of Sciences of the United States of America 104:12187–12192.

BOLY M, FAYMONVILLE M-E, PEIGNEUX P, LAMBERMONT B, DAMAS P, DEL FIORE G, DEGUELDRE C, FRANCK G, LUXEN A, LAMY M, MOONEN G, MAQUET P, LAUREYS S (2004) Auditory processing in severely brain injured patients: differences between the minimally conscious state and the persistent vegetative state. Archives of neurology 61:233–238.

BOLY M, FAYMONVILLE M-E, SCHNAKERS C, PEIGNEUX P, LAMBERMONT B, PHILLIPS C, LANCELLOTTI P, LUXEN A, LAMY M, MOONEN G, MAQUET P, LAUREYS S (2008) Perception of pain in the minimally conscious state with PET activation: an observational study. Lancet neurology 7:1013–1020.

BOLY M, GARRIDO MI, GOSSERIES O, BRUNO M -A. M-A, BOVEROUX P, SCHNAKERS C, MASSIMINI M, LITVAK V, LAUREYS S, FRISTON K (2011) Preserved Feedforward But Impaired Top-Down Processes in the Vegetative State. Science (New York, NY) 332:858–862.

BOLY M, TSHIBANDA L, VANHAUDENHUYSE A, NOIRHOMME Q, SCHNAKERS C, LEDOUX D, BOVEROUX P, GARWEG C, LAMBERMONT B, PHILLIPS C, LUXEN a, MOONEN G, BASSETTI C, MAQUET P, LAUREYS S (2009) Functional connectivity in the default network during resting state is preserved in a vegetative but not in a brain dead patient. Human brain mapping 30:2393–2400.

BONHOMME V, BOVEROUX P, VANHAUDENHUYSE A, HANS P, BRICHANT JF, JAQUET O, BOLY M, LAUREYS S (2011) Linking sleep and general anesthesia mechanisms: this is no walkover. Acta anaesthesiologica Belgica 62:161–171.

BONHOMME V, FISET P, MEURET P, BACKMAN S, PLOURDE G, PAUS T, BUSHNELL MC, EVANS AC (2001) Propofol Anesthesia and Cerebral Blood Flow Changes Elicited by Vibrotactile Stimulation: A Positron Emission Tomography Study. J Neurophysiol 85:1299–1308.

BOUCHARD KE, MESGARANI N, JOHNSON K, CHANG EF (2013) Functional organization of human sensorimotor cortex for speech articulation. Nature 495:327–332.

BOYER JL, HARRISON S, RO T (2005) Unconscious processing of orientation and color without primary visual cortex. Proceedings of the National Academy of Sciences of the United States of America 102:16875–16879.

BRADLEY C, MEDDIS R (1974) Arousal threshold in dreaming sleep. Physiological Psychology 2:109–110.

BRAUN AR, BALKIN TJ, WESENTEN NJ, CARSON RE, VARGA M, BALDWIN P, SELBIE S, BELENKY G, HERSCOVITCH P (1997) Regional cerebral blood flow throughout the sleep-wake cycle. An H2(15)O PET study. Brain 120 (Pt 7:1173–1197.

BREITMEYER BG, OGMEN H (2000) Recent models and findings in visual backward masking: a comparison, review, and update. Perception & psychophysics 62:1572–1595.

BRINDLEY GS, GAUTIER-SMITH PC, LEWIN W (1969) Cortical blindness and the functions of the non-geniculate fibres of the optic tracts. Journal of neurology, neurosurgery, and psychiatry 32:259–264.

BROADBENT DE (1957) A mechanical model for human attention and immediate memory. Psychological Review 64:205–215.

BROUWER GJ, HEEGER DJ (2009) Decoding and reconstructing color from responses in human visual cortex. The Journal of Neuroscience 29:13992–14003.

BRUALLA J, ROMERO MF, SERRANO M, VALDIZÁN JR (1998) Auditory event-related potentials to semantic priming during sleep. Electroencephalography and clinical neurophysiology 108:283–290.

BRUNO M-A, GOSSERIES O, LEDOUX D, HUSTINX R, LAUREYS S (2011a) Assessment of consciousness with electrophysiological and neurological imaging techniques. Current opinion in critical care 17:146–151.

BRUNO M-A, VANHAUDENHUYSE A, SCHNAKERS C, BOLY M, GOSSERIES O, DEMERTZI A, MAJERUS S, MOONEN G, HUSTINX R, LAUREYS S (2010) Visual fixation in the vegetative state: an observational case series PET study. BMC neurology 10:35.

BRUNO M-A, VANHAUDENHUYSE A, THIBAUT A, MOONEN G, LAUREYS S (2011b) From unresponsive wakefulness to minimally conscious PLUS and functional locked-in syndromes: recent advances in our understanding of disorders of consciousness. Journal of neurology 258:1373–1384.

BRUNO MA, FERNÁNDEZ-ESPEJO D, LEHEMBRE R, TSHIBANDA L, VANHAUDENHUYSE A, GOSSERIES O, LOMMERS E, NAPOLITANI M, NOIRHOMME Q, BOLY M, PAPA M, OWEN A, MAQUET P, LAUREYS S, SODDU A (2011c) Multimodal neuroimaging in patients with disorders of consciousness showing "functional hemispherectomy". Progress in brain research 193:323–333.

BRÁZDIL M, REKTOR I, DANIEL P, DUFEK M, JURÁK P (2001) Intracerebral event-related potentials to subthreshold target stimuli. Clinical neurophysiology 112:650–661.

BUCHSBAUM MS, HAZLETT E A, WU J, BUNNEY WE (2001) Positron emission tomography with deoxyglucose-F18 imaging of sleep. Neuropsychopharmacology 25:S50–6.

BUCKNER RL, ANDREWS-HANNA JR, SCHACTER DL (2008) The brain's default network: anatomy, function, and relevance to disease. Annals of the New York Academy of Sciences 1124:1–38.

BUSCH NA, DUBOIS J, VANRULLEN R (2009) The phase of ongoing EEG oscillations predicts visual perception. The Journal of Neuroscience 29:7869–7876.

BUSEMEYER JR, POTHOS EM, FRANCO R, TRUEBLOOD JS (2011) A quantum theoretical explanation for probability judgment errors. Psychological Review 118:193–218.

BUZSAKI G (2009) Rhythms of the Brain.

BYRNE S, HARDIMAN O, MONTI MM, VANHAUDENHUYSE A, COLEMAN MR, BOLY M, PICKARD JD, TSHIBANDA L, OWEN AM, LAUREYS S (2010) c or r e sp ondence Willful Modulation of Brain Activity in Disorders of Consciousness. The New England Journal of Medicine 326:1937; author reply 1937–1938.

CAO Y, TUNG W, GAO J, PROTOPOPESCU V, HIVELY L (2004) Detecting dynamical changes in time series using the permutation entropy. Physical Review E 70:046217.

CARLSON T, TOVAR DA, KRIEGESKORTE N (2013) Representational dynamics of object vision: The first 1000 ms. 13:1–19.

CARLSON TA (2011) High temporal resolution decoding of object position and category. 11:1–17.

CARMEL D, LAVIE N, REES G (2006) Conscious awareness of flicker in humans involves frontal and parietal cortex. Current biology 16:907–911.

CASALI AG, GOSSERIES O, ROSANOVA M, BOLY M, SARASSO S, CASALI KR, CASAROTTO S, BRUNO M-A. M-A, LAUREYS S, TONONI G, MASSIMINI M (2013) A Theoretically Based Index of Consciousness Independent of Sensory Processing and Behavior. Science Translational Medicine 5:198ra105–198ra105.

CATON R (1875) Electrical Currents of the Brain. Chicago Journal of nervous & Mental Diseases 2:610.

CAUDA F, MICON BM, SACCO K, DUCA S, D'AGATA F, GEMINIANI G, CANAVERO S (2009) Disrupted intrinsic functional connectivity in the vegetative state. Journal of neurology, neurosurgery, and psychiatry 80:429–431.

CAVANAGH P (2001) Seeing the forest but not the trees. Nature neuroscience 4:673–674.

CAVINATO M, FREO U, ORI C, ZORZI M, TONIN P, PICCIONE F, MERICO A (2009) Post-acute P300 predicts recovery of consciousness from traumatic vegetative state. Brain injury 23:973–980.

CHAITIN G (1974) Information-theoretic computation complexity. IEEE Transactions on Information Theory 20:10–15.

CHAITIN G (1995) The berry paradox. Complex Systems and Binary Networks.

CHALMERS DJ (1996) The Conscious Mind: In Search of a Fundamental Theory (Flanagan O, ed). Oxford University Press.

CHAN AM, HALGREN E, MARINKOVIC K, CASH SS (2011) Decoding word and category-specific spatiotemporal representations from MEG and EEG. NeuroImage 54:3028–3039.

CHANG C, LIN C (2001) LIBSVM: a library for support vector machines. Computer 2:1–30.

CHANG EF, RIEGER JW, JOHNSON K, BERGER MS, BARBARO NM, KNIGHT RT (2010) Categorical speech representation in human superior temporal gyrus. Nature neuroscience 13:1428–1432.

CHARLES L, KING J-R, DEHAENE S (n.d.) Decoding the dynamics of action, intention, and error-detection for conscious and subliminal stimuli. The Journal of Neuroscience.

CHARLES L, VAN OPSTAL F, MARTI S, DEHAENE S (2013) Distinct brain mechanisms for conscious versus subliminal error detection. NeuroImage 73C:80–94.

CHEESMAN J, MERIKLE PM (1984) Priming with and without awareness. Perception & psychophysics 36:387–395.

CHENNU S, NOREIKA V, GUEORGUIEV D, BLENKMANN A, KOCHEN S, IBÁÑEZ A, OWEN AM, BEKINSCHTEIN TA (2013) Expectation and Attention in Hierarchical Auditory Prediction. The Journal of Neuroscience 33:11194–11205.

CHILDS NL, MERCER WN, CHILDS HW (1993) Accuracy of diagnosis of persistent vegetative state. Neurology 43:1465–1467.

CHIPAUX M, VERCUEIL L, KAMINSKA A, MAHON S, CHARPIER S (2013) Persistence of cortical sensory processing during absence seizures in human and an animal model: evidence from EEG and intracellular recordings. PloS one 8:e58180.

CHRISTOFF K, GORDON AM, SMALLWOOD J, SMITH R, SCHOOLER JW (2009) Experience sampling during fMRI reveals default network and executive system contributions to mind wandering. Proceedings of the National Academy of Sciences of the United States of America 106:8719–8724.

CHRISTOPHEL TB, HEBART MN, HAYNES J-D (2012) Decoding the contents of visual short-term memory from human visual and parietal cortex. The Journal of Neuroscience 32:12983–12989.

CIMENSER A, PURDON PL, PIERCE ET, WALSH JL, SALAZAR-GOMEZ AF, HARRELL PG, TAVARES-STOECKEL C, HABEEB K, BROWN EN (2011) Tracking brain states under general anesthesia by

using global coherence analysis. Proceedings of the National Academy of Sciences of the United States of America 108:8832–8837.

COENEN AML, VENDRIK AJH (1972) Determination of the transfer ratio of cat's geniculate neurons through quasi-intracellular recordings and the relation with the level of alertness. Experimental brain research Experimentelle Hirnforschung Expérimentation cérébrale 14:227–242.

COHEN MX, VAN GAAL S, RIDDERINKHOF KR, LAMME VAF (2009) Unconscious Errors Enhance Prefrontal-Occipital Oscillatory Synchrony. Frontiers in human neuroscience 3:12.

COLE MW, REYNOLDS JR, POWER JD, REPOVS G, ANTICEVIC A, BRAVER TS (2013) Multi-task connectivity reveals flexible hubs for adaptive task control. Nature neuroscience 16:1348–1355.

COLEMAN MR, RODD JM, DAVIS MH, JOHNSRUDE IS, MENON DK, PICKARD JD, OWEN AM (2007) Do vegetative patients retain aspects of language comprehension? Evidence from fMRI. Brain 130:2494–2507.

COLOGAN V, DROUOT X, PARAPATICS S, DELORME A, GRUBER G, MOONEN G, LAUREYS S (2013) Sleep in the unresponsive wakefulness syndrome and minimally conscious state. Journal of neurotrauma 30:339–346.

COTE K A, EPPS TM, CAMPBELL KB (2000) The role of the spindle in human information processing of high-intensity stimuli during sleep. Journal of sleep research 9:19–26.

COTE KA, CAMPBELL KB (1999) P300 to high intensity stimuli during REM sleep. Clinical Neurophysiology 110:1345–1350.

COWEY A (2010) The blindsight saga. Experimental brain research Experimentelle Hirnforschung Expérimentation cérébrale 200:3–24.

COWEY A, STOERIG P (1995) Blindsight in monkeys. Nature 373:247–249.

CRICK F, KOCH C (1990a) Toward a neurobiological theory of consciousness. Seminars in Neuroscience 2:263–275.

CRICK F, KOCH C (1990b) Some reflections on visual awareness. Cold Spring Harbor symposia on quantitative biology 55:953–962.

CRICK F, KOCH C (1998) Consciousness and neuroscience. Cerebral cortex 8:97–107.

CRONE JS, LADURNER G, HÖLLER Y, GOLASZEWSKI S, TRINKA E, KRONBICHLER M (2011) Deactivation of the default mode network as a marker of impaired consciousness: an fMRI study. PloS one 6:e26373.

CRUSE D, CHENNU S, CHATELLE C, BEKINSCHTEIN T A, FERNÁNDEZ-ESPEJO D, PICKARD JD, LAUREYS S, OWEN AM (2012) Bedside detection of awareness in the vegetative state – Authors' reply. The Lancet 379:1702.

CRUSE D, CHENNU S, CHATELLE C, BEKINSCHTEIN T A, FERNÁNDEZ-ESPEJO D, PICKARD JD, LAUREYS S, OWEN AM (2013a) Reanalysis of "Bedside detection of awareness in the vegetative state: a cohort study" - Authors' reply. Lancet 381:291–292.

CRUSE D, CHENNU S, CHATELLE C, BEKINSCHTEIN TA, FERNÁNDEZ-ESPEJO D, PICKARD JD, LAUREYS S, OWEN AM (2011) Bedside detection of awareness in the vegetative state: a cohort study. Lancet 378:2088–2094.

CRUSE D, THIBAUT A, DEMERTZI A, NANTES JC, BRUNO M-A, GOSSERIES O, VANHAUDENHUYSE A, BEKINSCHTEIN TA, OWEN AM, LAUREYS S (2013b) Actigraphy assessments of circadian sleep-wake cycles in the Vegetative and Minimally Conscious States. BMC medicine 11:18.

CUL A DEL, NACCACHE L, VINCKIER F, COHEN L, DEHAENE S, GAILLARD RR, DEL CUL A (2006) Nonconscious semantic processing of emotional words modulates conscious access. Proceedings of the National Academy of Sciences of the United States of America 103:7524–7529.

CZISCH M, WEHRLE R, STIEGLER A, PETERS H, ANDRADE K, HOLSBOER F, SÄMANN PG (2009) Acoustic oddball during NREM sleep: a combined EEG/fMRI study. PloS one 4:e6749.

CZISCH M, WETTER TC, KAUFMANN C, POLLMÄCHER T, HOLSBOER F, AUER DP (2002) Altered processing of acoustic stimuli during sleep: reduced auditory activation and visual deactivation detected by a combined fMRI/EEG study. NeuroImage 16:251–258.

DALTROZZO J, CLAUDE L, TILLMANN B, BASTUJI H, PERRIN F (2012) Working memory is partially preserved during sleep. Zang Y-F, ed. PloS one 7:e50997.

DALTROZZO J, WIOLAND N, MUTSCHLER V, KOTCHOUBEY B (2007) Predicting coma and other low responsive patients outcome using event-related brain potentials: a meta-analysis. Clinical Neurophysiology 118:606–614.

DANG-VU TT, DESSEILLES M, LAUREYS S, DEGUELDRE C, PERRIN F, PHILLIPS C, MAQUET P, PEIGNEUX P (2005) Cerebral correlates of delta waves during non-REM sleep revisited. NeuroImage 28:14–21.

DANNLOWSKI U, OHRMANN P, BAUER J, DECKERT J, HOHOFF C, KUGEL H, AROLT V, HEINDEL W, KERSTING A, BAUNE BT, SUSLOW T (2008) 5-HTTLPR biases amygdala activity in response to masked facial expressions in major depression. Neuropsychopharmacology 33:418–424.

DANNLOWSKI U, OHRMANN P, BAUER J, KUGEL H, AROLT V, HEINDEL W, KERSTING A, BAUNE BT, SUSLOW T (2007) Amygdala reactivity to masked negative faces is associated with automatic judgmental bias in major depression: a 3 T fMRI study. Journal of psychiatry & neuroscience 32:423–429.

DAVE AS, MARGOLIASH D (2000) Song Replay During Sleep and Computational Rules for Sensorimotor Vocal Learning. Science 290:812–816.

DAVIDSON TJ, KLOOSTERMAN F, WILSON MA (2009) Hippocampal replay of extended experience. Neuron 63:497–507.

DAVIS H (1964) Enhancement of Evoked Cortical Potentials in Humans Related to a Task Requiring a Decision. Science 145:182–183.

DAVIS MH, COLEMAN MR, ABSALOM AR, RODD JM, JOHNSRUDE IS, MATTA BF, OWEN AM, MENON DK (2007) Dissociating speech perception and comprehension at reduced levels of awareness. Proceedings of the National Academy of Sciences of the United States of America 104:16032–16037.

DE GARDELLE V, CHARLES L, KOUIDER S (2011) Perceptual awareness and categorical representation of faces: Evidence from masked priming. Consciousness and Cognition 20:1–10.

DE JONG BM, WILLEMSEN A T, PAANS AM (1997) Regional cerebral blood flow changes related to affective speech presentation in persistent vegetative state. Clinical neurology and neurosurgery 99:213–216.

DE LANGE FP, VAN GAAL S, LAMME V A F, DEHAENE S (2011) How awareness changes the relative weights of evidence during human decision-making. PLoS biology 9:e1001203.

DECO G, PÉREZ-SANAGUSTÍN M, DE LAFUENTE V, ROMO R, PE M (2007) Perceptual detection as a dynamical bistability phenomenon: A neurocomputational correlate of sensation. Proceedings of the National Academy of Sciences of the United States of America 104:20073–20077.

DEHAENE S (1996) The organization of brain activations in number comparison: Event-related potentials and the additive-factors methods. Journal of Cognitive Neuroscience 8:47–68.

DEHAENE S (2009) Conscious and Nonconscious Processes: Distinct Forms of Evidence Accumulation? Engel C, Singer W, eds. Seminaire Poincare XII:89 – 114.

DEHAENE S, CHANGEUX J-P (2005) Ongoing spontaneous activity controls access to consciousness: a neuronal model for inattentional blindness. Abbott L, ed. PLoS biology 3:e141.

DEHAENE S, CHANGEUX J-P (2011) Experimental and theoretical approaches to conscious processing. Neuron 70:200–227.

DEHAENE S, CHANGEUX J-P, NACCACHE L, SACKUR J, SERGENT C (2006a) Conscious, preconscious, and subliminal processing: a testable taxonomy. Trends in cognitive sciences 10:204–211.

DEHAENE S, CHANGEUX JP, NACCACHE L, SACKUR J, SERGENT C (2006b) Conscious, preconscious, and subliminal processing: a testable taxonomy. Trends in Cognitive Sciences 10:204–211.

DEHAENE S, JOBERT A, NACCACHE L, CIUCIU P, POLINE J-B, LE BIHAN D, COHEN L (2004) Letter binding and invariant recognition of masked words: behavioral and neuroimaging evidence. Psychological science 15:307–313.

DEHAENE S, KERSZBERG M, CHANGEUX JP (1998a) A neuronal model of a global workspace in effortful cognitive tasks. Proceedings of the National Academy of Sciences of the United States of America 95:14529–14534.

DEHAENE S, NACCACHE L (2001) Towards a cognitive neuroscience of consciousness: basic evidence and a workspace framework. The cognitive neuroscience of consciousness:1–37.

DEHAENE S, NACCACHE L, COHEN L, BIHAN DL, MANGIN JF, POLINE JB, RIVIÈRE D (2001) Cerebral mechanisms of word masking and unconscious repetition priming. Nature neuroscience 4:752–758.

DEHAENE S, NACCACHE L, LE CLEC'H G, KOECHLIN E, MUELLER M, DEHAENE-LAMBERTZ G, VAN DE MOORTELE PF, LE BIHAN D (1998b) Imaging unconscious semantic priming. Nature 395:597–599.

DEHAENE S, SERGENT C, CHANGEUX J-P (2003) A neuronal network model linking subjective reports and objective physiological data during conscious perception. Proceedings of the National Academy of Sciences of the United States of America 100:8520–8525.

DEL CUL A, DEHAENE S, REYES P, BRAVO E, SLACHEVSKY A (2009) Causal role of prefrontal cortex in the threshold for access to consciousness. Brain 132:2531–2540.

DEL CUL A, BAILLET S, DEHAENE S, CUL A DEL (2007) Brain dynamics underlying the nonlinear threshold for access to consciousness. PLoS biology 5:e260.

DEL CUL A, DEHAENE S, LEBOYER M (2006) Preserved subliminal processing and impaired conscious access in schizophrenia. Archives of general psychiatry 63:1313–1323.

DENEVE S, LATHAM PE, POUGET A (1999) Reading population codes: a neural implementation of ideal observers. Nature neuroscience 2:740–745.

DENG S, SRINIVASAN R, LAPPAS T, D'ZMURA M (2010) EEG classification of imagined syllable rhythm using Hilbert spectrum methods. Journal of neural engineering 7:046006.

DENNETT DC (1992) Consciousness Explained. Back Bay Books.

DESMEDT JE, DEBECKER J, MANIL J (1965a) [Demonstration of a cerebral electric sign associated with the detection by the subject of a tactile sensorial stimulus. The analysis of cerebral evoked potentials derived from the scalp with the aid of numerical ordinates]. Bulletin de l'Académie royale de médecine de Belgique 5:887–936.

DESMEDT JE, DEBRECKER J, J. M (1965b) Mise en évidence d'un signe électrique cérébral associé à la détection par le sujet d'un stimulus sensoriel tactile. Bulletin et Mémoire de l'Academie Royale de Médecine de Belgique 5:887–936.

DESTEXHE A (2000) Modelling corticothalamic feedback and the gating of the thalamus by the cerebral cortex. Journal of physiology, Paris 94:391–410.

DEVLIN JT, JAMISON HL, MATTHEWS PM, GONNERMAN LM (2004) Morphology and the internal structure of words. Proceedings of the National Academy of Sciences of the United States of America 101:14984–14988.

DEVOLDER AG, GOFFINET AM, BOL A, MICHEL C, DE BARSY T, LATERRE C (1990) Brain glucose metabolism in postanoxic syndrome. Positron emission tomographic study. Archives of neurology 47:197–204.

DICARLO JJ, ZOCCOLAN D, RUST NC (2012) How does the brain solve visual object recognition? Neuron 73:415–434.

DIEKELMANN S, BORN J (2010) The memory function of sleep. Nature reviews Neuroscience 11:114–126.

DIEKHOF EK, BIEDERMANN F, RUEBSAMEN R, GRUBER O (2009) Top-down and bottom-up modulation of brain structures involved in auditory discrimination. Brain research 1297:118–123.

DIMITROV AG, LAZAR AA, VICTOR JD (2011) Information theory in neuroscience. Journal of computational neuroscience 30:1–5.

DONDERS FC (1969) On the speed of mental processes (translation). Acta Psychologica 30:412–431.

DOYA K (2007) Bayesian Brain: Probabilistic Approaches to Neural Coding (Doya K, Ishii S, Pouget A, Rao RPN, eds). MIT Press.

DRESLER M, KOCH SP, WEHRLE R, SPOORMAKER VI, HOLSBOER F, STEIGER A, SÄMANN PG, OBRIG H, CZISCH M (2011) Dreamed movement elicits activation in the sensorimotor cortex. Current Biology 21:1833–1837.

DRIVER J, VUILLEUMIER P, EIMER M, REES G (2001) Functional magnetic resonance imaging and evoked potential correlates of conscious and unconscious vision in parietal extinction patients. NeuroImage 14:S68–S75.

DUNCAN CC, MIRSKY AF, LOVELACE CT, THEODORE WH (2009) Assessment of the attention impairment in absence epilepsy: comparison of visual and auditory P300. International journal of psychophysiology 73:118–122.

DUNCAN KK, HADJIPAPAS A, LI S, KOURTZI Z, BAGSHAW A, BARNES G (2010) Identifying spatially overlapping local cortical networks with MEG. Human Brain Mapping 31:1003–1016.

DUPOUX E, DE GARDELLE V, KOUIDER S (2008) Subliminal speech perception and auditory streaming. Cognition 109:267–273.

EDDY MD, SCHNYER D, SCHMID A, HOLCOMB PJ (2007) Spatial dynamics of masked picture repetition effects. NeuroImage 34:1723–1732.

EDELMAN GM (1989) The remembered present: a biological theory of consciousness. Basic Books.

EDELMAN GM (1993) Neural Darwinism: selection and reentrant signaling in higher brain function. Neuron 10:115–125.

EDELMAN GM, TONONI G (2000) A universe of consciousness: How matter becomes imagination. Basic books.

ELTON M, WINTER O, HESLENFELD D, LOEWY D, CAMPBELL K, KOK A (1997) Event-related potentials to tones in the absence and presence of sleep spindles. Journal of sleep research 6:78–83.

ENGEL A K, FRIES P, SINGER W (2001) Dynamic predictions: oscillations and synchrony in top-down processing. Nature reviews Neuroscience 2:704–716.

ENGEL A K, SINGER W (2001) Temporal binding and the neural correlates of sensory awareness. Trends in cognitive sciences 5:16–25.

ENGEL J (2013) Seizures and Epilepsy.

ERIKSEN CW (1960) Discrimination and learning without awareness: A methodological survey and evaluation. Psychological Review 67:279–300.

FAHRENFORT JJ, SCHOLTE HS, LAMME V A F (2007) Masking disrupts reentrant processing in human visual cortex. Journal of cognitive neuroscience 19:1488–1497.

FAHRENFORT JJ, SNIJDERS TM, HEINEN K, VAN GAAL S, SCHOLTE HS, LAMME VAF, GAAL S VAN (2012) Neuronal integration in visual cortex elevates face category tuning to conscious face perception. Proceedings of the National Academy of Sciences of the United States of America 109:21504–21509.

FANG F, HE S (2005) Cortical responses to invisible objects in the human dorsal and ventral pathways. Nature neuroscience 8:1380–1385.

FAUGERAS F, ROHAUT B, WEISS N, BEKINSCHTEIN T A, GALANAUD D, PUYBASSET L, BOLGERT F, SERGENT C, COHEN L, DEHAENE S, NACCACHE L (2011) Probing consciousness with event-related potentials in the vegetative state. Neurology 77:264–268.

FAUGERAS F, ROHAUT B, WEISS N, BEKINSCHTEIN T, GALANAUD D, PUYBASSET L, BOLGERT F, SERGENT C, COHEN L, DEHAENE S, NACCACHE L (2012) Event related potentials elicited by violations of auditory regularities in patients with impaired consciousness. Neuropsychologia 50:403–418.

FELLINGER R, KLIMESCH W, SCHNAKERS C, PERRIN F, FREUNBERGER R, GRUBER W, LAUREYS S, SCHABUS M (2011) Cognitive processes in disorders of consciousness as revealed by EEG time-frequency analyses. Clinical neurophysiology□: official journal of the International Federation of Clinical Neurophysiology 122:2177–2184.

FERNANDEZ-DUQUE D, GROSSI G, THORNTON IM, NEVILLE HJ (2003) Representation of change: separate electrophysiological markers of attention, awareness, and implicit processing. Journal of cognitive neuroscience 15:491–507.

FERNÁNDEZ-ESPEJO D, BEKINSCHTEIN T, MONTI MM, PICKARD JD, JUNQUE C, COLEMAN MR, OWEN AM (2011) Diffusion weighted imaging distinguishes the vegetative state from the minimally conscious state. NeuroImage 54:103–112.

FERRARELLI F, MASSIMINI M, SARASSO S, CASALI A, RIEDNER B A, ANGELINI G, TONONI G, PEARCE R A (2010) Breakdown in cortical effective connectivity during midazolam-induced loss of consciousness. Proceedings of the National Academy of Sciences of the United States of America 107:2681–2686.

FIEZ JA, PETERSEN SE (1998) Neuroimaging studies of word reading. Proceedings of the National Academy of Sciences of the United States of America 95:914–921.

FINELLI LA, BORBELY AA, ACHERMANN P (2001) Functional topography of the human nonREM sleep electroencephalogram. European Journal of Neuroscience 13:2282–2290.

FINGELKURTS A A, FINGELKURTS A A, BAGNATO S, BOCCAGNI C, GALARDI G (2012a) EEG oscillatory states as neuro-phenomenology of consciousness as revealed from patients in vegetative and minimally conscious states. Consciousness and cognition 21:149–169.

FINGELKURTS AA, FINGELKURTS AA, BAGNATO S, BOCCAGNI C, GALARDI G (2012b) DMN Operational Synchrony Relates to Self-Consciousness: Evidence from Patients in Vegetative and Minimally Conscious States. The open neuroimaging journal 6:55–68.

FINS JJ, ILLES J, BERNAT JL, HIRSCH J, LAUREYS S, MURPHY E (2008) Neuroimaging and disorders of consciousness: envisioning an ethical research agenda. The American journal of bioethics 8:3–12.

FISCH L, PRIVMAN E, RAMOT M, HAREL M, NIR Y, KIPERVASSER S, ANDELMAN F, NEUFELD MY, KRAMER U, FRIED I, MALACH R (2009) Neural "ignition": enhanced activation linked to perceptual awareness in human ventral stream visual cortex. Neuron 64:562–574.

FISCHER C, LUAUTE J, ADELEINE P, MORLET D, LUAUTÉ J (2004) Predictive value of sensory and cognitive evoked potentials for awakening from coma. Neurology 63:669–673.

FISCHER C, LUAUTE J, MORLET D (2010) Event-related potentials (MMN and novelty P3) in permanent vegetative or minimally conscious states. Clinical neurophysiology 121:1032–1042.

FISCHER C, LUAUTÉ J (2005) Evoked potentials for the prediction of vegetative state in the acute stage of coma. Neuropsychological rehabilitation 15:372–380.

FISCHER C, MORLET D, BOUCHET P, LUAUTE J, JOURDAN C, SALORD F (1999) Mismatch negativity and late auditory evoked potentials in comatose patients. Clinical neurophysiology 110:1601–1610.

FISET P, PAUS T, DALOZE T, PLOURDE G, MEURET P, BONHOMME V, HAJJ-ALI N, BACKMAN SB, EVANS AC (1999) Brain mechanisms of propofol-induced loss of consciousness in humans: a positron emission tomographic study. The Journal of Neuroscience 19:5506–5513.

FISHER RS, VAN EMDE BOAS W, BLUME W, ELGER C, GENTON P, LEE P, ENGEL J (2005) Epileptic seizures and epilepsy: definitions proposed by the International League Against Epilepsy (ILAE) and the International Bureau for Epilepsy (IBE). Epilepsia 46:470–472.

FLEMING SM, WEIL RS, NAGY Z, DOLAN RJ, REES G (2010) Relating Introspective Accuracy to Individual Differences in Brain Structure. Science 329:1541–1543.

FODOR JA (1983) The Modularity of Mind: An Essay on Faculty Psychology (Livre numérique Google). MIT Press.

FORMISANO E, DE MARTINO F, BONTE M, GOEBEL R (2008) "Who" is saying "what"? Brain-based decoding of human voice and speech. Science (New York, NY) 322:970–973.

FOSTER DJ, WILSON M A (2006) Reverse replay of behavioural sequences in hippocampal place cells during the awake state. Nature 440:680–683.

FOX MD, CORBETTA M, SNYDER AZ, VINCENT JL, RAICHLE ME (2006) Spontaneous neuronal activity distinguishes human dorsal and ventral attention systems. Proceedings of the National Academy of Sciences of the United States of America 103:10046–10051.

FRANKS NP (2008) General anaesthesia: from molecular targets to neuronal pathways of sleep and arousal. Nature reviews Neuroscience 9:370–386.

FRANKS NP, ZECHARIA AY (2011) Sleep and general anesthesia. Canadian journal of anaesthesia = Journal canadien d'anesthésie 58:139–148.

FREEDMAN DJ, RIESENHUBER M, POGGIO T, MILLER EK (2002) Visual categorization and the primate prefrontal cortex: neurophysiology and behavior. Journal of neurophysiology 88:929–941.

FREEMAN J, BROUWER GJ, HEEGER DJ, MERRIAM EP (2011) Orientation decoding depends on maps, not columns. The Journal of neuroscience 31:4792–4804.

FRENCH JD (1952) Brain lesions associated with prolonged unconsciousness. AMA archives of neurology and psychiatry 68:727–740.

FRIES P (2005) A mechanism for cognitive dynamics: neuronal communication through neuronal coherence. Trends in cognitive sciences 9:474–480.

FRIES P, NEUENSCHWANDER S, ENGEL A K, GOEBEL R, SINGER W (2001) Rapid feature selective neuronal synchronization through correlated latency shifting. Nature neuroscience 4:194–200.

FRIES P, ROELFSEMA PR, ENGEL A K, KÖNIG P, SINGER W (1997) Synchronization of oscillatory responses in visual cortex correlates with perception in interocular rivalry. Proceedings of the National Academy of Sciences of the United States of America 94:12699–12704.

FRIES P, WOMELSDORF T, OOSTENVELD R, DESIMONE R (2008) The effects of visual stimulation and selective visual attention on rhythmic neuronal synchronization in macaque area V4. The Journal of Neuroscience 28:4823–4835.

FRISTON K (2005) A theory of cortical responses. Philosophical Transactions of the Royal Society of London - Series B: Biological Sciences 360:815–836.

FRISTON K (2010) The free-energy principle: a unified brain theory? Nature reviews Neuroscience 11:127–138.

FUENTEMILLA L, PENNY WD, CASHDOLLAR N, BUNZECK N, DÜZEL E (2010) Theta-coupled periodic replay in working memory. Current Biology 20:606–612.

FUSTER JM (2008) The Prefrontal Cortex (Raven, ed). Academic Press.

GAILLARD R, DEHAENE S, ADAM C, CLÉMENCEAU S, HASBOUN D, BAULAC M, COHEN L, NACCACHE L (2009) Converging intracranial markers of conscious access. PLoS Biology 7:1–21.

GALANAUD D ET AL. (2012) Assessment of White Matter Injury and Outcome in Severe Brain Trauma: A Prospective Multicenter Cohort. Anesthesiology 117:1300–1310.

GALLANT J, NASELARIS T, PRENGER R, KAY K, STANSBURY D, OLIVER M, VU A, NISHIMOTO S (2009) Bayesian Reconstruction of Perceptual Experiences from Human Brain Activity. In: Foundations of Augmented Cognition. Neuroergonomics and Operational Neuroscience, pp 393. Springer.

GARCIA JO, SRINIVASAN R, SERENCES JT (2013) Near-real-time feature-selective modulations in human cortex. Current Biology 23:515–522.

GARDELLE V DE, KOUIDER S (2009) Cognitive Theories of Consciousness. In: Encyclopedia of Consciousness.

GARRETT DD, KOVACEVIC N, MCINTOSH AR, GRADY CL (2010) Blood oxygen level-dependent signal variability is more than just noise. The Journal of neuroscience 30:4914–4921.

GARRIDO MI, FRISTON KJ, KIEBEL SJ, STEPHAN KE, BALDEWEG T, KILNER JM (2008) The functional anatomy of the MMN: a DCM study of the roving paradigm. NeuroImage 42:936–944.

GARRIDO MI, KILNER JM, KIEBEL SJ, STEPHAN KE, FRISTON KJ (2007) Dynamic causal modelling of evoked potentials: a reproducibility study. NeuroImage 36:571–580.

GARRIDO MI, KILNER JM, STEPHAN KE, FRISTON KJ (2009) The mismatch negativity: a review of underlying mechanisms. Clinical neurophysiology 120:453–463.

GAUCHET M (1992) L'Inconscient cérébral. Seuil.

GERSHMAN SJ, VUL E, TENENBAUM JB (2012) Multistability and Perceptual Inference. Neural Computation 24:1–24.

GIACINO JT, ASHWAL S, CHILDS N, CRANFORD R, JENNETT B, KATZ DI, KELLY JP, ROSENBERG JH, WHYTE J, ZAFONTE RD (2002) The minimally conscious state: Definition and diagnostic criteria. Neurology 58:349.

GIACINO JT, HIRSCH J, SCHIFF N, LAUREYS S (2006) Functional neuroimaging applications for assessment and rehabilitation planning in patients with disorders of consciousness. Archives of physical medicine and rehabilitation 87:S67–76.

GIACINO JT, KALMAR K (2005) Diagnostic and prognostic guidelines for the vegetative and minimally conscious states. Neuropsychological rehabilitation 15:166–174.

GIACINO JT, KALMAR K, WHYTE J (2004) The JFK Coma Recovery Scale-Revised: measurement characteristics and diagnostic utility. Archives of physical medicine and rehabilitation 85:2020.

GIACINO JT, SCHNAKERS C, RODRIGUEZ-MORENO D, KALMAR K, SCHIFF N, HIRSCH J (2009) Behavioral assessment in patients with disorders of consciousness: gold standard or fool's gold? Elsevier.

GIFANI P, RABIEE HR, HASHEMI M, GHANBARI M (2007) Dimensional characterization of anesthesia dynamic in reconstructed embedding space. Conference proceedings: . Annual International Conference of the IEEE Engineering in Medicine and Biology Society IEEE Engineering in Medicine and Biology Society Conference 2007:6484–6487.

GILBERT SJ, DUMONTHEIL I, SIMONS JS, FRITH CD, BURGESS PW (2007) Comment on "Wandering minds: the default network and stimulus-independent thought". Science (New York, NY) 317:43; author reply 43.

GILL-THWAITES H (2006) Lotteries, loopholes and luck: misdiagnosis in the vegetative state patient. Brain injury 20:1321–1328.

GILL-THWAITES H, MUNDAY R (2004) The Sensory Modality Assessment and Rehabilitation Technique (SMART): a valid and reliable assessment for vegetative state and minimally conscious state patients. Brain injury 18:1255–1269.

GILOVICH T, GRIFFIN D, KAHNEMAN D (2002) Heuristics and Biases: The Psychology of Intuitive Judgment Gilovich T, Griffin D, Kahneman DTSB, eds. System 29:695.

GIORDANO BL, MCADAMS S, ZATORRE RJ, KRIEGESKORTE N, BELIN P (2013) Abstract encoding of auditory objects in cortical activity patterns. Cerebral cortex 23:2025–2037.

GOLD JI, SHADLEN MN (2000) Representation of a perceptual decision in developing oculomotor commands. Nature 404:390–394.

GOLD JI, SHADLEN MN (2001) Neural computations that underlie decisions about sensory stimuli. Trends in Cognitive Sciences 5:10–16.

GOLD JI, SHADLEN MN (2007) The neural basis of decision making. Annual review of neuroscience 30:535–574.

GOLDFINE AM, BARDIN JC, NOIRHOMME Q, FINS JJ, SCHIFF ND, VICTOR JD (2013) Reanalysis of "Bedside detection of awareness in the vegetative state: a cohort study". Lancet 381:289–291.

GOLDFINE AM, VICTOR JD, CONTE MM, BARDIN JC, SCHIFF ND (2011) Determination of awareness in patients with severe brain injury using EEG power spectral analysis. Clinical Neurophysiology 122:2157–2168.

GOLDFINE AM, VICTOR JD, CONTE MM, BARDIN JC, SCHIFF ND (2012) Bedside detection of awareness in the vegetative state. Lancet 379:1701–2; author reply 1702.

GOLDSTEIN A, SPENCER KM, DONCHIN E (2002) The influence of stimulus deviance and novelty on the P300 and Novelty P3. Psychophysiology 39:781–790.

GOODALE MA, MILNER AD (2005) Sight Unseen: An Exploration of Conscious and Unconscious Vision. Oxford University Press, USA.

GOODALE MA, MILNER ADD (1992) Separate visual pathways for perception and action. Trends in neurosciences 15:20–25.

GOREA A, SAGI D (2000) Failure to handle more than one internal representation in visual detection tasks. Proceedings of the National Academy of Sciences of the United States of America 97:12380–12384.

GOREA A, SAGI D (2010) Using the unique criterion constraint to disentangle transducer nonlinearity from lack of noise constancy. Journal of Vision 1:437–437.

GOSSERIES O, SCHNAKERS C, LEDOUX D, VANHAUDENHUYSE A, BRUNO M-A, DEMERTZI A, NOIRHOMME Q, LEHEMBRE R, DAMAS P, GOLDMAN S, PEETERS E, MOONEN G, LAUREYS S (2011) Automated EEG entropy measurements in coma, vegetative state/unresponsive wakefulness syndrome and minimally conscious state. Functional neurology 26:25–30.

GRAHAM DI, ADAMS JH, MURRAY LS, JENNETT B (2005) Neuropathology of the vegetative state after head injury. Neuropsychological rehabilitation 15:198–213.

GRAMFORT A, PALLIER C, VAROQUAUX G, THIRION B (2012) Decoding Visual Percepts Induced by Word Reading with fMRI. 2012 Second International Workshop on Pattern Recognition in NeuroImaging 1:13–16.

GRAY CM, KÖNIG P, ENGEL AK, SINGER W (1989) Oscillatory responses in cat visual cortex exhibit inter-columnar synchronization which reflects global stimulus properties. Nature 338:334–337.

GRAY CM, SINGER W (1989) Stimulus-specific neuronal oscillations in orientation columns of cat visual cortex. Proceedings of the National Academy of Sciences of the United States of America 86:1698–1702.

GREEN DM, SWETS JA (1966) Signal detection theory and psychophysics. Wiley.

GREENWALD AG, DRAINE SC, ABRAMS RL (1996) Three cognitive markers of unconscious semantic activation. Science 273:1699.

GREGORIOU GG, GOTTS SJ, ZHOU H, DESIMONE R (2009a) High-frequency, long-range coupling between prefrontal and visual cortex during attention. Science 324:1207–1210.

GREGORIOU GG, GOTTS SJ, ZHOU H, DESIMONE R, ED NS (2009b) Long-range neural coupling through synchronization with attention. Elsevier.

GREICIUS MD, KIVINIEMI V, TERVONEN O, VAINIONPÄÄ V, ALAHUHTA S, REISS AL, MENON V (2008) Persistent default-mode network connectivity during light sedation. Human brain mapping 29:839–847.

GRILL-SPECTOR K, KUSHNIR T, HENDLER T, MALACH R (2000) The dynamics of object-selective activation correlate with recognition performance in humans. Nature neuroscience 3:837–843.

GROSS J, SCHMITZ F, SCHNITZLER I, KESSLER K, SHAPIRO K, HOMMEL B, SCHNITZLER A (2004) Modulation of long-range neural synchrony reflects temporal limitations of visual attention in humans. Proceedings of the National Academy of Sciences of the United States of America 101:13050–13055.

GUIASU S (1977) Information Theory with Applications. McGraw-Hill Inc.,US.

GUILLEMANT P, ABID C, REY M (2004) Activation dimension of EEG: a cue tool with a real time algorithm. Neurophysiologie Clinique 22:7–14.

GULDENMUND P, VANHAUDENHUYSE A, BOLY M, LAUREYS S, SODDU A (2012) A default mode of brain function in altered states of consciousness. Archives italiennes de biologie 150:107–121.

GUTSCHALK A, MICHEYL C, OXENHAM AJ (2008) Neural correlates of auditory perceptual awareness under informational masking Griffiths TD, ed. PLoS Biol 6:e138.

GUYE M, RÉGIS J, TAMURA M, WENDLING F, MCGONIGAL A, CHAUVEL P, BARTOLOMEI F (2006) The role of corticothalamic coupling in human temporal lobe epilepsy. Brain 129:1917–1928.

GÓMEZ CM, FLORES A, LEDESMA A (2007) Fronto-parietal networks activation during the contingent negative variation period. Brain Research Bulletin 73:40–47.

HAAS LF (2003) Hans Berger (1873-1941), Richard Caton (1842-1926), and electroencephalography. Journal of neurology, neurosurgery, and psychiatry 74:9.

HAIDER M, SPONG P, LINDSLEY DB (1964) Attention, Vigilance, and Cortical Evoked-Potentials in Humans. Science 145:180–182.

HALGREN E, BAUDENA P, CLARKE JM, HEIT G, MARINKOVIC K, DEVAUX B, VIGNAL J-P, BIRABEN A (1995) Intracerebral potentials to rare target and distractor auditory and visual stimuli. II. Medial, lateral and posterior temporal lobe. Electroencephalography and Clinical Neurophysiology 94:229–250.

HALGREN E, MARINKOVIC K, CHAUVEL P (1998) Generators of the late cognitive potentials in auditory and visual oddball tasks. Electroencephalography and clinical neurophysiology 106:156–164.

HANSLMAYR S, ASLAN A, STAUDIGL T, KLIMESCH W, HERRMANN CS, BÄUML K-H (2007) Prestimulus oscillations predict visual perception performance between and within subjects. NeuroImage 37:1465–1473.

HARE RM, BARNES J, CHADWICK H (1982) Founders of Thought. Oxford University Press.

HARI R, HÄMÄLÄINEN M, ILMONIEMI R, KAUKORANTA E, REINIKAINEN K, SALMINEN J, ALHO K, NÄÄTÄNEN R, SAMS M (1984) Responses of the primary auditory cortex to pitch changes in a sequence of tone pips: Neuromagnetic recordings in man. Neuroscience Letters 50:127–132.

HARNAD S (2003) Categorical Perception. Wiley Interdisciplinary Reviews Cognitive Science 1:69–78.

HAROUSH K, DEOUELL LY, HOCHSTEIN S (2011) Hearing while blinking: multisensory attentional blink revisited. The Journal of Neuroscience 31:922–927.

HARRISON S A, TONG F (2009) Decoding reveals the contents of visual working memory in early visual areas. Nature 458:632–635.

HASSLER R, ORE GD, DIECKMANN G, BRICOLO A, DOLCE G (1969) Behavioural and EEG arousal induced by stimulation of unspecific projection systems in a patient with post-traumatic apallic syndrome. Electroencephalography and clinical neurophysiology 27:306–310.

HAYNES J-D (2011) Multivariate decoding and brain reading: introduction to the special issue. NeuroImage 56:385–386.

HAYNES J-D, DEICHMANN R, REES G (2005a) Eye-specific effects of binocular rivalry in the human lateral geniculate nucleus. Nature 438:496–499.

HAYNES J-D, DRIVER J, REES G (2005b) Visibility reflects dynamic changes of effective connectivity between V1 and fusiform cortex. Neuron 46:811–821.

HAYNES J-DD, REES G (2006) Decoding mental states from brain activity in humans. Nature Reviews Neuroscience 7:523–534.

HE BJ, RAICHLE ME (2009) The fMRI signal, slow cortical potential and consciousness. Trends in Cognitive Sciences 13:302–309.

HE BJ, SNYDER AZ, ZEMPEL JM, SMYTH MD, RAICHLE ME (2008) Electrophysiological correlates of the brain's intrinsic large-scale functional architecture. Proceedings of the National Academy of Sciences of the United States of America 105:16039–16044.

HEALTH N, DWGO S, WILKINSON RT, SEALES DM (1978) EEG event-related potentials and signal detection. Biological psychology 7:13–28.

HEINKE W, KENNTNER R, GUNTER TC, SAMMLER D, OLTHOFF D, KOELSCH S (2004) Sequential effects of increasing propofol sedation on frontal and temporal cortices as indexed by auditory event-related potentials. Anesthesiology 100:617–625.

HENSON RN, MOUCHLIANITIS E, MATTHEWS WJ, KOUIDER S (2008) Electrophysiological correlates of masked face priming. NeuroImage 40:884–895.

HESTER R, FOXE JJ, MOLHOLM S, SHPANER M, GARAVAN H (2005) Neural mechanisms involved in error processing: a comparison of errors made with and without awareness. NeuroImage 27:602–608.

HILLYARD SA, SQUIRES KC, BAUER JW, LINDSAY PH (1971) Evoked potential correlates of auditory signal detection. Science 172:1357–1360.

HIPP JF, ENGEL AK, SIEGEL M (2011) Oscillatory synchronization in large-scale cortical networks predicts perception. Neuron 69:387–396.

HOLENDER D (1986) Semantic activation without conscious identification in dichotic listening, parafoveal vision, and visual masking: A survey and appraisal. Behavioral and Brain Sciences 9:1–66.

HOLMES MD, BROWN M, TUCKER DM (2004) Are "generalized" seizures truly generalized? Evidence of localized mesial frontal and frontopolar discharges in absence. Epilepsia 45:1568–1579.

HORIKAWA T, TAMAKI M, MIYAWAKI Y, KAMITANI Y (2013) Neural decoding of visual imagery during sleep. Science (New York, NY) 340:639–642.

HÄMÄLÄINEN M, HARI R, ILMONIEMI RJ, LOUNASMAA O V., KNUUTILA J (1993) Magnetoencephalography—theory, instrumentation, and applications to noninvasive studies of the working human brain. Reviews of Modern Physics 65:413–497.

IBÁÑEZ A, LÓPEZ V, CORNEJO C (2006) ERPs and contextual semantic discrimination: degrees of congruence in wakefulness and sleep. Brain and language 98:264–275.

IBÁÑEZ AM, MARTÍN RS, HURTADO E, LÓPEZ V (2009) ERPs studies of cognitive processing during sleep. International journal of psychology 44:290–304.

INOUE M, VAN LUIJTELAAR EL, VOSSEN JM, COENEN AM (1992) Visual evoked potentials during spontaneously occurring spike-wave discharges in rats. Electroencephalography and Clinical Neurophysiology/Evoked Potentials Section 84:172–179.

INOUYE T, SHINOSAKI K, SAKAMOTO H, TOI S, UKAI S, IYAMA A, KATSUDA Y, HIRANO M (1991) Quantification of EEG irregularity by use of the entropy of the power spectrum. Electroencephalography and Clinical Neurophysiology 79:204–210.

ISSA EB, WANG X (2011) Altered neural responses to sounds in primate primary auditory cortex during slow-wave sleep. The Journal of Neuroscience 31:2965–2973.

JAZAYERI M, MOVSHON JA (2007) A new perceptual illusion reveals mechanisms of sensory decoding. Nature 446:912–915.

JEHEE JFM, LAMME V A F, ROELFSEMA PR (2007) Boundary assignment in a recurrent network architecture. Vision research 47:1153–1165.

JENNETT B (2002) Medical facts, ethical and legal dilemma. In: The Vegetative State, pp 1–6.

JENNETT B (2005) Thirty years of the vegetative state: clinical, ethical and legal problems. Progress in brain research 150:537–543.

JENNETT B, PLUM F (1972) Persistent vegetative state after brain damage. A syndrome in search of a name. Lancet 1:734–737.

JENSEN O, BONNEFOND M, VANRULLEN R (2012) An oscillatory mechanism for prioritizing salient unattended stimuli. Trends in Cognitive Sciences 16:200–206.

JIANG Y, ZHOU K, HE S (2007) Human visual cortex responds to invisible chromatic flicker. Nature neuroscience 10:657–662.

JOKISCH D, JENSEN O (2007) Modulation of gamma and alpha activity during a working memory task engaging the dorsal or ventral stream. The Journal of Neuroscience 27:3244–3251.

JONES K (2007) Complex Partial Seizures. Aviation, Space, and Environmental Medicine 78:999–1000.

JORDAN D, STOCKMANNS G, KOCHS EF, PILGE S, SCHNEIDER G (2008) Electroencephalographic order pattern analysis for the separation of consciousness and unconsciousness: an analysis of approximate entropy, permutation entropy, recurrence rate, and phase coupling of order recurrence plots. Anesthesiology 109:1014–1022.

KAERNBACH C (1991) Simple adaptive testing with the weighted up-down method. Perception And Psychophysics 49:227–229.

KAISTI KK, LÅNGSJÖ JW, AALTO S, SC M, OIKONEN V, SIPILÄ H (2003) Oxide on Regional Cerebral Blood Flow , Oxygen Consumption , and Blood Volume in Humans. i.

KAISTI KK, METSÄHONKALA L, TERÄS M, OIKONEN V, AALTO S, JÄÄSKELÄINEN S, HINKKA S, SCHEININ H (2002) Effects of surgical levels of propofol and sevoflurane anesthesia on cerebral

blood flow in healthy subjects studied with positron emission tomography. Anesthesiology 96:1358–1370.

KAJIMURA N, UCHIYAMA M, TAKAYAMA Y, UCHIDA S, UEMA T, KATO M, SEKIMOTO M, WATANABE T, NAKAJIMA T, HORIKOSHI S, OGAWA K, NISHIKAWA M, HIROKI M, KUDO Y, MATSUDA H, OKAWA M, TAKAHASHI K (1999) Activity of midbrain reticular formation and neocortex during the progression of human non-rapid eye movement sleep. The Journal of Neuroscience 19:10065–10073.

KAMITANI Y, TONG F (2005) Decoding the visual and subjective contents of the human brain. Nature Neuroscience 8:679–685.

KANAI R, WALSH V, TSENG C-H (2010) Subjective discriminability of invisibility: A framework for distinguishing perceptual and attentional failures of awareness. Consciousness and cognition:2005–2009.

KANE NM, BUTLER SR, SIMPSON T (2000) Coma outcome prediction using event-related potentials: P(3) and mismatch negativity. Audiology neurootology 5:186–191.

KANE NM, CURRY SH, ROWLANDS CA, MANARA AR, LEWIS T, MOSS T, CUMMINS BH, BUTLER SR (1996) Event-related potentials — neurophysiological tools for predicting emergence and early outcome from traumatic coma. Intensive Care Medicine 22:39–46.

KANWISHER N, MCDERMOTT J, CHUN MM (1997) The fusiform face area: a module in human extrastriate cortex specialized for face perception. Journal of Neuroscience 17:4302.

KAY KN, GALLANT JL (2009) I can see what you see. Nature Neuroscience 12:245.

KAYSER J, TENKE CE (2006a) Principal components analysis of Laplacian waveforms as a generic method for identifying ERP generator patterns: II. Adequacy of low-density estimates. Clinical neurophysiology 117:369–380.

KAYSER J, TENKE CE (2006b) Principal components analysis of Laplacian waveforms as a generic method for identifying ERP generator patterns: I. Evaluation with auditory oddball tasks. Clinical neurophysiology 117:348–368.

KENTRIDGE RW, HEYWOOD CA, WEISKRANTZ L (1999) Attention without awareness in blindsight. Proceedings of the Royal Society B: Biological Sciences 266:1805.

KERSSENS C, HAMANN S, PELTIER S, HU XP, BYAS-SMITH MG, SEBEL PS (2005) Attenuated Brain Response to Auditory Word Stimulation with Sevoflurane. Anesthesiology 103:11–19.

KERSTEN D, MAMASSIAN P, YUILLE A (2004) Object perception as Bayesian inference Knill D, Richards W, eds. Annual Review of Psychology 55:271–304.

KERSTEN D, YUILLE A (2003) Bayesian models of object perception. Current Opinion in Neurobiology 13:150–158.

KIEFER M, BRENDEL D (2006) Attentional Modulation of Unconscious Automatic" Processes: Evidence from Event-related Potentials in a Masked Priming Paradigm. Journal of cognitive neuroscience 18:184–198.

KIM C, BLAKE R (2005) Psychophysical magic: rendering the visible "invisible". Trends in Cognitive Sciences 9:381–388.

KING J-R, BEKINSCHTEIN T, DEHAENE S (2011) Comment on "Preserved feedforward but impaired top-down processes in the vegetative state". Science (New York, NY) 334:1203.

KING J-R, FAUGERAS F, GRAMFORT A, SCHURGER A, EL KAROUI I, SITT JD, ROHAUT B, WACONGNE C, LABYT E, BEKINSCHTEIN T, COHEN L, NACCACHE L, DEHAENE S (2013a) Single-trial decoding of auditory novelty responses facilitates the detection of residual consciousness. NeuroImage 83C:726–738.

KING J-R, GRAMFORT A, SCHURGER A, NACCACHE L, DEHAENE S (2014) Two Distinct Dynamic Modes Subtend the Detection of Unexpected Sounds. PloS one.

KING J-R, SITT JD, FAUGERAS F, ROHAUT B, EL KAROUI I, COHEN L, NACCACHE L, DEHAENE S (2013b) Information Sharing in the Brain Indexes Consciousness In noncommunicative patients. Current Biology 23:1–37.

KINNEY HC, KOREIN J, PANIGRAHY A, DIKKES P, GOODE R (1994) Neuropathological findings in the brain of Karen Ann Quinlan. The role of the thalamus in the persistent vegetative state. The New England journal of medicine 330:1469–1475.

KISHIMOTO T, KADOYA C, SNEYD R, SAMRA SK, DOMINO EF (1995) Topographic electroencephalogram of propofol-induced conscious sedation. Clinical pharmacology and therapeutics 58:666–674.

KLEIN S A (1985) Double-judgment psychophysics: problems and solutions. Journal of the Optical Society of America A, Optics and image science 2:1560–1585.

KLIMESCH W, SAUSENG P, HANSLMAYR S (2007) EEG alpha oscillations: the inhibition-timing hypothesis. Brain research reviews 53:63–88.

KNILL DC, POUGET A (2004) The Bayesian brain: the role of uncertainty in neural coding and computation. Trends in Neurosciences 27:712–719.

KNILL DC, RICHARDS W (2008) Perception as Bayesian Inference. Cambridge Univ Pr.

KNOPS A, THIRION B, HUBBARD EM, MICHEL V, DEHAENE S (2009) Recruitment of an area involved in eye movements during mental arithmetic. Science (New York, NY) 324:1583–1585.

KO Y, LAU H (2012) A detection theoretic explanation of blindsight suggests a link between conscious perception and metacognition. Philosophical transactions of the Royal Society of London Series B, Biological sciences 367:1401–1411.

KOCH C (2004) The Quest for Consciousness: A Neurobiological Approach. Roberts & Company Publishers.

KOCH C, CRICK F (2003) Consciousness, neural basis of. John Benjamins.

KOELSCH S, HEINKE W, SAMMLER D, OLTHOFF D (2006) Auditory processing during deep propofol sedation and recovery from unconsciousness. Clinical Neurophysiology 117:1746–1759.

KOIVISTO M, REVONSUO A, LEHTONEN M (2006) Independence of visual awareness from the scope of attention: an electrophysiological study. Cerebral Cortex 16:415–424.

KOJIMA S, GOLDMAN-RAKIC PS (1982) Delay-related activity of prefrontal neurons in rhesus monkeys performing delayed response. Brain Research 248:43–50.

KOK P, JEHEE JFM, DE LANGE FP (2012) Less is more: expectation sharpens representations in the primary visual cortex. Neuron 75:265–270.

KOLMOGOROV A (1965) Three approaches to the quantitative definition of information. Problems of Information Transmission 1:1 – 7.

KOTCHOUBEY B, LANG S, MEZGER G, SCHMALOHR D, SCHNECK M, SEMMLER A, BOSTANOV V, BIRBAUMER N (2005) Information processing in severe disorders of consciousness: vegetative state and minimally conscious state. Clinical Neurophysiology 116:2441–2453.

KOTCHOUBEY B, LOTZE M (2013) Instrumental methods in the diagnostics of locked-in syndrome. Restorative neurology and neuroscience 31:25–40.

KOTCHOUBEY B, MERZ S, LANG S, MARKL A, MÜLLER F, YU T, SCHWARZBAUER C (2013) Global functional connectivity reveals highly significant differences between the vegetative and the minimally conscious state. Journal of neurology 260:975–983.

KOUIDER S, DE GARDELLE V, DEHAENE S, DUPOUX E, PALLIER C (2010) Cerebral bases of subliminal speech priming. NeuroImage 49:922–929.

KOUIDER S, DEHAENE S (2007) Levels of processing during non-conscious perception: a critical review of visual masking. Philosophical transactions of the Royal Society of London Series B, Biological sciences 362:857–875.

KRETSCHMER E (1940) Das apallische Syndrom. Zeitschrift für die gesamte Neurologie und Psychiatrie 169:576–579.

KRIEGESKORTE N, KIEVIT R A (2013) Representational geometry: integrating cognition, computation, and the brain. Trends in cognitive sciences 17:401–412.

KRIEGESKORTE N, SIMMONS WK, BELLGOWAN PSF, BAKER CI (2009) Circular analysis in systems neuroscience: the dangers of double dipping. Nature neuroscience 12:535–540.

KUMAR A, ANAND S, CHARI P, YADDANAPUDI LN, SRIVASTAVA A (2007) A set of EEG parameters to predict clinically anaesthetized state in humans for halothane anaesthesia. Journal of medical engineering & technology 31:46–53.

KUTAS M, FEDERMEIER KD (2011) Thirty years and counting: finding meaning in the N400 component of the event-related brain potential (ERP). Annual review of psychology 62:621–647.

KÖNIG P, ENGEL AK, SINGER W (1996) Integrator or coincidence detector? The role of the cortical neuron revisited. Trends in Neurosciences 19:130–137.

LACHAUX JP, RODRIGUEZ E, MARTINERIE J, VARELA FJ (1999) Measuring phase synchrony in brain signals. Human brain mapping 8:194–208.

LAITIO RM, KAISTI KK, LÅANGSJÖ JW, AALTO S, SALMI E, MAKSIMOW A, AANTAA R, OIKONEN V, SIPILÄ H, PARKKOLA R, SCHEININ H (2007) Effects of xenon anesthesia on cerebral blood flow in humans: a positron emission tomography study. Anesthesiology 106:1128–1133.

LAITIO RM, KASKINORO K, SÄRKELÄ MOK, KAISTI KK, SALMI E, MAKSIMOW A, LÅNGSJÖ JW, AANTAA R, KANGAS K, JÄÄSKELÄINEN S, OTHERS (2008) Bispectral index, entropy, and quantitative electroencephalogram during single-agent xenon anesthesia. Anesthesiology 108:63.

LAMBERT I, ARTHUIS M, MCGONIGAL A, WENDLING F, BARTOLOMEI F (2012) Alteration of global workspace during loss of consciousness: a study of parietal seizures. Epilepsia 53:2104–2110.

LAMME V A. F (2010) How neuroscience will change our view on consciousness. Cognitive Neuroscience 1:204–220.

LAMME VA., SUPÈR H, LANDMAN R, ROELFSEMA PR, SPEKREIJSE H (2000) The role of primary visual cortex (V1) in visual awareness. Vision research 40:1507–1521.

LAMME VAF (2003) Why visual attention and awareness are different. Trends in Cognitive Sciences 7:12–18.

LAMME VAF (2006a) Zap! Magnetic tricks on conscious and unconscious vision. Trends in cognitive sciences 10:193–195.

LAMME VAF (2006b) Towards a true neural stance on consciousness. Trends in Cognitive Sciences 10:494–501.

LAMME VAFF, ROELFSEMA PR (2000) The distinct modes of vision offered by feedforward and recurrent processing. Trends in Neurosciences 23:571–579.

LAMY D, SALTI M, BAR-HAIM Y (2009) Neural correlates of subjective awareness and unconscious processing: an ERP study. Journal of cognitive neuroscience 21:1435–1446.

LANDSNESS E, BRUNO M-A, NOIRHOMME Q, RIEDNER B, GOSSERIES O, SCHNAKERS C, MASSIMINI M, LAUREYS S, TONONI G, BOLY M (2011) Electrophysiological correlates of behavioural changes in vigilance in vegetative state and minimally conscious state. Brain 134:2222–2232.

LANGFORD GW, MEDDIS R, PEARSON AJD (1974) Awakening Latency From Sleep For Meaningful and Non-Meaningful Stimuli. Psychophysiology 11:1–5.

LAU H (2008) A higher order Bayesian decision theory of consciousness. Progress in Brain Research 168:35–48.

LAU H, ROSENTHAL D (2011) Empirical support for higher-order theories of conscious awareness. Trends in cognitive sciences 15:365–373.

LAU HC, PASSINGHAM RE (2006) Relative blindsight in normal observers and the neural correlate of visual consciousness. Proceedings of the National Academy of Sciences of the United States of America 103:18763–18768.

LAU HC, PASSINGHAM RE (2007) Unconscious activation of the cognitive control system in the human prefrontal cortex. Journal of Neuroscience 27:5805.

LAUREYS S (2005a) The Boundaries of Consciousness: Neurobiology and Neuropathology. Elsevier.

LAUREYS S (2005b) The neural correlate of (un)awareness: lessons from the vegetative state. Trends in cognitive sciences 9:556–559.

LAUREYS S, CELESIA GG, COHADON F, LAVRIJSEN J, LEÓN-CARRIÓN J, SANNITA WG, SAZBON L, SCHMUTZHARD E, VON WILD KR, ZEMAN A, DOLCE G (2010) Unresponsive wakefulness syndrome: a new name for the vegetative state or apallic syndrome. BMC medicine 8:68.

LAUREYS S, FAYMONVILLE ME, DEGUELDRE C, FIORE GD, DAMAS P, LAMBERMONT B, JANSSENS N, AERTS J, FRANCK G, LUXEN A, MOONEN G, LAMY M, MAQUET P (2000a) Auditory processing in the vegetative state. Brain 123 (Pt 8:1589–1601.

LAUREYS S, FAYMONVILLE ME, LUXEN A, LAMY M, FRANCK G, MAQUET P (2000b) Restoration of thalamocortical connectivity after recovery from persistent vegetative state. Lancet 355:1790–1791.

LAUREYS S, FAYMONVILLE MEE, PEIGNEUX P, DAMAS P, LAMBERMONT B, DEL FIORE G, DEGUELDRE C, AERTS J, LUXEN A., FRANCK G, LAMY M, MOONEN G, MAQUET P (2002) Cortical Processing of Noxious Somatosensory Stimuli in the Persistent Vegetative State. NeuroImage 17:732–741.

LAUREYS S, GOLDMAN S, PHILLIPS C, VAN BOGAERT P, AERTS J, LUXEN A, FRANCK G, MAQUET P (1999a) Impaired effective cortical connectivity in vegetative state: preliminary investigation using PET. NeuroImage 9:377–382.

LAUREYS S, LEMAIRE C, MAQUET P, PHILLIPS C, FRANCK G (1999b) Cerebral metabolism during vegetative state and after recovery to consciousness. Journal of neurology, neurosurgery, and psychiatry 67:121.

LAUREYS S, OWEN AM, SCHIFF ND (2004) Brain function in coma, vegetative state, and related disorders. The Lancet Neurology 3:537–546.

LAUREYS S, SCHIFF ND (2011) Coma and consciousness: Paradigms (re)framed by neuroimaging. NeuroImage 61:478–491.

LAUREYS S, TONONI G (2008) The neurology of consciousness: cognitive neuroscience and neuropathology (Laureys S, Tononi G, eds). Academic Press.

LECHINGER J, BOTHE K, PICHLER G, MICHITSCH G, DONIS J, KLIMESCH W, SCHABUS M (2013) CRS-R score in disorders of consciousness is strongly related to spectral EEG at rest. Journal of neurology.

LEE AK, WILSON MA (2002) Memory of sequential experience in the hippocampus during slow wave sleep. Neuron 36:1183–1194.

LEE S-H, KRAVITZ DJ, BAKER CI (2012) Disentangling visual imagery and perception of real-world objects. NeuroImage 59:4064–4073.

LEE U, KU S, NOH G, BAEK S, CHOI B, MASHOUR GA (2013) Disruption of Frontal-Parietal Communication by Ketamine, Propofol, and Sevoflurane. Anesthesiology 118:1264–1275.

LEE U, MASHOUR G A, KIM S, NOH G-J, CHOI B-M (2009) Propofol induction reduces the capacity for neural information integration: implications for the mechanism of consciousness and general anesthesia. Consciousness and cognition 18:56–64.

LEHEMBRE R, BRUNO M-A, VANHAUDENHUYSE A, CHATELLE C, COLOGAN V, LECLERCQ Y, SODDU A, MACQ B, LAUREYS S, NOIRHOMME Q (2012) Resting-state EEG study of comatose patients: a connectivity and frequency analysis to find differences between vegetative and minimally conscious states. Functional neurology 27:41–47.

LEITE FP, RATCLIFF R (2010) Modeling reaction time and accuracy of multiple-alternative decisions. Attention, perception & psychophysics 72:246–273.

LEMIEUX JF, BLUME WT (1986) Topographical evolution of spike-wave complexes. Brain research 373:275–287.

LEMM S, BLANKERTZ B, DICKHAUS T, MÜLLER K-R (2011) Introduction to machine learning for brain imaging. NeuroImage 56:387–399.

LEMPEL A, ZIV J (1976) On the Complexity of Finite Sequences. IEEE Transactions on Information Theory 22:75–81.

LEON-CARRION J, LEON-DOMINGUEZ U, POLLONINI L, WU M-H, FRYE RE, DOMINGUEZ-MORALES MR, ZOURIDAKIS G (2012) Synchronization between the anterior and posterior cortex determines consciousness level in patients with traumatic brain injury (TBI). Brain research.

LEV M, YEHEZKEL O, POLAT U (2013) Temporal processing overcomes spatial crowding in the fovea. Journal of Vision 13:574–574.

LEVY DE, SIDTIS JJ, ROTTENBERG DA, JARDEN JO, STROTHER SC, DHAWAN V, GINOS JZ, TRAMO MJ, EVANS AC, PLUM F (1987) Differences in cerebral blood flow and glucose utilization in vegetative versus locked-in patients. Annals of neurology 22:673–682.

LEWIS LD, WEINER VS, MUKAMEL E A, DONOGHUE JA, ESKANDAR EN, MADSEN JR, ANDERSON WS, HOCHBERG LR, CASH SS, BROWN EN, PURDON PL (2012) Rapid fragmentation of neuronal networks at the onset of propofol-induced unconsciousness. Proceedings of the National Academy of Sciences of the United States of America 109:E3377–86.

LI X, CUI S, VOSS LJ (2008) Using permutation entropy to measure the electroencephalographic effects of sevoflurane. Anesthesiology 109:448–456.

LIU T, PLESKAC TJ (2011) Neural correlates of evidence accumulation in a perceptual decision task. Journal of neurophysiology 106:2383–2398.

LIU X, LAUER KK, WARD BD, RAO SM, LI S-J, HUDETZ AG (2012) Propofol disrupts functional interactions between sensory and high-order processing of auditory verbal memory. Human brain mapping 33:2487–2498.

LLINÁS R, RIBARY U, CONTRERAS D, PEDROARENA C (1998) The neuronal basis for consciousness. Philosophical transactions of the Royal Society of London Series B, Biological sciences 353:1841–1849.

LLINÁS RR, PARÉ D (1991) Of dreaming and wakefulness. Neuroscience 44:521–535.

LOGOTHETIS NK, LEOPOLD DA, SHEINBERG DL (1996) What is rivalling during binocular rivalry? Nature 380:621–624.

LOPEZ V, CARMENATE L, ALVAREZ A (2001) N400 effect during different sleep stages. Clinical neurophysiology 112:12–51.

LOUIE K, WILSON MA (2001) Temporally structured replay of awake hippocampal ensemble activity during rapid eye movement sleep. Neuron 29:145–156.

LUAUTÉ J, FISCHER C, ADELEINE P, MORLET D, TELL L, BOISSON D (2005) Late auditory and event-related potentials can be useful to predict good functional outcome after coma. Archives of physical medicine and rehabilitation 86:917–923.

LUMER ED (1998) Neural Correlates of Perceptual Rivalry in the Human Brain. Science 280:1930–1934.

LUMER ED, REES G (1999) Covariation of activity in visual and prefrontal cortex associated with subjective visual perception. Proceedings of the National Academy of Sciences of the United States of America 96:1669–1673.

LUO Q, MITCHELL D, CHENG X, MONDILLO K, MCCAFFREY D, HOLROYD T, CARVER F, COPPOLA R, BLAIR J (2009) Visual awareness, emotion, and gamma band synchronization. Cerebral cortex 19:1896–1904.

MACK A (2003) Inattentional blindness. Current Directions in Psychological Science 12:180.

MACK A, ROCK I (1998) Inattentional blindness: Perception without attention. Visual attention 8:55–76.

MACKAY DJC (2003) Information Theory, Inference and Learning Algorithms. Cambridge University Press.

MAGNIN M, BASTUJI H, GARCIA-LARREA L, MAUGUIÈRE F (2004) Human thalamic medial pulvinar nucleus is not activated during paradoxical sleep. Cerebral cortex 14:858–862.

MAGNIN M, REY M, BASTUJI H, GUILLEMANT P, MAUGUIÈRE F, GARCIA-LARREA L (2010) Thalamic deactivation at sleep onset precedes that of the cerebral cortex in humans. Proceedings of the National Academy of Sciences of the United States of America 107:3829–3833.

MAIER A, WILKE M, AURA C, ZHU C, YE FQ, LEOPOLD DA (2008) Divergence of fMRI and neural signals in V1 during perceptual suppression in the awake monkey. Nature neuroscience 11:1193–1200.

MAKSIMOW A, SÄRKELÄ M, LÅNGSJÖ JW, SALMI E, KAISTI KK, YLI-HANKALA A, HINKKA-YLI-SALOMÄKI S, SCHEININ H, JÄÄSKELÄINEN SK (2006) Increase in high frequency EEG activity explains the poor performance of EEG spectral entropy monitor during S-ketamine anesthesia. Clinical Neurophysiology 117:1660–1668.

MANNI R (2005) Rapid eye movement sleep, non-rapid eye movement sleep, dreams, and hallucinations. Current psychiatry reports 7:196–200.

MAQUET P (1997) Positron emission tomography studies of sleep and sleep disorders. Journal of neurology 244:S23–8.

MAQUET P (2000) Functional neuroimaging of normal human sleep by positron emission tomography. Journal of sleep research 9:207–231.

MAQUET P, PHILLIPS C (1998) Functional brain imaging of human sleep. Journal of sleep research 7 Suppl 1:42–47.

MAQUET P, PÉTERS J, AERTS J, DELFIORE G, DEGUELDRE C, LUXEN A, FRANCK G (1996) Functional neuroanatomy of human rapid-eye-movement sleep and dreaming. Nature 383:163–166.

MAROIS R, YI D-J, CHUN MM (2004) The neural fate of consciously perceived and missed events in the attentional blink. Neuron 41:465–472.

MARSHALL JC, HALLIGAN PW (1993) Visuo-spatial neglect: a new copying test to assess perceptual parsing. Journal of neurology 240:37–40.

MARTI S, SIGMAN M, DEHAENE S (2012) A shared cortical bottleneck underlying Attentional Blink and Psychological Refractory Period. NeuroImage 59:2883–2898.

MARTINI M, KRANZ T, WAGNER T, LEHNERTZ K (2011) Inferring directional interactions from transient signals with symbolic transfer entropy. Physical Review E 83:1–6.

MARTUZZI R, RAMANI R, QIU M, RAJEEVAN N, CONSTABLE RT (2010) Functional connectivity and alterations in baseline brain state in humans. NeuroImage 49:823–834.

MASON MF, NORTON MI, VAN HORN JD, WEGNER DM, GRAFTON ST, MACRAE CN (2007) Wandering minds: the default network and stimulus-independent thought. Science 315:393–395.

MASSIMINI M, FERRARELLI F, ESSER SK, RIEDNER B A, HUBER R, MURPHY M, PETERSON MJ, TONONI G (2007) Triggering sleep slow waves by transcranial magnetic stimulation. Proceedings of the National Academy of Sciences of the United States of America 104:8496–8501.

MASSIMINI M, FERRARELLI F, HUBER R, ESSER SK, SINGH H, TONONI G (2005) Breakdown of cortical effective connectivity during sleep. Science 309:2228–2232.

MASSIMINI M, FERRARELLI F, MURPHY M, HUBER R, RIEDNER B, CASAROTTO S, TONONI G (2010) Cortical reactivity and effective connectivity during REM sleep in humans. Cognitive neuroscience 1:176–183.

MASSIMINI M, FERRARELLI F, SARASSO S, TONONI G (2012) Cortical mechanisms of loss of consciousness: insight from TMS/EEG studies. Archives italiennes de biologie 150:44–55.

MATHEWSON KE, GRATTON G, FABIANI M, BECK DM, RO T (2009) To see or not to see: prestimulus alpha phase predicts visual awareness. The Journal of neuroscience 29:2725–2732.

MAXWELL WL, MACKINNON MA, SMITH DH, MCINTOSH TK, GRAHAM DI (2006) Thalamic nuclei after human blunt head injury. Journal of neuropathology and experimental neurology 65:478–488.

MCCARLEY R, SINTON C (2008) Neurobiology of sleep and wakefulness. Scholarpedia 3:3313.

MCCLELLAND JL (1979) On the time-relations of mental processes: An examination of systems of processes in cascade. Psychological Review 86:287–330.

MCCORMICK PA (1997) Orienting attention without awareness. Journal of Experimental Psychology-Human Perception and Performance 23:168–179.

MELLONI L, MOLINA C, PENA M, TORRES D, SINGER W, RODRIGUEZ E (2007) Synchronization of neural activity across cortical areas correlates with conscious perception. The Journal of Neuroscience 27:2858–2865.

MELLONI L, SCHWIEDRZIK CM, MÜLLER N, RODRIGUEZ E, SINGER W (2011) Expectations change the signatures and timing of electrophysiological correlates of perceptual awareness. The Journal of neuroscience 31:1386–1396.

MENON DK, OWEN AM, WILLIAMS EJ, MINHAS PS, ALLEN CM, BONIFACE SJ, PICKARD JD (1998) Cortical processing in persistent vegetative state. Wolfson Brain Imaging Centre Team. Lancet 352:200.

MERIKLE PM (1982) Unconscious perception revisited. Perception and Psychophysics 31:298–301.

MEYERS EM, FREEDMAN DJ, KREIMAN G, MILLER EK, POGGIO T, EM M, DJ F, EK M (2008) Dynamic population coding of category information in inferior temporal and prefrontal cortex. Journal of neurophysiology 100:1407–1419.

MILLER KJ, SORENSEN LB, OJEMANN JG, DEN NIJS M (2009) Power-law scaling in the brain surface electric potential. Sporns O, ed. PLoS computational biology 5:e1000609.

MITRA P, BOKIL H (2007) Observed Brain Dynamics. Oxford University Press, USA.

MIYAWAKI Y, UCHIDA H, YAMASHITA O, SATO M, MORITO Y, TANABE HC, SADATO N, KAMITANI Y (2008) Visual image reconstruction from human brain activity using a combination of multiscale local image decoders. Neuron 60:915–929.

MOELLER S, NALLASAMY N, TSAO DY, FREIWALD W A (2009) Functional connectivity of the macaque brain across stimulus and arousal states. The Journal of Neuroscience 29:5897–5909.

MONTI MM, VANHAUDENHUYSE A, COLEMAN MR, BOLY M, PICKARD JD, TSHIBANDA L, OWEN AM, LAUREYS S (2010) of Consciousness. The New England Journal of Medicine 362:579–589.

MOONEY CM (1957) Age in the Development of Closure Ability in Children. Canad J Psychol 11:219–226.

MORENO-BOTE R, KNILL DC, POUGET A (2011) Bayesian sampling in visual perception. Proceedings of the National Academy of Sciences of the United States of America 108:1–6.

MORLET D, FISCHER C (2013) MMN and Novelty P3 in Coma and Other Altered States of Consciousness: A Review. Brain topography.

MORRIS JS, OHMAN A, DOLAN RJ (1999) A subcortical pathway to the right amygdala mediating "unseen" fear. Proceedings of the National Academy of Sciences of the United States of America 96:1680–1685.

MULLER-GASS A, MACDONALD M, SCHRÖGER E, SCULTHORPE L, CAMPBELL K (2007) Evidence for the auditory P3a reflecting an automatic process: Elicitation during highly-focused continuous visual attention. Brain research 1170:71–78.

MURPHY M, RIEDNER B A, HUBER R, MASSIMINI M, FERRARELLI F, TONONI G (2009) Source modeling sleep slow waves. Proceedings of the National Academy of Sciences of the United States of America 106:1608–1613.

NACCACHE L (2006) Psychology. Is she conscious? Science (New York, NY) 313:1395–1396.

NACCACHE L (2009) Le nouvel inconscient: Freud, Christophe Colomb des neuroscience.

NACCACHE L, DEHAENE S (2001a) The priming method: imaging unconscious repetition priming reveals an abstract representation of number in the parietal lobes. Cerebral cortex 11:966–974.

NACCACHE L, DEHAENE S (2001b) Unconscious semantic priming extends to novel unseen stimuli. Cognition 80:215–229.

NACCACHE L, PUYBASSET L, GAILLARD R, SERVE E, WILLER JC (2005) Auditory mismatch negativity is a good predictor of awakening in comatose patients: a fast and reliable procedure. Clinical neurophysiology 116:988.

NAKAMURA K, DEHAENE S, JOBERT A, LE BIHAN D, KOUIDER S (2005) Subliminal convergence of Kanji and Kana words: further evidence for functional parcellation of the posterior temporal cortex in visual word perception. Journal of cognitive neuroscience 17:954–968.

NASHIDA T, YABE H, SATO Y, HIRUMA T, SUTOH T, SHINOZAKI N, KANEKO S (2000) Automatic auditory information processing in sleep. Sleep 23:821–828.

NEUROSCIENCE H, LIU Y, PARADIS A, YAHIA-CHERIF L, TALLON-BAUDRY C, STRANGE BA (2012) Activity in the lateral occipital cortex between 200 and 300 ms distinguishes between physically identical seen and unseen stimuli. Frontiers in human neuroscience 6:211.

NEWCOMBE VFJ, WILLIAMS GB, SCOFFINGS D, CROSS J, CARPENTER TA, PICKARD JD, MENON DK (2010) Aetiological differences in neuroanatomy of the vegetative state: insights from diffusion tensor imaging and functional implications. Journal of neurology, neurosurgery, and psychiatry 81:552–561.

NIEDEGGEN M, WICHMANN P, STOERIG P (2001) Change blindness and time to consciousness. The European journal of neuroscience 14:1719–1726.

NIEDERMEYER E (2003) Electrophysiology of the frontal lobe. Clinical EEG (electroencephalography) 34:5–12.

NIELSEN-BOHLMAN L, KNIGHT RT, WOODS DL, WOODWARD K (1991) Differential auditory processing continues during sleep. Electroencephalography and Clinical Neurophysiology 79:281–290.

NIESSING J, FRIEDRICH RW (2010) Olfactory pattern classification by discrete neuronal network states. Nature 465:47–52.

NIKOLIĆ D, HÄUSLER S, SINGER W, MAASS W (2009) Distributed fading memory for stimulus properties in the primary visual cortex. PLoS biology 7:e1000260.

NISHIMOTO S, VU AT, NASELARIS T, BENJAMINI Y, YU B, GALLANT JL (2011) Reconstructing visual experiences from brain activity evoked by natural movies. Current Biology 21:1641–1646.

NISHITANI N, HARI R (2002) Viewing lip forms: cortical dynamics. Neuron 36:1211–1220.

NOLTE G, BAI O, WHEATON L, MARI Z, VORBACH S, HALLETT M (2004) Identifying true brain interaction from EEG data using the imaginary part of coherency. Clinical Neurophysiology 115:2292–2307.

NOMURA M, OHIRA H, HANEDA K, IIDAKA T, SADATO N, OKADA T, YONEKURA Y (2004) Functional association of the amygdala and ventral prefrontal cortex during cognitive evaluation of facial expressions primed by masked angry faces: an event-related fMRI study. NeuroImage 21:352–363.

NORMAN DA, SHALLICE T (1986) Attention to action. Consciousness and self-regulation 4:1–18.

NORTHOFF G (2012) What the brain's intrinsic activity can tell us about consciousness? A tri-dimensional view. Neuroscience and biobehavioral reviews.

NURY H, VAN RENTERGHEM C, WENG Y, TRAN A, BAADEN M, DUFRESNE V, CHANGEUX J-P, SONNER JM, DELARUE M, CORRINGER P-J (2011) X-ray structures of general anaesthetics bound to a pentameric ligand-gated ion channel. Nature 469:428–431.

NÄÄTÄNEN R, ASTIKAINEN P, RUUSUVIRTA T, HUOTILAINEN M (2010) Automatic auditory intelligence: an expression of the sensory-cognitive core of cognitive processes. Brain Research Reviews 64:123–136.

NÄÄTÄNEN R, GAILLARD AWK, MÄNTYSALO S (1978) Early selective-attention effect on evoked potential reinterpreted. Acta Psychologica 42:313–329.

NÄÄTÄNEN R, PAAVILAINEN P, RINNE T, ALHO K (2007) The mismatch negativity (MMN) in basic research of central auditory processing: a review. Clinical Neurophysiology 118:2544–2590.

NÄÄTÄNEN R, PICTON T (1987) The N1 wave of the human electric and magnetic response to sound: a review and an analysis of the component structure. Psychophysiology 24:375–425.

OLOFSEN E, SLEIGH JW, DAHAN A (2008) Permutation entropy of the electroencephalogram: a measure of anaesthetic drug effect. British journal of anaesthesia 101:810–821.

OOSTENVELD R, FRIES P, MARIS E, SCHOFFELEN J-M (2011) FieldTrip: Open source software for advanced analysis of MEG, EEG, and invasive electrophysiological data. Computational intelligence and neuroscience 2011:156869.

ORREN MM (1978) Evoked potential studies in petit mal epilepsy. Visual information processing in relation to spike and wave discharges. Electroencephalography and clinical neurophysiology Supplement:251–257.

OSWALD I, TAYLOR AM, TREISMAN M (1960) Discriminative responses to stimulation during human sleep. Brain 83:440–453.

OVERGAARD M, SANDBERG K (2012) Kinds of access: different methods for report reveal different kinds of metacognitive access. Philosophical transactions of the Royal Society of London Series B, Biological sciences 367:1287–1296.

OWEN A, SCHIFF N, LAUREYS S (2009a) The Assessment of Conscious Awareness in the Vegetative State. In: The neurology of consciousness: cognitive neuroscience and neuropathology, pp 163–172.

OWEN AM (2008) Disorders of consciousness. Annals of the New York Academy of Sciences 1124:225–238.

OWEN AM, COLEMAN MR, BOLY M, DAVIS MH, LAUREYS S, PICKARD JD (2006) Detecting awareness in the vegetative state. Science (New York, NY) 313:1402.

OWEN AM, COLEMAN MR, MENON DK, JOHNSRUDE IS, RODD JM, DAVIS MH, TAYLOR K, PICKARD JD (2005) Residual auditory function in persistent vegetative state: a combined PET and fMRI study. Neuropsychological rehabilitation 15:290–306.

OWEN AM, SCHIFF ND, LAUREYS S (2009b) A new era of coma and consciousness science. Progress in brain research 177:399–411.

O'REGAN JK (2006) Change Blindness. Encyclopedia of Cognitive Science.

PAAVILAINEN P, CAMMANN R, ALHO K, REINIKAINEN K, SAMS M, NÄÄTÄNEN R (1987) Event-related potentials to pitch change in an auditory stimulus sequence during sleep. Electroencephalography and clinical neurophysiology Supplement 40:246–255.

PALVA S, LINKENKAER-HANSEN K, NÄÄTÄNEN R, PALVA JM (2005) Early neural correlates of conscious somatosensory perception. The Journal of Neuroscience 25:5248–5258.

PARKES L, LUND J, ANGELUCCI A, SOLOMON J A, MORGAN M (2001) Compulsory averaging of crowded orientation signals in human vision. Nature neuroscience 4:739–744.

PASCUAL-LEONE A, WALSH V (2001) Fast backprojections from the motion to the primary visual area necessary for visual awareness. Science (New York, NY) 292:510–512.

PASHLER H (1994) Dual-task interference in simple tasks: data and theory. Psychol Bull 116:220–44.

PASLEY BN, MAYES LC, SCHULTZ RT (2004) Subcortical discrimination of unperceived objects during binocular rivalry. Neuron 42:163–172.

PEDREGOSA F, WEISS R, BRUCHER M (2011) Scikit-learn: Machine Learning in Python. Journal of Machine Learning Research 12:2825–2830.

PENROSE R, HAMEROFF S (2011) Consciousness in the Universe: Neuroscience, Quantum Space-Time Geometry and Orch OR Theory. Journal of Cosmology 14:1–28.

PERRIN F, BASTUJI H, GARCIA-LARREA L (2002) Detection of verbal discordances during sleep. Neuroreport 13:1345–1349.

PERRIN F, GARCÕ L, MAUGUIE Ë (1999) A differential brain response to the subject's own name persists during sleep. Clinical Neurophysiology 110:2153–2164.

PERRIN F, SCHNAKERS C, SCHABUS M, DEGUELDRE C, GOLDMAN S, BREDART S, FAYMONVILLE M-EE, LAMY M, MOONEN G, LUXEN A, BRÉDART S, MAQUET P, LAUREYS S (2006) Brain response to one's own name in vegetative state, minimally conscious state, and locked-in syndrome. Archives of neurology 63:562–569.

PERSAUD N, MCLEOD P, COWEY A (2007) Post-decision wagering objectively measures awareness. Nat Neurosci 10:257–261.

PESSIGLIONE M, PETROVIC P, DAUNIZEAU J, PALMINTERI S, DOLAN RJ, FRITH CD (2008) Subliminal instrumental conditioning demonstrated in the human brain. Neuron 59:561–567.

PESSIGLIONE M, SCHMIDT L, DRAGANSKI B, KALISCH R, LAU H, DOLAN RJ, FRITH CD (2007) How the Brain Translates Money into Force: a Neuroimaging Study of Subliminal Motivation. Science 316:904–906.

PFEIFFER BE, FOSTER DJ (2013) Hippocampal place-cell sequences depict future paths to remembered goals. Nature 497:74–79.

PINS D (2003) The Neural Correlates of Conscious Vision. Cerebral Cortex 13:461–474.

PITTS M A, MARTÍNEZ A, HILLYARD S A (2012) Visual processing of contour patterns under conditions of inattentional blindness. Journal of cognitive neuroscience 24:287–303.

PLATT JC (1999) Probabilistic Outputs for Support Vector Machines and Comparisons to Regularized Likelihood Methods Smola AJ, Bartlett PL, Schölkopf B, Schuurmans D, eds. Advances in Large Margin Classifiers 10:61–74.

PLOURDE G, BELIN P, CHARTRAND D, FISET P, BACKMAN SB, XIE G, ZATORRE RJ (2006) Cortical processing of complex auditory stimuli during alterations of consciousness with the general anesthetic propofol. Anesthesiology 104:448–457.

POE GR, NITZ DA, MCNAUGHTON BL, BARNES CA (2000) Experience-dependent phase-reversal of hippocampal neuron firing during REM sleep. Brain research 855:176–180.

POLICH J (2007) Updating P300: an integrative theory of P3a and P3b. Clinical neurophysiology 118:2128–2148.

POLICH J, CRIADO JR (2006) Neuropsychology and neuropharmacology of P3a and P3b. International journal of psychophysiology 60:172–185.

POLICH J, MARGALA C (1997) P300 and probability: comparison of oddball and single-stimulus paradigms. International Journal of Psychophysiology 25:169–176.

POLONSKY A, BLAKE R, BRAUN J, HEEGER DJ (2000) Neuronal activity in human primary visual cortex correlates with perception during binocular rivalry. Nature neuroscience 3:1153–1159.

POPPER K, ECCLES JC (1984) The Self and Its Brain: An Argument for Interactionism. Routledge.

PORTAS CM, KRAKOW K, ALLEN P, JOSEPHS O, ARMONY JL, FRITH CD (2000) Auditory processing across the sleep-wake cycle: simultaneous EEG and fMRI monitoring in humans. Neuron 28:991–999.

POSNER JB, SAPER CB, SCHIFF N, PLUM F (2007) Plum and Posner's diagnosis of stupor and coma. In. Oxford University Press, USA.

POSNER MI, ROTHBART MK (1991) Les mécanismes de l'attention et l'expérience consciente. Revue de Neuropsychologie 2:85–115.

POSNER MI, ROTHBART MK (1998) Attention, self-regulation and consciousness. Philosophical transactions of the Royal Society of London Series B, Biological sciences 353:1915–1927.

POSNER MI, SCENCESS D (1994) Review Attention: The mechanisms of consciousness. Proceedings of National Academy of Science USA 91:7398–7403.

POSNER MI, SNYDER CRR (1975) Attention and cognitive control. In: Information processing and cognition The Loyola Symposium (Solso RL, ed), pp 55–85. Erlbaum.

POUGET A, DENEVE S, DUHAMEL JR (2002) A computational perspective on the neural basis of multisensory spatial representations. Nature Reviews Neuroscience 3:741–747.

PRESS WH, TEUKOLSKY SA, VETTERLING WT, FLANNERY BP (2007) Numerical Recipes 3rd Edition: The Art of Scientific Computing. Cambridge University Press.

PÖPPEL E, HELD R, FROST D (1973) Residual Visual Function after Brain Wounds involving the Central Visual Pathways in Man. Nature 243:295–296.

QIAO E, VINCKIER F, SZWED M, NACCACHE L, VALABRÈGUE R, DEHAENE S, COHEN L (2010) Unconsciously deciphering handwriting: subliminal invariance for handwritten words in the visual word form area. NeuroImage 49:1786–1799.

QUIAN QUIROGA R, PANZERI S (2009) Extracting information from neuronal populations: information theory and decoding approaches. Nature reviews Neuroscience 10:173–185.

QUIROGA RQ, MUKAMEL R, ISHAM EA, MALACH R, FRIED I (2008) Human single-neuron responses at the threshold of conscious recognition. Proceedings of the National Academy of Sciences of the United States of America 105:3599–3604.

RAGAZZONI A, PIRULLI C, VENIERO D, FEURRA M, CINCOTTA M, GIOVANNELLI F, CHIARAMONTI R, LINO M, ROSSI S, MINIUSSI C (2013) Vegetative versus minimally conscious states: a study using TMS-EEG, sensory and event-related potentials. PloS one 8:e57069.

RAHNEV D A, BAHDO L, DE LANGE FP, LAU H (2012a) Prestimulus hemodynamic activity in dorsal attention network is negatively associated with decision confidence in visual perception. Journal of neurophysiology 108:1529–1536.

RAHNEV D A, HUANG E, LAU H (2012b) Subliminal stimuli in the near absence of attention influence top-down cognitive control. Attention, perception & psychophysics 74:521–532.

RAHNEV D, MANISCALCO B, GRAVES T, HUANG E, DE LANGE FP, LAU H (2011) Attention induces conservative subjective biases in visual perception. Nature neuroscience 14:1513–1515.

RAICHLE ME, MACLEOD A M, SNYDER AZ, POWERS WJ, GUSNARD D A, SHULMAN GL (2001) A default mode of brain function. Proceedings of the National Academy of Sciences of the United States of America 98:676–682.

RAMANI R, QIU M, REKKAS V, RAJEEVAN N, CONSTABLE RT (2007) Effect of 0.25 MAC and 0.5 MAC Sevoflurane on Memory--A Functional MRI Study in Healthy Volunteers. Anesthesiology:1890.

RAMKUMAR P, JAS M, PANNASCH S, HARI R, PARKKONEN L (2013) Feature-specific information processing precedes concerted activation in human visual cortex. The Journal of neuroscience 33:7691–7699.

RAMPIL IJ (1998) A primer for EEG signal processing in anesthesia. Anesthesiology 89:980–1002.

RAO RP, BALLARD DH (1999) Predictive coding in the visual cortex: a functional interpretation of some extra-classical receptive-field effects. Nature neuroscience 2:79–87.

RATCLIFF R, MCKOON G (2008) The Diffusion Decision Model: Theory and Data for Two-Choice Decision Tasks.

RATCLIFF R, ROUDER JN (1998) Modeling Response Times for Two-Choice Decisions. Psychological Science 9:347–356.

RATCLIFF R, VAN ZANDT T, MCKOON G (1999) Connectionist and diffusion models of reaction time. Psychological Review 106:261–300.

RAYMOND JE, SHAPIRO KL, ARNELL KM (1997) The attentional blink. Trends in cognitive sciences 1:291–296.

REBER TP, LUECHINGER R, BOESIGER P, HENKE K (2012) Unconscious relational inference recruits the hippocampus. The Journal of Neuroscience 32:6138–6148.

RECHTSCHAFFEN A, HAURI P, ZEITLIN M (1966) Auditory awakening thresholds in REM and NREM sleep stages. Perceptual and motor skills 22:927–942.

REDCAY E, KENNEDY DP, COURCHESNE E (2007) fMRI during natural sleep as a method to study brain function during early childhood. NeuroImage 38:696–707.

REES G, KREIMAN G, KOCH C (2002) Neural correlates of consciousness in humans. Nature reviews Neuroscience 3:261–270.

REY M, BASTUJI H, GARCIA-LARREA L, GUILLEMANT P, MAUGUIÈRE F, MAGNIN M (2007) Human thalamic and cortical activities assessed by dimension of activation and spectral edge frequency during sleep wake cycles. Sleep 30:907–912.

REYNOLDS JH, CHELAZZI L, DESIMONE R (1999) Competitive mechanisms subserve attention in macaque areas V2 and V4. The Journal of neuroscience 19:1736–1753.

RIBARY U, IOANNIDES AA, SINGH KD, HASSON R, BOLTON JP, LADO F, MOGILNER A, LLINÁS R (1991) Magnetic field tomography of coherent thalamocortical 40-Hz oscillations in humans. Proceedings of the National Academy of Sciences of the United States of America 88:11037–11041.

RIHS TA, MICHEL CM, THUT G (2009) A bias for posterior alpha-band power suppression versus enhancement during shifting versus maintenance of spatial attention. NeuroImage 44:190–199.

RISSMAN J, GREELY HT, WAGNER AD (2010) Detecting individual memories through the neural decoding of memory states and past experience. Proceedings of the National Academy of Sciences 107:9849–9854.

RO T, BREITMEYER B, BURTON P, SINGHAL NS, LANE D (2003) Feedback contributions to visual awareness in human occipital cortex. Current Biology 13:1038–1041.

RODRIGUEZ E, GEORGE N, LACHAUX JP, MARTINERIE J, RENAULT B, VARELA FJ (1999) Perception's shadow: long-distance synchronization of human brain activity. [London: Macmillan Journals], 1869-.

ROELFSEMA PR, LAMME V A F, SPEKREIJSE H (2004) Synchrony and covariation of firing rates in the primary visual cortex during contour grouping. Nature neuroscience 7:982–991.

ROELFSEMA PR, LAMME V A F, SPEKREIJSE H, BOSCH H (2002) Figure-ground segregation in a recurrent network architecture. Journal of cognitive neuroscience 14:525–537.

ROELFSEMA PR, LAMME VA, SPEKREIJSE H (1998) Object-based attention in the primary visual cortex of the macaque monkey. Nature 395:376–381.

ROGERS BP, MORGAN VL, NEWTON AT, GORE JC (2007) Assessing functional connectivity in the human brain by fMRI. Magnetic resonance imaging 25:1347–1357.

ROHAUT B, FAUGERAS F, BEKINSCHTEIN T -A., WASSOUF A., CHAUSSON N, DEHAENE S, NACCACHE L (2009) Prédiction du réveil et détection de la conscience : intérêt des potentiels évoqués cognitifs. Réanimation 18:659–663.

ROMEI V, BRODBECK V, MICHEL C, AMEDI A, PASCUAL-LEONE A, THUT G (2008a) Spontaneous fluctuations in posterior alpha-band EEG activity reflect variability in excitability of human visual areas. Cerebral cortex 18:2010–2018.

ROMEI V, RIHS T, BRODBECK V, THUT G (2008b) Resting electroencephalogram alpha-power over posterior sites indexes baseline visual cortex excitability. Neuroreport 19:203–208.

ROMO R, BRODY CD, HERNÁNDEZ A, LEMUS L (1999) Neuronal correlates of parametric working memory in the prefrontal cortex. Nature 399:470–473.

ROSAHL SK, KNIGHT RT (1995) Role of Prefrontal Cortex in Generation of the Contingent Negative Variation. Cerebral Cortex 5:123–134.

ROSANOVA M, GOSSERIES O, CASAROTTO S, BOLY M, CASALI AG, BRUNO M-A, MARIOTTI M, BOVEROUX P, TONONI G, LAUREYS S, MASSIMINI M (2012) Recovery of cortical effective connectivity and recovery of consciousness in vegetative patients. Brain 135:1308–1320.

ROSENBLATH W (1899) Uber einen bemerkenswerten Fall von Hirnerschutterung. Dtch Arch Klein Med 64:406–420.

ROSENTHAL DM (1997) A theory of consciousness. The nature of consciousness:729–753.

ROUNIS E, MANISCALCO B, ROTHWELL JCJ, PASSINGHAM RERRE, LAU H (2010) Theta-burst transcranial magnetic stimulation to the prefrontal cortex impairs metacognitive visual awareness. Cognitive neuroscience 1:165–175.

RUDOLF J, SOBESKY J, GROND M, HEISS WD (2000) Identification by positron emission tomography of neuronal loss in acute vegetative state. Lancet 355:115–116.

SAALMANN YB, PINSK MA, WANG L, LI X, KASTNER S (2012) The pulvinar regulates information transmission between cortical areas based on attention demands. Science (New York, NY) 337:753–756.

SADAGHIANI S, HESSELMANN G, KLEINSCHMIDT A (2009) Distributed and antagonistic contributions of ongoing activity fluctuations to auditory stimulus detection. The Journal of Neuroscience 29:13410–13417.

SADAGHIANI S, SCHEERINGA R, LEHONGRE K, MORILLON B, GIRAUD A-L, KLEINSCHMIDT A (2010) Intrinsic connectivity networks, alpha oscillations, and tonic alertness: a simultaneous electroencephalography/functional magnetic resonance imaging study. The Journal of Neuroscience 30:10243–10250.

SAHRAIE A, WEISKRANTZ L, BARBUR JL, SIMMONS A, WILLIAMS SCR, BRAMMER MJ (1997) Pattern of neuronal activity associated with conscious and unconscious processing of visual signals. Proceedings of the National Academy of Sciences 94:9406–9411.

SALEK-HADDADI A, LEMIEUX L, MERSCHHEMKE M, FRISTON KJ, DUNCAN JS, FISH DR (2003) Functional magnetic resonance imaging of human absence seizures. Annals of neurology 53:663–667.

SALISBURY D, SQUIRES NK, IBEL S, MALONEY T (1992) Auditory event-related potentials during stage 2 NREM sleep in humans. Journal of sleep research 1:251–257.

SALLINEN M, KAARTINEN J, LYYTINEN H (1996) Processing of auditory stimuli during tonic and phasic periods of REM sleep as revealed by event-related brain potentials. Journal of sleep research 5:220–228.

SALOMON D (2007) Data Compression: The Complete Reference (Vol. 10). Springer-Verlag.

SALTI M, BAR-HAIM Y, LAMY D (2012) The P3 component of the ERP reflects conscious perception, not confidence. Consciousness and cognition 21:961–968.

SAMS M, PAAVILAINEN P, ALHO K, NÄÄTÄNEN R (1985) Auditory frequency discrimination and event-related potentials. Electroencephalography and Clinical Neurophysiology/Evoked Potentials Section 62:437–448.

SANDBERG K, BIBBY BM, TIMMERMANS B, CLEEREMANS A, OVERGAARD M (2011) Measuring consciousness: task accuracy and awareness as sigmoid functions of stimulus duration. Consciousness and cognition 20:1659–1675.

SCHAEFER RS, FARQUHAR J, BLOKLAND Y, SADAKATA M, DESAIN P (2010) Name that tune: Decoding music from the listening brain. NeuroImage.

SCHIFF N, PLUM F (1999) Cortical function in the persistent vegetative state. Trends in cognitive sciences 3:43–44.

SCHIFF ND, GIACINO JT, KALMAR K, VICTOR JD, BAKER K, GERBER M, FRITZ B, EISENBERG B, BIONDI T, O'CONNOR J, KOBYLARZ EJ, FARRIS S, MACHADO A, McCAGG C, PLUM F, FINS JJ, REZAI A R (2007) Behavioural improvements with thalamic stimulation after severe traumatic brain injury. Nature 448:600–603.

SCHIFF ND, RODRIGUEZ-MORENO D, KAMAL A, KIM KHS, GIACINO JT, PLUM F, HIRSCH J (2005) fMRI reveals large-scale network activation in minimally conscious patients. Neurology 64:514–523.

SCHNAKERS C, GIACINO J, KALMAR K, PIRET S, LOPEZ E, BOLY M, MALONE R, LAUREYS S (2006) Does the FOUR score correctly diagnose the vegetative and minimally conscious states? Annals of neurology 60:744–5; author reply 745.

SCHNAKERS C, LEDOUX D, MAJERUS S, DAMAS P, DAMAS F, LAMBERMONT B, LAMY M, BOLY M, VANHAUDENHUYSE A, MOONEN G, LAUREYS S (2008a) Diagnostic and prognostic use of bispectral index in coma, vegetative state and related disorders. Brain injury 22:926–931.

SCHNAKERS C, MAJERUS S, GIACINO J, VANHAUDENHUYSE A, BRUNO M-A, BOLY M, MOONEN G, DAMAS P, LAMBERMONT B, LAMY M, DAMAS F, VENTURA M, LAUREYS S (2008b) A French validation study of the Coma Recovery Scale-Revised (CRS-R). Brain injury 22:786–792.

SCHNAKERS C, PERRIN F, SCHABUS M, HUSTINX R, MAJERUS S, MOONEN G, BOLY M, VANHAUDENHUYSE A, BRUNO M-A, LAUREYS S (2009a) Detecting consciousness in a total locked-in syndrome: an active event-related paradigm. Neurocase 15:271–277.

SCHNAKERS C, VANHAUDENHUYSE A, GIACINO J, VENTURA M, BOLY M, MAJERUS S, MOONEN G, LAUREYS S (2009b) Diagnostic accuracy of the vegetative and minimally conscious state: clinical consensus versus standardized neurobehavioral assessment. BMC neurology 9:35.

SCHOENLE PW, WITZKE W (2004) How vegetative is the vegetative state? Preserved semantic processing in VS patients--evidence from N 400 event-related potentials. NeuroRehabilitation 19:329–334.

SCHOLTE HS, WITTEVEEN SC, SPEKREIJSE H, LAMME VAF (2006) The influence of inattention on the neural correlates of scene segmentation. Brain research 1076:106–115.

SCHROUFF J, PERLBARG V, BOLY M, MARRELEC G, BOVEROUX P, VANHAUDENHUYSE A, BRUNO M-A, LAUREYS S, PHILLIPS C, PÉLÉGRINI-ISSAC M, MAQUET P, BENALI H (2011) Brain functional integration decreases during propofol-induced loss of consciousness. NeuroImage 57:198–205.

SCHRÖTER MS, SPOORMAKER VI, SCHORER A, WOHLSCHLÄGER A, CZISCH M, KOCHS EF, ZIMMER C, HEMMER B, SCHNEIDER G, JORDAN D, ILG R (2012) Spatiotemporal reconfiguration of large-scale brain functional networks during propofol-induced loss of consciousness. The Journal of Neuroscience 32:12832–12840.

SCHURGER A, COWEY A, TALLON-BAUDRY C (2006) Induced gamma-band oscillations correlate with awareness in hemianopic patient GY. Neuropsychologia 44:1796–1803.

SCHURGER A, PEREIRA F, TREISMAN A, COHEN JD, SCHURGER PEREIRA, F.,TREISMAN, A., COHEN, J. A (2010) Reproducibility Distinguishes Conscious From Non-conscious Neural Representations. Science 327:97–99.

SCHWIEDRZIK CM, SINGER W, MELLONI L (2009) Sensitivity and perceptual awareness increase with practice in metacontrast masking. Journal of vision 9:18.1–18.

SCHYNS PG, THUT G, GROSS J (2011) Cracking the code of oscillatory activity. PLoS biology 9:e1001064.

SCULTHORPE LD, OUELLET DR, CAMPBELL KB (2009) MMN elicitation during natural sleep to violations of an auditory pattern. Brain research 1290:52–62.

SEBEL PS, BOWDLE TA, GHONEIM MM, RAMPIL IJ, PADILLA RE, GAN TJ, DOMINO KB (2004) The incidence of awareness during anesthesia: a multicenter United States study. Anesthesia & Analgesia 99:833–839, table of contents.

SEKAR K, FINDLEY WM, POEPPEL D, LLINÁS RR (2013) Cortical response tracking the conscious experience of threshold duration visual stimuli indicates visual perception is all or none. Proceedings of the National Academy of Sciences of the United States of America 110:5642–5647.

SERGENT C, BAILLET S, DEHAENE S (2005) Timing of the brain events underlying access to consciousness during the attentional blink. Nature Neuroscience 8:1391–1400.

SERGENT C, DEHAENE S (2004) Is consciousness a gradual phenomenon? Evidence for an all-or-none bifurcation during the attentional blink. Psychological Science 15:720–728.

SERGENT C, NACCACHE L (2012) Imaging neural signatures of consciousness: "what", "when", "where" and "how" does it work? Archives italiennes de biologie 150:91–106.

SERGENT C, WYART V, BABO-REBELO M, COHEN L, NACCACHE L, TALLON-BAUDRY C (2013) Cueing attention after the stimulus is gone can retrospectively trigger conscious perception. Current Biology 23:150–155.

SETH A (2007) Models of consciousness. Scholarpedia 2:1328.

SETH AK, BARRETT AB, BARNETT L (2011) Causal density and integrated information as measures of conscious level. Philosophical transactions Series A, Mathematical, physical, and engineering sciences 369:3748–3767.

SETH AK, DIENES Z, CLEEREMANS A, OVERGAARD M, PESSOA L (2008) Measuring consciousness: relating behavioural and neurophysiological approaches. Trends in cognitive sciences 12:314–321.

SETH AK, IZHIKEVICH E, REEKE GN, EDELMAN GM (2006) Theories and measures of consciousness: an extended framework. Proceedings of the National Academy of Sciences of the United States of America 103:10799–10804.

SETH AK, MCKINSTRY JL, EDELMAN GM, KRICHMAR JL (2004) Visual binding through reentrant connectivity and dynamic synchronization in a brain-based device. Cerebral cortex 14:1185–1199.

SHADLEN MN, KIANI R, HANKS TD, CHURCHLAND AK (2008) Neurobiology of Decision Making An Intentional Framework. In: Better than Conscious?, pp 71–101.

SHADLEN MN, MOVSHON JA (1999) Synchrony Unbound: Review A Critical Evaluation of the Temporal Binding Hypothesis. Neuron 24:67–77.

SHALBAF R, BEHNAM H, SLEIGH JW, STEYN-ROSS A, VOSS LJ (2013) Monitoring the depth of anesthesia using entropy features and an artificial neural network. Journal of neuroscience methods 218:17–24.

SHAW FZ, CHEN RF, TSAO HW, YEN CT (1999) Algorithmic complexity as an index of cortical function in awake and pentobarbital-anesthetized rats. Journal of neuroscience methods 93:101–110.

SHEINBERG DL, LOGOTHETIS NK (1997) The role of temporal cortical areas in perceptual organization. Proceedings of the National Academy of Sciences of the United States of America 94:3408–3413.

SHIEL A, HORN SA, WILSON BA, WATSON MJ, CAMPBELL MJ, MCLELLAN DL (2000) The Wessex Head Injury Matrix (WHIM) main scale: a preliminary report on a scale to assess and monitor patient recovery after severe head injury. Clinical rehabilitation 14:408–416.

SIEGEL M, DONNER TH, OOSTENVELD R, FRIES P, ENGEL AK (2008) Neuronal synchronization along the dorsal visual pathway reflects the focus of spatial attention. Neuron 60:709–719.

SILVA S, ALACOQUE X, FOURCADE O, SAMII K, MARQUE P, WOODS R, MAZZIOTTA J, CHOLLET F, LOUBINOUX I (2010) Wakefulness and loss of awareness: brain and brainstem interaction in the vegetative state. Neurology 74:313–320.

SILVANTO J, COWEY A, LAVIE N, WALSH V (2005) Striate cortex (V1) activity gates awareness of motion. Nature neuroscience 8:143–144.

SIMONS DJ, CHABRIS CF (1999) Gorillas in our midst: sustained inattentional blindness for dynamic events. Perception 28:1059–1074.

SIMPSON TP, MANARA AR, KANE NM, BARTON RL, ROWLANDS CA, BUTLER SR (2002) Effect of propofol anaesthesia on the event-related potential mismatch negativity and the auditory-evoked potential N1. British journal of anaesthesia 89:382–388.

SINGER W (1993) Synchronization of cortical activity and its putative role in information processing and learning. Annual review of physiology 55:349–374.

SINGER W, GRAY CM (1995a) Visual feature integration and the temporal correlation hypothesis. Annual review of neuroscience 18:555–586.

SINGER W, GRAY CM (1995b) Integration and the Temporal Correlation Hypothesis.

SITT JD, KING J-R, NACCACHE L, DEHAENE S (2013) Ripples of consciousness. Trends in cognitive sciences 17:552–554.

SLIGTE IG, VANDENBROUCKE ARE, SCHOLTE HS, LAMME V A F (2010) Detailed sensory memory, sloppy working memory. Frontiers in psychology 1:175.

SNODGRASS M (2002) Disambiguating conscious and unconscious influences: Do exclusion paradigms demonstrate unconscious perception? American Journal of Psychology 115:545–579.

SNODGRASS M, SHEVRIN H (2006) Unconscious inhibition and facilitation at the objective detection threshold: replicable and qualitatively different unconscious perceptual effects. Cognition 101:43–79.

SODDU A, VANHAUDENHUYSE A, BAHRI MA, BRUNO M-A, BOLY M, DEMERTZI A, TSHIBANDA J-F, PHILLIPS C, STANZIANO M, OVADIA-CARO S, NIR Y, MAQUET P, PAPA M, MALACH R, LAUREYS S, NOIRHOMME Q (2012) Identifying the default-mode component in spatial IC analyses of patients with disorders of consciousness. Human brain mapping 33:778–796.

SOFTKY WR, KOCH C (1993) The highly irregular firing of cortical cells is inconsistent with temporal integration of random EPSPs. The Journal of Neuroscience 13:334–350.

SPERLING G (1960) The information available in brief visual presentations. Psychological Monographs General and Applied 74:1–29.

SPONG P, HAIDER M, LINDSLEY DB (1965) Selective attentiveness and cortical evoked responses to visual and auditory stimuli. Science 148:395–397.

SPORNS O, GALLY JA A, REEKE GNN, EDELMAN GM (1989) Reentrant signaling among simulated neuronal groups leads to coherency in their oscillatory activity. Proceedings of the National Academy of Sciences of the United States of America 86:7265–7269.

SPORNS O, TONONI G, EDELMAN GM (1991) Modeling perceptual grouping and figure-ground segregation by means of active reentrant connections. Proceedings of the National Academy of Sciences of the United States of America 88:129–133.

SPORNS O, TONONI G, EDELMAN GM (2000) Connectivity and complexity: the relationship between neuroanatomy and brain dynamics. Neural Networks 13:909–922.

SQUIRES KC, HILLYARD S A., LINDSAY PH (1973a) Vertex potentials evoked during auditory signal detection: Relation to decision criteria. Perception & Psychophysics 13:25–31.

SQUIRES KC, HILLYARD S A., LINDSAY PH (1973b) Cortical potentials evoked by confirming and disconfirming feedback following an auditory discrimination. Perception & Psychophysics 13:25–31.

SQUIRES KC, SQUIRES NK, HILLYARD SA (1975a) Vertex evoked potentials in a rating-scale detection task: relation to signal probability. Behavioral Biology 13:21–34.

SQUIRES KC, WICKENS C, SQUIRES NK, DONCHIN E (1976) The effect of stimulus sequence on the waveform of the cortical event-related potential. Science (New York, NY) 193:1142–1146.

SQUIRES NK, SQUIRES KC, HILLYARD SA (1975b) Two varieties of long-latency positive waves evoked by unpredictable auditory stimuli in man. Electroencephalography and Clinical Neurophysiology 38:387–401.

STAM CJ (2005) Nonlinear dynamical analysis of EEG and MEG: review of an emerging field. Clinical neurophysiology 116:2266–2301.

STAM CJ, NOLTE G, DAFFERTSHOFER A (2007) Phase lag index: assessment of functional connectivity from multi channel EEG and MEG with diminished bias from common sources. Human brain mapping 28:1178–1193.

STANIEK M, LEHNERTZ K (2008) Symbolic transfer entropy. Physical review letters 100:158101.

STEPPACHER I, EICKHOFF S, JORDANOV T, KAPS M, WITZKE W, KISSLER J (2013) N400 predicts recovery from disorders of consciousness. Annals of neurology 73:594–602.

STERIADE M, MCCORMICK D A, SEJNOWSKI TJ (1993) Thalamocortical oscillations in the sleeping and aroused brain. Science 262:679–685.

STERNBERG S (1969) The discovery of processing stages: Extensions of Donders' method Koster WG, ed. Acta Psychologica 30:276–315.

STOERIG P, COWEY A (2009) Blindsight. The Oxford Companion to Consciousness:112–115.

STOERIG P, HÜBNER M, PÖPPEL E (1985) Signal detection analysis of residual vision in a field defect due to a post-geniculate lesion. Neuropsychologia 23:589–599.

STOKES MG, KUSUNOKI M, SIGALA N, NILI H, GAFFAN D, DUNCAN J (2013) Dynamic coding for cognitive control in prefrontal cortex. Neuron 78:364–375.

STRICH SJ (1956) Diffuse degeneration of the cerebral white matter in severe dementia following head injury. Journal of neurology, neurosurgery, and psychiatry 19:163–185.

STURM W, WILLMES K (2001) On the functional neuroanatomy of intrinsic and phasic alertness. NeuroImage 14:S76–84.

STUSS DT, PICTON TW, CERRI AM, LEECH EE, STETHEM LL (1992) Perceptual closure and object identification: electrophysiological responses to incomplete pictures. Brain and cognition 19:253–266.

SUDRE G, POMERLEAU D, PALATUCCI M, WEHBE L, FYSHE A, SALMELIN R, MITCHELL T (2012) Tracking neural coding of perceptual and semantic features of concrete nouns. NeuroImage 62:451–463.

SUMMERFIELD C, JACK AI, BURGESS AP (2002) Induced gamma activity is associated with conscious awareness of pattern masked nouns. International journal of psychophysiology 44:93–100.

SUMMERFIELD C, KOECHLIN E (2008) A neural representation of prior information during perceptual inference. Neuron 59:336–347.

SUPP GG, SIEGEL M, HIPP JF, ENGEL AK (2011) Supplemental Information Cortical Hypersynchrony Predicts Breakdown of Sensory Processing during Loss of Consciousness. Current Biology 21:1988–1993.

SUPÈR H, SPEKREIJSE H, LAMME V A (2001) Two distinct modes of sensory processing observed in monkey primary visual cortex (V1). Nature neuroscience 4:304–310.

SUTTON S, BRAREN M, ZUBIN J, JOHN ER (1965) Evoked-Potential Correlates of Stimulus Uncertainty. Science 150:1187–1188.

TALLON-BAUDRY C (2009) The roles of gamma-band oscillatory synchrony in human visual cognition. Frontiers in bioscience (Landmark edition) 14:321–332.

TALLON-BAUDRY C, BERTRAND O (1999) Oscillatory gamma activity in humans and its role in object representation. Trends in Cognitive Sciences 3:151–162.

TALLON-BAUDRY C, BERTRAND O, DELPUECH C, PERNIER J (1997) Oscillatory gamma -Band (30-70 Hz) Activity Induced by a Visual Search Task in Humans. J Neurosci 17:722–734.

TALLON-BAUDRY C, BERTRAND O, FISCHER C (2001) Oscillatory synchrony between human extrastriate areas during visual short-term memory maintenance. The Journal of Neuroscience 21:RC177.

TAMIETTO M, GEMINIANI G, GENERO R, DE GELDER B (2007) Seeing fearful body language overcomes attentional deficits in patients with neglect. Journal of Cognitive Neuroscience 19:445–454.

TANAKA H, FUJITA N, TAKANASHI M, HIRABUKI N, YOSHIMURA H, ABE K, NAKAMURA H (2003) Effect of stage 1 sleep on auditory cortex during pure tone stimulation: evaluation by functional magnetic resonance imaging with simultaneous EEG monitoring. AJNR American journal of neuroradiology 24:1982–1988.

TASKIN B, HOLTZE S, KRAUSE T, VILLRINGER A (2008) Inhibitory impact of subliminal electrical finger stimulation on SI representation and perceptual sensitivity of an adjacent finger. NeuroImage 39:1307–1313.

TAULU S, KAJOLA M, SIMOLA J (2004) Suppression of interference and artifacts by the Signal Space Separation Method. Brain topography 16:269–275.

THIRION B, DUCHESNAY E, HUBBARD E, DUBOIS J, POLINE J-B, LEBIHAN D, DEHAENE S (2006) Inverse retinotopy: inferring the visual content of images from brain activation patterns. NeuroImage 33:1104–1116.

TIITINEN H, MAY P, REINIKAINEN K, NÄÄTÄNEN R (1994) Attentive novelty detection in humans is governed by pre-attentive sensory memory. Nature 372:90–92.

TOMMASINO C, GRANA C, LUCIGNANI G, TORRI G, FAZIO F (1995) Regional cerebral metabolism of glucose in comatose and vegetative state patients. Journal of neurosurgical anesthesiology 7:109–116.

TONG F, MENG M, BLAKE R (2006) Neural bases of binocular rivalry. Trends in cognitive sciences 10:502–511.

TONG F, NAKAYAMA K, VAUGHAN JT, KANWISHER N (1998) Binocular rivalry and visual awareness in human extrastriate cortex. Neuron 21:753–759.

TONONI G (2004) An information integration theory of consciousness. BMC neuroscience 5:42.

TONONI G (2008) Consciousness as Integrated Information: a provisional manifesto. :216–242.

TONONI G, EDELMAN GM (1998) Consciousness and Complexity. Science 282:1846–1851.

TONONI G, EDELMAN GM, SPORNS O (1998) Complexity and coherency: integrating information in the brain. Trends in cognitive sciences 2:474–484.

TONONI G, KOCH C (2008) The neural correlates of consciousness: an update. Annals of the New York Academy of Sciences 1124:239–261.

TONONI G, SPORNS O (2003) Measuring information integration. BMC Neuroscience 4:31.

TONONI G, SPORNS O, EDELMAN GM (1994) A measure for brain complexity: relating functional segregation and integration in the nervous system. Proceedings of the National Academy of Sciences 91:5033–5037.

TOWNSEND JT (1990) Serial vs. Parallel Processing: Sometimes They Look Like Tweedledum and Tweedledee but They Can (and Should) be Distinguished. Psychological Science 1:46–54.

TSHIBANDA L, VANHAUDENHUYSE A, GALANAUD D, BOLY M, LAUREYS S, PUYBASSET L (2009) Magnetic resonance spectroscopy and diffusion tensor imaging in coma survivors: promises and pitfalls. Progress in brain research 177:215–229.

TURVEY MT (1973) On peripheral and central processes in vision: inferences from an information-processing analysis of masking with patterned stimuli. Psychological review 80:1–52.

TZOVARA A, ROSSETTI AO, SPIERER L, GRIVEL J, MURRAY MM, ODDO M, DE LUCIA M (2012) Progression of auditory discrimination based on neural decoding predicts awakening from coma. Brain.

URSU S, CLARK K A, AIZENSTEIN HJ, STENGER VA, CARTER CS (2009) Conflict-related activity in the caudal anterior cingulate cortex in the absence of awareness. Biological psychology 80:279–286.

UUSITALO MA, ILMONIEMI RJ (1997) Signal-space projection method for separating MEG or EEG into components. Medical & Biological Engineering & Computing 35:135–140.

VAKKURI A, YLI-HANKALA A, TALJA P, MUSTOLA S, TOLVANEN-LAAKSO H, SAMPSON T, VIERTIO-OJA H (2004) Time-frequency balanced spectral entropy as a measure of anesthetic drug effect in central nervous system during sevoflurane, propofol, and thiopental anesthesia. Acta Anaesthesiologica Scandinavica 48:145–153.

VAN AALDEREN-SMEETS SI, OOSTENVELD R, SCHWARZBACH J (2006) Investigating neurophysiological correlates of metacontrast masking with magnetoencephalography. Advances in Cognitive Psychology 2:21–35.

VAN DEN BUSSCHE E, VAN DEN NOORTGATE W, REYNVOET B (2009) Mechanisms of masked priming: a meta-analysis. Psychological bulletin 135:452–477.

VAN DIJK H, SCHOFFELEN J-M, OOSTENVELD R, JENSEN O (2008) Prestimulus oscillatory activity in the alpha band predicts visual discrimination ability. The Journal of Neuroscience 28:1816–1823.

VAN GAAL S, LAMME V A F (2011) Unconscious High-Level Information Processing: Implication for Neurobiological Theories of Consciousness. The Neuroscientist 18:287–301.

VAN GAAL S, LAMME V A F, FAHRENFORT JJ, RIDDERINKHOF KR (2011) Dissociable brain mechanisms underlying the conscious and unconscious control of behavior. Journal of cognitive neuroscience 23:91–105.

VAN GAAL S, RIDDERINKHOF KR, FAHRENFORT JJ, SCHOLTE HS, LAMME V A F, GAAL S VAN (2008) Frontal cortex mediates unconsciously triggered inhibitory control. Journal of Neuroscience 28:8053.

VAN GAAL S, RIDDERINKHOF KR, SCHOLTE HS, LAMME V A F (2010) Unconscious activation of the prefrontal no-go network. The Journal of Neuroscience 30:4143–4150.

VAN GAAL S, RIDDERINKHOF KR, VAN DEN WILDENBERG WPM, LAMME VAF (2009) Dissociating consciousness from inhibitory control: Evidence for unconsciously triggered response inhibition in the stop-signal task. Journal of Experimental Psychology: Human Perception and Performance 35:1129–1139.

VAN GERVEN M A J, KOK P, DE LANGE FP, HESKES T (2011) Dynamic decoding of ongoing perception. NeuroImage 57:950–957.

VAN HOOFF JC, DE BEER NA, BRUNIA CH, CLUITMANS PJ, KORSTEN HH (1997) Event-related potential measures of information processing during general anesthesia. Electroencephalography and clinical neurophysiology 103:268–281.

VANHAUDENHUYSE A, NOIRHOMME Q, TSHIBANDA LJ-F, BRUNO M-A, BOVEROUX P, SCHNAKERS C, SODDU A, PERLBARG V, LEDOUX D, BRICHANT J-F, MOONEN G, MAQUET P, GREICIUS MD, LAUREYS S, BOLY M (2010) Default network connectivity reflects the level of consciousness in non-communicative brain-damaged patients. Brain 133:161–171.

VAROTTO G, FAZIO P, ROSSI SEBASTIANO D, DURAN D, D'INCERTI L, PARATI E, SATTIN D, LEONARDI M, FRANCESCHETTI S, PANZICA F, D'INCERTI L (2013) Altered resting state effective connectivity in long-standing vegetative state patients: An EEG study. Clinical Neurophysiology.

VELLY LJ, REY MF, BRUDER NJ, GOUVITSOS FA, WITJAS T, REGIS JM, PERAGUT JC, GOUIN FM (2007) Differential dynamic of action on cortical and subcortical structures of anesthetic agents during induction of anesthesia. Anesthesiology 107:202–212.

VIERTIÖ-OJA H, MAJA V, SÄRKELÄ M, TALJA P, TENKANEN N, TOLVANEN-LAAKSO H, PALOHEIMO M, VAKKURI A, YLI-HANKALA A, MERILÄINEN P (2004) Description of the Entropy algorithm as applied in the Datex-Ohmeda S/5 Entropy Module. Acta anaesthesiologica Scandinavica 48:154–161.

VIGGIANO MP, KUTAS M (2000) Overt and covert identification of fragmented objects inferred from performance and electrophysiological measures. Journal of Experimental Psychology: General 129:107–125.

VINCENT JL, PATEL GH, FOX MD, SNYDER AZ, BAKER JT, VAN ESSEN DC, ZEMPEL JM, SNYDER LH, CORBETTA M, RAICHLE ME (2007) Intrinsic functional architecture in the anaesthetized monkey brain. Nature 447:83–86.

VOGEL EK, LUCK SJ, SHAPIRO KL (1998) Electrophysiological evidence for a postperceptual locus of suppression during the attentional blink. Journal of experimental psychology Human perception and performance 24:1656–1674.

VOGT BA, LAUREYS S (2005) Posterior cingulate, precuneal and retrosplenial cortices: cytology and components of the neural network correlates of consciousness. Progress in brain research 150:205–217.

VOGT F, KLIMESCH W, DOPPELMAYR M (1998) High-frequency components in the alpha band and memory performance. Journal of clinical neurophysiology 15:167–172.

VON DER MALSBURG C, SCHNEIDER W (1986) A neural cocktail-party processor. Biological cybernetics 54:29–40.

VON WILD K, LAUREYS ST, GERSTENBRAND F, DOLCE G, ONOSE G (2012) The vegetative state--a syndrome in search of a name. Journal of medicine and life 5:3–15.

VORBERG D, MATTLER U, HEINECKE A, SCHMIDT T, SCHWARZBACH J (2003) Different time courses for visual perception and action priming. Proceedings of the National Academy of Sciences of the United States of America 100:6275–6280.

VUILLEUMIER P, SAGIV N, HAZELTINE E, POLDRACK R A, SWICK D, RAFAL RD, GABRIELI JD (2001) Neural fate of seen and unseen faces in visuospatial neglect: a combined event-related functional MRI and event-related potential study. Proceedings of the National Academy of Sciences of the United States of America 98:3495–3500.

VUL E, HANUS D, KANWISHER N (2009a) Attention as inference: selection is probabilistic; responses are all-or-none samples. Journal of experimental psychology General 138:546–560.

VUL E, HARRIS C, WINKIELMAN P, PASHLER H (2009b) Puzzlingly High Correlations in fMRI Studies of Emotion, Personality, and Social Cognition. Perspectives on Psychological Science 4:274–290.

WACONGNE C, CHANGEUX J-P, DEHAENE S (2012) A neuronal model of predictive coding accounting for the mismatch negativity. The Journal of neuroscience 32:3665–3678.

WACONGNE C, LABYT E, VAN WASSENHOVE V, BEKINSCHTEIN T, NACCACHE L, DEHAENE S (2011) Evidence for a hierarchy of predictions and prediction errors in human cortex. Proceedings of the National Academy of Sciences of the United States of America 108:20754–20759.

WALTER WG, COOPER R, ALDRIDGE VJ, MCCALLUM WC, WINTER AL (1964) Contingent Negative Variation: an electric sign of sensorimotor association and expectancy in the human brain. Nature 203:380–384.

WANG X-J (2008) Decision making in recurrent neuronal circuits. Neuron 60:215–234.

WARD LM (2011) The thalamic dynamic core theory of conscious experience. Consciousness and cognition 20:464–486.

WEISKRANTZ L (1986) Blindsight: A case study and implications. Oxford University Press, USA.

WELCH P (1967) The use of fast Fourier transform for the estimation of power spectra: A method based on time averaging over short, modified periodograms. IEEE Transactions on Audio and Electroacoustics 15:70–73.

WELFORD AT (1952) The psychological refractory period and the timing of high-speed performance - A review and a theory. British Journal of Psychology 43:2–19.

WHALEN PJ, RAUCH SL, ETCOFF NL, MCINERNEY SC, LEE MB, JENIKE MA (1998) Masked presentations of emotional facial expressions modulate amygdala activity without explicit knowledge. The Journal of Neuroscience 18:411–418.

WHITNEY D, LEVI DM (2011) Visual crowding: a fundamental limit on conscious perception and object recognition. Trends in cognitive sciences 15:160–168.

WIJDICKS EFM, BAMLET WR, MARAMATTOM B V, MANNO EM, MCCLELLAND RL (2005) Validation of a new coma scale: The FOUR score. Annals of neurology 58:585–593.

WIJNEN VJM, VAN BOXTEL GJM, EILANDER HJ, DE GELDER B (2007) Mismatch negativity predicts recovery from the vegetative state. Clinical neurophysiology 118:597–605.

WILKE M, LOGOTHETIS NK, LEOPOLD DA (2006) Local field potential reflects perceptual suppression in monkey visual cortex. Proceedings of the National Academy of Sciences of the United States of America 103:17507–17512.

WILSON MA, MCNAUGHTON BL (1994) Reactivation of hippocampal ensemble memories during sleep. Science (New York, NY) 265:676–679.

WINDEY B, GEVERS W, CLEEREMANS A (2013) Subjective visibility depends on level of processing. Cognition 129:404–409.

WINKLER I (2007) Interpreting the Mismatch Negativity. 21:147–163.

WINTER O, KOK A, KENERNANS JL, ELTON M, KENEMANS JL (1995) Auditory event-related potentials to deviant stimuli during drowsiness and stage 2 sleep. Electroencephalography and clinical neurophysiology 96:398–412.

WOLFE J (1999) Inattentional Amnesia. Fleeting Memories: Cognition of brief visual stimuli:71.

WOMELSDORF T, FRIES P, MITRA PP, DESIMONE R (2006) Gamma-band synchronization in visual cortex predicts speed of change detection. Nature 439:733–736.

WOOD JN, GRAFMAN J (2003) Human prefrontal cortex: processing and representational perspectives. Nature reviews Neuroscience 4:139–147.

WOODMAN GF, LUCK SJ (2003) Dissociations among attention, perception, and awareness during object-substitution masking. Psychological science 14:605–611.

WYART V, DE GARDELLE V, SCHOLL J, SUMMERFIELD C (2012) Rhythmic Fluctuations in Evidence Accumulation during Decision Making in the Human Brain. Neuron 76:847–858.

WYART V, DEHAENE S, TALLON-BAUDRY C (2011) Early dissociation between neural signatures of endogenous spatial attention and perceptual awareness during visual masking. Frontiers in human neuroscience 6:16.

WYART V, TALLON-BAUDRY C (2008) Neural dissociation between visual awareness and spatial attention. Journal of Neuroscience 28:2667.

WYART V, TALLON-BAUDRY C (2009) How ongoing fluctuations in human visual cortex predict perceptual awareness: baseline shift versus decision bias. The Journal of Neuroscience 29:8715–8725.

WYGNANSKI-JAFFE T, PANTON CM, BUNCIC JR, WESTALL CA (2009) Paradoxical robust visual evoked potentials in young patients with cortical blindness. Documenta ophthalmologica Advances in ophthalmology 119:101–107.

YAMAGISHI N, CALLAN DE, GODA N, ANDERSON SJ, YOSHIDA Y, KAWATO M (2003) Attentional modulation of oscillatory activity in human visual cortex. NeuroImage 20:98–113.

ZEKI S (2003) The disunity of consciousness. Trends in Cognitive Sciences 7:214–218.

ZHANG J, KRIEGESKORTE N, CARLIN JD, ROWE JB (2013) Choosing the rules: distinct and overlapping frontoparietal representations of task rules for perceptual decisions. The Journal of Neuroscience 33:11852–11862.

ZHANG Y, MEYERS EM, BICHOT NP, SERRE T, POGGIO TA, DESIMONE R (2011) Object decoding with attention in inferior temporal cortex. Proceedings of the National Academy of Sciences of the United States of America 108:8850–8855.

ZHAO L, LI J (2006) Visual mismatch negativity elicited by facial expressions under non-attentional condition. Neuroscience letters 410:126–131.

ZHOU J, LIU X, SONG W, YANG Y, ZHAO Z, LING F, HUDETZ AG, LI S-J (2011) Specific and nonspecific thalamocortical functional connectivity in normal and vegetative states. Consciousness and cognition 20:257–268.

ZUNG WW, WILSON WP (1961) Response to Auditory Stimulation During Sleep: Discrimination and Arousal as Studied with Electroencephalography. Archives of General Psychiatry 4:548.

ZYLBERBERG A, FERNÁNDEZ SLEZAK D, ROELFSEMA PR, DEHAENE S, SIGMAN M (2010) The brain's router: a cortical network model of serial processing in the primate brain. PLoS computational biology 6:e1000765.

SUPPLEMENTARY MATERIALS

COMMENT 1

TECHNICAL COMMENT ON "PRESERVED FEEDFORWARD BUT IMPAIRED TOP-DOWN PROCESSES IN THE VEGETATIVE STATE"

Jean-Rémi King [1, 2, 3, 4], Tristan Bekinschtein [5], Stanislas Dehaene [1, 5, 6, 7].

[1] Commissariat à l'Energie Atomique et aux Energies Alternatives, Division of Life Sciences, Institute of Bioimaging, Neurospin, Gif sur Yvette, 91191 France ; [2] Ecole Doctorale Cerveau Cognition Comportement, Université Pierre et Marie Curie-Paris 6, Paris, 75005 France ; [3] Institut National de la Santé et de la Recherche Médicale, Cognitive Neuroimaging Unit, Gif sur Yvette, 91191 France ; [4] Institut National de la Santé et de la Recherche Médicale, Institut du Cerveau et de la Moelle Épinière, UMRS 975, Paris, 75013 France ; [5] Medical Research Council, Cognition and Brain Sciences Unit, 15 Chaucer Road, Cambridge, CB2 7EF United Kingdom ; [6] Université Paris 11, Orsay, 91400 France ; [7] Collège de France, 11 Place Marcelin Berthelot, Paris, 75005 France

ABSTRACT

Boly et al (2011) investigated cortical connectivity patterns in patients suffering from a disorder of consciousness (DOC), using electro-encephalography in an auditory oddball paradigm. We point to several inconsistencies in their data, including a failure to replicate the classical mismatch negativity. Data quality, source reconstruction and statistics would need to be improved in order to support their conclusions.

ARTICLE

Using electro-encephalography (EEG) combined with an auditory odd-ball paradigm, Boly and collaborators [1] investigated the cortical connectivity pattern amongst 21 patients suffering from disorders of consciousness. Activities from the bilateral primary auditory cortices (A1), the bilateral superior temporal gyri (STG) and the right inferior frontal gyrus (IFG) were estimated, and connection strengths inferred with Dynamic Causal Modelling (DCM). It was concluded that vegetative (VS) patients differ from normal subjects and minimally conscious (MCS) patients in a single aspect: reduced top-down feedback from IFG to STG.

While such a top-down anomaly would be compatible with several converging theories of conscious processing [2-4], the data presented so far do not provide unambiguous support for the conclusions.

First, only a small and heterogeneous sample of patients is studied (13 MCS and only 8 VS with different etiologies and recorded from 12 days to 27 years post onset). Their EEG recordings seem noisy, judging from the fact that the classical mismatch negativity (MMN), which is frequently detectable in individual subjects with MCS, VS and even coma [5-8], does not appear to be present (see figures 2 and S1 in the original paper). Instead, their event related potentials (ERPs) are abnormal both in terms of topography and time course, with significant effects appearing too early for the MMN. For instance, across only 8 VS patients, an effect of sound deviancy is reported as shortly as 48 ms after the tone change (their figure 2), with a surprisingly high significance level of $p < 10^{-3}$ given that, at this time, their figure S1 does not even indicate consistent signs for all patients (indeed, the group statistics appears dominated by a single individual, patient VS1). The small ERP component found around 50 ms has been previously observed in healthy subjects performing identical paradigms (*e.g.* [9]), but is believed to reflect stimulus-specific adaptation rather than genuine mismatch detection. Individually, the vast majority of their patients failed to present a significant MMN at any latency (their figure S1). Although bed-side recordings may be noisy and lesions may distort the ERPs, we and our colleagues routinely record the MMN with satisfactory latencies and standard topographies in similar patients (see Fig. 1). Detection of this ERP component should be an indispensable quality check prior to source reconstruction and *a fortiori* to DCM.
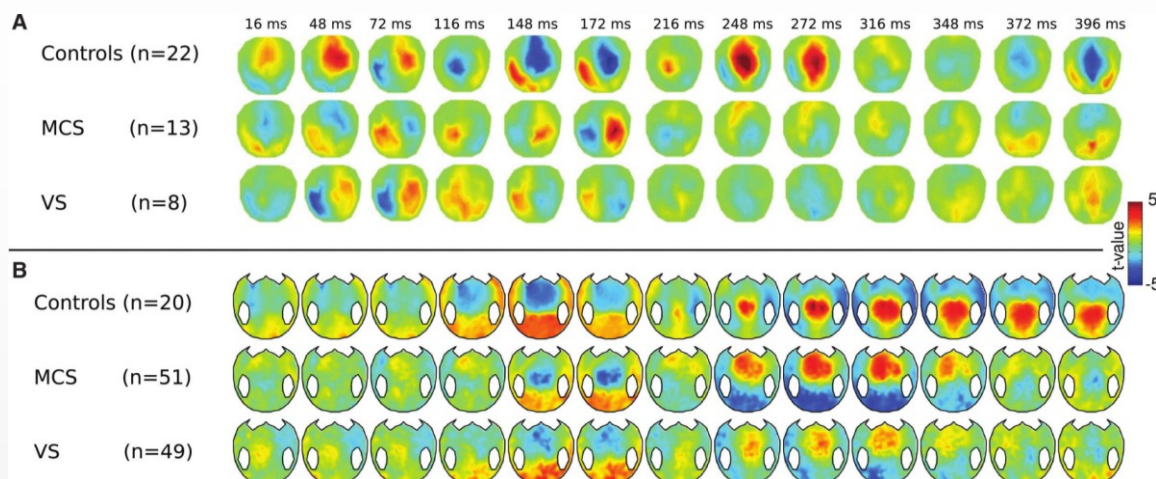

FIGURE 0.1 *MMN TOPOGRAPHY IN DOC PATIENTS AND HEALTHY CONTROLS.*

Comparison of a) Boly et al [1]'s t-test maps for the MMN (comparison of deviant–standard trials) with b) similar maps obtained from 120 recordings collected in the last three years in Lionel Naccache's laboratory, Hôpital de la Salpêtrière, Paris (Intermediate results published in [5, 7], full data set described in [16]). Note that we kept the uneven temporal spaces from Boly et al [1]'s figure 2. The higher resolution data and larger numbers of patients lead to a quiescent period (up to ~100 ms) followed by a classical fronto-central MMN (~100-200 ms) and P3a (~200-300 ms), with similar topography in all groups.

Secondly, from these scalp data, the authors attempted to reconstruct the activation of five distinct but close cortical regions, using MMN source localizations previously reported in healthy subjects. Yet accurate resolution of forward and inverse problems, even with the help of the strong priors imposed by the DCM method, should be particularly difficult with noisy bed-side EEG recordings and variably damaged skulls and brains. In fact, the source reconstructions presented in their figure 3 for a single VS

patient show several implausible features: (a) activity two to five times greater than in the control subject in most regions (note the different scales); (b) an almost entirely left-lateralized A1 response, which is unexplained and inconsistent with the claim of preserved feedforward activity; (c) greater frontal activity for the standard tones than for the deviant tones, which is inconsistent with all previous fMRI and ERP results on the MMN [6, 10]. It would be reassuring if the accuracy of DCM source reconstruction was first validated in every individual, for instance by demonstrating a consistent localization of early auditory ERPs to bilateral superior temporal regions.

Finally, the statistical tests that are reported do not exclude an additional impairment of feedforward processes in VS patients. The conclusions are based solely on the non-significance of a corrected-level two-sample t-test on individual feedforward connections. Yet such an insensitive test does not prove an absence of impairment. The authors should report the critical interaction needed to test whether the feedback connection from IFG is significantly more impaired than other feedforward connections.

Prima facie, the massive lesions typical of VS patients, which frequently involve distributed white matter anomalies [*11*], are likely to affect both feedforward and feedback connections from PFC. *A contrario,* the existence of a feedforward impairment in bringing auditory information to associative and prefrontal cortices is strengthened by the frequent absence of P3a and especially P3b ERP components in VS patients [*5-8*]. Indeed, previous work by the same team demonstrated that auditory stimuli failed to evoke activation beyond auditory cortices in VS patients, suggesting either a feedforward disconnection or direct lesions of higher cortices [*12, 13*]. In normal subjects, intracranial recordings suggest that both feedforward and feedback causal relations of posterior regions to prefrontal cortex are involved in conscious access [*14*]. We believe that bidirectional disconnections and, in many cases, direct PFC, thalamic and brain stem lesions are likely to provide a more complex but more realistic picture of the vegetative state [*11, 15*].

REFERENCES:

1. M. BOLY *ET AL.*, *Science* **332**, 858 (May 13, 2011).
2. H. C. LAU, *Prog Brain Res* **168**, 35 (2007).
3. S. DEHAENE, J. P. CHANGEUX, *Neuron* **70**, 200 (2011).
4. V. A. LAMME, *Trends Cogn Sci* **10**, 494 (Nov, 2006).
5. F. FAUGERAS *ET AL.*, *Neurology*, (published online May, 2011).
6. T. A. BEKINSCHTEIN *ET AL.*, *Proc Natl Acad Sci U S A* **106**, 1672 (Feb 3, 2009).
7. J. DALTROZZO *ET AL.*, *Clin Neurophysiol* **118**, 606 (Mar, 2007).
8. C. FISCHER, ET AL., *Neurology* **63**, 669 (Aug 24, 2004).
9. C. HAENSCHEL *ET AL.*, *J. of Neuroscience* **25**, 45 (Nov. 2005).
10. R. NÄÄTÄNEN, *ET AL.*, *Clin Neurophysiol* **118**, 2544 (Dec, 2007).
11. L. TSHIBANDA *ET AL.*, *Prog Brain Res* **177**, 215 (2009).
12. S., LAUREYS *ET AL.*, *Brain* **123**, 8 (2000)
13. M., BOLY *ET AL.*, *Arch Neurol* **61**, (Feb 2004)
14. R. GAILLARD *ET AL.*, *PLoS Biol* **7**, e61 (Mar 17, 2009).
15. D. FERNANDEZ-ESPEJO *ET AL.*, *Neuroimage* **54** , 103 (2010).
16. F. FAUGERAS, *ET AL.*, *Neuropsychologia*, under revision.

COMMENT 2

RIPPLES OF CONSCIOUSNESS

Sitt, Jacobo D. [1,2,3], King, Jean-Rémi [1,2,3], Naccache, Lionel [3,4,5], Dehaene, Stanislas [7,1,2,6]

1. Cognitive Neuroimaging Unit, Institut National de la Santé et de la Recherche Médicale, U992, F-91191 Gif/Yvette, France; 2. NeuroSpin Center, Institute of BioImaging Commissariat à l'Energie Atomique, F-91191 Gif/Yvette, France; 3. Institut du Cerveau et de la Moelle Épinière Research Center, Institut National de la Santé et de la Recherche Médicale, U975 Paris, France; 4. AP-HP, Groupe hospitalier Pitié-Salpêtrière, Department of Neurophysiology, Paris, France 5. Faculté de Médecine Pitié-Salpêtrière, Université Paris 6, Paris, France 6. Université Paris 11, Orsay, France; 7. Collège de France, F-75005 Paris, France

ABSTRACT

Casali et al. recently showed that the complexity of the electrophysiological brain response to a transcranial magnetic stimulation pulse distinguishes conscious from unconscious humans, in a variety of conditions. Beyond its theoretical implications, this novel method paves the way to a quantitative assessment of the states of consciousness.

ARTICLE

Every minute, millions of people lose (and recover) consciousness, because of the natural sleep-wake cycle, but also because of abnormal conditions such as coma, vegetative state, complex epileptic seizures or general anaesthesia. Yet, the precise neuronal mechanisms responsible for consciousness are poorly understood, and detecting whether a person is conscious therefore remains a major challenge.

In an exciting recent paper, Casali *et al.* [1] introduced a quantitative assay of the state of consciousness. Their work capitalizes on the electroencephalography (EEG) response evoked by a cortical transcranial magnetic stimulation (TMS) pulse. Previous research by the same group [2] demonstrated that, in conscious subjects, TMS pulses systematically elicit a complex spatiotemporal pattern of activation, whereas when the subjects are anesthetized, asleep, or in a vegetative state, TMS induces only a short and undifferentiated response. In their new publication [1], the authors quantify the complexity of this EEG response. They first reconstruct its cortical sources, then use algorithmic information theory tools to estimate the complexity of its spatiotemporal dynamics. They term the outcome Perturbational Complexity Index (PCI), a number ranging between 0 (no complexity) and 1 (maximal complexity).

Casali *et al.* applied this method to a large panel of subjects (n=32), obtaining recordings during wakefulness, light deep and REM sleep, and anaesthesia with midazolam, xenon or propofol. While all awake subjects presented a PCI above 0.44, all unconscious sleeping and anesthetized patients systematically showed values below 0.31. Thus, remarkably, the proposed index was distributed bimodally and

separated every conscious and unconscious individual. Furthermore, the authors tested this method in twelve patients with disorders of consciousness (DOC) and eight conscious brain-injured subjects. Vegetative state patients (n=6) had PCIs similar to the anaesthesia and sleeping groups, yet patients in a minimally conscious state (n=6) or emerging from it (n=6) had significantly higher PCIs (although they remained smaller than those of awake subjects). Finally, conscious but paralyzed patients ("locked-in syndrome", n=2), whose behavior may be confounded with a vegetative state, presented PCIs similar to healthy awake controls. These findings represent a major advance in the search for an empirical quantitative metric for consciousness, with important theoretical and clinical implications.

Theoretical implications

Casali *et al.* argue that PCI was designed to detect *integration* and *differentiation*, two central properties of the information integration theory of consciousness (IIT) [3]. According to the authors, integration can, in practice, be assessed by the global spread of cortical activation evoked by focal TMS, while differentiation relates to the fact that distinct regions are successively activated, without temporal redundancy. It should be noted, however, that EEG does not have the spatial resolution needed to evaluate the microdifferentiation of cell assemblies postulated in IIT, and that PCI is not directly related to Tononi's Phi measure (a formal quantification of the integrated information in a given network) proposed by IIT as a marker of consciousness. Although the technique was inspired by IIT ideas, the results so far merely show that TMS elicits a complex series of ripples across different brain areas only in conscious subjects. As such, they remain compatible with other models that associate consciousness with a preserved functional thalamocortical system able to "broadcast" a local activation to many distant cortical sites or to entertain long-lasting reverberating states [4,5].

A remarkable finding is that PCI is quantitatively identical regardless of the initial site of TMS application [1]. This finding fits with IIT's hypothesis that only information integration matters for the measurement of consciousness, while the specific anatomical areas involved can be disregarded. Nonetheless, this aspect of the research limits the interpretation of the precise neural mechanisms at work during conscious states. It would be important to know whether prefrontal, cingular or precuneus cortices as well as thalamocortical loops are systematically involved, as predicted by previous studies [4].

One important methodological aspect is the length of the time window used for PCI computation. Here the analysis was done on a 300-ms window following TMS. Although this choice may have been optimal, it seems arbitrary, as IIT theory does not specify the time scale at which information integration should take place. Conscious processing might be significantly slower in patients with diffuse white-matter lesions, demyelinating diseases, or during development. Indeed, a recent study showed that human infants present the same electrophysiological signatures of visual conscious perception as adults, but at much slower time scale [6]. It will important to verify whether PCI is robust to such temporal changes.

Clinical implications

Although Casali et al.'s patient sample remains small; their approach holds great promise for the diagnosis of vegetative state patients and the monitoring of anaesthesia. TMS stimulation has the clear advantage of directly perturbing the cortex with a strong stimulus, thus generating large EEG signals without requiring the integrity of a particular sensory pathway. Furthermore, unlike other paradigms previously tested to detect consciousness (see [7] for a review), this passive method does not depend on attention, task instructions or language comprehension. Nevertheless, because TMS-compatible EEG is not available in most clinics, it would be valuable to investigate if the TMS pulse is necessary, or if it could be replaced by another sensory stimulus. Supp *et. al.* [8] showed that the sequence of EEG responses to median nerve stimulation decreases dramatically under propofol anaesthesia. Similarly, the late long-lasting

event-related potentials evoked by an auditory oddball provides a tentative marker of consciousness in DOC patients [9]. Perhaps one might even get rid of the stimulus altogether and simply evaluate the presence of distributed and durable activation patterns in ongoing EEG. In recent work, King et al. show that a new EEG marker of the sharing of information across long cortical distances provides a sensitive index of consciousness in a large cohort of DOC patients (n=167) [10].

Finally, hundreds of TMS pulses are needed to compute a single value of PCI. This limitation may become relevant for minimally conscious patients in whom consciousness fluctuates over time, or for the real-time monitoring of anaesthesia. Could future research provide higher temporal resolution, faster acquisition and computation times, and ultimately a single-trial index of consciousness? Casali et al.'s research demonstrates that the dream of such a quantitative "consciousness-o-meter" may not be out of reach.

REFERENCES

1   CASALI, A.G. *ET AL.* (2013) A Theoretically Based Index of Consciousness Independent of Sensory Processing and Behavior. *Science Translational Medicine* 5, 198ra105–198ra105

2   MASSIMINI, M. *ET AL.* (2012) Cortical mechanisms of loss of consciousness: insight from TMS/EEG studies. *Archives italiennes de biologie* 150, 44–55

3   TONONI, G. (2004) An information integration theory of consciousness. *BMC neuroscience* 5, 42

4   DEHAENE, S. AND CHANGEUX, J.-P. (2011) Experimental and theoretical approaches to conscious processing. *Neuron* 70, 200–227

5   LAMME, V.A.F. AND ROELFSEMA, P.R. (2000) The distinct modes of vision offered by feedforward and recurrent processing. *Trends in Neurosciences* 23, 571–579

6   KOUIDER, S. *ET AL.* (2013) A neural marker of perceptual consciousness in infants. *Science* 340, 376–80

7   HARRISON, A.H. AND CONNOLLY, J.F. (2013) Finding a way in: A review and practical evaluation of fMRI and EEG for detection and assessment in disorders of consciousness. *Neuroscience and biobehavioral reviews* DOI: 10.1016/j.neubiorev.2013.05.004

8   SUPP, G.G. *ET AL.* (2011) Cortical hypersynchrony predicts breakdown of sensory processing during loss of consciousness. *Current biology* 21, 1988–93

9   KING, J-R. *ET AL.* (2013) Single-trial decoding of auditory novelty responses facilitates the detection of residual consciousness. *NeuroImage* 83C, 726–738

10   KING, J-R. *ET AL.* (2013) Cortical information sharing indexes the state of consciousness. *Current biology,* in press